THE UNIVERSITY
of EDINBURGH

New Optimal Power Flow Techniques to Improve Integration of Distributed Generation in Responsive Distribution Networks

Institute for Energy Systems

School of Engineering

University of Edinburgh

a thesis submitted for the degree of Doctor of Philosophy

March 2015

James Robertson

Abstract

Climate change has brought about legally-binding targets for Scotland, the U.K. and the E.U. to reduce greenhouse gas emissions and source a share of overall energy consumption from renewable energy resources by 2020. With severe limitations in the transport and heating sectors the onus is on the electricity sector to provide a significant reduction in greenhouse gas emissions and introduce a substantial increase in renewable energy production.

The most attractive renewable energy resources are located in the geographic extremes of the country, far from the large population densities and high voltage, high capacity transmission networks. This means that the majority of renewable generation technologies will need to connect to the conventionally passive, lower voltage distribution networks. The integration of Distributed Generation (DG) is severely restricted by the technical limitations of the passively managed lower voltage infrastructure. Long lead times and the capital expenditure of traditional electricity network reinforcement can significantly delay or make the economics of some renewable generation schemes unviable. To be able to quickly and cost-effectively integrate significant levels of DG, the conventional fit-and-forget approach will have to be evolved into a ‘connect-and-manage’ system using active network management (ANM) techniques.

ANM considers the real-time variation in generation and demand levels and schedules electricity network control settings to alleviate system constraints and increase connectable capacity of DG. This thesis explores the extent to which real time adjustments to DG and network asset controller set-points could allow existing networks to accommodate more DG.

This thesis investigates the use of a full AC OPF technique to operate and schedule in real time variables of ANM control in distribution networks. These include; DG real and reactive power output and on-load-tap-changing transformer set-points. New formulations of the full AC OPF problem including multi-objective functions,

penalising unnecessary deviation of variable control settings, and a Receding-Horizon formulation are assessed.

This thesis also presents a methodology and modelling environment to explore the new and innovative formulations of OPF and to assess the interactions of various control practices in real time.

Continuous time sequential, single scenario, OPF analyses at a very short control cycle can lead to the discontinuous and unnecessary switching of network control set-points, particularly during the less onerous network operating conditions. Furthermore, residual current flow and voltage variation can also gave rise to undesirable network effects including over and under voltage excursion and thermal overloading of network components. For the majority of instances, the magnitude of constraint violation was not significant but the levels of occurrence gave occasional cause for concern. The new formulations of the OPF problem were successful in deterring any extreme and unsatisfactory effects.

Results have shown significant improvements in the energy yield from non-firm renewable energy resources. Initial testing of the real time OPF techniques in a simple demonstration network where voltage rise restricted the headroom for installed DG capacity and energy yield, showed that the energy yield for a single DG increased by 200% from the fit-and-forget scenario. Extrapolation of the OPF technique to a network with multiple DGs from different types of renewable energy resources showed an increase of 216% from the fit-and-forget energy yield. In a much larger network case study, where thermal loading limits constrained further DG capacity and energy yield, the increase in energy yield was more modest with an average increase of 45% over the fit-and-forget approach. In the large network where thermal overloading prevailed there was no immediate alternative to real power curtailment.

This work has demonstrated that the proposed ANM OPF schemes can provide an intelligent, more cost effective and quicker alternative to network upgrades. As a result, DNOs can have a better knowledge and understanding of the capabilities and technical limitations of their networks to absorb DG safely and securely, without the expense of conventional network reinforcement.

Declaration of Originality

I hereby declare that the research presented in this thesis is entirely my own work, conducted and composed by myself in the Institute for Energy Systems, School of Engineering at The University of Edinburgh.

James Robertson

Acknowledgments

I would like to thank Robin Wallace and Gareth Harrison for their support, wisdom and advice.

My thanks also go out to all of my colleagues in the Institute for Energy Systems for their support and encouragement. I am particularly grateful to the advice of Jeff Steynor and Tom Davey, who in the early stages if this work helped me to acquire the tools and develop the skills necessary to see me through.

Further mention is also due to Randy (Sun Wei), Nando Ochoa and Paul Trodden for their insight and recommendations. Their advice and discussions have been invaluable and your assistance was greatly appreciated.

Special thanks are also reserved for the EPSRC UK-China Network of Clean Energy Research for providing financial support for this work and the opportunity to travel and experience the Chinese culture.

Final mention must however, go to my family, friends and partner Francesca who, in particular, has endured *'with such grace'* the best and the worst of my Jekyll-and-Hyde 'weegie' attitude during the highs and lows of this work.

Short Contents

Contents

List of Figures

List of Tables

Acronyms and Abbreviations

AMI	Advanced Metering Infrastructure
ANM	Active Network Management
APFM	Active Power Flow Management
AR(p)	Auto Regressive
ARIMA	Auto Regressive Integrated Moving Average
ARMA	Auto Regressive Moving Average
AVC	Automatic Voltage Control
AVR	Automatic Voltage Regulator
BAU	Business-As-Usual
CMA	Centred Moving Average
CVC	Coordinated Voltage Control
DA	Distribution Automation
DFIG	Doubly Fed Induction Generator
DFR	Distributed Frequency Response
DG	Distributed Generator
DMS	Distribution Management System
DNO	Distribution Network Operator
DPCR5	Fifth Electricity Distribution Price Control Review
DSM	Demand Side Management
ENSG	Electricity Networks Steering Group
EU	European Union
EV	Electric Vehicle
FG	Firm Generation
FLCOPF	Fault Level Constrained Optimal Power Flow
G8	Group of Eight
GHG	greenhouse gas
GSP	Grid Supply Point
IFI	Innovation Funding Incentive
IGBT	Insulated Gate Bipolar Transistor
ISO	Independent System Operator
LCNF	Low Carbon Networks Fund
LIFO	Last-In, First-OFF
MA(q)	Moving Average (forecast)

MPC	Model Predictive Control
NFG	Non Firm Generation
NIA	Network Innovation Alliance
OLTC	On Load Tap Changer
OPF	AC Optimal Power Flow
PFC	Power Factor control
PV	Photo-Voltaic
q MA	Moving Average (smoothing)
RD&D	Research Development and Deployment
RH	Receding-Horizon
RHOPF	Receding-Horizon Optimal Power Flow
RIIO	Revenues = Incentives + Innovation + Outputs
ROC	Renewables Obligation Certificate
ROCOF	Rate of Change of Frequency
RPZ	Registered Power Zone
RTU	Remote Terminal Unit
TSO	Transmission System Operator
UN	United Nations
UNFCCC	United Nations Framework Convention on Climate Change
UoE	University of Edinburgh
V2G	Vehicle to Grid
VPP	Virtual Power Plant
VR	Voltage Regulator
WCMA	Weighted Centred Moving Average
WEC	Wave Energy Converter
WTG	Wind Turbine Generator

Chapter 1

Introduction

1.1 THESIS BACKGROUND

Around the world, meeting the significant international targets for the reduction of greenhouse gas (GHG) emissions [1],[5] will require substantial decarbonisation of the conventional electricity generating mix as well as large scale reductions in demand. Substantial decarbonisation beckons towards high levels of sustainable but more variable renewable energy resources. The UK, and Scotland in particular, has a rich and abundant resource of renewable energy potential such as wind, wave and tidal energy. However, accepting a high proportion of renewable energy resources into the electricity generating mix is a scientific and engineering challenge [41],[42].

Renewable energy resources are typified by low energy density and are highly dependent on geographical and environmental conditions. This generally means the best potential resources are available in remote areas of the country, typically located far from the load demand centres of the nation's cities and towns. Renewable energy resources are also harvested by modular units of small capacity and their geographic dispersion means that they are remote from the more heavily reinforced sections of the electricity network. Connection to the electricity network is typically achieved in the lower voltage distribution network.

Distribution networks are designed to transfer electricity from the high voltage transmission network to industrial, commercial and domestic users. In the geographically remote locations of abundant renewable energy resources, the distribution networks are generally structured radially, with passive control practices and are tapered in cross-sectional area with a continually diminishing voltage level and capacity to carry electrical power. Generating units connected to the lower voltage supply side of the electricity network are not currently centrally controlled or dispatched

and are referred to as Distributed Generation (DG). Other widely recognised terms include embedded or dispersed generation.

Currently new capacities of DG are permitted to connect to distribution networks provided they do not conflict with or degrade the existing network operating conditions. This is known as, the business as usual (BAU) 'fit-and-forget' approach, and in practice can significantly restrict the capacity of DG development that can be connected to the existing distribution network. Additional DG capacity can be accommodated but has previously required traditional reinforcement of the electricity network at high capital cost to the DG developer. With the high levels of renewable energy resources in the generation mix required to meet ambitious renewable energy targets, this is a significant economic challenge. The desire to see the integration of high penetrations of intermittent and spatially variable DG capacity mandates a reconsideration of the passive operating principles of conventional distribution networks. In order to establish the ability of the existing distribution networks to facilitate the increases in DG capacity, new and innovative approaches to the operation and control of distribution networks are required [47]. Electricity networks at large are in a phase of major redevelopment under the combined influences of ageing infrastructure, growing demand and changing generation mix. This further adds to the financial strain of up-rating the peripheries of electricity networks.

Research is exploring the challenges that decarbonisation of the electricity generation mix brings. The current research in power systems planning and operation is developing new ways of understanding how to connect more generation from renewable energy resources into electricity networks. Existing research has highlighted the benefits to be found from the application of active network management (ANM) techniques and promoted the use of futuristic smart-grid technologies. In the work to date, a number of Optimal Power Flow (OPF) techniques have been used to investigate the network benefits from integrating multiple ANM techniques [59]. This work has focused upon the, "off-line" planning phase of power systems operation.

The work reported in this thesis investigated the next phase of challenges in developing and modelling appropriate solutions for scheduling variable network control settings "on-line" to provide real time active homeostatic network operation. In a related theme,

the maturation of the current onshore wind energy sector, improvements in energy yield prediction techniques and reductions in uncertainties for renewable resources makes the ability to anticipate power production levels in pseudo-real time conceivable, and therefore desirable. This project developed from the existing research and explored a new dimension, investigating the benefits and system consequences that arise from the real time deployment of integrated ANM techniques and investigated new OPF based techniques and methodologies to improve the scheduling of ANM control settings.

1.2 PROJECT OBJECTIVES AND SCOPE

Mapping the application of modern, more intelligent control techniques onto the existing vertically integrated electricity systems is most likely to be implemented through a series of multi-level control systems with differing functionality, coordination and range of control.

The aim of this PhD study was to investigate the novel use of Optimal Power Flow (OPF) techniques to establish the best distribution network control presets for pseudo-real time scheduling of generation and other network assets in responsive distribution networks to better facilitate high penetrations of intermittent and spatially variable DG sources within the existing network framework.

The main objectives for the project were:

- To establish generic distribution network models that would have the ability to allow implementation of innovative control procedures and exploration of the technical limitations of the existing electrical systems.
- To establish new OPF techniques to better integrate renewable generation sources and maximise the network benefit from DG.
- To investigate the benefits of real, or pseudo-real, time optimisation of distribution networks in terms of network hosting capacity, energy losses and improved use of existing assets.
- To explore hybrid methods of generation and network control to coordinate the implementation of OPF control presets in real time.

This thesis reports the research methods and findings in each of these areas.

1.3 THESIS AND CONTRIBUTION TO KNOWLEDGE

This project set out to test the hypothesis that:

"OPF techniques can be used in real time to determine appropriate active network control set-points to integrate more DG from renewable energy resources within the existing network infrastructure."

Whilst considerable attention has been paid to the opportunities for ANM in distribution networks, there is no corresponding investigation of the real time network impacts and potential viability of implementation.

This thesis reports the successful application of OPF techniques in distribution networks with high penetrations of variable DG. Control of generation and network assets under the advisory action of new OPF and forecasting techniques led to significantly increased yield in constrained networks.

Furthermore, while the relationship between the centralised scheduling of assets and the active localised control practices is becoming better understood, this thesis adds to that body of knowledge within the context of OPF techniques.

1.4 THESIS OUTLINE

This chapter provided an introduction to the thesis. It presented a high level overview of the case for ANM and identified a need for analysing and interpreting the real time application and system consequences of applying progressively more active strategies to distribution networks.

Chapter 2 begins with an extensive literature review of the environmental, political and commercial influences driving significant change in the electricity industry. It continues with a review of electricity network, power flow and optimal power flow theory.

The technical challenges of integrating renewable DG are also discussed followed by a survey of existing ANM techniques and projects. Development of existing active management activities is also reviewed with an emphasis on progressing state of the art concepts, extending their capabilities and providing flexibility to accommodate future technological developments.

A new modelling environment and OPF technique for active scheduling (and control) of variable DG and responsive network asset control settings was developed and is described in Chapter 3. Specification of the fully integrated ANM scheme is presented alongside a package of interchangeable software elements, defined to facilitate real time performance assessment, and reflecting the 'hardware-in-the-loop' application of an ANM solution.

Test case simulations are presented in Chapters 4 and 5, beginning from proof of concept in Chapter 4 and extending to validation in further network configurations with higher numbers of DGs from multiple renewable energy resources in Chapter 5. Performance of the OPF technique to prescribe progressively more active and coordinated control settings was tested against increased energy capture and harmonisation of control settings.

In the later section of Chapter 5 an interactive network case study with the centralised optimal scheduling of active DG and responsive network control assets in combination with autonomous decentralised (or local) control intelligence is presented.

Finally Chapter 6 further discusses the results and outcomes of Chapters 4 and 5 and reflects on the work in a wider system context, reviewing the strengths and limitations of the proposed techniques and detailing key issues for future work.

1.5 Associated Published Work

James Robertson, Gareth P. Harrison & A. Robin Wallace, *"A Pseudo-Real Time Distribution Network Simulator for Analysis of Coordinated ANM Control Strategies"*, Proceedings CIRED workshop 2012: Integration of Renewables into the Distribution Grid, no. 0285.

James Robertson, Gareth P. Harrison & A. Robin Wallace, *"A Receding-Horizon OPF for Active Network Management"*, *CIRED 22nd International Conference on Electricity Distribution*, no. 1412, 2013.

James Robertson and A. Robin Wallace, *"Evaluation of Finite Horizon Active Network Management"*, International Conference on Sustainable Power Generation and Supply (SUPERGEN) 2012.

Chapter 2

Literature Review and Basic Theory

2.1 INTRODUCTION

This chapter reviews the findings from an extensive literature survey on the UK electricity system and renewable energy resources. It starts with a general description of the UK electricity system and a detailed overview of the theory of power flow and Optimal Power Flow (OPF). A review of the key technical impacts and restrictions on DG developments in typical UK distribution networks is presented along with consideration of known engineering development within the sector. The political pressures driving change in the electricity supply sector are also addressed. Finally, assertions are made on the likely future objectives for the operation of distribution networks and utilised to provide a formative picture for the progression of this work.

2.2 CLIMATE DRIVERS AND POLITICAL RESPONSE

Based on consistent scientific evidence about the detrimental consequences of climate change there is an increased international awareness of the need to reduce greenhouse gas emissions. As a result the energy sector is in the early stages of a period of prolonged change.

In the UK, changes in energy policy have been influenced by the United Nations Framework Convention on Climate Change (UNFCCC), the European Union (EU) and the G8.

At the United Nations (UN) Conference on Environment and Development in 1992, 195 nations, including the UK as a member of the European Community, negotiated a treaty that introduced the first preliminary measures to reduce greenhouse gas emissions. This

treaty known as, the UNFCCC, was ratified to stabilise greenhouse gas concentrations emitted as a result of human activity, to ideally reach pre-1990 levels.

This was followed by the Kyoto Protocol in 1997, which only came into force in 2005, and concerned a period of commitment between 2008 and 2012, that created an international incentive to introduce legally-binding targets for emission reductions. With a strong appreciation for the integral link between energy and economic development, and given that current greenhouse gas emissions are inflated from more than 150 years of industrial activity principally in nations now regarded as developed countries, the Kyoto Protocol retained a *"common but differentiated responsibilities"* approach placing more substantial accountability on developed nations [1]. As a result of these measures and as a member of the European Community, which assumed its responsibility for a gross percentage reduction in emissions spread throughout its member states, the UK was committed to reducing its GHG to 12.5% below 1990 levels.

Furthermore, as president of the G8 summit in 2005, the UK government extended its international commitment, albeit non-obligatory, to address climate change with the Gleneagles Plan of Action: Climate Change, Clean Energy and Sustainable Development [2].

The plan acknowledged extended benefits from a transition to a more sustainable international energy portfolio and reaffirmed the importance of developing long-term national and inter-national policy frameworks. The document detailed strong commitments to increase energy efficiency across a wide range of commercial and residential sectors. Development and commercialisation of renewable energy technologies would, alongside facilitating nuclear power, cleaner fossil fuels and Carbon Capture and Storage (CCS) technologies, improve security of energy supplies. The document confirmed favourable support for a market-led approach to financing the transition, via incentives, investment and policy approaches subject to each country's national circumstances.

More importantly in the context of this work, the document was first to acknowledge the potential challenges of integrating renewable energy resources into electricity networks. The outcomes from this part of the discussion highlighted the need for

drawing together research and evaluating ways and means to overcome technical, regulatory and commercial barriers.

The Energy White Paper: “Meeting the Energy Challenge” by the former Department of Trade and Industry (DTI) [3] accumulated the research outcomes on climate change and additional energy security issues and initiated discussions on how the UK could meet its international obligations on climate change. The paper supported the findings from the G8 summit in 2005 to pursue a market-led approach to future electricity supplies, and acknowledged the need for incentivising mechanisms to stimulate renewable energy developments. The 2007 Energy White Paper also indicated the UK intention for a minimum 60% reduction in greenhouse gas emissions against the 1990 baseline and, amongst other strategies, committed increased funding allowances and incentives for substantial investment in the electricity networks to meet growth in electricity demand, enable connection of renewable energy technologies and replace rapidly ageing infrastructure.

A parliamentary bill to make the 2007 Energy White Paper target legally binding was passed in the UK Climate Change Act of 2008 [4]. This bill made the UK the first country in the world to have a legally binding-long term framework to cut carbon emissions, and increased the UK target of reducing its emissions from 60% to 80% by 2050. Further dissemination of the Act 2008 highlighted an interim target of 26% in 2020.

In relation, the European Council introduced legally-binding targets for all EU member states to reduce greenhouse gas emissions with the publication of the “20 20 by 2020: Europe’s climate change opportunity package” [5]. The package set out two key accumulative targets for the EU member states:

- A reduction of at least 20% in greenhouse gases by 2020.
- A 20% share of renewable energies in EU energy consumption by 2020.

The second target commits the EU member states to meet 20% of their overall energy consumption in 2020 from renewable energy resources, regardless of any reductions in greenhouse gas emissions. The term energy consumption implies the energy required for heating and cooling, electricity and transport. In line with the *"common but*

differentiated responsibilities" approach the UK's national target for final energy consumption from renewable energy resources is 15%. While this does not represent the largest percentage contribution of any member state, it does represent the single largest percentage point increase supplied from renewable energy resources, with the UK only achieving 1.3% of final energy consumption from renewables in 2005 [6]. In the EU 20 20 by 2020 directive, member states were free to encourage their share of the renewables targets in any of the heating and cooling, electricity or transport sectors. At the time of issue, the UK's final energy usage comprised of 41% from heating and cooling, 22% electricity and 37% from transport, with only 4.5% of 2006 electricity generation from renewable energy resources and 0.6% and 0.5% of energy from renewable sources in the heating and cooling and transport sectors respectively.

Substantial gains in renewable transport are severely hampered by contentions in the sustainability of bio-fuel crops. Moreover, the support for electric vehicles and further electrification of the railways redirects the burden of renewable energy production onto the electricity sector. Increasing the contribution of large scale renewable heat sources would be inefficient and require transmission infrastructure and policy that is unlikely to be available in the specified time frame. This implies that the electricity sector, despite playing the smallest contribution to overall energy consumption, is set to make the largest contribution to renewable energy production, with somewhere between 30% and 40% of electricity generated coming from renewable sources depending on achievements in the heating and cooling and transport sectors.

Under the ordinance of the Gleneagles Plan of Action; the UK Climate Change Act; and, the EU 20 20 by 2020 Directive coupled with an anticipated increase in overall electricity demand there is a need for the drastic integration of renewable energy generating technologies. In Scotland, political agendas and an abundance of the most concentrated renewable energy resources in the whole of Europe, have encouraged self-imposed voluntary targets that make a disproportionate contribution to UK and EU renewable energy targets. Given the rapid development of renewable technologies, the latest announcement of Scotland's renewables strategy [7] has committed the country to the most ambitious targets in the EU, aiming for 100% of equivalent electricity demand, and 30% of its overall energy consumption to come from renewable sources in 2020.

The UK government published its response to the EU 20 20 by 2020 directive in October 2008 [6] and in 2009, issued the UK's Renewable Energy Strategy [8] that set out the country's plan to meet the legally-binding targets on renewable energy generation. The strategy acknowledged that the electricity system, from network infrastructure to electricity markets, was not designed for the large influx of renewable energy technologies. Existing market and regulatory statutes were designed with the needs of large, centrally connected generators presenting issues with market penetration, encouraging innovation and a lack of grid access [9].

In the privatised UK Electricity Market, the price and supply of energy is determined by market action and therefore, in theory, under the principles of perfect competition and the free market economy, the price of energy is set at the level of its economic worth, providing the best value for the consumer. Whilst fossil fuels are an initial cheap source of energy, and uncertainties with the availability of renewable energy resources persist, the market economy initially, did not favour the integration of renewable energy technologies and failed to deliver a feasible mechanism for substantial investment in their research and development

Multiple incentive schemes, including Non Fossil Fuel Obligations, Fossil Fuel Levies, Certificated Renewables Obligations and Feed-In-Tariffs that offer financial support for high cost renewable energy developments have been introduced and worked well to incentivise renewable energy developments. Renewables Obligation Certificates (ROCs), the primary support mechanism for generation of power from renewable sources in the UK, compels electricity suppliers to certify that a certain percentage of the electricity they sell is sourced from renewable generators. The required percentage rises year-on-year to support continued development of renewable energy in line with projected targets. Amendments to the system, such as varying levels of support for different renewable technologies assist the development of new resources and diversification of the electricity generation mix.

Nevertheless, each incentive directly rewards the production of renewable energy and their emphasis is based on levellising the cost of renewable and immature technologies in the electricity market and does not directly or in-directly support the development of the required network infrastructure or supply chains. With long waiting lists for grid

connections for new wind farm developments; the Government introduced the concept of “connect and manage” grid connections for renewables projects. Given the intermittent and variable nature of wind energy means that most developments only operate with a capacity factor of 30-40%, the most onerous system conditions are only experienced for a limited number of times per year. Connect-and-manage (or non-firm) grid connections allow renewable developments to connect prior to the necessary grid reinforcement by curtailing generator production when network power flows become problematic.

It was reported in [8] that around 1GW of the 10-14GW noted in [6] of renewable developments were offered the opportunity for early connection using this approach.

Support for a ‘connect-and-manage’ approach in the distribution networks, marked a major transition and evolution from the stable passive approach and, given the privatisation of the electricity networks, requires substantial support and incentives to change the technical mindset of DNOs. The government department and national regulatory authority, Office of Gas and Electricity Markets (Ofgem), has introduced a series of initiatives and additional subsidy to DNOs including the Innovation Fund Incentive, Registered Power Zone and the Low Carbon Networks fund, which are detailed further below.

2.2.1 INNOVATION FUND INCENTIVE

From early 2002, due to a lack of natural market pressures on DNOs to invest in research, development and deployment activities, Ofgem began consultation on funding mechanisms to encourage such activities and help prepare the networks for the low-carbon economy.

In 2005 the Innovation Funding Incentive (IFI) scheme was introduced and was initially scheduled to run until 2010. The Innovation Funding Incentive provides funding for research, development and deployment (RD&D) activities relating to innovation and technical development in the design and operation of distribution networks up to and including 132 kV.

The IFI mechanism allows DNOs to recover from its customers a significant proportion of the investment it makes in IFI RD&D projects. This portion began at 90% in 2005

and tapered steadily until 2010 when it stood at 70%. Total IFI expenditure was capped at 0.5% of the DNOs distribution network revenue.

In 2006 the scheme was extended to run until the end of the next price control period in 2015, when it will be replaced by the Network Innovation Alliance (NIA), which is specifically designed to function within the new price control model for electricity distribution networks RIIO (Revenue = Incentive + Innovation + Outputs), and will provide funding for smaller technical, commercial and operational projects.

2.2.2 REGISTERED POWER ZONES

The Registered Power Zone (RPZ) scheme differs from the IFI in that the mechanism is used to promote RD&D specifically targeted at the integration of renewable DG. It was designed to encourage DNOs to integrate technically innovative concepts as part of their wider business development.

There were four 'connect-and-mange' concepts piloted through the RPZ scheme. These concepts include the active regulation of primary substation voltage control measures in Martham and Steyning, metering and active regulation of the thermal capacity of overhead lines in Skegness, curtailment of wind power production in order to maximise generation capacity in the Orkney Isles and energy storage projects in the Shetland Isles. More detail is provided on these schemes and concepts in the review of Active Network Management in Chapter 2.7.

2.2.3 LOW CARBON NETWORKS FUND

The RPZ scheme acted as a pre-cursor for a Low Carbon Networks Fund (LCNF), which was established under the fifth distribution electricity price control review (DPCR5) as a means of introducing incentives for DNOs to research and develop innovative solutions that will prepare and advance their networks to facilitate legally binding targets on renewable energy resources. The LCNF provides up to £500million of financial support over five years for DNOs to investigate the potential for new technology and the challenges facing their networks under a future low carbon generation mix. Subsidy for the LCNF is provided through the new price control model for distribution revenues, RIIO, whereby the subsidy that DNOs receive from the LCNF

is a redistribution of revenues from the traditional use of system charges applied to electricity suppliers.

2.3 RENEWABLE ENERGY RESOURCES

In the drive to reduce carbon emissions and introduce renewable sources of energy into the electricity sector, a significant amount of time and effort has been devoted to developing means of electricity generation from a rich mix of sustainable, low-carbon energy sources. The vast majority of the technology associated with these renewable energy resources has advanced to the stage where it is, or has the potential to; contribute significantly to the electricity generation of most of the developed world. Given the wide variety of renewable energy resources considered the availability, location and scale can vary significantly. This section provides a brief introduction to the primary properties of each resource, the characteristics of the supply and the associated connection to electricity networks.

2.3.1 HYDROPOWER

The most developed of all the renewable energy resources; hydropower is the oldest form of modern renewable power generation. Now ranking fourth, in 2001 hydropower was the second largest source of electricity generation in the world [9]. While world-wide growth is set to continue, it is believed that all large scale resources in the UK have been exhausted. However, there is still good potential for small or mini-hydro developments [11]. These developments will require connection to the electricity network as DG.

Hydropower involves exploiting the gravitational potential energy in volumes of water stored or running at different heights in a river or stream. In terms of production capabilities, the generation output is principally dependent on the height difference, or head, that the water flows through and the volumetric water flow rate. There are three distinct types of hydropower stations: run-of-river, impoundment and impoundment pumped storage. Run-of-river stations divert a percentage of running water in a stream and drop it through a turbine and back into the river downstream. Impoundment stations generate electricity in the same way but hold back the stream of water in either a natural or man-made reservoir. Pumped storage is a variation on impoundment that is

particularly useful in balancing system load as the reservoir can be drained at periods of high demand and pumped back-up from the free stream in periods of load demand. Hydropower in general is very useful for system balancing as the ramp-rate of production is very short and additional power can be brought online in the order of minutes.

2.3.2 WIND

In the 1970s, a new era for wind energy technology, saw it develop into the strongest market ready renewable generation technology. Installed capacities and trajectories of wind energy deployment show it to be currently, and for the foreseeable future, the largest producer of renewable energy in the UK. The current onshore wind energy capacity stands at 4 GW, producing 7 TWh of energy annually, with a further 11 GW of onshore wind energy capacity in the pipeline. It is likely that up to and around 13 GW of onshore wind energy will be connected by 2020 [9]. A further 3.6 GW of offshore wind energy is currently connected to the UK electricity network producing around 8 TWh of electricity annually [12]. Governmental targets indicate that up to 18 GW could be connected by 2020.

This poses some significant challenges for the Transmission System Operator (TSO) who is responsible for the continuous supply-demand balance. Power output from wind turbine generators (WTG) is proportional to and varies with the cube of the prevailing wind speed magnifying its spatial and temporal variability. A typical power curve of a WTG, shown in Figure 2.1, highlights this, with only wind speeds between 12-24 m/s producing maximum power generation. Above 24 m/s WTG are shut down to avoid damage and between 4-12 m/s power production ramps up sharply. With mean wind speeds for UK developments generally between 5-8 m/s this can introduce great variability in the power delivered.

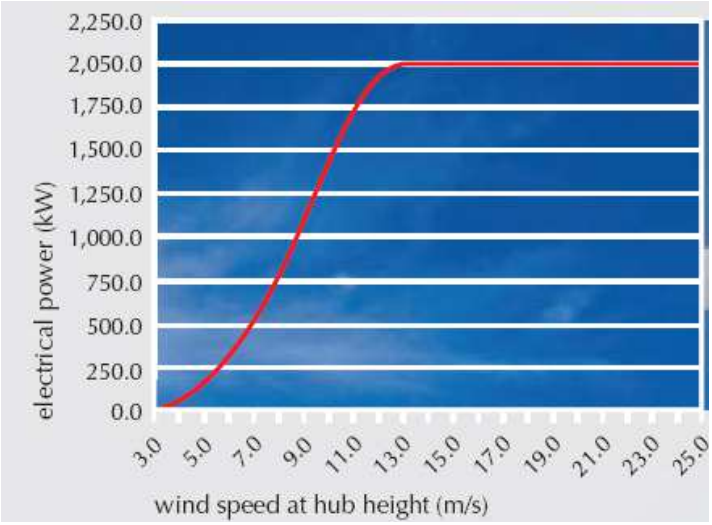

Figure 2.1: Power curve from the REpower MM82 WTG [13]

2.3.3 WAVE & TIDAL

Marine energy resources, developed by wave energy converters (WECs) and tidal current-turbines are an extremely important component to future electricity supplies in the UK given the climate and geographical position of the country. It is well regarded that the UK has the best potential for marine energy resources in Europe, and the sector is now moving to multiple machine array deployment.

Waves are generated over open bodies of water through friction between the water surface and the air molecules of wind blowing over the surface. The amount of energy in waves is dependent on the wind speed, the duration of the wind and the expanse of water the wind blows over [14]. Given that prevailing winds flow across the Atlantic Ocean from west to east, the prospect for wave energy in the UK looks promising. The potential for marine energy generation has been examined in some detail and forecasts have put the potential energy resource for electricity generation in the UK at 5.7 TWh/year for the near-shore wave energy conversion, and 70 TWh/year for the total UK practical resource [15].

Tidal current flows are driven by the gravitational interaction between the Earth, Sun and Moon. Because of this, although variable with time, tidal energy production patterns can be reliably predicted on both short and long timescales making tidal energy the most predictable of all renewable generation sources. There remain two primary methods for extracting power from the tides: tidal barrages and tidal currents.

A tidal barrage is the more conventional method of extracting power from tides. It consists of trapping high volumes of water at high tide using a barrage (or dam) to create a substantial head difference in the water level and then releasing it through a turbine.

Tidal current devices resemble underwater wind turbine generators extracting power from specific locations with high tidal current velocities. High velocity tidal currents are formed primarily in narrow channels through a combination of local geographic factors. Tidal turbines can be arranged singly or in arrays, allowing a range of power outputs to be produced. In the UK, this technology is currently under a great deal of research and development and is favoured to become the next commercially viable renewable energy resource after onshore wind. The tidal current resource has also been examined in great detail with the practical potential for electricity generation estimated to be around 30 TWh/year [15]. The best resources for tidal current devices are focused on a relatively small number of sites, which in Scotland, are located at the peripheries of the electricity network.

2.3.4 SOLAR

There exist two primary forms of solar energy conversion: thermal and electrical. The simplest form of solar energy conversion is the heating of water from the suns radiation. The second more valuable form comes as electricity generated through Photo-Voltaic (PV) panels. PV panels generate an electrical current from the movement of electrons in a photoelectric cell induced by the light energy incident on the cell surface.

The potential worldwide for electricity generation from solar energy is vast, however due to climatic conditions, installation of solar energy in Scotland and the UK is likely to be restricted to small scale domestic developments installed on the roofs of houses, or commercial buildings, known as micro-generation. The term micro-generation covers any electrical or heat generation development up to 50 kW for electricity and 45 kW for heat connected in parallel with public low voltage networks. Across the UK the overall solar PV capacity at the end of 2013 was 2.84 GW [16]. From the viewpoint of this thesis, the nature of small scale generation such as solar PV, cannot be aggregated or controlled at a distribution network level. Hence, the integration of micro-generation

has been perceived as an energy saving or load reduction measure and is not directly controllable as part of the ANM scheme as considered in this work.

2.3.5 BIOENERGY

According to the International Energy Agency (IEA) Bioenergy is the fourth largest energy source in the World after oil, coal and gas.

Bio-energy is the generic term for all energy types that have been derived from the decomposition of organic matter in the relatively recent past. This encompasses liquid and gas bio fuels, plant biomass, wood burning and animal by-products.

Biomass has an enormous advantage and distinction from most other renewable energy resources; it can be stockpiled in much the same way as coal to provide energy in a more continuous and dispatchable fashion. This can help to smooth out fluctuations in production.

In Scotland, biomass is likely to be largely employed to help achieve the Scottish Government 2020 targets on renewable heat [7]. This is also likely at the UK level, although indications are that total electrical capacity from biomass could rise from 2.5 GW (generating approximately 11.9 TWh) in 2010 to 6 GW in 2020 [18].

2.4 ELECTRICITY NETWORKS AND POWER FLOW

2.4.1 ELECTRICITY NETWORKS

This work focuses on UK electricity networks in particular, but the challenges identified and the solutions proposed are mirrored in power systems around the world. Electricity networks vary significantly across different countries; however the general structure of conventional systems remains unchanged. A standard model and the original UK electrical power systems structure, shown in Figure 2.2, is vertically integrated and composed from four main components: i) Generation; ii) Transmission; iii) Distribution; and, iv) Supply. The vertical structure is illustrated in Figure 2.2 and operates on a *'supply follows demand'* philosophy.

The emergence of large volumes of connected renewable generation can fundamentally alter the location and magnitude of power flow in the electricity network mandating increased understanding of the effects and potential mitigations of any adverse effects.

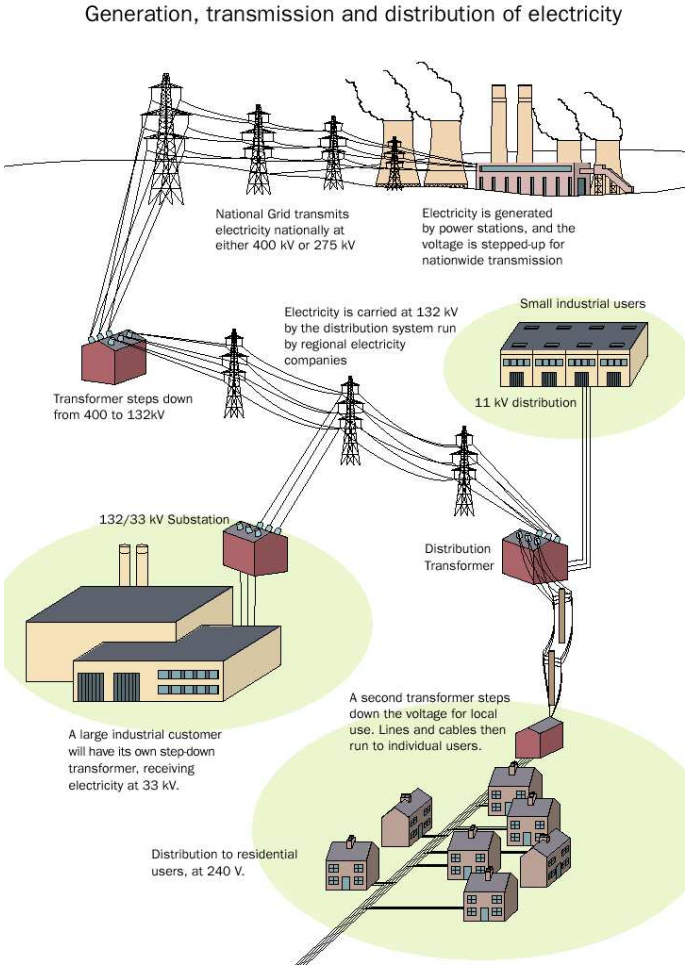

Figure 2.2: Structure and conventional composition of the UK electricity network [17]

Firstly, as evident in Figure 2.3, generation in the UK was traditionally served by large scale power plants utilising fossil fuel resources such as coal, gas and oil, as well as nuclear power stations and some hydropower in the north of Scotland and Wales. Power stations, by necessity, are always located in areas of good resource and relatively close to demand, as is evident in Figure 2.4. In practice this means that nuclear stations are restricted to the coast for a source of cooling water and gas plants require close links to large pipelines. Conveniently, in the case of coal, population densities also followed this principle, accumulating geographically in areas of high energy resources during the 19th and 20th centuries. Meaning much of the UK population clusters found outside of London and the south east of England are in areas with large scale coal resources and close to rivers or the sea for condenser cooling water. Emerging from these historical climates most of the generation capacity is located close to spikes population densities.

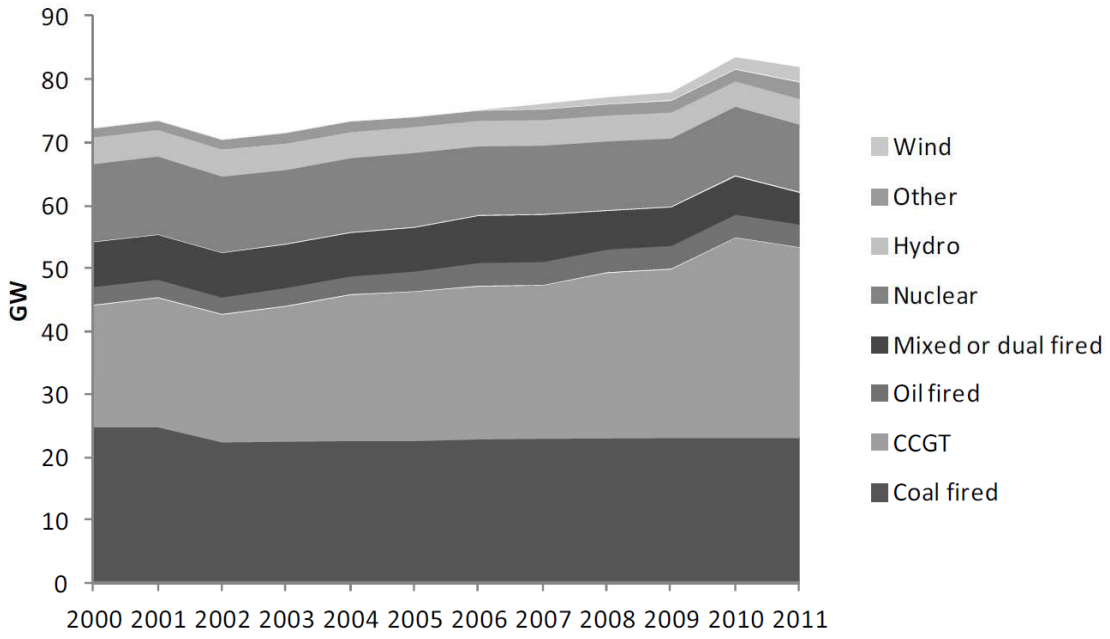

(1) 'Other' includes: Gas turbines, oil engines and renewables other than hydro.
(2) 'Hydro' includes Natural flow and pumped storage.
(3) 'Mixed or dual fired' includes non-CCGT stations that can be fuelled by a combination of gas, coal and oil
(4) Wind included from 2007

Figure 2.3: Generating capacity of major power producers 2000-2011 [18]

Connection of the various power generating stations to load centres is made over the transmission network, shown in Figure 2.4. The transmission network was built for bulk power transfer around the country. There is a very apparent historical phenomenon in the UK with the vast majority of power flowing from north towards the centre and south east of England. This is evident in the reduction of transmission system voltage levels, highlighted by the reduction in size and capacity of power lines in Scotland.

National Grid Electricity Transmission plc (NGET), as the licensed independent system operator, is responsible for balancing the system and maintaining security and quality of supply. The balance of electrical power demand and supply must be met on a second-by-second basis. Generation is scheduled to match forecasted demand trends, with lightly (or partly) loaded generation, referred to as spinning reserve, waiting to supply any short falls in real time supply.

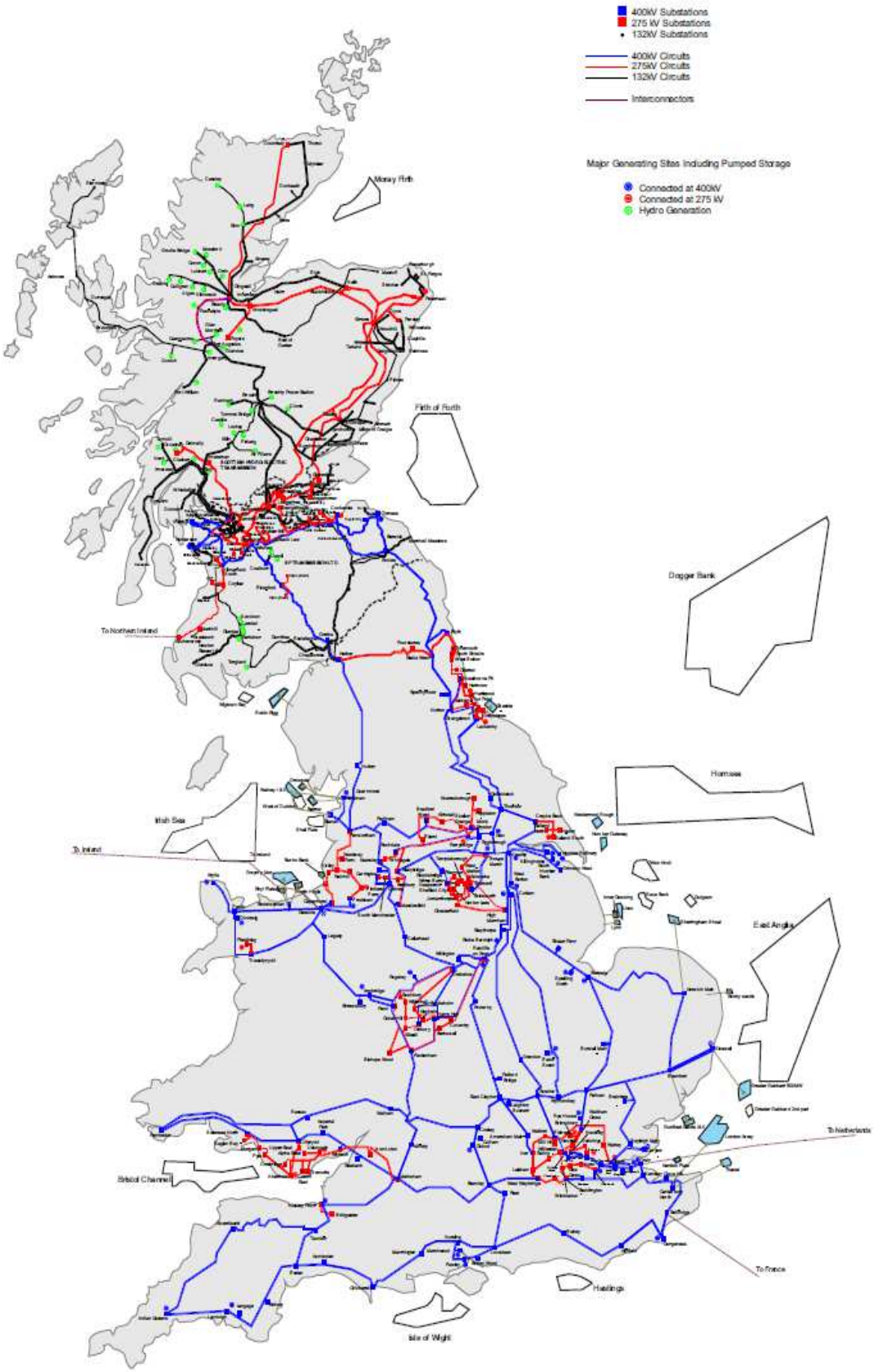

Figure 2.4: Map of the UK electricity transmission network 2013 [19]

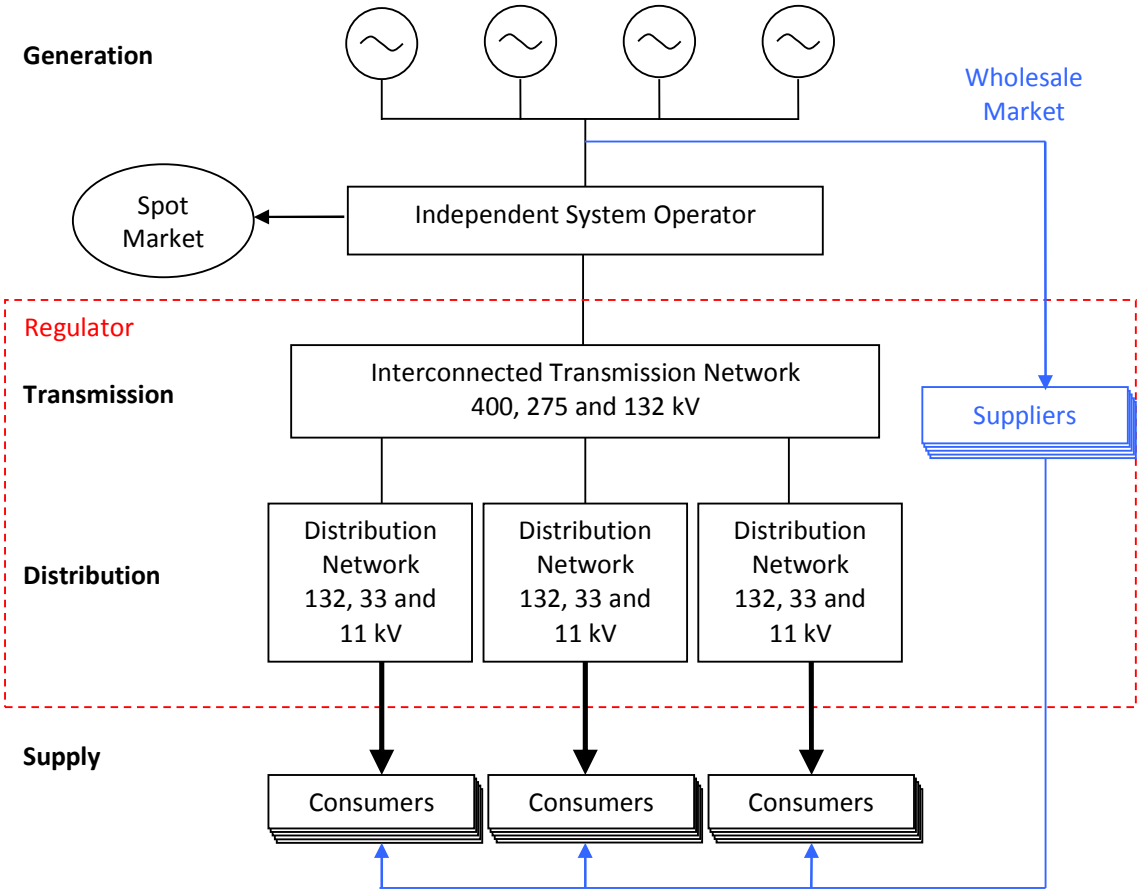

Figure 2.5: Structure of the UK electricity network industry

The structure of the UK electricity industry is illustrated in Figure 2.5, wherein electricity supply companies buy electricity on a wholesale market, administered by a Market Operator (Elexon), and sell it on to consumers. Suppliers pay use of system charges, set by the electricity regulator OFGEM, for their electricity to be transmitted across the national grid and the local distribution networks to their consumers.

The transmission network infrastructure in England and Wales is owned by NGET, while the network in Scotland is sub-divided into two parts, owned by ScottishPower in the south and SSE in the north. The entire system is operated by NGET.

2.4.2 DISTRIBUTION NETWORK

Sections of medium to low voltage networks known as distribution networks, not shown in Figure 2.4, convey electricity on to demand centres and individual customers at the appropriate voltage levels, connecting electricity supplies. This is shown in Figure 2.2

where commercial consumers are supplied at the higher voltage levels of the distribution network, and residential consumers at the lower, domestic voltage levels.

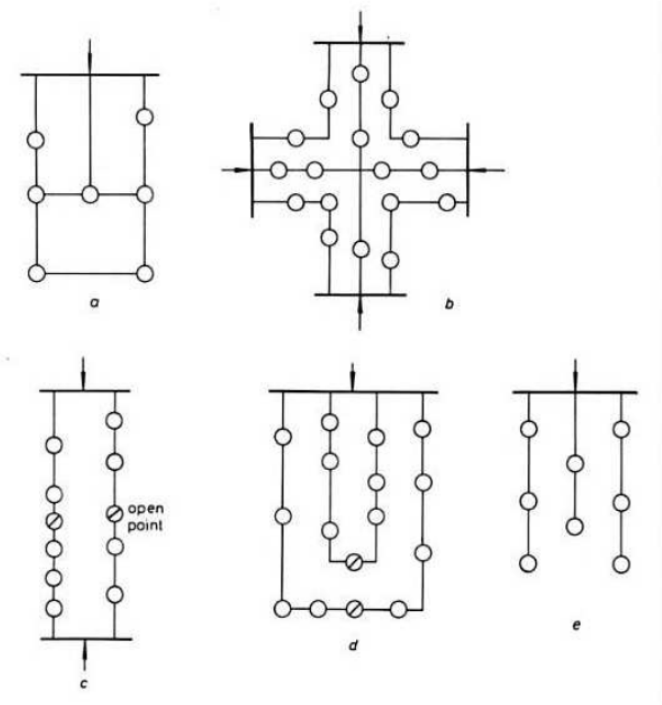

Figure 2.6: Distribution network configurations [20]

Distribution networks have a more varied structure and are classified based on the nature of the interconnecting substations. Five standard categories illustrated in Figure 2.6 were identified by Lakervi and Homes [20] to distinguish circuit construction. In each classification the configuration of the network is set-up to maximise the security of supply whilst minimising the complexity of the network. Urban and sub-urban areas are predominantly supplied by underground cables in a meshed structure like those shown in groups (a) and (b) in Figure 2.6. These provide the greatest level of security of supply. In rural areas, distribution networks are typically structured in a radial pattern of sometimes multiple feeders. Groups (c)-(e) in Figure 2.6 are more representative of these networks. Some interconnection between feeders is common to increase security of supply in rural locations with comparatively high levels of demand.

Distribution networks which, for the most part, did not contain generation were designed and originally operated in a passive manner. Power flow through these

networks was driven entirely by electricity demand, meaning power flows were unidirectional, and directly proportional to electricity demand of connected customers.

Since unbundling of the UK electricity network, distribution networks are maintained in 14 licensed zones, operated by six different companies: SSE Power Distribution; ScottishPower Energy Networks; Electricity North West; Northern Powergrid; Western Power Distribution; and UK Power Networks. These companies are known as the Distribution Network Operator (DNO).

It is an inherent characteristic of renewable energy resources that the best locations for harvesting the energy are usually at geographically remote and extreme (rural) locations. Therefore much of the analysis presented in this thesis relates to the integration of DG to radial distribution networks identified by (e) in Figure 2.6.

The introduction of DG at the edges of the distribution network can have implications for power flow, fault levels and supply quality. Meeting the substantial renewable energy targets within the existing networks will exaggerate the effects and require careful study of the integration of new DG in the distribution network to maximise energy production from renewable energy resources and minimise impact on the network.

2.4.3 COMPLEX POWER

Complex power, *S*, is the product of rms voltage phasor, $|V|\angle\theta_v$, and rms current phasor, $|I|\angle\theta_i$.

$$S = V\,I^* = |V||I|\angle\theta_v - \theta_i = |V||I|\angle\theta$$

$$= |V||I|\cos\theta + j|V||I|\sin\theta$$

where $\theta = \theta_v - \theta_i$.

The in-phase (or real) component is the average real power, *P*, and the out-of-phase (or imaginary) component is the reactive power *Q*.

Thus: $$S = V\,I^* = P + jQ \quad (1)$$

The ratio of real to apparent power is known as the power factor.

$$\frac{P}{S} = \cos(\theta_v - \theta_i) \tag{2}$$

For inductive loads, where the current lags the voltage, θ_i is less than θ_v, the power factor is said to be lagging. For capacitive loads, the current leads the voltage θ_i is greater than θ_v the power factor is said to be leading.

2.4.4 COMPLEX POWER TRANSFER

The flow of complex power in electricity networks is best illustrated by a simple 2-bus example. Consider the analysis as presented by Saadat [21] depicting the transfer of power along a standard overhead line *1-2*.

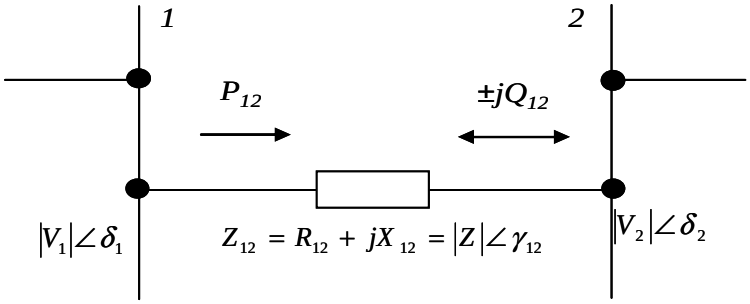

Figure 2.7: Two-bus electricity network

Let the assumed sending end phasor voltage at *1* be $|V_1|\angle\delta_1$ and the assumed receiving end, *2*, be $|V_2|\angle\delta_2$. The line current can be determined via Ohm's law as:

$$I_{12} = \frac{|V_1|\angle\delta_1 - |V_2|\angle\delta_2}{|Z|\angle\gamma} = \frac{|V_1|}{|Z|}\angle(\delta_1 - \gamma) - \frac{|V_2|}{|Z|}\angle(\delta_2 - \gamma) \tag{3}$$

The complex (or apparent) power flow into the line, S_{12}, is the product of rms voltage and rms current:

$$S_{12} = V_1 I_{12}^* = P_{12} + jQ_{12}$$

$$S_{12} = V_1 I_{12}^* = |V_1|\angle\delta_1 \left[\frac{|V_1|}{|Z|}\angle(\gamma - \delta_1) - \frac{|V_2|}{|Z|}\angle(\gamma - \delta_2)\right]$$

$$= \frac{|V_1|^2}{|Z|}\angle\gamma - \frac{|V_1||V_2|}{|Z|}\angle(\gamma + \delta_1 - \delta_2) \tag{4}$$

From which the transfer of real and reactive power across the overhead line can be determined 'in-phase' and in 'quadrature' as the $\Re e$ and $\Im m$ components respectively:

$$P_{12} = \Re e(S) = \frac{|V_1|^2}{|Z|}\cos\gamma - \frac{|V_1||V_2|}{|Z|}\cos(\gamma + \delta_1 - \delta_2) \tag{5}$$

$$Q_{12} = \Im m(s) = \frac{|V_1|^2}{|Z|}\sin\gamma - \frac{|V_1||V_2|}{|Z|}\sin(\gamma + \delta_1 - \delta_2) \tag{6}$$

Real and reactive powers are in quadrature and can flow independently of each other in either direction. The power flows, both real and reactive, must be carefully controlled for a power system to operate within acceptable system operating limits.

To illustrate, Kirchhoff's voltage law is applied to the two-bus example:

$$\bar{V}_2 = \bar{V}_1 - (R_{12} + jX_{12})\bar{I}_{12} \tag{7}$$

For the assumed sending end bus *1*, the line current can be expressed from as:

$$S_{12} = P_{12} + jQ_{12} = \bar{V}_1\bar{I}_{12}^* \;\Rightarrow\; \bar{I}_{12} = \frac{P_{12} - jQ_{12}}{\bar{V}_1^*}$$

Using this expression for the line current in the application of Kirchhoff's voltage law above it is possible to determine voltage level on bus *2* and the voltage drop between bus *1* and bus *2* as complex power leaves bus *1* flowing towards bus *2*. Assuming $\bar{V}_1 = V_1\angle 0°$:

$$\bar{V}_2 = V_1 - (R_{12} + jX_{12})\left(\frac{P_{12} - jQ_{12}}{V_1^*}\right)$$

$$= V_1 - \frac{R_{12}P_{12} + X_{12}Q_{12}}{V_1^*} - j\frac{X_{12}P_{12} - R_{12}Q_{12}}{V_1^*}$$

$$\bar{V}_2 - V_1 = -\frac{R_{12}P_{12} + X_{12}Q_{12}}{V_1^*} - j\frac{X_{12}P_{12} - R_{12}Q_{12}}{V_1^*}$$

And:

$$V_1 - \bar{V}_2 = \frac{R_{12}P_{12} + X_{12}Q_{12}}{V_1^*} + j\frac{X_{12}P_{12} - R_{12}Q_{12}}{V_1^*} \tag{8}$$

Resolving the in-phase and quadrature terms yields:

$$\Delta V = \frac{R_{12}P_{12} + X_{12}Q_{12}}{V_1^*} \quad \& \quad j\delta V = j\frac{X_{12}P_{12} - R_{12}Q_{12}}{V_1^*} \qquad (9)\ \&\ (10)$$

At the transmission level typically X >> R and the change in voltage magnitude and phase can be (13) approximated as:

$$\Delta V \approx \frac{X_{12}Q_{12}}{V_1^*} \quad \& \quad j\delta V \approx j\frac{X_{12}P_{12}}{V_1^*}$$

And it can be deduced as a rule of thumb that the transfer of real power is the driven by the change in voltage angle between network nodes and the transfer of reactive power can give rise to substantial voltage changes across a system. This means that it is necessary to maintain reactive power balances between sources of generation and points of demand; this is typically achieved on a zonal basis.

In distribution networks the ratio of transmission line reactance to resistance is closer to one and the transfer of real power can give rise to substantial changes in voltage magnitude. Hence, it is necessary to consider the full derivation of the power flow equations as detailed above. This mandates that all power flow and optimal power flow analyses in the lower voltage networks is conducted using the full AC power flow equations and not in a simplified model referred to as the DC power flow equations, where the resistance property is neglected amongst other things.

2.4.5 POWER FLOW EQUATIONS

Steady-state analysis of an interconnected power system during normal operation can be performed via the extrapolation of the theory presented above in a system known as the power flow equations. For the most part, the analysis assumes that the network is balanced and can therefore be represented by a single-phase (or one-line) network. The network equations can be formulated systematically in a variety of forms; however the most common approach is the node-voltage method as detailed in [21]. The steady-state solution of an AC electrical network is governed by the matrix equation:

$$\bar{I} = \bar{\bar{Y}}\bar{V} \tag{11}$$

Where: I is an n-dimensional vector of network currents injected on each system bus; V is an n-dimensional vector of system voltages at each system bus; and, Y is an n x n matrix of network admittance; which is a convenient representation of the inverted network complex impedances. The diagonal elements of the admittance matrix are the sum of all the admittances connected to each node, known as the self-admittance:

$$Y_{ii} = \sum_{j=0}^{n} y_{ij} \quad j \neq i$$

The off-diagonal elements are equal to the negative of the mutual admittance between network nodes.

$$Y_{ij} = Y_{ji} = -y_{ij}$$

To demonstrate, consider a typical system busbar, i, connected to n others as shown in Figure 2.8.

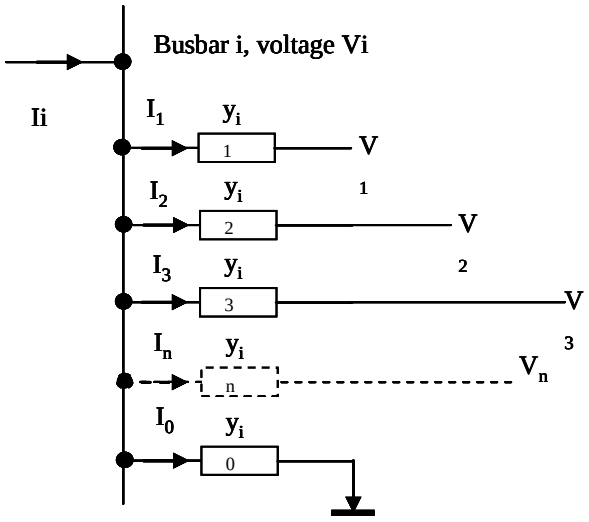

Figure 2.8: A typical electrical power system bus

The network busbars are all connected via the intervening impedance of each respective circuit branch, Z_{i1}, Z_{i2}, Z_{i3} … Z_{in}. The system impedances are inverted to form the system admittances, y_{i1}, y_{i2}, y_{i3} … y_{in}.

Application of Kirchhoff's Current Law (KCL) then yields:

$$I_i = y_{io}V_i + y_{i1}(V_i - V_1) + y_{i2}(V_i - V_2) + y_{i3}(V_i - V_3) + ... + y_{in}(V_i - V_n)$$
$$= (y_{io} + y_{i1} + y_{i2} + y_{i3} + \ldots + y_{in})V_i - y_{i1}V_1 - y_{i2}V_2 - y_{i3}V_3 - ... - y_{in}V_n$$

Or:
$$I_i = V_i \sum_{j=0}^{n} yij - V_j \sum_{j=1}^{n} y_{ij} \quad j \neq i \tag{12}$$

The formulation of the network equations in the nodal admittance form results in complex linear simultaneous equations in terms of node currents. However, in a power system it is typically the system power injections and absorptions that are known, not the currents.

Given the real and reactive power injections at bus *i* are:

$$P_i + jQ_i = V_i I_i^* \quad \text{or} \quad I_i = \frac{P_i - jQ_i}{V_i^*} \tag{13}$$

Substituting for I_i in (12) gives:

$$\frac{P_i - jQ_i}{V_i^*} = V_i \sum_{j=0}^{n} yij - V_j \sum_{j=1}^{n} y_{ij} \quad j \neq i \tag{14}$$

Therefore the resulting mathematical formulation, in terms of power, is a system of non-linear equations, which can only be solved by iterative means subject to the nodal power balance criteria.

After an iterative solution of the system node voltages, network line currents to and from each system node are calculated via (12) and the complex power flow in each direction determined by (1). The real power losses and reactive power charge in each network line and transformer are then deducted from the sum of the determined power flows. Where the complex power S_{ij} from bus *i* to *j* and S_{ji} from bus *j* to *i* are:

$$S_{ij} = V_i I_{ij}^* \ \& \ S_{ji} = V_j I_{ji}^* \tag{15) \& (16}$$

The power loss in line *i-j* is the algebraic sum of the power flows:

$$S_{L\,ij} = S_{ij} + S_{ji} \tag{17}$$

For larger power systems networks, particularly for high resolution time sequential solutions, this is only feasible by computational methods.

2.4.6 *POWER FLOW AND GENERATOR CONTROL*

In solving the power flow problem, four quantities are associated with each bus. These are: voltage magnitude, voltage phase angle, real power and reactive power (P, Q, V, δ_v).

Network system buses are classified into one of three types: Slack bus, P-Q (or Load) bus and P-V bus. The classification of each bus is dependent on whether a generator or a load is connected and in what control mode each generator operates.

The slack bus is a special case with two important functions necessary for successful solution if the power flow assessments. It provides a reference point for the network voltage levels, typically at 1.00 pu and 0.00˚, and an infinite resource of active and reactive power, in order to ensure the network supply demand balance criterion. The inputs to the power flow equation at the slack bus are the voltage magnitude and phase angle (V, δ_v). In this case, the system slack bus will be the GSP of each distribution network.

P-Q (or load) buses are network nodes which do not contain generation units (or potentially responsive network loads) operating in voltage control mode and actively regulating the node voltage level. Although generation may be connected to these network buses, it operates in a fixed power factor control mode where its real and reactive power output is fixed at a prescribed level. The input data to the power flow equations from these nodes will be the net node steady-state real and reactive power generation or demand (P, Q). Where the net complex power flow from buses containing both generation and demand is $P_{net} = P_{gen} - P_{load}$ and $Q_{net} = Q_{gen} - Q_{load}$. The iterative power flow solution method is used to determine the resultant voltage level and angle (V, δ_v).

P-V buses are network nodes that do contain generating units, switched shunt capacitor systems or tap-changing transformers which actively regulate network voltage levels. On these system buses, the real power injections (or drains) and the target voltage setting (P, V) is specified and the iterative power flow solution will compute the resultant reactive power flow and voltage phase angle (Q, θ_v).

The ability of each generator in the network to actively regulate the network voltage levels is dependent on the technology deployed, connection level and capacity. The operational aspects of synchronous generator real and reactive power output can be explained by the simple Thévenin equivalent model of a generator below [23], where V_t is the generator terminal voltage, E is the induced stator voltage, δ is the power angle, and X_g is the positive sequence synchronous reactance of the generator. From the figure, the generator current is:

$$I = \frac{E\angle\delta - V_t\angle 0}{jX_g} \tag{18}$$

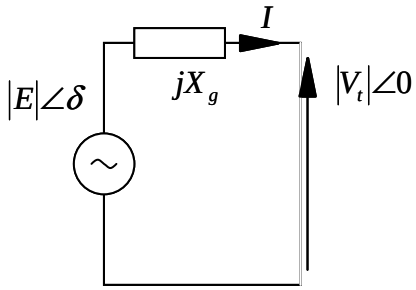

Figure 2.9: Synchronous generator Thévenin equivalent model

And the complex power delivered by the generator is:

$$S = V_t I^* = V_t\left(\frac{E\angle -\delta - V_t}{-jX_g}\right)$$

$$= \frac{V_t E(j\cos\delta + \sin\delta) - jV_t^2}{X_g} \tag{19}$$

The real and reactive power output as viewed from the network perspective[1] is then:

$$P = \Re e(S) = \frac{EV_t}{X_g}\sin(\delta) \tag{20}$$

$$Q = \Im m(S) = \frac{V_t}{X_g}(E\cos(\delta) - V_t) \tag{21}$$

From this it can be deduced that the real power, P, delivered at the generator terminal is dependent predominantly on the machine rotor load angle δ. The power angle of the generator is a function of the mechanical driving torque on the prime-mover, where an increase in prime-mover power delivers an increase in P at constant terminal voltage V_t.

[1] For the purposes of clarity, all outputs and definitions of generator terms are stated from the network perspective.

For small angle δ, cos(δ) is close to unity and (18) can be approximated as:

$$Q \approx \frac{V_t}{X_g}(E - V_t) \tag{22}$$

This shows that the flow of reactive power Q is governed predominantly by the difference in the induced stator voltage E and the machine terminal voltage V_t. The induced stator voltage in a synchronous generator can be increased and decreased by adjusting rotor excitation while holding the prime mover power constant (although a small decrease is required to hold P constant in (20). If the induced stator voltage E is greater than the terminal V_t, the generator produces reactive power and exports it to the connecting network. In this condition, from the network perspective, the generator is said to be overexcited and operating at a 'leading' power factor. If E is less than V_t, the generator draws reactive power down from the connecting network. The generator is said to be under-excited and therefore from the network perspective is operating at a 'lagging' power factor. The special case is when the power factor angle is zero and there is no transfer of reactive power between the generator and connecting network. In this condition the generator is said to be operating at 'unity' power factor.

While synchronous generators have the ability to operate at both leading and lagging power factor and can control the injection or absorption of reactive power, induction (or asynchronous) generators are excited via the stator winding and therefore require a source of reactive power to develop the magnetic field. This means they are not capable of producing reactive power and can only operate at a lagging, or unity power factor. The exception to this is a doubly-fed induction generator (DFIG), where the rotor has a secondary set of windings. The secondary magnetic field created by the secondary windings on the rotor allows the DFIG through the use of power electronics to inject, as well as absorb reactive power, from the grid once the generator has energised and can therefore operate the machine in voltage control mode.

Synchronous generators and DFIGs can both operate in voltage or power factor control mode. In voltage control mode (P,V) the generator AVR are actively engaged to hold the machine terminal voltage and real power output at a constant level. In power factor control mode (P,Q) the ratio of real to apparent power is maintained and the values of real and reactive power are varied together to keep this ratio.

Synchronous generators are more common in conventional hydropower and fossil fuel generating plant where the power delivered from the turbine prime mover is at a fixed speed. In generating applications such as wind power, induction generators or DFIGs, tend to be favoured as they can more readily absorb the high temporal variation in resource by operating at varying speed. Most modern day wind power developments utilise DFIG technology and can therefore be considered available for voltage control.

At the transmission level, the national electricity grid code [24] states that all plant must be:

'capable of contributing to frequency control by continuous modulation of active power' and *'capable of contributing to voltage control by continuous changes to the reactive power supplied to the National Electricity Transmission System*'.

For a synchronous generator each device must be able to provide a constant terminal voltage level via a continuously-acting automatic excitation control system. With induction (or asynchronous) generators the plant is required to maintain zero transfer of reactive power (unity power factor), unless otherwise instructed to do so. In some cases induction generators are instructed to operate at a fixed power factor within the range of 0.95 leading to 0.95 lagging.

At the distribution level, DNOs are obliged as part of their electricity distribution business licence to comply with a Distribution Code detailing the technical parameters and considerations relating to connection to, and use of, their electrical networks [25]. However, detailed connection practices are not standardised at this level due to the many network configurations and existing operating conditions. For the most part, DNOs are reluctant to allow third parties to operate equipment that could potentially interfere with the operation of their system. DNOs require DG to limit their capacity to a level that can be comfortably accommodated by the existing system infrastructure or finance the necessary reinforcement to the network infrastructure required to support the passive business as usual (BAU) approach to network operation. The BAU translates into DG developments being afforded, a 'firm' generation contract, operating in a fixed power factor control mode and exporting as much power output as possible at all times. In this arrangement, the generator does not regulate the system voltage and the point of

connection is still considered as a P-Q node in the power flow assessments. This arrangement is referred to throughout as the ‘fit-and-forget’ scenario.

2.4.7 DISTRIBUTION NETWORK VOLTAGE REGULATION

The statutory legislation governing the quality of electricity supply in the UK [25], stipulates the maximum allowable voltage variation from nominal. In the case of the distribution networks operating below 132 kV, voltage levels must not exceed a variation of ±6% of the nominal rated voltage level. For low voltage supply below 1 kV used in domestic customer connections, the voltage levels must not exceed 10% above or 6% below the nominal voltage level. Voltage regulation in the distribution networks is achieved, predominantly, by tap-changing transformers and line voltage regulators. Line voltage regulators are a special form of tap-changing transformer with a 1:1 voltage ratio. This, in part, is due to a historical absence of generation in these networks and the one-directional power flow.

There are two types of tap-changing transformers used in distribution networks, on-load tap changing (OLTC) and off-load tap changing. OLTC transformers have the built in voltage and current sensing circuitry which allows them to automatically actuate tap changes in response to changing loading levels while the transformer is energised and operating under load. OLTC transformers monitor and regulate the voltage level on the secondary (customer or demand) side and their operation traditionally relies on the flow of power down the voltage gradient from the higher voltage (supply) side. Off-load tap changing transformers require isolation, disconnection and manual alteration of the transformer tap settings by moving links. OLTC transformers are found in most high and medium voltage (132/33/11 kV) distribution networks, whilst off load tap-changing transformers are more common in the lower voltage (11/0.4 kV) domestic supply side.

Variable loading patterns have resulted in voltage regulation practices that operate autonomously to maintain the pre-defined system set-points. Therefore despite the perception and classification of distribution networks as passive, at the high and medium voltage level, the automatic OLTC transformers have been operating actively in response to variable demand patterns for many years. The passive control philosophy and original unidirectional power flows have meant that steady-state analysis of the most onerous network power flow conditions (worst case scenario) was sufficient to

demonstrate satisfactory network regulation under all operating conditions. Principally this came from the idea that, providing the plant infrastructure was sufficiently rated to deal with peak demand power flows, there was only a need for active regulation to compensate for the voltage drop down overhead lines and across transformers. Given that the voltage drop is most significant during peak demand and least significant during minimum demand; satisfactory network regulation could be proven by demonstrating acceptable operation of the network under both these conditions for a single network configuration.

A typical tap range for an OLTC transformer is +/-10%, and is effectively comprised of 32 incremental tap steps of 0.625% each [21]. The embedded voltage sensing circuitry, Automatic Voltage Control (AVC), compares measured voltage magnitude to a reference or set-point voltage and initiates tap changes on the high-voltage side to bring the secondary or low voltage back in line with the set-point voltage. Inside this AVC relay, two functions are maintained to minimise tap changing operations and prevent unnecessary tap actions. Firstly, an operational tolerance or deadband (typically about 2%) around the reference voltage is used to prevent hunting of a fixed voltage level that may exist between incremental tap steps. Secondly, a time-delay mechanism is installed to stop unnecessary tap changing operations resulting from momentary voltage spikes.

To demonstrate the functionality and configuration of OLTC transformer operation consider the four bus distribution network example of Figure 2.10. Voltage level at bus A is regulated by the two OLTC substation transformers, in a master and slave relationship. In addition the voltage at bus C is regulated by the OLTC capabilities of a 33/11-kV distribution transformer. The time delay deployed in the substation transformer is 60 seconds, while the time delay deployed in the distribution transformer is 90 seconds. Both OLTC transformers have a target voltage setting of 1.03 pu.

For this example, the network loads are subject to a daily demand curve, as shown in Figure 2.11, which is based on linear interpolation of average demand levels over half-hourly intervals. The resultant network voltage levels and transformer tap positions are shown in Figure 2.12 and Figure 2.13 respectively.

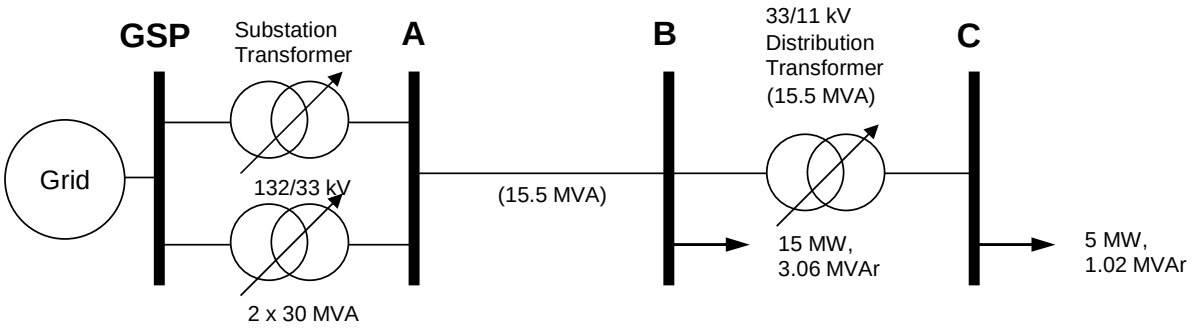

Figure 2.10: 4-bus distribution network with two coordinated OLTC transformers

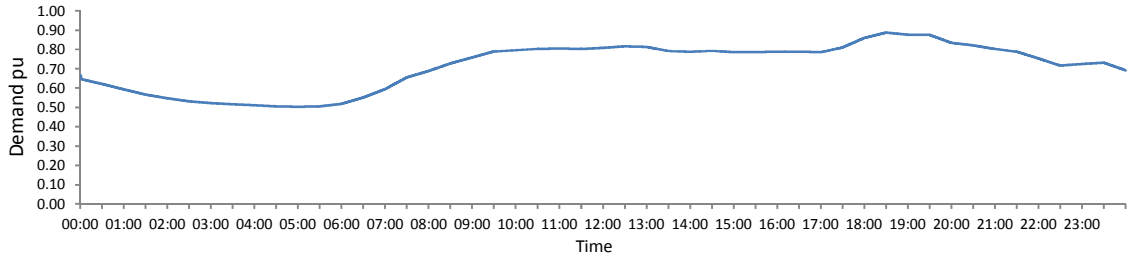

Figure 2.11: Daily demand profile

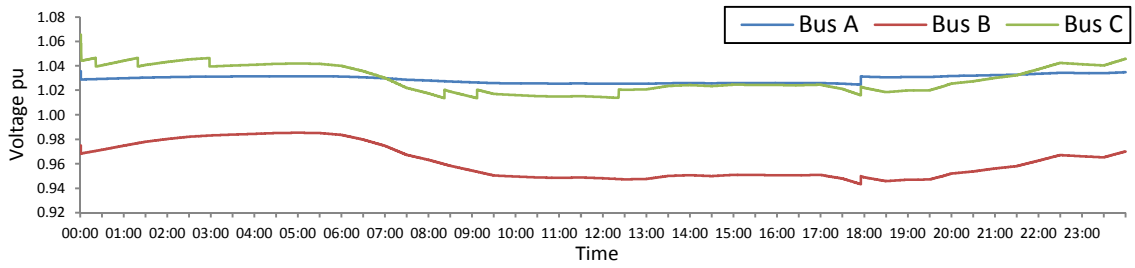

Figure 2.12: Distribution network voltage levels

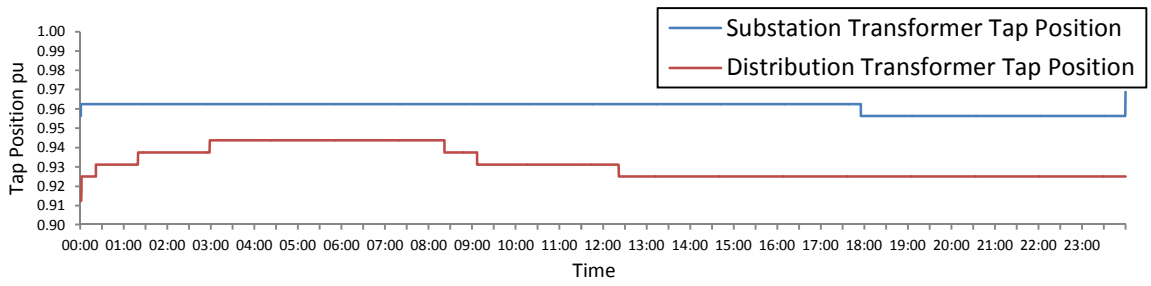

Figure 2.13: OLTC transformers tap positions

An example of typical OLTC deadband and delay functions is demonstrated in Figure 2.14, which shows a short term operating window of the 33/11-kV distribution transformer response to time varying demand levels. The corresponding voltage levels for this example are shown in Table I. With a target voltage level of 1.03 pu, the upper limit of the voltage deadband in this example was 1.04622 pu. Over the observed 5-minute period, system demand decreases, raising the voltage level at bus C. The measured voltage level breaches the upper limit of the regulation deadband at 00:20:10. After a delay of 90 seconds in this example, the AVC relay initiates a tap change at 00:21:30 bringing the voltage level back within the deadband. If the voltage level had dropped back within the voltage deadband during this delay, the imminent tap action would be cancelled and the delay time reset.

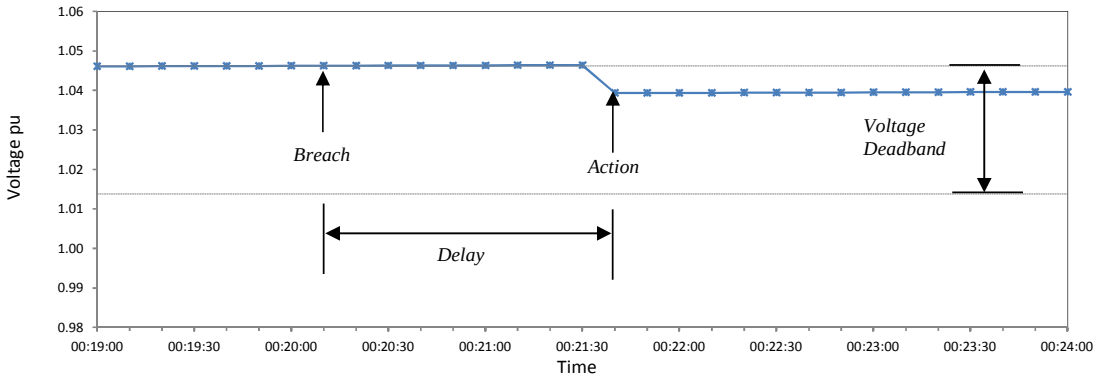

Figure 2.14: 33/11-kV distribution transformer OLTC control cycle

Time delays can be set depending on the overall network time-voltage coordination. These are typically staggered and proportional to distance from the GSP. This means that if a voltage excursion is large enough to initiate change at the head of the feeder, the OLTC on the substation transformer should move first, restoring the voltage profile from the source and mitigating the need for tap operations on each individual downstream transformer.

This is demonstrated in the above example and highlighted in Figure 2.15 to Figure 2.17 and Table II. Figure 2.15 and Figure 2.16 show the concurrent voltage levels on the two OLTC controlled network buses, A and C.

Table I: Section of results from the 4-bus distribution network with two coordinated OLTC transformers

Time	Voltage (pu)	Tap Position (pu)
00:19:00	1.04609	0.925
00:19:10	1.04611	0.925
00:19:20	1.04613	0.925
00:19:30	1.04615	0.925
00:19:40	1.04617	0.925
00:19:50	1.04619	0.925
00:20:00	1.04621	0.925
00:20:10	1.04623	0.925
00:20:20	1.04625	0.925
00:20:30	1.04627	0.925
00:20:40	1.04629	0.925
00:20:50	1.04631	0.925
00:21:00	1.04633	0.925
00:21:10	1.04635	0.925
00:21:20	1.04637	0.925
00:21:30	1.04639	0.925
00:21:40	1.03935	0.93125
00:21:50	1.03936	0.93125
00:22:00	1.03938	0.93125
00:22:10	1.03940	0.93125
00:22:20	1.03942	0.93125
00:22:30	1.03944	0.93125
00:22:40	1.03946	0.93125
00:22:50	1.03948	0.93125
00:23:00	1.03950	0.93125
00:23:10	1.03952	0.93125
00:23:20	1.03954	0.93125
00:23:30	1.03956	0.93125
00:23:40	1.03958	0.93125
00:23:50	1.03960	0.93125
00:24:00	1.03962	0.93125

Figure 2.17 shows the corresponding tap positions for each OLTC transformer. At 17:50:10 the voltage levels on both regulated buses falls below the lower limits of the voltage deadband, 1.02473 pu and 1.01703 pu respectively. After the 60 second delay substation transformer 'taps-up' the voltage level at bus A, raising the voltage level down the entire feeder and bringing the voltage level at bus C back within the deadband and negating the need for an additional tap-change by the distribution transformer.

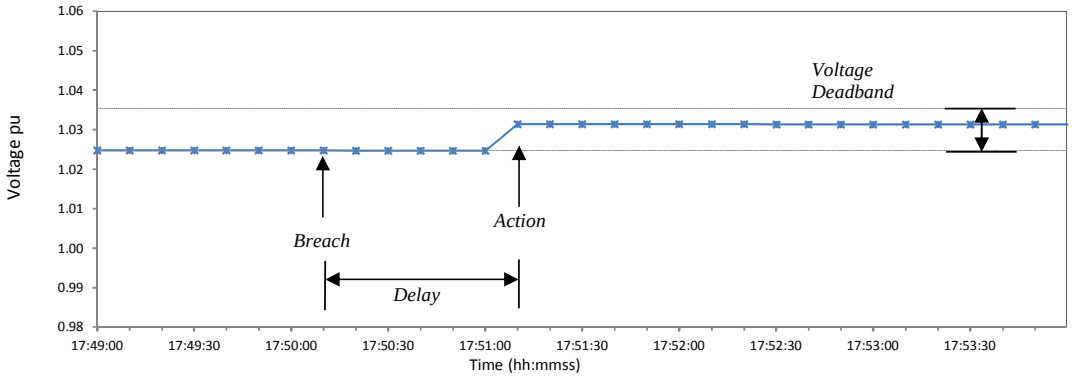

Figure 2.15: Voltage level at bus A

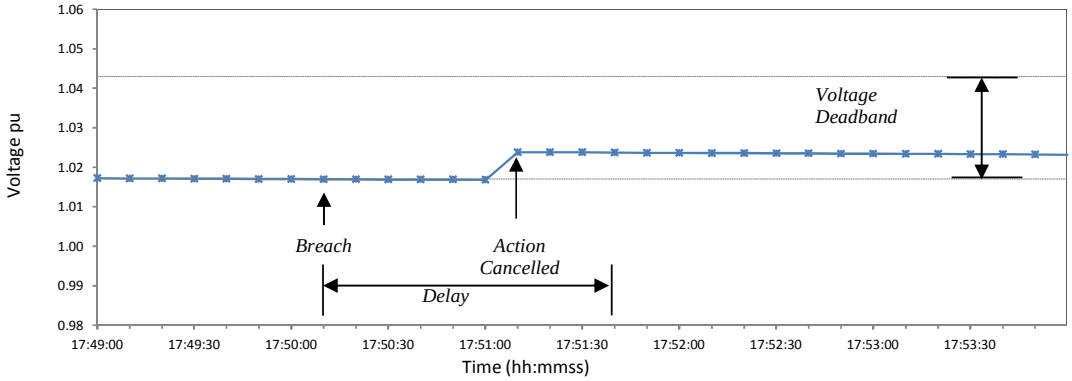

Figure 2.16: Voltage level at bus C

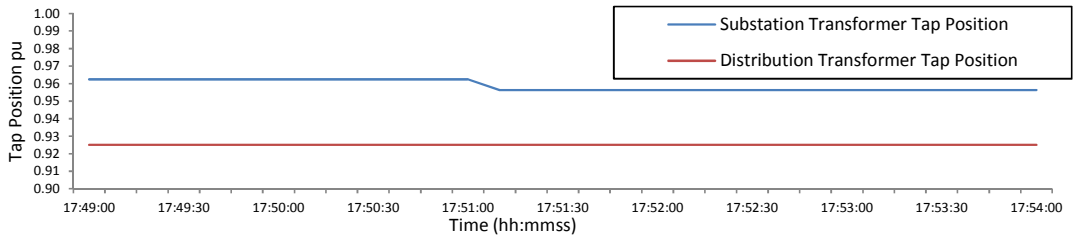

Figure 2.17: 4-bus distribution network tap positions

Table II: Section of results from the 4-bus distribution network with two coordinated OLTC transformers

Time	Bus A Voltage (pu)	Bus C Voltage (pu)	Substation Transformer Tap Position (pu)	Distribution Transformer Tap Position (pu)
17:49:00	1.02477	1.01723	0.9625	0.925
17:49:10	1.02476	1.01720	0.9625	0.925
17:49:20	1.02475	1.01717	0.9625	0.925
17:49:30	1.02475	1.01713	0.9625	0.925
17:49:40	1.02474	1.01710	0.9625	0.925
17:49:50	1.02474	1.01706	0.9625	0.925
17:50:00	1.02473	1.01703	0.9625	0.925
17:50:10	1.02473	1.01700	0.9625	0.925
17:50:20	1.02472	1.01696	0.9625	0.925
17:50:30	1.02472	1.01693	0.9625	0.925
17:50:40	1.02471	1.01689	0.9625	0.925
17:50:50	1.02471	1.01686	0.9625	0.925
17:51:00	1.02470	1.01683	0.9625	0.925
17:51:10	1.03140	1.02385	0.95625	0.925
17:51:20	1.03139	1.02383	0.95625	0.925
17:51:30	1.03139	1.02379	0.95625	0.925
17:51:40	1.03138	1.02375	0.95625	0.925
17:51:50	1.03138	1.02371	0.95625	0.925
17:52:00	1.03137	1.02367	0.95625	0.925
17:52:10	1.03136	1.02363	0.95625	0.925
17:52:20	1.03136	1.02359	0.95625	0.925
17:52:30	1.03135	1.02355	0.95625	0.925
17:52:40	1.03135	1.02351	0.95625	0.925
17:52:50	1.03134	1.02347	0.95625	0.925
17:53:00	1.03133	1.02343	0.95625	0.925
17:53:10	1.03133	1.02339	0.95625	0.925
17:53:20	1.03132	1.02335	0.95625	0.925
17:53:30	1.03132	1.02331	0.95625	0.925
17:53:40	1.03131	1.02327	0.95625	0.925
17:53:50	1.03130	1.02323	0.95625	0.925
17:54:00	1.03129	1.02319	0.95625	0.925

2.5 NETWORK IMPACTS OF DISTRIBUTED GENERATION

The integration of DG to the conventionally passive sections of the electricity network can bring about changes to supply quality and operation that present some significant challenges for DNOs to address. The maximum level of DG capacity that can be safely accommodated without network reinforcement is sometimes referred to as the *'headroom'* of the distribution network. The headroom for DG capacity is often limited, particularly in rural distribution networks, by voltage rise [33] and thermal loading constraints [40], although further restrictions can arise due to other effects such as fault level violation. The technical impacts of DG are well understood and documented [32]-[42].

Figure 2.18 illustrates the important network impacts apportioned to DG. The severity of the following issues will vary on a case by case basis therefore it is extremely important from a planning and operational perspective to be aware of the possible issues and the known engineering alternatives. The following sub-sections discuss these and additional consequences in further detail.

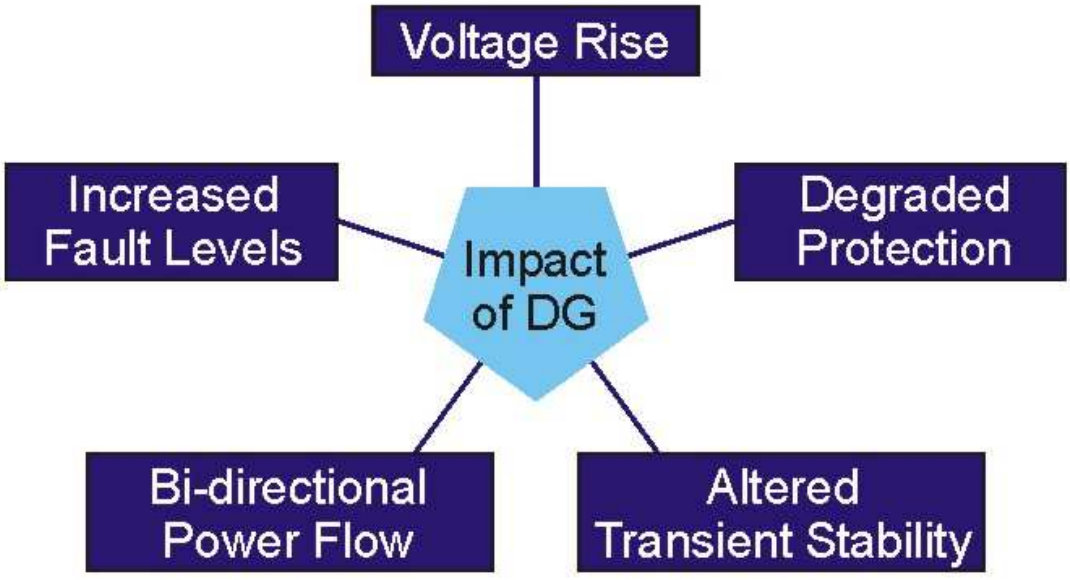

Figure 2.18: Key impacts of distributed renewable energy generation [32]

2.5.1 *VOLTAGE RISE*

By far the most prolific technical constraint to the integration of DG is the effect on the local voltage profiles, particularly on long radial distribution feeders. The occurrence of this issue was well demonstrated by Masters [36], which has inspired the following example.

The 33 kV distribution feeder, shown in Figure 2.19, connected to a primary substation is evenly distributed with 2 residential loads of the same size. Prior to the connection of the DG, the voltage level falls with increasing electrical distance from the primary substation. With a 1.00 pu nominal voltage level at the primary substation, the voltage level drops below 0.94 pu at the far end of the feeder, as shown in Figure 2.20. To correct for voltage drops in the network and ensure statutory voltage levels are maintained, it is common practice for the DNO to raise the primary substation voltage level from nominal, typically above 1.03 pu. Figure 2.19 also shows the resultant voltage profile for three pre-set voltage targets at the primary substation, nominal, 1.03 pu and 1.06 pu.

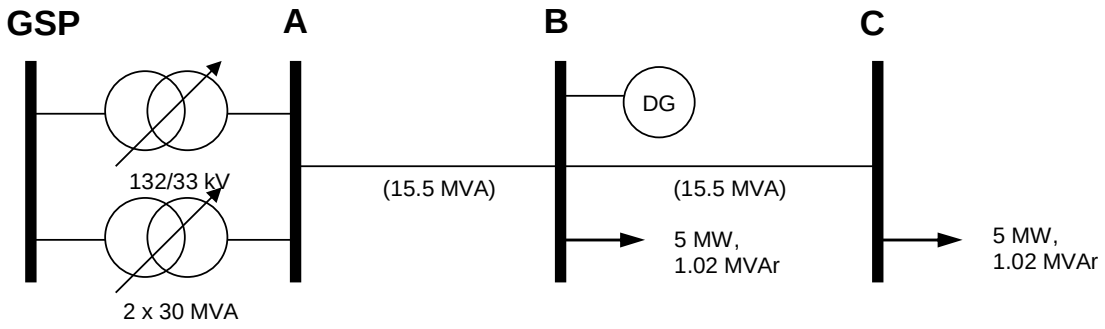

Figure 2.19: 4-bus distribution network example

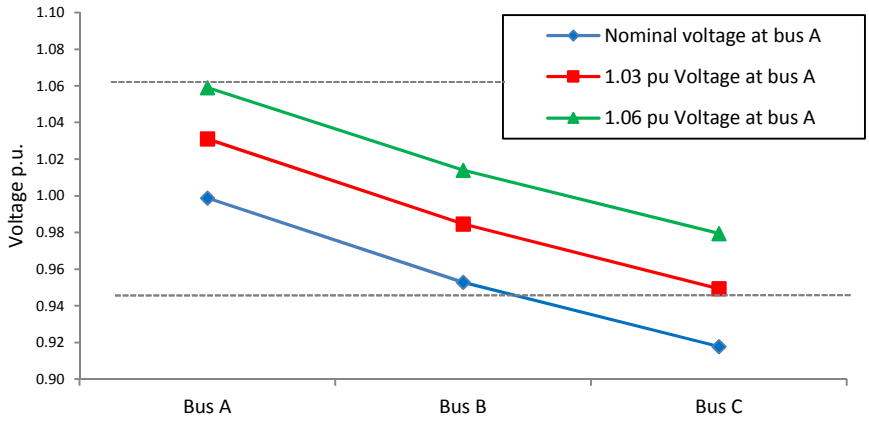

Figure 2.20: Voltage profile along a heavily loaded example 33 kV overhead line

A DG was connected mid-way down the feeder operating at unity power factor (i.e. with zero generation or absorption of reactive power). With the export of real power the voltage level at the point of connection rose, as indicated by (9). This restricted the capacity of DG that could be connected within the statutory voltage envelope of ± 6%. To demonstrate the effect of voltage rise, two sizes of DG were connected at full rated power with the resultant voltage profiles for maximum and minimum demand conditions illustrated in Figure 2.21.

Initially a DG capacity of 5 MW, equal to the downstream demand level, was connected with a pre-set voltage setting of 1.03 pu at the primary substation. For the maximum demand scenario the magnitude of power flow from the primary substation was significantly reduced but direction was not altered and the voltage level continued to drop with increasing distance from the substation, although not as severely as before.

Next a DG capacity of 20 MW was connected at unity power factor, which reversed the flow and increased the magnitude of real power back along the feeder. The voltage level at the DG was therefore lifted above the primary substation pre-set voltage level of 1.03 pu. In the given example, this caused the voltage level at the point of connection to breach the 1.06 pu upper voltage under the minimum demand condition.

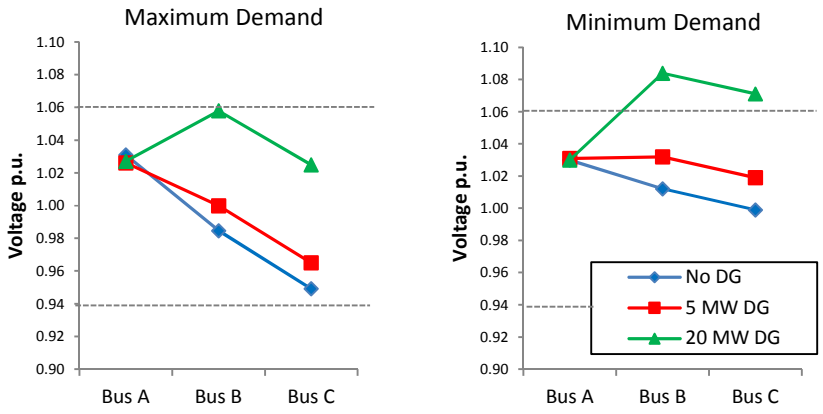

Figure 2.21: Voltage profiles after connection of a DG [36]

When integrating DG, unless the DG is capable and permitted to operate in voltage control mode, the voltage level at the point of connection will increase with the export of real power. This has the effect of increasing the voltage levels back up the distribution network from the point of injection towards the primary substation [37].

In conventional radial distribution systems, where the primary substation is the sole source of power, the voltage profile is normally regulated using OLTC transformers at the substations, with supplementary line regulators and switched capacitors on the feeders [39]. The voltage rise issue caused from the integration of DG will vary depending on the size and location of DG, length and impedance per km of radial feeder, size and variance of load, voltage regulating plant and, regulating measures implemented. The extent of the effect can be quantified with consideration given to all of the above listed dependencies that are appropriate for specific individual sections of distribution networks.

2.5.2 Bi-Directional Power Flow

The most apparent impact from the integration of particularly high levels of DG is the direction of power flow with the potential inception of reverse and bi-directional flows in the conventional uni-directional distribution networks.

To illustrate, consider the 4-bus radial distribution feeder example of [11], shown in Figure 2.22. The network consists of a single distribution feeder, with an OLTC transformer at the feeder head, a long radial feeder and an off load tap changing transformer, which operates at a fixed tap position. Prior to the connection of DG,

power flow was unidirectional and the voltage drop along the feeder varied with the time series pattern of demand for real and reactive power.

Connecting fixed output DG to variable demand unloads the feeder and adjusts the steady state voltage, shifting the demand pattern and power flow may then become bidirectional at times, depending on the relative magnitudes of generation and demand.

Connecting variable output DG with fixed demand can result in bidirectional flow and a voltage profile determined by the time series of DG production.

Combining the connection of variable DG on top of variable demand combines the temporal variation of both to result in network power flows which are bidirectional and voltage envelopes whose time series is determined by production and demand patterns.

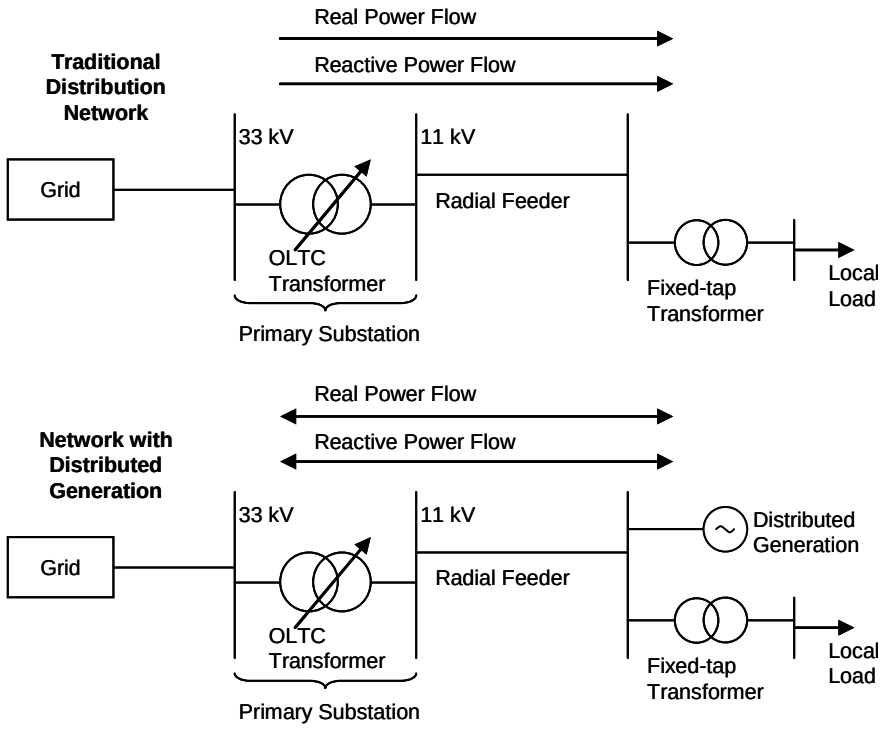

Figure 2.22: Changing distribution networks [11]

The capability of the network plant to safely transmit power in the opposite direction is limited by both the thermal rating of the network plant and the control settings of the OLTC network transformers. For example, consider the operation of an OLTC under the action of forward power flow (i.e. from high voltage supply side to low voltage demand side) the AVC relays are measuring the secondary voltage level only and actuating tap changes to hold this voltage level at a pre-defined set point. Under reverse

power flow the transfer of power back along the feeder could lift the nominal voltage level on the low voltage demand side above the set-point and cause the OLTC to 'tap down' the secondary voltage level. If the supply side voltage level is not closely regulated by the upstream network this may result in irregular voltage levels on the primary winding of the transformer.

In addition, typically due to network protection schemes, some distribution network transformers may have limited capacity or not be capable of supporting reverse power flow.

2.5.3 INCREASED NETWORK LOSSES

Real power losses and reactive power storage in a transmission line or transformer are caused by the ohmic resistance and reactance. The real power losses P_L can be calculated by:

$$P_L = I_i I_i^* R \tag{23}$$

Where the current injected from a system sending end bus *i* is given by (13)

$$I_i = \frac{P_i - jQ_i}{V_i^*}$$

And:
$$P_L = \frac{(P_i + jQ_i)(P_i - jQ_i)}{V_i V_i^*}.R = \frac{P_i^2 + Q_i^2}{V_i^2}.R \tag{24}$$

Real power losses incurred in the transfer of electrical power are therefore proportional to the square of the complex power flow.

A perceived benefit from low levels of DG in the system is the potential to serve demand locally, reducing the magnitude of power flow in the line and proportional system losses. Once the penetration level becomes comparable with or greater than twice the pre-existing network demand level, network losses increase with the reverse transfer (export) of greater complex power than was previously imported. Hence, in situations where DG production dominates network power flows there is little alternative to increase system losses.

2.5.4 *Fault Level Contributions*

In the event of a short-circuit network fault, all generating plant connected to the network will contribute to the resultant fault current. The magnitude of fault current is determined by the intervening network impedance between the system voltage sources and the fault location. The connection of DG introduces an additional voltage source and will inject additional fault currents leading to higher fault levels globally, but with the greatest increase at the area surrounding the point of connection. The fault rating of existing network switchgear can introduce a significant constraint on the headroom of distribution networks. If sufficient DG capacity is added to the network, the fault current may become large enough to increase fault levels above safe fault capacities, which will be make the local switchgear vulnerable. The type, capacity and location of DG all have significant effects on the final fault contribution.

If DG is connected close to a feeder substation or within urban areas, where the existing fault level is likely to be high, or close to the rating of the switchgear, the increase in fault level contributions caused by the generator can limit the permitted headroom. Additionally, the existing high network fault levels may make connected DG plant vulnerable.

If however, the DG is connected at the far-end of long radial feeders or in rural areas (where wind energy DG developments are most likely to be located) the higher impedance of the network may reduce the fault levels experienced at more distant sections of the network and increase the headroom for DG. With low levels of penetration increased fault level contributions are likely to be small, however high penetrations of DG will combine to cause an increase in the fault level contributions across the entire system.

The magnitude of the fault level contribution from DG is also dependent on the type of generator deployed and the type of network coupling [38]. With induction generators, which require excitation from the power system, a shorting of the machine terminals causes a collapse in the excitation, which in turn results in a collapse of the fault current contribution. This means that the typical fault current contributions become negligible very quickly. The fault contribution from DFIGs is dependent on the generator and power electronics design. Power electronic devices cannot handle large currents over a

long period of time, therefore control electronics stop firing the semiconductor valves when a sudden increase in the current is detected. This means that the sustained fault contribution from DFIG wind turbines and any other generating unit connected through a power electronic interface is minimal. The fault contribution of conventional synchronous generators, on the other hand, is considerable.

2.5.5 DEGRADED PROTECTION

Protection equipment in distribution networks is required to protect customers against unsafe electricity supplies and to prevent damage to the network infrastructure in the event of overload or fault. When electrical faults do occur they are subject to very high currents at the fault location and critically at the connection point of generators that feed the fault current into the network.

The operational current rating for protective switchgear is derived based on the range of maximum and minimum system fault currents at individual network locations that arise from the variable demand patterns and their projected growth. The presence of DG may directly degrade the existing protection in electricity network by alteration of the network fault currents for which the existing protection was specified. The increase in total fault current can increase the fault levels beyond the existing switchgear capacity, especially in close proximity to the DG itself.

It is more difficult to provide and specify protection settings across all protective relays that provide protection in the presence and absence of DG with time-dependent nominal currents and bi-directional power flows. In most cases the cost of the upgrading previously adequate switchgear will be determined by the DNO and recovered from the developer. Where future revision of the protection settings to benefit a third party is possible, an agreement will be sought.

Anti-islanding protection is commonly provided through Rate of Change of Frequency (ROCOF) or vector shift relays. While these protective relays are set to detect islanding, the sensitive settings employed mean that other major system disturbances (e.g. loss of a large system load) can cause nuisance tripping. With the large scale integration of DG, nuisance tripping can instigate further tripping of additional DGs, which is likely to cause more severe system disturbance and initiate protection stability concerns.

2.6 OPTIMAL POWER FLOW

Reliable electrical power systems feature multiple power generation stations supplying an interconnected system of transmission lines. Security of supply is increased by having a greater generation capacity than is required to meet demand plus delivery losses at all times. But there is a need to schedule the generation plant so that supply and demand balance at all times. Very early in the power systems literature [26] - [27] the idea of scheduling generation to minimise the total fuel cost associated with electricity generation, known as economic dispatch, came to the forefront of generating plant scheduling.

Economic dispatch was initially calculated using only the fuel costs of generating plant, disregarding the cost of transmission losses and more or less extensive use of the system. As an extension to the economic dispatch problem, transmission losses and thermal loading constraints were included by coupling the economic dispatch formulation with the power flow equations. This formulation provided an optimised steady state solution to the complex economic dispatch and power flow problem that is now regarded as optimal power flow (OPF). Conventionally OPF studies were used in the dispatch of generating units at the transmission level, where the ratio of resistance to reactance was very low and the power flow equations could be simplified by the DC power flow approximation. The OPF techniques presented in this thesis are intended for use at the lower voltage distribution networks, where the ratio of resistance to reactance is closer to one and the flow of reactive power has a very significant effect on the power flow regime, Therefore all OPF techniques investigated are full AC OPF solutions.

The classical formulation of the OPF is best presented by Dommel and Tinney [28]. The nonlinear problem formulation used the Newton-Raphson methodology to solve the power flow and computed an optimal solution via iteration along the path of steepest descent, also known as the gradient method.

The general statement of a constrained mathematically optimisation problem may be represented as:

Minimise: $f(u,x)$ (25)

Subject to: $g(u,x)=0$ (26)

And: $h(u,x)\geq 0$ (27)

Where u is a set of independent variables and x is the set of dependent variables. This general optimisation problem consists of; a single function of measurability, parameters that can be adjusted in order to achieve the best objective, and restrictions on the form and extent of the allowed variation.

In the case of power systems optimisation, the independent or adjustable control variables, u, represent the system control presets and can include: the active and reactive power injections; tap and phase changer settings and switched shunt or static compensation devices. The dependent or state variables x represent the resultant network state characteristics, namely the voltage magnitude and phase angle at each system bus. The equality constraints (26) maintain the active and reactive power balance at each system bus, while the inequality constraints (27) implement the physical limitations of the power system as restrictions on the variables.

Thus, the standard formulation of the economic dispatch OPF problem is as follows.

The objective function to be minimised is the total cost of real power generation.

$$\text{Minimise: } \sum_{i=1}^{n} C_{gi}(P_{gi}) \tag{28}$$

The power flow in a network of n buses is modelled as a system of $2n$ equality constraints that reflect the nodal power balance. Using the notation $P_l(V,\delta)+jQ_l(V,\delta)$ to indicate the complex power injection (or drain) along each connecting transmission line in the set L; at each system node:

$$P_{gi}-P_{di}=\sum_{l=1}^{L}P_l(V,\delta);\ Q_{gi}-Q_{di}=\sum_{l=1}^{L}Q_l(V,\delta) \tag{29); (30}$$

Where P_{gi},Q_{gi} are P_{di},Q_{di} the real and reactive power generation and demand at each system node.

The limits of variable system operational parameters such as generator operating capacity (31)-(32), the statutory voltage envelope (or prescribed limits of voltage operation on a P-V node) (33) and infrastructure thermal capacity limits (34) are included in the optimisation inequality constraints.

$$P_{gi}^{\min} \le P_{gi} \le P_{gi}^{\max}; \quad Q_{gi}^{\min} \le Q_{gi} \le Q_{gi}^{\max} \qquad (31); (32)$$

$$V^{\min} \le V \le V^{\max} \qquad (33)$$

$$S_l \le S_l^{\max} \qquad (34)$$

While this traditional statement of OPF is a form of economic dispatch, subject to the physical and operational constraints of the electricity network, OPF studies are also commonly used in a range of power system operation and planning applications. Other conventional OPF objectives can exhibit greater focus on the operation of the network in conjunction with the scheduling of generation. Some examples of additional OPF tasks include: minimum active power transmission losses; minimum deviation from a specified operating point; minimum post contingency violations; minimum post contingency load shedding and maximum load-ability of a network [29].

OPF techniques for improving operation of the network beyond the economic dispatch of active power, began with the decomposition and minimisation of real and reactive power flows. Dopazo et al [30] developed a method for planning the economic dispatch of reactive power by attributing the levels of real power losses with the respective reactive power injections at each bus. In a similar vein, Peschon et al [31] worked on a method of scheduling generator excitation and transformer tap settings in a system of fixed generator real power settings to minimise transmission losses. The benefits that were established from the use of such techniques included the reduction of power production costs, unloading of power systems equipment, reduction in network losses and improvements to the voltage profile of transmission networks. Conveniently, much of these benefits are now desirable in distribution networks to support further integration of DG. For example, decreased component loading can reduce the stresses exerted on network operation, which in turn can increase the available hosting capacity and energy yield from new DG.

2.7 ACTIVE NETWORK MANAGEMENT

While the first option among DNOs to improve the headroom of distribution networks would imply up rating of the existing infrastructure, it might be argued that the limiting factor is not the infrastructure but the passive operational mode and the fit-and-forget control practices that exist. In this section the concept of “connect-and-manage” or active (smart) network management (ANM) to better integrate DG with variable supply is reviewed and discussed.

2.7.1 ACTIVE NETWORK MANAGEMENT BACKGROUND

ANM is not a new concept in the power systems literature with homeostatic distribution automation and control contemplated as far back as the 1980s. Schweppe et al [44] proposed the principle of making supply and demand respond to each other in a continuous state of equilibrium in previously unregulated sections of electricity networks as a means of improving efficiency, costs and social impacts. In more recent times, ageing infrastructure, changing distribution network participants, increased system demands and governmental incentives have driven a significant rise globally in research and development of ANM as a quicker more cost effective alternative to infrastructure upgrades.

An indication of these and the transition from passive to a fully responsive, actively managed distribution networks was reported by the Embedded Generator Working Group (EGWG) [45] and categorised in Table III.

Table III: Changing the technical focus of network operation [45]

Level	Operator Behaviour	Infrastructure Requirements
1 Passive	Reactive to abnormal situations	Existing monitoring and control at key nodes only
2 Basic	Reactive to planned abnormalities or longer term restrictions (e.g. seasonal)	Selective extension of existing monitoring and control infrastructure on restricted number of circuits
3 Intermediate	Some real time network monitoring, scheduling / constraining of generation and load management across parts of network. Automatic interaction between DNO plant and embedded generation.	Further extension of monitoring and control systems but still on restricted number of circuits. Communication between key network plant and generator for voltage control together with intertripping for load flow and fault level management
4 Fully Active	Real time network monitoring, scheduling / constraining of generation, load management across all network	Monitoring and control at key network nodes, communication with controllable generators and, loads. Real time modelling capability of power, active power, voltage, fault levels & security.

Table III presents what was perceived as the typical network practices and the necessary changes to monitoring and control infrastructure

According to [45], the initial integration of basic active elements to the passive distribution network would see localised extension to the distribution control automation inherent in the system already. It is believed that this basic level of automation would see the network control pre-sets altered manually by DNOs based on a long term operational time scale. This is likely to accommodate better regulation over seasonal fluctuations in network demands, but will not provide sufficient flexibility to improve the integration of highly intermittent renewable generation.

An intermediate or transitional stage is likely to see some real time control over DG real and reactive power output and automatic interaction with network infrastructure. It usually consists of independent localised control schemes that adjust automatically the most prevalent system constraints through programmable logic controllers. This would be achieved with minimal development of advanced metering or communication

systems. One issue with these developments is that their application may be limited by operational conflict with existing system controls and must therefore be carefully considered.

The final functionality required for transition to a 'fully active' distribution network includes the real time measurement of system operating parameters. In principle, this should see an increase in the communication and operation of the network controls and an end or reduction of independent localised control schemes. It will require the development of monitoring and control systems on key sections of distribution network and communication protocols between DNO and DG development.

This transition is in keeping with much of the recent literature, where there is a general consensus over the 'active' network philosophy. The term 'ANM' is commonly used to represent that, but the interpretation can vary significantly and ANM does not have a simple formal definition.

In the early stages of ANM research and development in the UK, EA Technology Ltd on behalf of the DTI's Electrical Networks Steering Group (ENSG) defined ANM as [46]:

"ANM is understood to mean systems that operate to take action automatically to maintain networks within their normal operating parameters. … ANM operates pre-emptive action to maintain networks within their normal operating parameters."

Another definition of ANM operation was introduced by the Department for Energy and Climate Change (DECC) [47] where 'Active Control' is referred to and considered as:

"A system covering the monitoring, decision making and actioning stages required to manage the DNO's Licence Obligations in a real time control timeframe (i.e. seconds). It is designed to proactively manage network / generator constraints currently achieved either by the DNO's Control Engineer or through hard-wired logic. … Active Control involves a continuous cycle of:

- *Taking regular measurements from the live network.*
- *Performing rule based assessments, to compare the input measurements with a predetermined network model or sequence.*

- *An output to a final control element (generator control module/interface, circuit breaker, transformer tap changer, etc).*
- *Feedback to report actions as complete."*

A criticism of the above definition is that it implies that active control decision simply hold system operation within a 'predetermined' network state or sequence. With this approach active technologies are merely permitting an extension of the existing control regimes without any evolution of the passive network modus operandi.

A better description of the functionality required from a truly ANM alternative is more in-line with the refined sequence presented by [48], where ANM is envisaged as:

- The ability to view a wide range of operational indicators in real-time;
- Optimisation of the power system enabling the large scale use of intermittent renewable generation sources in a controlled manner;
- Introduction of a certain level of homeostatic 'intelligence'; and,
- Working with existing systems and compatible with other devices.

It is this functionality that was considered to represent the state-of-the-art vision for ANM and was adopted as the working vision of the work reported in this thesis.

With the integration of independent active controllers and regulators, considered here as a catalyst of change, becoming more readily practised (as discussed in the following section), there is a need to investigate possible techniques for the optimisation of these assets in a transparent and controllable manner. A distinguishing characteristic of future electricity supplies that needs to be addressed is the ability to provide in real time, optimal scheduling of network control set-points.

2.7.2 ACTIVE NETWORK MANAGEMENT ACTIVITIES

Thanks to the external influence of governmental incentives: research, development and installation of real time ANM techniques has begun to increase the headroom of distribution networks. Several methods of responsive network and active DG control can enhance the operation of distribution networks [45] and create a more supportive environment for DG connections. Active control techniques include: curtailment, where the generator output is regulated by the system operator and can be curtailed to maintain

power flows within technical and statutory operating limits, and Coordinated Voltage Control (CVC), where terminal voltage settings are updated in real time between AVC and AVR relays. In addition, Dynamic Line Ratings (DLR), Distributed Frequency Response (DFR), Demand Side Management (DSM) and the integration of future technologies such as Electric Vehicles (EV) or localised energy storage are seen as important components of a futuristic fully integrated ANM system.

Curtailment

The concept of real power curtailment was first identified by Collinson et al [49] as the last of three methods which offer a more financially attractive alternative to network reinforcement for connecting DG with a capacity greater than the headroom of the upstream network to which it is connected. The alternative connection schemes provide a real time, short term technique to mitigate problematic power flow regimes in both the post-fault and normal operating conditions. The concept for all three schemes was based on extending the DG capacity on distribution networks where the headroom was limited by the N-1 network criteria, which states that the network should not be subjected to system overloads as a result of the loss of the most heavily loaded connecting network branch. Fundamentally, this means that under normal operating conditions there should always be sufficient spare capacity in the network to redirect network power flows in the event of a critical circuit outage. The schemes presented in [49] proposed violation of this constraint under normal operating conditions by allowing new levels of DG to access this otherwise spare capacity. In the event of a system fault or loss of a network branch the new DG capacity is tripped off or curtailed (‘trimmed’) to maintain pre-existing system security. The three compositions, in growing order of complexity, were:

- Direct intertripping;
- Generation trip based on power flow measurements; and
- Generator power output control based on power flow measurements (Curtailment).

Direct intertripping involves the automatic opening of the DG circuit breaker and tripping of the new DG capacity in the event of any activation of the upstream network circuit breakers. In this situation the new DG capacity can continue to operate as before

under normal operating conditions but is tripped off post fault to protect the N-1 network contingency.

Generator tripping based on power flow measurements is illustrated in Figure 2.23. In this arrangement a more calculated approach was proposed to determine when to trip off new DG production. Again during a circuit outage on the upstream network, instead of directly tripping off the additional DG capacity, real time measurement of the resultant system power flows are utilised to determine whether or not the post-fault power flows result in a breach of the thermal network limits. If an excursion does occur the new DG capacity is automatically tripped off.

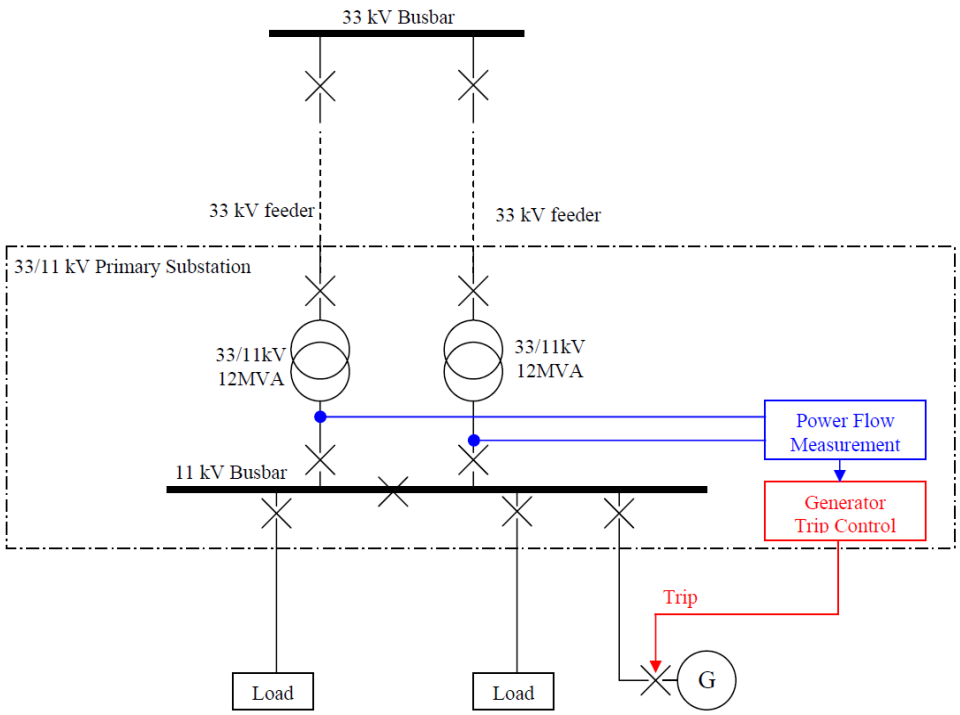

Figure 2.23: Generator trip based on power flow measurements [49]

Curtailment of DG power output was proposed as part of the final scheme: generator power output control based on power flow measurements. Curtailment was proposed as a means of avoiding excessive, often unnecessary, restrictions to DG power output during system post-fault conditions. The methodology is the same as the generator trip scheme discussed above; instead this time further consideration is given to the existing load flow conditions and incremental reductions in DG power production (or

progressive curtailment) are instigated to mitigate an impending overcurrent or thermal violation and reduce the occurrence of tripping new DG capacity.

To address growing limitations on the headroom for new DG capacity on the Orkney Isles distribution network, the theory behind the post-fault curtailment of DG production was extended to normal operating conditions and implemented in the ANM scheme incentivised by the RPZ initiative [50]. The scheme allowed significant new levels of DG capacity to connect via a strategic ANM technique to alleviate thermal loading constraints. The scheme was referred to as 'Active Power Flow Management (APFM)' and utilises a single fundamental component of full ANM scheme. In the APFM scheme, new levels of DG capacity, based on the 'best case' scenario, were permitted to connect under the supervision and restriction of a centralised distribution management system (DMS). New DG developments were termed 'non-firm' DG and referred explicitly to DG units whose real power production level is subject to reduction or disconnection in either normal or post-fault operating conditions. The scheme applies reduction (*'trimming'*) and shut down (*'tripping'*) of non-firm DG output levels within connected power zones, if and when the thermal network limitations are approached at the boundaries to each zone. The system decisions for *'trimming and tripping'* were determined on a last-in, first-out basis of connected non-firm DGs. A substantial milestone was achieved with the deployment of the Orkney Isles APFM scheme, as it was the first scheme to apply an ANM technique featuring multiple DG units. Figure 2.24 demonstrates the performance of the Orkney Isles APFM scheme. It illustrates the continuous and successful curtailment of the wind farm power output at 5 minute intervals, referred to as a control cycle.

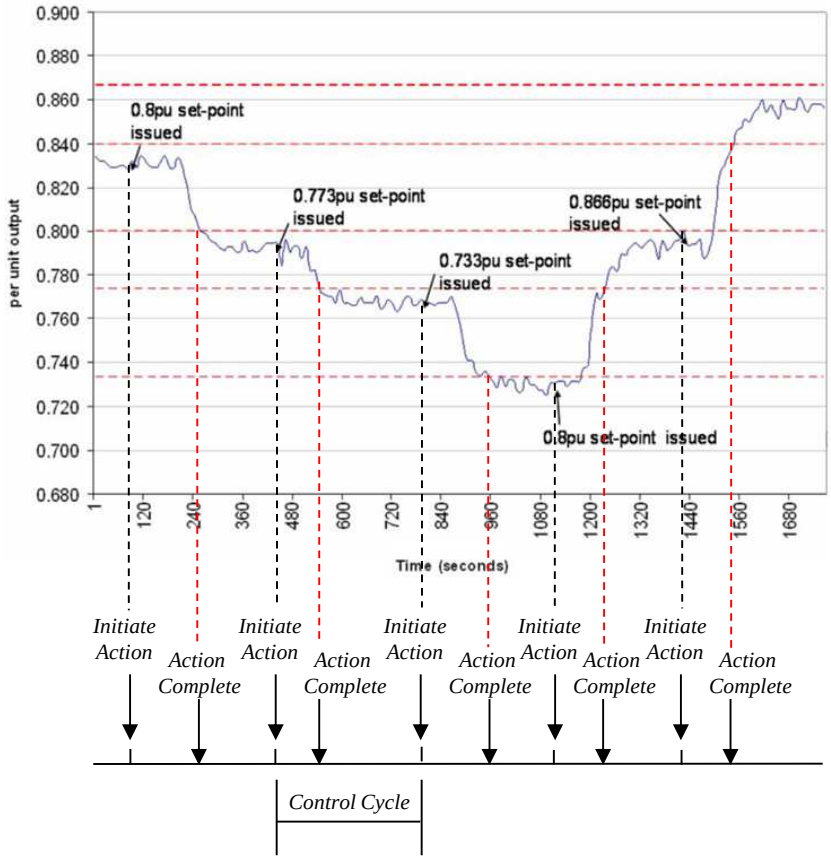

Figure 2.24: Wind farm output during trial of ANM [50]

Curtailment of real power generation was also proposed by Zhou and Bialek [51] as a means of voltage control in distribution networks. The technique was promoted as an option of last resort to deal with voltage constraints arising from the integration of intermittent renewable DG. Should the traditional measures of passive voltage control fail to ensure operation within statutory voltage limits under all conditions of renewable power generation, an optimal curtailment strategy based on the network sensitivity matrix, could then be implemented to minimise the amount of renewable generation curtailed. The authors also touched on one of the commercial considerations that such a scheme would pose. Given that the scheme has a strictly technical objective it could prove contentious and deemed discriminatory in a market context. For example, while the level of curtailment may be correctly apportioned to the DG directly causing a thermal overload or voltage excursion, this condition may be reached systematically by the presence of additional DG units not in direct violation of technical or statutory limits. One possible alternative proposed by the authors would be to introduce a

proportioned method of curtailment compensation between generators. This would result in the benefits of an optimally prescribed curtailment strategy being distributed fairly for all DGs contributing to the APFM scheme.

Generator Voltage Control

Basic generator voltage control functions, as used for regulating operation of the transmission networks, are also technically feasible, albeit resource dependent and predominantly non-dispatchable with DG. Previously operation of DG in voltage control mode has been forbidden by DNOs as this can, under the influence of reverse power flows, inadvertently cause conflicts between the DG and the AVC circuitry sensing relays deployed in tap-changing transformers. In addition, the use of localised voltage control measures are limited by: current planning regulations, the potential for the independent circulation of reactive power, the associated increase in network losses due to higher line currents and the unknown implications for existing and future network assets [49]. For these reasons, conventional connection practices generally requires DGs to operate in fixed power factor control (PFC) mode; where the ratio of real and reactive power is maintained constant and the voltage level is determined by the resulting power flow.

Voltage management at the point of DG connection can be induced by active control of the power factor setting. This regulates the flow of reactive power in a controlled manner. Active management of DG reactive power flow has previously been proposed as a means of improving the connection practices for DG and reducing the need for traditional network reinforcement [49]. The predominant constraint on distribution network headroom is often voltage rise. Several methods of active DG control have been proposed to mitigate network constraints during periods of high DG output, whilst preserving the original passive operation of the distribution network control presets. Individual solutions may exist depending on specific network constraints.

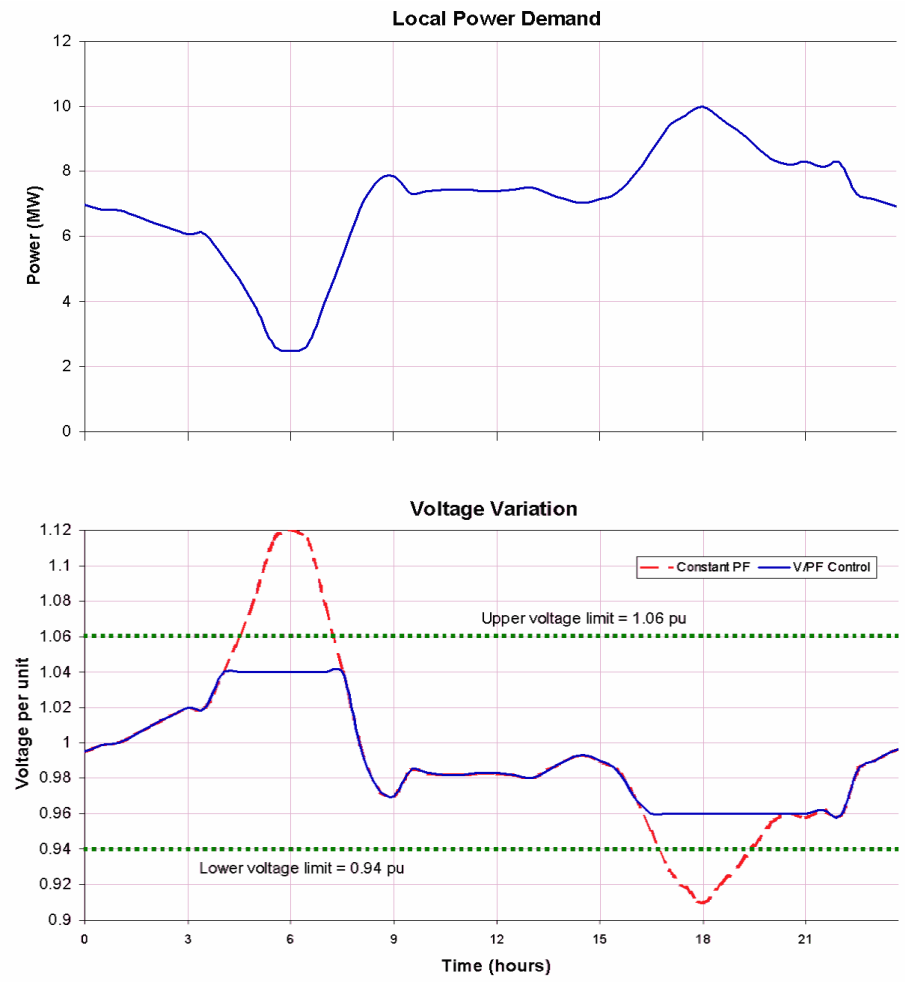

Figure 2.25: Functionality of the AVPFC scheme [52]

A hybrid control technique, proposed by Kiprakis and Wallace [52], termed AVPFC implemented voltage control on DG units only when necessary to prevent bus voltage excursion. The AVPFC system maintains constant power factor operation at a DG unit while the network voltage is within the statutory envelope. When voltage levels approach statutory limits due to varying demand patterns the DG unit switches to voltage control mode. This operation is demonstrated in Figure 2.25. The addition of '*trimming and tripping*' curtailment to the hybrid AVPFC of [52] was proposed by Sansawatt et al [53] as a means of further extending the operational reach for variable DG.

Application of a similar control scenario was examined as a high level off-line assessment by Strbac et al [54], where a priority list and OPF study were investigated as viable methods for scheduling active control of DG. Reactive power flow

compensation, via static VAr compensators (SVC), at the point of DG connection was quantified for an annual simulation period and compared with alternative voltage control strategies. The provision of real power curtailment was required to ensure successful convergence of the OPF during periods when alternative control strategies were not sufficient to yield an appropriate solution. The results of the particular network case study showed that, while reactive power compensation does prevent instances of real power curtailment, there was not a substantial increase in the energy yield over a straight real power curtailment scheme. However, it was stressed that the effect of reactive power compensation may be more considerable on alternative network case studies.

Coordinated Voltage Control

Another technique for alleviating voltage rise in distribution networks would be to introduce active management of the AVCs in OLTC transformer. Introducing lower voltage settings at OLTC transformers could better accommodate DG. However, due to the intermittent nature of renewable DG resources and the potential voltage difference between parallel feeders not containing DG, it may not be possible to guarantee compliance with statutory voltage limits for all generation and supply conditions under a passive, fit-and-forget philosophy. Introducing real-time feedback and active decision making to the AVC relay can allow it to determine in real time, the most appropriate network voltage settings to support the retrospective addition of high levels of DG whilst maintaining statutory voltage levels in all supply and demand variations.

An area-based voltage control system of this type was proposed by [49]. The mechanisms of the scheme were defined in line with the works of [54] and the then current developments made by Hird et al [55]. This comprised of two functional components; state estimation and control scheduling. Their arrangement is illustrated in Figure 2.26.

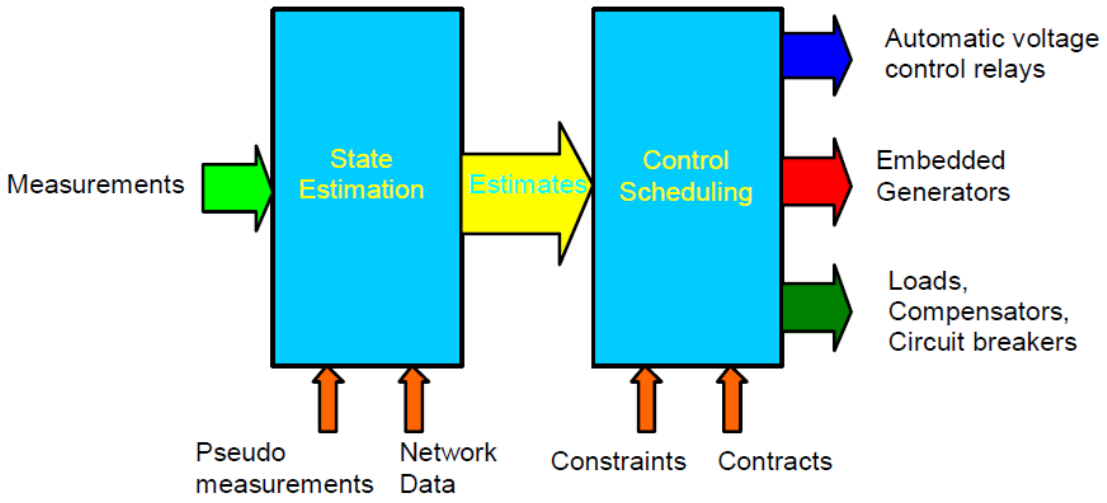

Figure 2.26: Block diagram of DMS controller software [54]

As the basis for informing real time control decisions the real time operating state of the electricity network was calculated from a combination of strategic real time power and voltage measurements, pseudo measurements derived from historical data, network topology and impedance data. Following state estimation, scheduling of the network control settings was determined by a number of methods. In [54] an optimisation technique was utilised to determine appropriate control settings, against a 'priority list' of pre-determined corrective actions.

Examples of two further CVC systems that have been developed and tested on UK distribution network include; the SuperTAPP n+ system by Fundamentals Ltd [56], and the GenAVC^{TM} developed by Econnect [57] as part of the RPZ incentive.

Functional diagrams of each system are shown in Figure 2.27 and Figure 2.28. Both introduced a form of negative load drop compensation to the decision process of the AVC relay. The control scheduling in each system was comparatively simple; following state estimation should any network voltage level fall out-with the deadband of their respective 'control-range', a corrective voltage target is issued to the set point of the AVC relay.

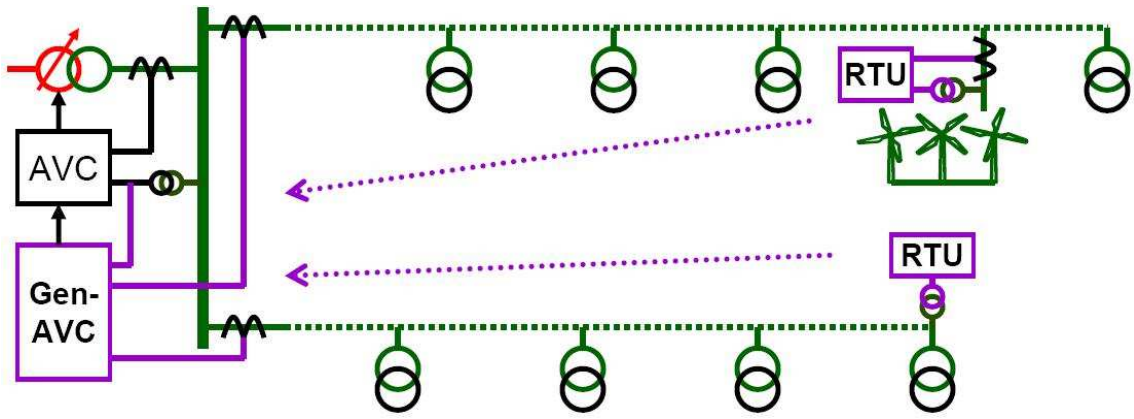

Figure 2.27: GenAVC scheme arrangement [57]

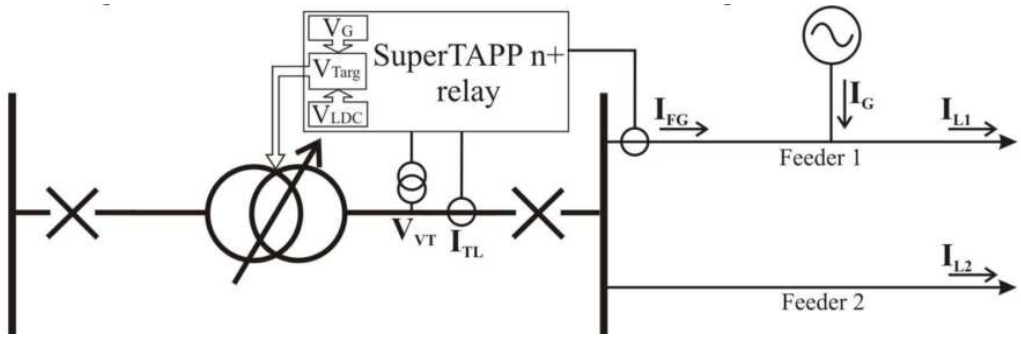

Figure 2.28: SuperTAPP n+ scheme arrangement [56]

One notable difference between the two systems lies in the position of the real-time data measurements. As shown in Figure 2.27, the GenAVC^{TM} device employs Remote Terminal Units (RTU)s located on the feeders and a communications network to feedback real-time data measurements. The SuperTAPP n+ does not require a communications infrastructure and performs state estimation of the DG output through an additional measure of current on the sending end of the radial feeder. Field trials of both systems have been completed and confirmed successful implementation of both approaches.

A number of studies such as [54], Liew and Strbac [58] & Ochoa et al [59] have compared the benefit of increased hosting capacity and energy yield that can be achieved against the various control strategies discussed thus far. In each of these studies, the level of last resort real power curtailment necessary to prevent system voltage excursion was significantly reduced with the incorporation of a CVC strategy. In all studies, CVC was identified as the most effective mechanism of any ANM

technique in alleviating voltage rise issues in distribution networks. However, scaling of the corrective CVC techniques developed in [56] and [57] to larger more complex distribution networks, as considered in these studies, has not yet been addressed.

Dynamic Thermal Ratings

Up till now, ANM techniques considered have focused on new and responsive control techniques. Alongside more active means of network control, real time system monitoring can also facilitate greater utilisation of existing capacity in network lines and transformers. A highly respected technique in this respect was dynamic line ratings (DLRs). DLRs epitomise the philosophy of intelligent or *'smart'* electricity networks and can significantly improve use of the existing infrastructure assets. The thermal capacity of network infrastructure is limited by a number of environmental and atmospheric conditions. Traditional thermal capacity limits were determined from static off-line assessments based on conservative estimates of the environmental and atmospheric variables. Techniques have been proposed by Michiorri et al [60] and a demonstration project by Yip et al [61] that use real time weather measurements to calculate the actual thermal capacity of network infrastructure, permitting greater magnitudes of power flow depending on weather conditions.

The thermal rating of overhead lines is likely to become a more common constraint on the distribution network headroom as active voltage control techniques are deployed. Besides employing greater levels of real power curtailment, which is at odds with the efforts of active voltage control techniques, DLRs offer the only known alternative to expensive network upgrades.

Demand Side Management

The future of electricity supply in Scotland, the UK and beyond will undoubtedly see the introduction of 'Smart Energy Meters' to residential customers. The role of these smart energy meters could be to form the basis for an Advanced Metering Infrastructure (AMI) that can allow the collection and aggregation of real time network demand data. This will play a vital role in informing system operators of the loading on the networks and aid the control and scheduling of the future generation mix.

In addition to this, smart energy meters will provide some of the functionality required to pursue and implement active Demand Side Management (DSM) strategies. DSM refers to the use of load control to ensure statutory supply quality in constrained networks or during generation shortfall. The traditional form of load control used by system operators is load shedding, where industrial customers are incentivised to have their electricity supply cut or curtailed during extreme or abnormal network conditions.

An alternative method of DSM was proposed by Scott et al [62] to actively regulate voltage levels on distribution networks with wind power DG. Here, voltage levels at the point of DG connection were monitored and in the event of voltage rise beyond the pre-set target, switchable thermal consumer loads were turned on, increasing the steady state demand and returning the voltage level below its target threshold. Although not modelled specifically, the paper identified consumer thermal loads such as thermal storage heaters and hot water storage systems as the most appropriate technology for DSM. Results witnessed a shifting of the varying demand pattern to match wind power production levels. Although feasible, it was concluded that the low levels of intermittent use of this technology meant pay-back periods were too long and ANM technologies such as curtailment and PFC were likely to be more cost-effective.

Another DSM strategy was proposed by Westermann and John [63]. Here it was suggested that mass consumer applications for personal comfort, such as air-conditioning, could be actively regulated by the DNO. In this situation, loading levels were adapted to normalise the power flows across GSPs and through transmission network corridors. This could be used to balance deviations from energy contracts, avoiding spot market expenses for reserve power and postpone investment in transmission network reinforcement.

There are multiple studies of DSM involving load scheduling, shifting or control. This includes the use of optimisation techniques, such as that proposed by Longenthiran et al [64]. A significant limitation to standard optimisation formulations for the real time scheduling of dispatchable system loads is that there is limited scope to identify to an 'optimal' service point.

Another potential source of DSM could be the use of stationary Electric Vehicles (EV) in a future technology known as vehicle-to-grid (V2G) storage. From the early inception of EV load in the distribution networks, the potential for adverse system impacts such as a lack of system generation and transfer capacity to meet high EV penetration levels poses significant difficulties for DNOs. The potential for load shifting of EV charging was investigated by Rahman and Shrestha [65] as a potentially meaningful and lucrative means of flattening the daily demand profile by means of off-peak charging and peak time deferral.

Electric Vehicles

The idea has been extended to the point that plug-in EVs can behave as loads or as a distributed energy resource, exporting power back to the electricity grid. This V2G concept has the potential to provide better utilisation of distribution networks, improving efficiency, stability and reliability. Significant issues related to consumer opinion, commercial arrangements as well as technical and regulatory standards are still to be addressed as highlighted by Yilmaz and Krein [66] and Ustun et al [67].

It is conceivable that a collection of active DSM schemes may become visible to and controllable by DNOs in the future. This has the potential to provide a mechanism for 'shifting' peak demand and flattening the varying demand pattern. In the extreme case, DSM could facilitate a scenario where generation no longer follows demand, but demand follows generation.

Distribution Network Aggregation and Future Network Strategies

Since the long term projection is that renewable energy technologies will make a large contribution to the future generation mix, it is also conceivable that distribution networks will have to act as an aggregator for the embedded DG that they host. In this vision of future electricity supplies, distribution networks will resemble a virtual power plant (VPP), comprising of both renewable energy DG and DSM and be responsible not

only, for the power flow within network boundaries, but the power flow across their boundaries into the transmission network, as suggested by [63].

Furthermore, by deliberately curtailing DG output by a certain percentage of available 'optimised' resource, a 'reserve' power source could be created to provide a near instantaneous real power supply for the purpose of maintaining frequency of supply. This is likely to be reserved for larger scale DG developments.

In this scenario, it is probable that the TSO would call upon the DNOs to regulate boundary power flows for load balancing purposes. While this is deemed to be a long-term strategy that is yet to be considered seriously, contemplation of this functionality was, like DSM, V2G and energy storage, retained while building the OPF technique presented in this thesis.

2.7.3 Active Network Management Development

ANM activities are concerned with the real time determination and communication of network control set-points to maintain network operating conditions within statutory limits. There has been limited research on (i) the coordinated use of ANM technology to better integrate multiple control schemes and (ii) the issues surrounding the real time application. There is therefore a need to develop appropriate scheduling algorithms to coordinate and optimise the use of ANM techniques in real time.

Building on the literature survey of ANM activities, a number of real time operational concepts were given consideration to help refine the potential operational functionality provided by an integrated ANM scheme. These are used to inform the subsequent research presented in this thesis for optimal real time ANM scheduling algorithms. The following discussions examine these in detail.

Steady-State and Real Time Management

As highlighted previously, the key characteristic in the development of ANM and evolution of distribution network operation is the change of state which determines necessary adjustments to network control settings. Conventional electricity distribution networks have been operating with minimal real time intervention by using fixed network pre-sets determined from steady-state 'worst-case' scenario conditions. With the transition to real time system monitoring and control in a fully integrated ANM

scheme, evaluation and determination of the network control settings will be conducted 'on-line' in real, or pseudo-real time.

The primary criterion for real time analysis and scheduling is the determination of DG output levels and network control presets based on prevailing network conditions rather than the speed of operation (as is commonly misunderstood). Real time analysis evaluates network power flow constraints and determines an appropriate response based on the current network conditions through wide area measurement and/or state estimation.

Centralised and Decentralised Approaches

The second management approach to consider is the geographical system area that a full ANM scheme will operate within and how the control variables in that system will be determined relative to each other. Methods to increase DG capacity levels in distribution networks include a range of centralised architectures, where individual elements of control are scheduled to improve collective network operation, as well as more decentralised or distributed methods of responsive network control that are only operated for their own individual benefit.

With the decentralised automation and intelligence of distribution network controllers, the major advantage over centralised ANM architecture is that it can operate on purely localised measurements at its own terminals and does not require any communication between network devices, as seen in [52],[53],[55],[56],[61],[62],[69]. However, decentralised controllers need careful consideration to prevent any conflicts with other interacting control systems. A further issue with embedding voltage regulation methods in a decentralised control scheme is the potential for large and unchecked amounts of reactive power to circulate in the network, which can cause overheating of generator and other network components.

Centralised ANM schemes provide greater network flexibility and can therefore enable the accommodation of greater levels of DG capacity [59]. The primary disadvantage of centralised schemes lies in the additional cost required to implement them and the unknown interactions in real time.

Much of the potential benefit from a fully integrated ANM scheme is suggested by the principle of centralised monitoring and scheduling of distribution automation.

Decentralised distributed automation schemes could be deployed in distribution networks and operated to maintain targets that are continuously re-evaluated via a centralised decision engine. Under this method, a fully integrated, centrally controlled and synergetic ANM scheme could be achieved through decentralised control techniques implementing and maintaining power flow and network variations within the statutory limits.

Given the advantages and disadvantages associated with each strategy, an attempt to quantify and compare the gain in hosting capacity from centralised coordination of DG voltage regulation and distributed active voltage control measures was conducted by Vovos et al [71] for worst case scenario conditions. The analysis showed that both approaches had a significant impact on the potential integration of DG, and while a centralised approach could facilitate a greater level of DG connection, particularly in rural networks, the increase over active distributed control measures would be unlikely to merit the investment required in a communications infrastructure and energy management system.

This assertion can now be disputed, when considering more recent work that took into account the annual variation of generation and supply combinations [59], where the increased uptake of ANM schemes in a centralised control infrastructure indicated a greater increase in the network headroom than was suggested by the earlier study. A clear conclusion from the study is that the worst case scenario approach to power flow management is no longer sufficient when dealing with variable and intermittent sources of generation.

The conclusions from [59] are consistent with similar work [58], which quantifies the energy and financial benefits from connecting renewable DG with three methods of active distribution network control. The study applied a bespoke OPF formulation to minimise the amount of curtailed real power at each time interval in a constrained network. The OPF was applied to defined levels of DG connection and studied more progressive methods of centralised active control.

Re-Active and Pro-Active control

Control methods can also be classified into one of two categories: re-active or pro-active. The difference being that the latter invokes control actions based on upcoming

system constraints, as opposed to adjusting control in response to system or control setting excursions. Re-active control techniques would afford the same opportunities as conventional OLTC.

In the literature, most of the developed ANM techniques operate re-actively, initiating corrective control actions following an excursion of system or control limits. However, in much of the literature regarding the design and principles of ANM, it was envisaged that these techniques would operate pro-actively, and take *'pre-emptive action'* as power flow conditions approach statutory and operational boundaries

2.8 ADDITIONAL RELATED RESEARCH

Over the last half century since OPF techniques were first established, their contribution to the understanding and improved operation of power systems has been substantial. Variations in the OPF formulation, applications and computational solution methods have featured heavily in research publications, from which [72]- [78] is a selection.

In a succession of research studies leading up to the work reported in this thesis, feasibility studies using augmented OPF functions for assessing a number of new network planning problems and congestion issues in the distribution network were conducted. The objectives of these include maximising the network headroom capacity for DG connections, optimising network investment and improving the integration of ANM technology.

One such application was reverse load-ability by Harrison and Wallace [79]–[80], which was designed to examine the shortcomings of conventional DNO practice in connecting DG. Customarily DNOs would evaluate DG capacity on a location by location basis and under worst-case scenario operating conditions to ensure continuing quality of supply to its customers. This conventional practice has generally been accepted for individual DG connections, where the impact could be clearly identified and mitigated. However, in a complex and highly interdependent system, location by location analysis does not ensure the best utilisation and operation of the network. Major limitations in the conventional practice included i) exhaustive search techniques were only feasible in small systems, and ii) there was a significant possibility of sterilising network capacity or stranding assets, given the first come, first served approach to connection agreements. As a means of improving connection practices

network wide, reverse load-ability modelled DG as negative load and used an OPF algorithm to minimise load shedding, therefore identifying the maximum connection capacity of DGs. This established a more efficient algorithm for assessing the complexities and interdependencies of distribution networks and highlighted the existence, or otherwise, of spare headroom capacity. This work improved the knowledge and understanding of distribution networks that contain a huge number of possible DG connection points, but where voltage, thermal and fault level constraints significantly limited the network headroom. However the approach maintained analysis under one-off worst-case operating conditions, failing to acknowledge how spatial and temporal variability of renewable energy resources would effect operation, and could relieve constraints.

The early reverse load-ability approach also failed to include fault level restrictions on maximising DG capacities, but reverted to post analysis fault studies to explore violations. Further work by Vovos et al [81] included the development of the fault level-constrained OPF (FLCOPF). The FLCOPF embedded the post-hoc fault analysis in an iterative process. The process reviewed the results from a capacity allocation OPF to determine if, and which, DGs would contribute fault currents that violated existing switchgear fault capacities before redefining the affected generation bounds in the capacity allocation OPF and repeating until a satisfactory solution was found. The FLCOPF which utilised proprietary OPF solvers continued a methodology present in the reverse-load ability formulation by augmenting the OPF with negative cost coefficients to favour DG.

OPF with operational changes in distribution networks was introduced by Boehme et al [82]. With time series power flow analysis, concurrent patterns of various generation and demand profiles were used to scale respective DG capacities and peak loading levels at hourly time increments, depicting the temporal and spatial variation of power flows in the network. Non-firm DG connections were allocated to new renewable DGs and an OPF algorithm was used to minimise the level of generator power curtailment required at each time step. The OPF algorithm again utilised cost multipliers to emulate a pseudo-merit order of dispatching generation plant, in this case wind, wave and tidal generation. To maximise the potential output from these renewable DGs, the time series analysis actively scheduled the maximum possible output at each renewable generator

for each incremental time step to determine the power production derived from the resource and allowed the OPF algorithm to minimise the required level of generator power curtailment to maintain power flows and supply quality within statutory limits. The study provided a preliminary appraisal of non-firm DG connections, estimating the frequency and duration of potential incidents of curtailment.

Additional ANM techniques were included in the OPF formulation of [58]. In one of the earliest and most widely-citied papers, an OPF technique was developed to compare and contrast the benefit of alternative ANM control techniques on the energy capture of DG from wind. The paper demonstrated three ANM strategies: Curtailment, CVC and the installation of reactive power compensation. The study investigated the hour-by-hour time series variation in generation and demand with results showing considerable improvements in potential DG penetration levels and energy yield. Systematic reductions in the required real power curtailment at various fixed capacity levels were demonstrated initially with the control of reactive power, and then with CVC of all network OLTC transformers in combination with real power curtailment.

Further changes in distribution network operation were then investigated with the development of a multi-period OPF [59]. The multi-period approach was developed to reduce the computational burden of performing full annual time series evaluation, while the OPF introduced further flexibility in the network simulation by converting constraints associated with passive control variables into variables of ANM. The specific ANM technologies employed were CVC, adaptive PFC and Curtailment. Outcomes of the work identified substantial margins for capacity expansion through operational changes that could lead to avoiding or postponing asset reinforcement. Results from the work also highlighted clearly the potential issue of increased losses with maximised utilisation and loading of networks. The methodology employed was extremely flexible with a bespoke optimisation environment as opposed to the optimisation solvers embedded in proprietary power flow packages. This allowed extensive application of the method to address further issues relating to ANM and enhanced distribution network usage, including: where an additional constraint reflecting the restriction on the sudden voltage step that occurs with the unplanned disconnection of DG was included in the OPF formulation [83]; where the OPF

framework was used to minimise energy losses [84] and reduce the reactive power demand in distribution networks with substantial DG penetration levels [85].

Ahmadi and Green [86] developed an OPF technique for autonomous network control as part of the AuRA-NMS concept. The OPF algorithm exhibited the potential to optimise DG capacity in different types of constrained networks but did not consider the ability of DG and network assets to implement variable control settings. More recent work on online operational modes of OPF includes a “corrective” management technique, by Dolan et al [87], to schedule real power curtailment. For the OPF to comply with proven last-in, first-out (LIFO) generator connection agreements, priority generators were favoured with the biasing of real power production costs. The practical application of OPF to operate within a real time, closed loop scenario was demonstrated. Simulation results highlighted deficiencies in the OPF algorithm which include; non-conformity of the LIFO connection regime during more onerous power flow congestion issues and discontinuous real time power curtailment settings.

A high level OPF was proposed in Czarkowski and Leon [88] for voltage regulation by means of DG set-point scheduling in large highly-meshed distribution networks. Similar to the approach taken in the Orkney RPZ scheme, networks were divided functionally into small sub-networks, with monitoring and communication systems deployed at these sub-network boundaries. While the approach of coordinating DGs in subdivisions of neighbouring DG units is seemingly promising, the results presented in this paper were limited in their consideration of the future high levels of renewable DG resources. The study is comprised of two manifestations of the OPF algorithm depending on the power factor regulation employed by the DGs; unity power factor (UPF) and off unity PFC modes. Constraints on the voltage regulation optimisation also included reverse power flow through network transformers, preventing external supply from DG.

In PFC mode, voltage drops arising from the loss of a DG unit were compensated for by increased reactive power production from neighbouring DGs.

In UPF mode, voltage drops are compensated for by increases in DG active power output from neighbouring DGs. The study therefore assumed that DG power is dispatchable, and operates with margins of reserve capacity. While this approach promoted a new philosophy for maintaining voltage regulation within limits in future

electricity systems, it lacked the functionality of maximising the benefit from renewable DG resources.

It was clear from the above literature survey, that there has been a great deal of activity in OPF techniques with ANM. Evidently there is also a general trend and natural progression of studies from planning algorithms – investigating and estimating the benefit of ANM, to real time control scheduling algorithms for the online environment. A consensus of the research reported suggests that there is significant scope for improving network operation and the integration of DG with ANM and that OPF scheduling has the considerable potential for real time implementation, but, at the time of writing, none of the above research has proposed an OPF algorithm that is capable of performing 'optimised' network scheduling in a fashion that embodies the continual time varying aspects of renewable electricity generation and ANM.

2.9 RESEARCH GAP

The need to find new technological and innovative responses to the growing challenges of ageing system assets and high volume integration of renewable energy resources in distribution networks has brought about development and consensus in ANM activities. OPF studies have been identified for many years as an appropriate tool for network analysts to study the steady state operating conditions of electricity networks. Recent advances in the use of OPF techniques to study the potential contribution of ANM techniques in distribution networks have illustrated that there are substantial advances in network operation to be found in the systematic coordination of ANM techniques. There is yet to be a significant development in the real time scheduling of multiple ANM techniques in an on-line environment. Individual ANM techniques have been demonstrated to work independently and in real time however, there is a need to examine the collaborative and synergetic interaction of these techniques in real time. This includes an examination of the potential network impacts and system consequences. The spatial and temporal variation pattern of production of DG from renewable energy resources and the stresses that it might exhibit on real time control practices are not truly reflected in the coarse, high level OPF studies covered in the literature surveyed.

Finally a key issue that continued to be evident within many sections of the literature was the establishment of appropriate market mechanisms and commercial arrangements (principles of access) around new network concepts and operating conditions across the spectrum of ANM activities. This is not an issue that is addressed specifically in this thesis. However, an assertion has been made regarding this issue in that, as there is currently a precedent for DNOs to dictate the control settings for a DG development within their network, any variation on those set-points, be that fixed or active, is commercially acceptable provided that there is an inherent benefit to that developer over the long term. With this in mind, provided some arrangement can be made to share the costs and benefits achieved from an ANM scheme across all participants, the adoption of fully integrated ANM schemes is not likely to be stalled by commercial constraints.

The work reported in the remainder of this thesis sets out to explore, prove and test the extent to which real-time adjustments to DG and network asset controller set-points could allow existing networks to accommodate more DG and increase energy yield from additional or existing DG capacity. New optimal power flow techniques have been developed to define the time-variation of control settings.

2.10 CHAPTER SUMMARY

This chapter has introduced the primary concepts of power flow in electricity networks and briefly reviewed some of the industry analysis tools used to plan and control network operation. It went on to review the drivers behind current developments and changes to the sector goals and initiatives.

From the literature review in this field, it became evident that the nature of electricity distribution networks will be required to change drastically in the near future. The high integration of DG from renewable and dispersed energy resources to best serve consumers dictates that the passive control philosophy will have to be evolved into one of ANM. In addition, in order to maximise the potential headroom in distribution networks it is important that future ANM schemes contain some form of centralised coordination of automated distribution control measures.

A potential long term solution to the centralised scheduling and control of ANM schemes may be to deploy one or more OPF techniques to deliver real time determination and appropriation of new control set-points. Distributed controllers will

then be operating autonomously to maintain the scheduled set-points in a re-active manner. The application of real time OPF techniques could also be extended to coordinate power flows over several tiers of network infrastructure for a variety of evolving network concepts maximising the overall system good. The intention of this study was therefore:

- To investigate new formulations of OPF for the real time scheduling of electricity network control settings to increase connectable capacity and energy yield from renewable energy resources and,
- To examine the real time network impact of multiple ANM techniques under the direction of OPF control and identify the potential consequences to system operation.

Chapter 3

Specification and Simulation Architecture

3.1 INTRODUCTION

Chapter 2 identified a need for new methods of scheduling in real (or pseudo-real) time active DG and responsive network controller set-points. The purpose of this chapter is to define the parameters of the problem and introduce the concepts and simulation procedures presented in this thesis.

The chapter begins by reiterating the high level principles, ANM and OPF. This includes a statement of the concepts and the potential limitations to the approach. New models introduced in this chapter that may be advantageous to real time application, such as the Receding-Horizon principle, are introduced. The specifics of the ANM OPF technique and examination of the consequences on system operation are then presented; including an overview of the simulation procedure; Receding-horizon principle; OPF formulations; time series input data and two distribution network case studies of growing complexity.

Finally, 'open-loop' testing of the ANM OPF techniques was performed to clarify the suitability and robustness of the new formulations.

3.2 SPECIFICATION

In Chapter 2, the need for research into ways of scheduling active DG and responsive network control settings in a collaborative and synergetic manner was identified. Central to these needs, is the proper quantification of system consequences from wide spread active management in previously passive distribution networks. A high-level specification for evolving distribution networks was outlined:

- ANM techniques based on the real-time regulation of network asset and DG controllers can increase the headroom capacity of distribution networks.
- ANM considers the real-time variation in generation and demand levels, rather than assuming the most onerous system conditions.
- ANM involves pro-active (preventive) and re-active (corrective) control actions to manage network constraints.
- Real time scheduling of variable controller settings will minimise unnecessary switching actions.
- OPF techniques provide a simple but effective tool to the scheduling problem that is well known, transparent and adaptable.
- OPF techniques should consider the probable fluctuations in generation and demand rather than the current resource and loading levels.
- OPF techniques can be implemented in a range of network sizes and types for a multitude of network operating applications.

The work presented in this thesis meets this high-level specification through the determination of appropriate network control settings in real time to increase the energy yield from distributed renewable energy resources and minimise the impact on DG and network asset controllers. To properly determine the impact of OPF studies on DG and network controller settings requires modelling of the independent control loops.

The introduction of OPF techniques to the real time control environment provides a means of increasing the scope for wide area operation of active DG and network controllers. Existing studies of OPF techniques for the real time control environment have often produced undesirable results such as spurious and unnecessary control switching [87]-[89]. In most cases the lack of time dependent analysis in the OPF formulation often contributed to poor temporal stability, categorised by discontinuous switching of control settings between successive solutions. This is demonstrated by an extract of results from [87], shown in Figure 3.1, where the per-unit DG set-point issued to DG 4 switches frequently between time steps at the beginning of the observational test case.

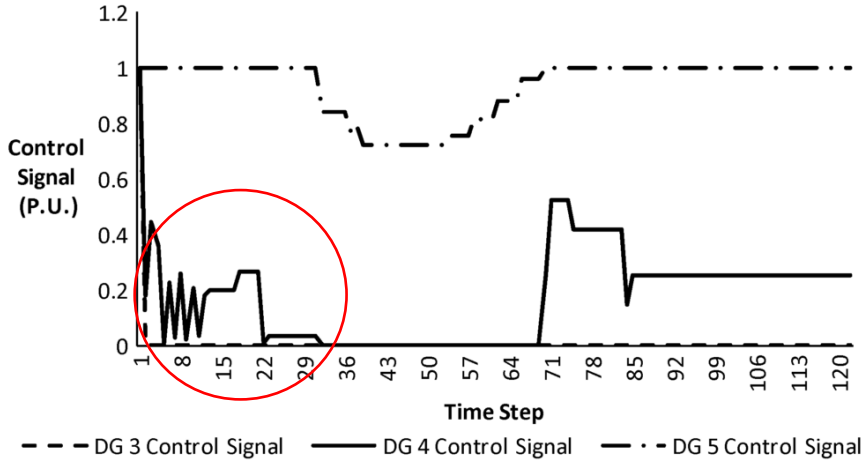

Figure 3.1: DG per unit set points [87]

In this study, new formulations of OPF were desired to ensure no unnecessary increase in network switching actions. Multi-objective functions and the Receding-Horizon principle were identified as potential alterations to the standard OPF formulation that could stabilise control actions in time sequential OPF solutions. These are discussed in the following chapter subsections as part of the formal OPF formulation in section 3.5.

As a stand-alone package no simple software environment was capable of formulating the advanced OPF algorithms and could address the need to model the real time functionality of independent DG and network asset control loops. Therefore, a novel and customised simulation environment was required where new OPF formulations could be formulated and the network power flow could be solved successively at higher resolution (shorter time steps) than the OPF, in order to follow and interpret the real time actions and system response to new optimally prescribed control settings. The customised simulation architecture is introduced in the next section.

3.3 Defining the Simulation Architecture

Most proprietary power flow software packages provide system add-ons to model the standard OPF problem. The freedom to express new ideas and define bespoke OPF formulations is often denied by the limited number of available problem parameters that can be defined. In addition the OPF add-ons can only be formulated over individual steady state scenarios and successive solutions automatically install new network

control variables removing the possibility to review the real time implementation and model system consequences. Hence implementation of the OPF algorithm and examination of the likely real time network impacts required a new approach to modelling system operation and the OPF problem. Formulation of bespoke and custom optimisation algorithms can be achieved on many other more general computer programs.

In a real life scenario, ANM on distribution networks can be separated into two distinct operating systems: (a) the physical network and, (b) the additional intelligence embodied for determining appropriate control actions. In this work, a suite of interconnected model elements, illustrated in Figure 3.2, was developed [90] to facilitate simulation of the real time network operation and enable the real time transfer of data between a 'proxy' distribution network and a centralised distribution management system (DMS).

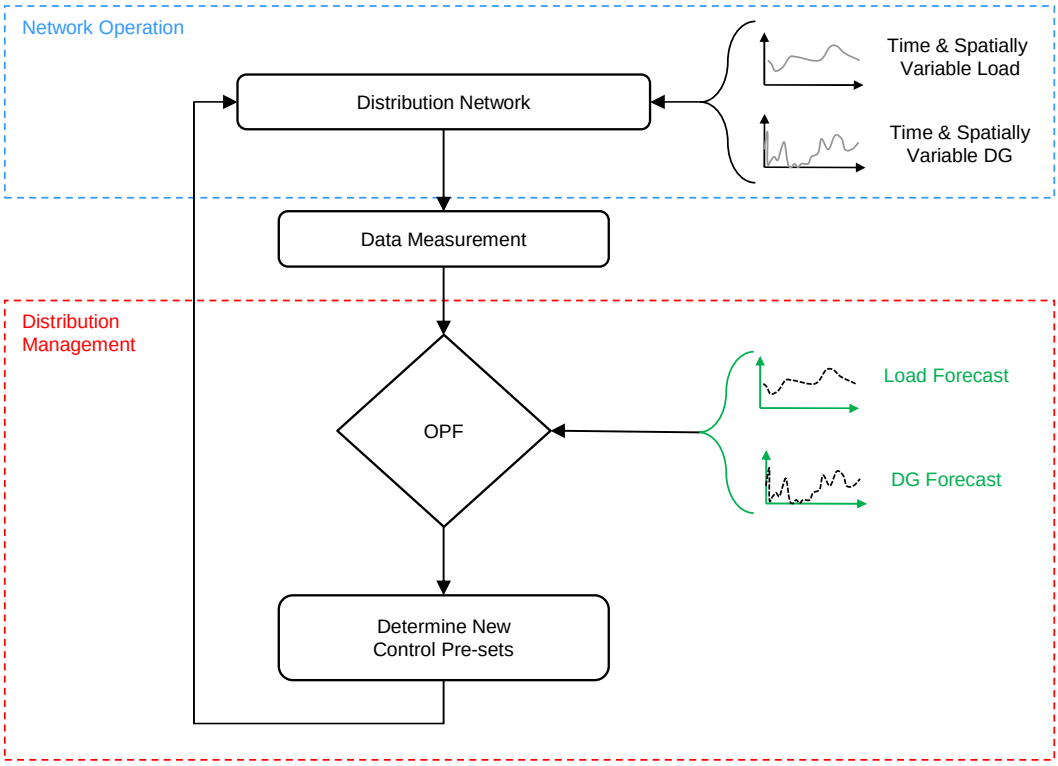

Figure 3.2: Architecture of the distribution network simulation environment

The system architecture is composed of three interfaced elements: (i) a distribution management system within which a range of management approaches can be articulated; (ii) a distribution network simulator that translates commands within

specific infrastructure referred to as the ‘proxy’ distribution network; and, (iii) a dedicated optimisation platform, which forms part of the distribution management system, hosting the full ANM OPF technique presented below.

The optimisation platform AIMMS [91] was used to build the various ANM OPF formulations. The AIMMS optimisation environment is a new and distinct platform for formulating the advanced OPF techniques presented in this work. Successive time sequential solutions of the OPF were automated with MATLAB via the COM interface. A detailed formulation of the real time ANM OPF algorithm is presented in section 3.5 alongside the various augmentations investigated in this thesis. While these model elements were by necessity in software form, the ultimate intention is that they would be interchangeable with hardware-in-the-loop components or the real network.

The system provides the opportunity to programme and interpret new formulations of OPF with the added dimension of time and without acting directly on control settings in the power flow. In addition, it allows the active regulation of DG and network asset controllers to be modelled explicitly in the power flow solution so that the network response and system consequences under varying power flow injections can be observed.

Variable power flow conditions are modelled by the time series profiles of generation and demand. The time series input data is introduced in section 3.6. As shown in Figure 3.2, the time series of load and DG production levels are fed exclusively to the power flow solutions of the ‘proxy’ distribution network. Sampling of load and generation values, as well as prevailing network conditions, is articulated in the distribution management system (i) and used as input data to the OPF.

The exception to this is the receding-horizon formulation where synthetic load and generation forecast data were pre-prepared and fed directly to the distribution management element for real time transfer to the OPF engine. The creation of forecast data for the receding-horizon application is discussed in detail in section 3.7.

Sampling of real time network information in this manner is considered sufficiently representative of an Advanced Metering Infrastructure (AMI) providing remote measurement of real time information to a centralised management system.

In the work presented, the open source software program OpenDSS [22] was utilised to perform time sequential solutions of the power flow equations. This software program was selected after careful consideration of alternative proprietary packages. Programs such as PSS/E, PowerWorld and MATLAB, were all available and offered sufficient feasible alternatives, but did not match the flexibility, speed and ease of use provided by the OpenDSS environment. Furthermore, the potential of OpenDSS to model as yet unknown system complications, such as network unbalance, made it the obvious choice for this and for further work in this vein.

Power flow in continuous time is simulated as a series of short term steady state power flow solutions in OpenDSS with the network control infrastructure operating autonomously. Periodically the network control settings are updated via commands from the DMS, the time step between these intervals is referred to as the control cycle. The time frame of concurrent OPF and power flow solutions is depicted in Figure 3.3. For the majority of this thesis, the control cycle was set at 5 minutes with power flow solutions at every 5 seconds in the intervening and concurrent time steps. The only exception is in section 5.4, where the control cycle was 15 minutes. In section 5.4 the longer control cycle and a coarser, 5 minute, interval of power flow solutions were employed to allow a longer overall period of analysis.

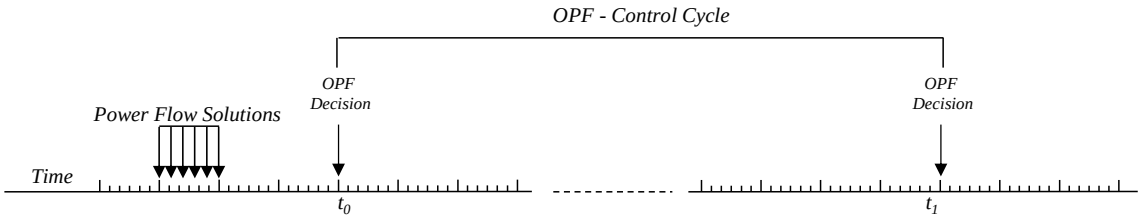

Figure 3.3: Power flow solutions and control cycle of simulation architecture

MATLAB was used as a middle management agent to drive the system simulations and control the real time exchange of data between the ‘proxy’ distribution network in OpenDSS and the OPF algorithm in AIMMS.

The use of OpenDSS, controlled and driven by MATLAB, is considered and later shown to provide a sufficient platform to emulate the application to a real life system. The separation of the simulator and control algorithms reflects a realistic evolution of the network by mapping modern, more intelligent control techniques onto the

conventional passive sections of the network. The segregated OpenDSS power flow solver is used solely to replicate the time dependent response of the physical network infrastructure and resultant power flows. The OpenDSS block is said to be representative of the *'real'* distribution network.

In this scenario, the OPF technique is used to schedule network control set-points continuously in discrete time regardless of whether or not network constraints were violated. This approach was specifically chosen to optimise network response in new bi-directional power flow regimes.

At each time sequential solution of the ANM OPF, prevailing network configuration and state are sampled from the OpenDSS environment and the information is exchanged through MATLAB with the OPF algorithm. After successful convergence of the OPF, the resulting network control set-points are prescribed by the DMS and issued to the control infrastructure in the OpenDSS software. The real time implementation of continuous and new system set-points are then resolved by the OpenDSS environment as described below.

OLTC transformers

The real time voltage regulating functionality of OLTCs, as described in [92], is embedded in the OpenDSS software package. OLTC transformers are fitted with a voltage regulator control object in the software that is designed to emulate standard utility voltage regulation control practices. Under normal operating procedures, fluctuations of voltage are tolerated within a deadband, and tap-changing actions are subject to time delays as designated in accordance with the pre-existing coordination of voltage regulation. When actively prescribing new voltage targets through the ANM OPF, the response of the OLTCs to comply with the new target is subject to a short communication time delay, Δt, and the time delay, d, of the transformer OLTC control circuitry as illustrated in Figure 3.4.

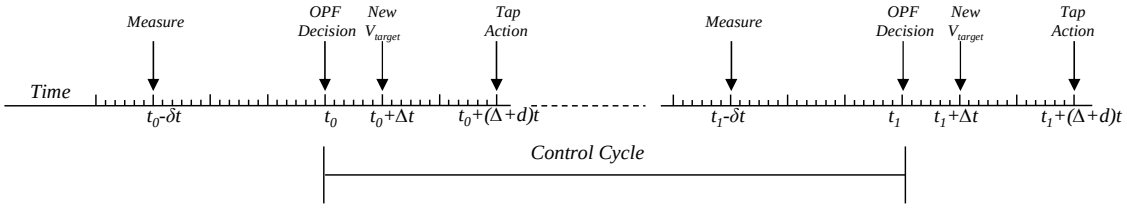

Figure 3.4: Control cycle of OLTC transformers in the ANM OPF

DG

Modelling the active DG controller concepts, such as variable PFC and curtailment, in a self-governing manner was not feasible in the OpenDSS environment. This is because ANM operating practices are not yet established or standardised in power system modelling. To circumvent this shortcoming, the DMS is programmed to script generator set-points that emulate the functionality of these active control measures. In this approach the variable PFC control scheme is replicated by running the generator in PFC mode and actively updating the power factor set-point as required. In a similar manner, active regulation of the generator power output required for curtailment is achieved by limiting the capacity of the generator along a per-unit basis. Hence, the resource based variation of output is unaffected but the maximum DG output is limited to levels identified as satisfactory network regulation.

In deriving the real time response of DG to new control set points, certain assertions were made after careful consideration of the literature. The power flow solutions of the distribution network continue uninterrupted at a high resolution, i.e. with a shorter time step than the OPF control cycle. Prior to each control cycle period, new measurements of network state information are recorded from the power flow solutions. At the beginning of each control cycle when there is a new configuration of DG set points issued, dispatch of the DG set points is subject to a short communication delay, Δt, and a further period of generator ramping, Δt, between previous and newly issued set points. This is demonstrated in Figure 3.5. The communication delay and ramping time are only representative and are assumed constant at 30 seconds each.

In the first instance, the case is made in each network, for the short term real time control dispatch where the control cycle operates on a rolling 5 minute window, while the time sequential power flow solutions of the ‘proxy’ distribution network are

performed at 5 second intervals, to show the real time interactions of multiple control practices and the network implications.

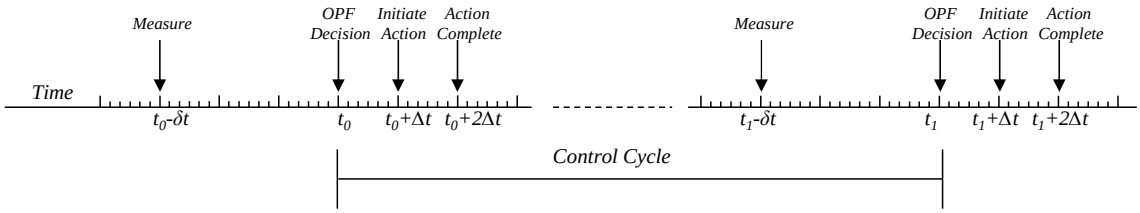

Figure 3.5: Control cycle of DG controllers

The DG transition from current state to a new prescribed dispatch is traced linearly, both up and down, in incremental steps as demonstrated in Figure 3.6. Again this approximation is only considered to be representative of the likely real time rate-of-change of DG power production instigated by centralised ANM schemes.

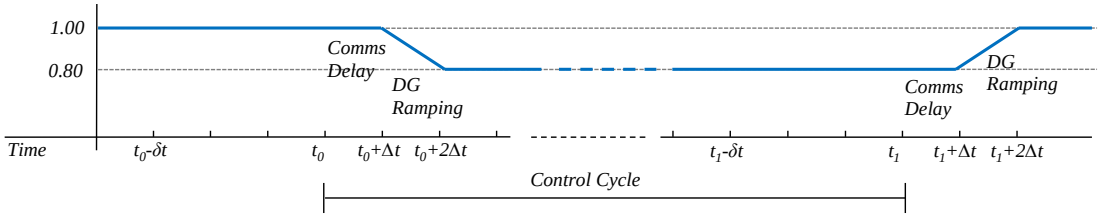

Figure 3.6: Control switching of DG

Changes to the reactive power dispatch occur in tandem with the active power dispatch, as the DG operates in power factor control mode, but the switch between variable PFC control settings occur almost instantaneously (or within the 5 second simulation window of the power flow solutions).

The work then progressed to assess wider variation and more progressive changes in supply and demand variation, with simulations conducted over a longer time frame with power flow solutions at 5 minute intervals and an OPF control cycle of 15 minutes. In this instance the real time interactions of various network control practices are not modelled. This longer, coarser time steps are only applicable to section 5.4.

Thus in this novel application of OpenDSS, key functionalities of both conventional responsive, but passively operated, distribution network assets and intelligent active distributed control practices can be modelled. This establishes a bespoke distribution

network simulator for fully assessing the introduction of both decentralised and centralised novel control practices in distribution networks.

Some of the key functionalities of the full simulation environment include:

- Flexibility over distribution network cases to implement active DG and network control.
- Flexibility of the DMS to accept new means of supervisory control decision engines.
- Ability of the DMS to mask, or suppress information on current network state to any supervisory control decision engines, replicating a loss of communication from AMIs.
- Ability to supply forecast (and erroneous) data to the supervisory control decision engine and view the implications of imbalances between the input data and the real time network inputs.
- Ability to view and analyse interactions and conflicts between the existing network autonomous control functionality and retrospective ANM techniques.
- The ability to perform and investigate, like for like, reactive and proactive ANM control techniques.

3.4 THE RECEDING HORIZON PRINCIPLE

With the specification of a new OPF formulation for real time ANM control in distribution networks, new avenues and potential adaptations of the standard OPF model were investigated to improve the application of the ANM OPF and the impacts on network operation. One of the adaptations considered was the Receding Horizon principle [93].

The receding or ‘rolling’ horizon principle is applied in one class of real-time control approaches, known as Model Predictive Control (MPC). MPC methods are designed to implement optimisation strategies within the control loop (i.e. in real time). Classical control schemes can define parameters that lead to sub-optimal plant operation due to conservative operational margins imposed by a lack of knowledge and vision of

temporal constraints. MPC control techniques have the advantage of being able to estimate upcoming temporal constraints, including them in the control evaluation and therefore determining better set-points closer to an optimal configuration.

MPC is practiced in a time sequential feedback control loop. For each time step, an MPC will:

1) Record a measurement of the system state or outputs.
2) Compute a control sequence over an upcoming finite control horizon via an internal model depicting system behaviour, and an optimisation algorithm.
3) Implement the first stages of the optimal sequence.

The receding-horizon component of MPC is the continual automation of this process. Historically, the application of MPC control techniques has been limited to 'slow' process systems such as petrochemical or pulp and paper industries due to the length of computational time steps [93]. With advances in computing, processes with a computational time of approximately one minute in 1990, can now be computed in less than a second, making MPC control techniques applicable to faster moving problems such as the control of electricity networks.

In the OPF case, the receding-horizon approach operates continually in real time using forecast generation and demand data to compute the optimal network set points over a finite control horizon of arbitrary chosen discrete time steps. With the advancement of each discrete time step, initial action(s) in the projected control sequence are implemented and optimal network control set points are computed for the next finite control horizon. The control horizon is continually receding and the system settings are actively and progressively tracking optimal set points. Recent literature on the MPC and the receding-horizon principle has shown that the techniques can improve continuity and stability in time sequential solutions of OPF techniques [94]-[96].

Xie et al [94] used a MPC OPF algorithm to solve a hybrid economic-environmental dispatch problem in electricity systems with intermittent resources. The proposed OPF algorithm reduced total generation costs by dispatching generation from intermittent resources to compensate for temporal load fluctuations (load-following). Results showed that MPC can be used to balance generation from intermittent resources against

short term fluctuations in demand. When compared to standard (snapshot) economic dispatch, the MPC approach reduced the need for short-lived expensive dispatch of natural gas (balancing) plants.

Ramp rate violations incurred by the sequential implementation of conventional static OPF solutions were considered by Xia et al [95]. Studies showed the output of successive economic dispatch OPF solutions depend on the initial system conditions. As time elapses, variations to the initial system conditions can cause a large discrepancy between OPF solutions from the initial system conditions and those from a flat start. This has the potential to violate system ramp rate constraints. The study showed that the MPC approach can prevent the OPF algorithm from configuring network settings into a problematic network state and improve the temporal stability of OPF for real time dispatch.

Glavic et al [96] presented a receding-horizon OPF technique to correct voltage excursion and prevent long term voltage instability in transmission networks following major circuit events. Using adjustments to shunt capacitor settings, generator terminal voltage settings and load shedding, the receding-horizon OPF achieved an acceptable control response to correct voltage excursion and stabilise system operation. When compared to a single step (snapshot) optimisation the receding-horizon approach prevented additional load shedding or switching actions which lead to further voltage oscillations and increased settling times.

3.5 DEFINING THE ACTIVE NETWORK MANAGEMENT AC OPF

In this section an OPF algorithm is specified to actively regulate existing and new control settings in distribution networks, minimising the level of curtailment necessary to maintain statutory supply quality under varying power flows and minimising the impact on network control settings.

3.5.1 PROBLEM FORMULATION

Conventional formulations of the OPF problem solve the problem for a single scenario (or snapshot) of power flow injections. In this work, the OPF is formulated over a "control horizon" of arbitrary length and arbitrary discrete time steps, chosen to best suit the unique circumstances of differing network cases and technologies.

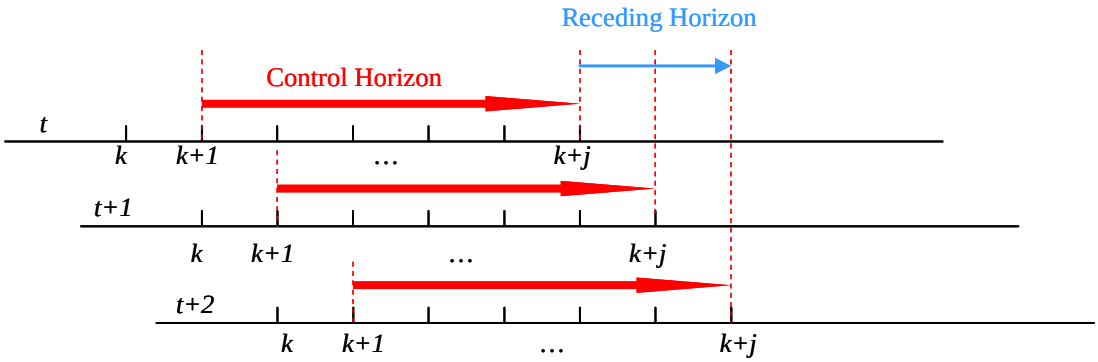

Figure 3.7: Visual representation of the Receding-Horizon OPF

Figure 3.7 demonstrates how the OPF technique is proposed to operate sequentially for each control horizon. In this approach, the time series analysis of network power flows is divided into a sequence of short windows of time depicted here by *(k + j|k)*. Each window represents a period of time or a 'control horizon' composed of *j* discrete time steps from current time *k*. The OPF algorithm is formulated over the control horizon and returns projected solution at each time step, subject to current network conditions at *k*. The OPF is solved over the entire finite control horizon determining appropriate configurations of ANM control schemes for every projected moment in time. Testing of the standard, single scenario OPF formulations was conducted using the same OPF models, by reducing the window of control horizon to one discrete time step (j=1). This means the OPF is solving selectively at snapshots of time based on sampled levels of generation and demand.

The proposed OPF formulations are solved continuously and provide periodic updates to the ANM control schemes. It was considered advantageous to pre-condition the network control set-points in the run-up to challenging power flow conditions. This progressive conditioning of network control measures during periods where network power flows were not problematic is intended to reduce significant spurious changes to network configuration and improve quality of supply.

In the following, the mathematical formulation of the optimisation is referred to throughout as the OPF. Later the OPF is solved over snapshots of time and over multiple periods of time with the use of synthetic forecast data. When considering the traditional form of the OPF model, where the optimisation is computed for a single scenario of steady-state power flow conditions, referred to as a snapshot, the technique

is referred to as 'OPF', whereas formulation of the OPF over a control horizon of progressive discrete time steps with the use of synthesised forecast data is referred to exclusively as Receding-Horizon OPF or 'RHOPF'.

The real time ANM OPF technique was based on an existing robust formulation of a multi-period OPF technique [59] developed to evaluate the hosting capacity of a distribution network with active controls under variable supply and demand combinations. In this work, the OPF is formulated over the finite control horizon, as described above, and not in an assortment of representative supply and demand combinations.

In the work reported in this thesis two new objective functions are defined over varying system control horizons:

OPF1: $$Min \sum_{g \in G} p_g^{curt}(k+j|k) \tag{35}$$

Where: $p_g^{curt}(k+j|k)$ is the real power curtailed in each discrete time step.

In this basic expression of the objective function, the formulation is a minimisation of the real power curtailment for all time variable distributed generators g in the set, G to maximise the real power output at discrete time intervals and consequently energy yield across the finite control time horizon.

An additional objective function to discourage unnecessary and spurious changes to voltage settings at tap changing transformers is also introduced:

OPF2: $$Min \sum_{g \in G} p_g^{curt}(k+j|k) + \sum_{b \in B} (V_{OLTC}(k+j|k) - V_{OLTC}^{target})^2 \tag{36}$$

Where: $V_{OLTC}(t)$ is the time dependent voltage level on the secondary winding of existing network OLTC transformers and V_{OLTC}^{target} are the pre-defined voltage settings for the fit-and-forget passive control arrangement. This prevents the inception of unnecessary tap changing actions. Other means of trading off minimal levels of energy curtailment in favour of reducing the level of switching actions incurred are possible, such as direct penalisation of tap changes. The benefits to this, minimum deviation by least squares approach include its simplicity and scalability, as well as the fact that it is well known and trusted means of minimising deviation in power flow studies.

A third formulation of the objective function, termed OPF3, where the internal OPF pre-defined operational voltage settings V_{OLTC}^{target} for the second objective function are re-defined to specialise the OPF technique against the unique circumstances of each network test case, was investigated later in this thesis.

As the formulation of the control horizon time period is in progressive discrete steps of steady state power flow, the on-line formulation of the OPF can be structured in the same manner as the standard OPF, but with the added dimension of time, as depicted with the finite control horizon.

The parameters of the OPF problem were as follows.

The fixed system input parameters include:

- Peak demand at each node *b*,: $d_b^{P,Q}$.
- Installed DG capacity for each generating unit, p_g.

The variable system inputs which mandate change to the system control settings were:

- Variable demand, $\eta(t)$.
- Variable generation, $\omega_g(t)$.

The network model is subject to the technical and statutory system constraints including:

The statutory voltage envelope:

$$V_b^- \le V_b(t) \le V_b^+ \quad \forall b \in B \tag{37}$$

The power balance equations:

$$\sum_{l \in L \mid \beta_l^{1,2} = b} p_b^L(t) + d_b^P \eta(t) = \sum_{g \in G \mid \beta_g = b} \left[p_g \omega_g(t) - p_g^{curt}(t) \right] + \sum_{x \in X \mid \beta_g = b} p_x(t) \tag{38}$$

$$\sum_{l \in L \mid \beta_l^{1,2} = b} q_b^L(t) + d_b^Q \eta(t) = \sum_{g \in G \mid \beta_g = b} \left[p_g \omega_g(t) - p_g^{curt}(t) \right] \tan(\phi_g(t)) + \sum_{x \in X \mid \beta_g = b} q_x(t) \tag{39}$$

And the thermal limits of the network infrastructure:

$$(p_{b_i b_j}(t))^2 + (q_{b_i b_j}(t))^2 \leq (s_l)^2 \quad (40)$$

Where: $p_x(t), q_x(t)$ are the time dependent levels of external power supply, such as the GSP and interconnections and, $p^L_{b_i b_j}(t), q^L_{b_i b_j}(t)$ are the time dependent network power losses. A full derivation of the ANM OPF technique is provided in Appendix A.

Three potentially active control settings, introduced in chapter 2, that DNOs currently have the opportunity to actively influence were adopted as new optional measures of active control, all acting on independent control loops. These were: A. Curtailment, B. Variable PFC and C. CVC.

A. Curtailment

At each discrete time step the maximum level of real power curtailment necessary at the DG is a function of the prevailing resource level.

$$0 \leq p^{curt}_g(t) \leq p_g \omega_g(t) \quad \forall g \in G \quad (41)$$

In the OPF solution, the value of power curtailment is not a function of prevailing resource, instead it is a blank subtraction of power production required to keep voltage and thermal loading levels within limits under varying power flow injections, as shown in (38). In order to maximise power production from DG, the set-point issued to the actual distribution network simulation is a per-unit setting of the maximum power output over the forecasted resource dependent power production level, $p_g \omega_g(t)$.

Hence, the per-unit set-point issued to the DG controller is not a portion of maximum allowable power output, but a calculated measure of anticipated power output based on the projected level of available resource at each DG, $\omega_g(t)$. The reasoning behind this is that the ANM scheme is not simply a means of mitigating the most severe impacts of DG integration but a supporting system to network regulation, facilitating more intelligent operation over a wide network area. In which case, localised pockets of ANM set-points may be reliant on appropriate levels of DG production at each moment in time to ensure voltages across the network are within statutory limits.

B. Adaptive Power Factor Control

Currently, the obligation of DGs to provide network support and ancillary services is dependent on plant size and contractual connection. The functionality is also dependent on technology. Here, all DG plants are assumed to possess the technological and thermal capability and are initially installed in the optimisation to provide network support in the form of adaptive reactive power compensation, termed variable Power Factor Control (PFC). PFC regulates the voltage level at the point of connection of a DG by actively adjusting the DG power factor angle ϕ_g to absorb or inject reactive power as required to optimise network operation.

$$\phi_g^- \leq \phi_g(t) \leq \phi_g^+ \tag{42}$$

C. Coordinated Voltage Control

Existing distribution network infrastructure possesses the ability to run responsively to alterations in the network voltage profile. Based on steady-state pre-set voltage targets, OLTC transformers are used to maintain voltage levels under variable load patterns. With CVC this principle is extended to allow dynamic control of OLTCs and Voltage Regulators (VR) to meet the evolving needs of distribution networks. The OPF permits a variable tap position that emulates the range of incremental steps in a tap changing transformer.

$$V_{OLTC}^- \leq V_{OLTC}(t) \leq V_{OLTC}^+ \tag{43}$$

within the bounds of the tap positions in the OLTC transformers:

$$\tau_l^- \leq \tau_l(t) \leq \tau_l^+ \tag{44}$$

3.5.2 Analyses and Acronyms

Throughout this thesis three specific formulations of the ANM OPF technique were investigated. For the purposes of clarity, variations in the objective function are denoted numerically with the following acronyms:

I. Minimise energy curtailment - OPF1.

II. Minimise curtailment and deviation from ‘fit-and-forget’ pre-sets - OPF2.

III. Minimise curtailment and deviation from the new voltage targets - OPF3.

In addition, two formulations of the control horizon are denoted textually with the following acronyms:

I. Snapshot - OPF.

II. Receding-Horizon - RHOPF.

Finally, two interpretations and utilisation of the time series of input forecast data in the RHOPF analysis are studied. These are denoted:

I. RHOPF-A

II. RHOPF-B

Where, RHOPF-A refers to studies where the RHOPF follows the time series of the pre-processed stream of forecast data explicitly. RHOPF-B solves the RHOPF problem over a linearly interpolated trajectory between the last measured network data and the linearly interpolated half hourly forecasted value. Further detail on these different utilisation of available forecast data is described in section 4.5.

3.6 DEFINING THE TIME SERIES INPUT DATA

System demand varies continuously with notable seasonal and diurnal fluctuations. Modelling of the demand profiles in this research would have ideally, been as close to disaggregated reality as possible. However, load diversity beyond the 33/11-kV substation transformers has been of little concern to DNOs and is not widely monitored or documented. For the purposes of this research, the important consideration in the demand modelling was the time-wise variation of load demand in the system and it was considered sufficient to scale each load in the network along the single normalised demand pattern. The normalised half-hourly demand for central Scotland, illustrated by a one-month sample in Figure 3.8, was taken from [97] and used for this purpose across all the test networks.

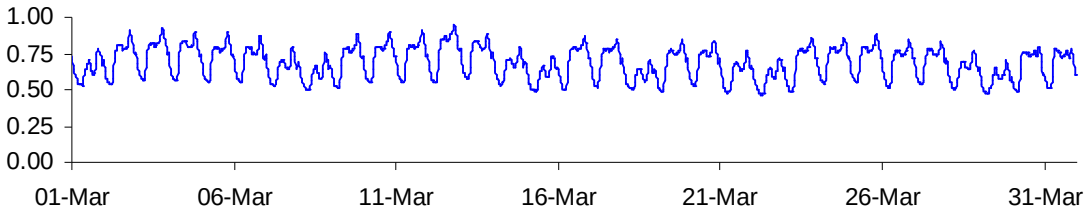

Figure 3.8: Example of the temporal demand pattern

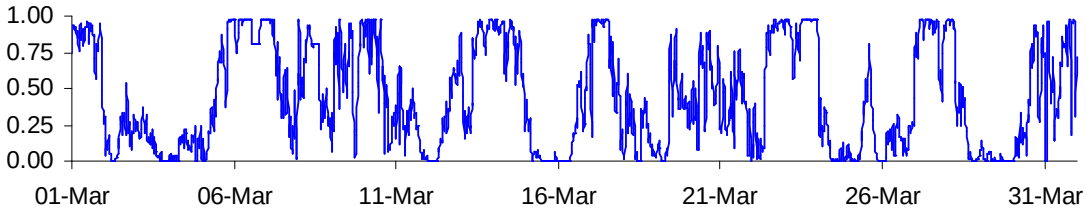

Figure 3.9: Example of the wind power production pattern

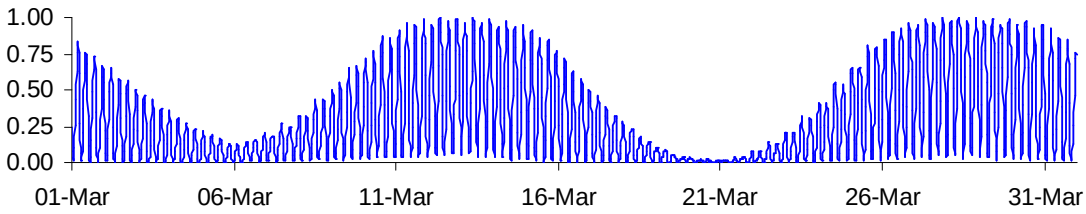

Figure 3.10: Example of the tidal power production pattern

The potential power output profile of each renewable energy resource is quite specific as discussed in Section 2.3. Coincident hours of wind production patterns based on measured wind speed data from the U.K. Meteorological Office and a generic wind power curve were taken from the work of [97]. Similarly, an approximate time-wise variation of tidal generation production was synthesised from the work presented in [98]. All data sets were linearly interpolated to between the 30 minute windows down to the necessary resolution for each simulation test case.

For the purposes of this research, it is not the site specific values of the generation output that is pertinent to the results but the challenge of variability. Electricity demand level and the temporal variation in wind and tidal production were represented by the

time series of normalised values and scaled linearly across the installed peak demand level and the locally installed capacity of each resource. DGs of each type were also bundled into regional clusters, which were considered close enough in the network analysed to be following the same resource production profile. Figure 3.9 and Figure 3.10 illustrate an example of the temporal variation in generator production level from wind and tidal resources.

The linear up-scaling of resource along the generic resource profile and spatial transposition in regional clusters is considered sufficient for the concept-proof and testing of the proposed technique. In the event that the proposed technique is developed for implementation, site specific variations, such as time shifts across regional clusters are actually envisaged as beneficial attributes to the data forecasts and could improve determination of the forecast data in a receding-horizon application.

3.7 FORECAST DATA

The use of forecast data in the power systems industry is common-place for load balancing in the higher voltage transmission system. However, within distribution networks there has been little operational requirement or a substantial benefit from the use of forecast data within the passive control regimes deployed.

The integration of significant levels of highly spatial and temporally variable renewable DG has established a need to evolve the passive management philosophy of distribution networks into one of ANM. A common concern regarding the introduction of ANM to distribution networks is the potential for variable control settings that lead the network into a challenging network state, which requires drastic action to rectify, using generation or load shedding. The primary cause of concern stems from the inherent variability of renewable energy resources. From the viewpoint of any network operator, uncertainties and fluctuations in power production levels of significant magnitude and, or rates of change, are likely to cause scheduling and control difficulties in the operation of network plant, such as transformer tap changing and degradation of protection schemes.

In the work presented in this thesis, one formulation of the OPF technique is designed to operate with the receding horizon application as described earlier in an attempt to improve the temporal stability of the active control settings prescribed by the time

sequential solutions of the OPF algorithm. The principle of this proposed technique provides a means of pro-active or pre-emptive network control, such that the Receding Horizon OPF (RHOPF) can actively and progressively prescribe optimal network control settings through time. This requires advanced notice of the fluctuation in power system demand as well as the supply from distributed renewable energy resources. The performance of the RHOPF algorithm is dependent on the availability of forecast data. With the receding-horizon application the important parameter of forecast data is the correlation between the forecast and real time variations. One primary advantage to the receding-horizon application is that the accuracy of the distant projected value of the forecast is not of significant importance, but even a simple forecast can help substantially. This is because the OPF solution is reassessed and re-evaluated at the next intermediate time step and the distant forecast value provides only a trajectory to improve the time sequential solutions of OPF. In essence, this has the potential to alleviate some of the concern held by DNOs over the uncertainty in power production forecasts as the certainty required diminishes along the length of the horizon. One further potential advantage to the long horizon period is the avoidance of driving the network configuration into an unstable situation.

A brief survey of some recent literature on short term forecasting has illustrated that there is currently substantial research being undertaken into deterministic methods of short term power production from renewable energy resources, with particular reference to wind and solar energy [99]-[103].

Of the literature surveyed, the terminology of short-term forecasting was used to categorise forecast predictions from anything between 30 minutes to 36 hours ahead, with the majority of forecasting techniques predicting power production or wind speed measurements at hourly intervals. The projected benefit from forecasting over this period was to provide either a reliable mechanism for frequency regulation and system balancing or enabling renewable energy technologies to participate in electricity trading markets.

Forecast horizons of less than half an hour have not been viewed as particularly important or beneficial. The standard method of providing short term forecast data in power systems studies within the half hour time frame is called persistence forecasting.

Persistence forecasting is regarded as the best method of informing control decisions in slow moving power systems studies. This is based on the relatively slow shifts in the aggregate demand level, however half an hour is a long time to assume wind power output levels will not change. In the persistence forecasting method, current values of generation and demand are presumed to be the same at the next time step.

With the enhanced integration of renewable energy resources in distribution networks under ANM techniques, electricity networks are anticipated to be operated and consequently controlled within tighter operating margins, persistence forecasting was not thought to represent the most efficient approach to network scheduling in this scenario, particularly for the short term, 5 minute control cycles, of the ANM OPF technique. Furthermore, in the context of this thesis, the use of persistence forecasting with the proposed RHOPF technique undermines the philosophy of the receding horizon application.

Testing and assessment of the RHOPF technique requires an input stream of forecast data to perform the look-ahead horizon scanning component. A full study into the methods of real time short-term forecasting is considered a more specialised project that goes beyond the boundaries of the work presented in this thesis. However, a brief summary of potential forecasting methods was conducted.

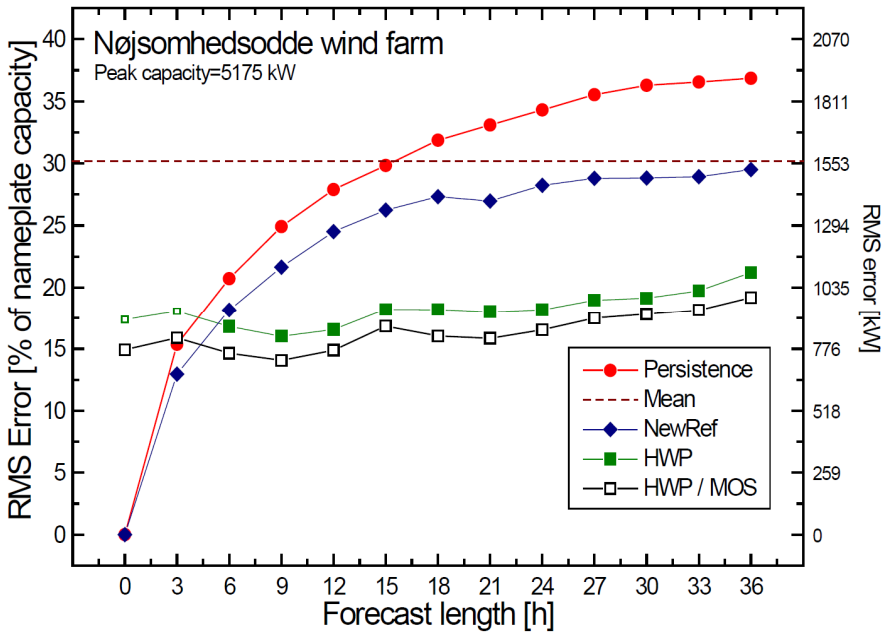

Figure 3.11: Root Mean Square (RMS) error of different forecast lengths and different prediction methods [99]

Typical results from an array of short-term wind power prediction techniques were compared in [99] on a Danish wind farm in the mid-nineties. Figure 3.11 shows the typical behaviour of the residual errors observed for different forecast lengths and different prediction methods. The prediction methodologies employed in the study were: Persistence, NewRef, HWP and HWP/MOS. Persistence forecasting has already been discussed. The NewRef model refers to a New Reference Model [100] which is essentially a hybrid persistence forecast which considers the last recorded observation and the time series (running) mean. The HWP results are generated from the 'raw' output from a Numerical Weather Prediction (NWP) model and finally the HWP / MOS model is a coupled model of the 'raw' NWP results and a post processing routine termed Model Output Statistics (MOS). The HWP/MOS model is now known as the commercially available system, 'Prediktor'.

As is inferred in Figure 3.11, persistence forecasting methods are far superior to advanced NWP models for short prediction horizons (below 3 hours). However one class of forecasting methodology missing from the study is a representation of current regressive statistical processing methods and a hybrid coupling of these with NWP methods. In theory this class of model would use past observations and current

climatologic conditions to approximate current trends and predict the upcoming pattern of change. In [99] the probable results of such a methodology were stated to be a horizon-dependent weighting of the persistence and HWP/MOS results, meaning that while it is not likely to do much better than persistence for immediate projections and will be limited by the NWP model over longer horizons, it is better equipped to predict potential patterns and shifts in the one to three hour horizon. Furthermore the findings of [101] also highlight improvements in persistence forecasting in the sub 30 minute horizon.

In order to function properly, sophisticated methods of forecasting applications such as NWP, Neural Networks and Artificial Intelligence would require intimate knowledge of a specific location as well as environmental factors associated with the time series data that are not available through the current data sources. Naïve methods of forecasting likely trends in the system near term performance, were thought to be possible through the processing of historical time series data from real time monitoring of the distribution system power flows and could satisfy the requirement for suitable forecast data. A more thorough examination of regressive statistical forecasting methods was conducted and is discussed in the following subsections.

3.7.1 Regressive Time Series Forecasting

More often than we realise, not only the production levels of electricity from renewable energy resources but our own electricity use, is underpinned by natural occurrences that feature seasonal and cyclical characteristics. Medium and long term trends that fluctuate around a steady horizontal mean also feature in the make-up of renewable energy resources and electricity demand.

A number of basic statistical forecasting tools are derived from what might appear as a time series of random data values by the decomposition of these characteristics and trends into distinguished patterns identifying individual components of the time series [102]. From this information there are a number of well established techniques that can be used to estimate how the sequence of each pattern will continue into the future. Based on the projection of each of these individual behaviours, it is possible to determine a highly accurate forecast of how the overall time series will progress at future time intervals.

The well established modelling techniques considered here to estimate the future projections of the decomposed time series include regression and time series methods. Regression methods are used to define the relationship between an individual, or a series of independent variables, and a dependent variable. For example, in the modelling of wind speed as the dependent forecast variable, independent variables may include; wind direction, temperature, time of day, month of year etc.

The regression model, in its simplest form, is a standard linear projection of the correlation between an independent and the dependent variable. Multiple Linear Regression (MLR) is an extrapolated form of the simple linear regression which features the transposition of each of the individual linear trends associated with each independent variable into a single equation. The form of a single linear regression and MLR model are show below.

$$Y_t = \beta_1 + \beta_2(X_2) + \varepsilon_t \tag{45}$$

$$Y_t = \beta_1 + \beta_2(X_2) + \beta_3(X_3) + ... + \beta_n(X_n) + \varepsilon_t \tag{46}$$

where $X_2,...,X_n$ are the independent variables of the dependent forecast variable Y_t, at time t, and $\beta_2,...,\beta_n$ are their regression coefficients that must be estimated. The symbol ε_t represents the random error term which typically has zero mean and constant variance (i.e., white noise).

A series of special forms of regressive forecast models where the dependent variables are regressed on a time lagged series of itself are more commonly referred to as time series methods, known as *auto*regressive models, as they correlate time-varying relationships between previous values of the series. Autoregressive models exhibit a distinct advantage over more general regression models due to their simplicity. However they also suffer from the distinct disadvantage that they do not directly describe a 'cause and effect' relationship, only one of the time dependency [105].

Based on the data available to a stand-alone distribution management system, namely historical time series records of observed power demand and generation outputs, without a stream of incoming independent variables, forecasting of demand and generation production levels in this work was restricted to time series methods. Four variations of autoregressive time series methods were investigated: Autoregressive

(AR), Moving Average (MA), Autoregressive Moving Average (ARMA) and Autoregressive Integrated Moving Average (ARIMA).

Autoregressive (AR) Method

In an Autoregressive (AR) model, forecasted variables of a time series are estimated as a linear progression of the regressive correlation between one or more previous values of the time series. An AR process of order p, denoted AR(p), is defined by:

$$Y_t = \phi_1 Y_{t-1} + \phi_2 Y_{t-2} + ... + \phi_p Y_{t-p} + \varepsilon_t \quad (47)$$

Where: $Y_{t-1}, {}_2\, Y_{t-2}, ..., Y_{t-p}$ are previous values of the time series Y_t, and $\phi_1, \phi_2, ..., \phi_p$ are autoregressive model parameters (correlations) [106].

Moving Average (MA) Method

The second method of forecasting from an observed univariate time series is the finite moving average method. The well established moving average (MA) process as defined in [106] is given below, which denotes an MA process of order q, MA(q).

$$Y_t = \varepsilon_t - \theta_1 \varepsilon_{t-1} - \theta_2 \varepsilon_{t-2} - ... - \theta_q \varepsilon_{t-q} \quad (48)$$

Where: $\theta_1, \theta_2, ..., \theta_q$ are the moving average coefficients.

As illustrated by the MA process the nomenclature "*moving average*" can be somewhat misleading as the current value Y_t of the time series is based on a relationship of a finite horizon of previous deviations, or error $\varepsilon_{t-1}, \varepsilon_{t-2}, ..., \varepsilon_{t-q}$, from the mean about which the time series varies. Therefore the MA(q) method does not arise from averaging of a finite section of historical time series itself.

The more obvious interpretation of the term "*moving average*", referred to above, is in essence a smoothing process that computes a simple mean of preceding values in the time series and is generally referred to as q MA to denote a moving average *smoother* of order q.

Autoregressive Moving Average (ARMA) Methods

Coupling the basic processes of the AR and MA methods, can define a class of slightly more complex time series models that benefit from greater flexibility known as Autoregressive Moving Average (ARMA). It captures both the self-correcting nature of the moving average method whilst expressing the projection of a time series as a function of auto regression. ARMA of order (p,q) take the form:

$$Y_t = \phi_1 Y_{t-1} + \phi_2 Y_{t-2} + ... + \phi_p Y_{t-p} + \varepsilon_t - \theta_1 \varepsilon_{t-1} - \theta_2 \varepsilon_{t-2} - ... - \varepsilon_q a_{t-q} \qquad (49)$$

Autoregressive Integrated Moving Average (ARIMA) Methods

ARMA models are only applicable when the input time series data is stationary. A data set is defined as stationary when the data values fluctuate around a constant mean. ARMA models can be extended to non-stationary series by allowing differencing of the data series. Differencing of the time series is achieved by computing the change between each observation of the time series, like so:

$$Y_t^{'} = Y_t - Y_{t-1} \qquad (50)$$

ARMA models on a differenced data set are known as Autoregressive Integrated Moving Average (ARIMA) models. They take the general notation of ARIMA (p,d,q), where:

AR: p = order of the autoregressive part.

I: d = degree of the first differencing involved.

MA: q = order of the moving average part.

As the differencing component adds significantly to the algebraic statement of the model a backward shift operator, B, depicting the time shift operation is commonly utilised in the statement of the ARIMA model. Where:

$$BY_t = Y_{t-1} \qquad (51)$$

Hence B notifies a backward shift of a variable, in the case Y_t. Higher order backward shifting is characterised by B to the power of the order of backward shift (i.e. $B^{12}Y_t$ is equivalent to Y_{t-12}). This simplifies the ARIMA model statement considerably.

In the simplest case, ARIMA (1,1,1) the model takes the form:

$$(1-\phi_1 B)(1-B)Y_t = c + (1-\theta_1 B)e_t \qquad (52)$$

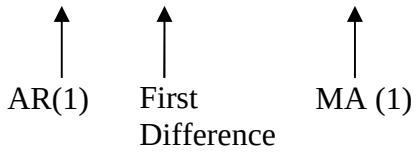

3.7.2 FORMULATION OF FORECAST DATA

Having reviewed potential means of forecasting, load, wind and tidal production patterns in the literature, attempts were made to derive approximate forecast models at half hourly intervals for each data stream into the RHOPF technique. The time series of the input forecast data had to have a greater time step than the operational control cycles, such that it depicts the longer term trend in generation and demand patterns. For this reason, time series forecast data was generated on the half hourly time frame. A single month of the sample data set was selected and analysis conducted to identify suitable models for the purpose of this research. Whilst reasonably acceptable tentative models were identified for demand and tidal power forecasts, the tasks involved for wind power forecasting grew beyond scope of this thesis.

An example of one forecasting model output for load based on a simple logic oriented ARMA (1,1) type model with a 24 hour backshift is shown below. Figure 3.12 and Table IV compare the results of the forecasting technique with the half-hourly persistence forecast.

$$Y_t = \phi Y_{t-1} + \theta(Y_{t-48} - Y_{t-49}) \tag{53}$$

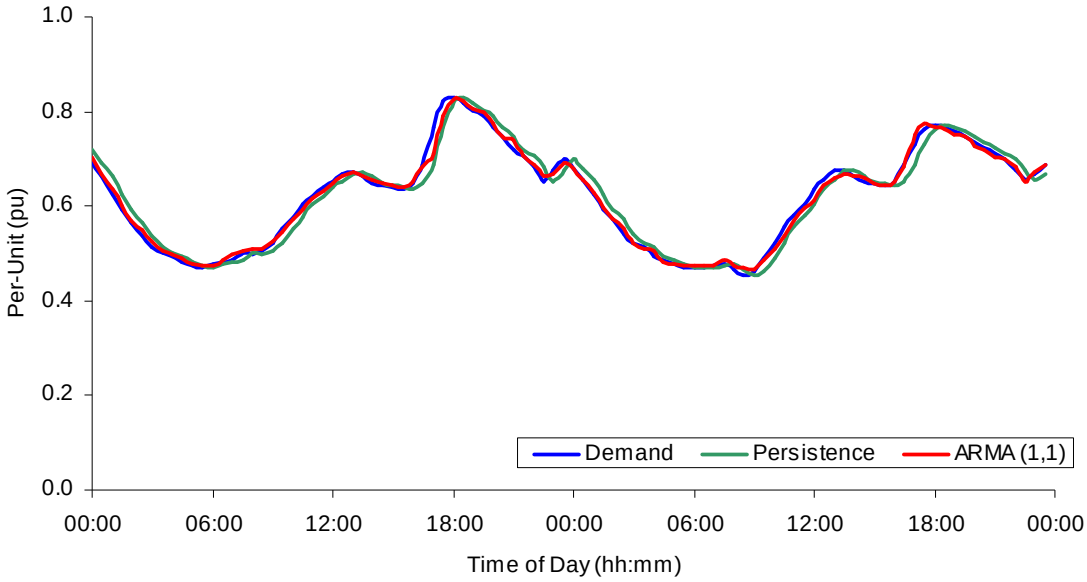

Figure 3.12: Illustration of demand forecasting

Table IV: Statistics of demand forecasting

	Persistence	ARMA(1,1)
Mean Squared Error	0.000	0.000
Mean Absolute Deviation	0.000	-0.001
Correlation Coefficient	0.970	0.994
R	98.5%	99.7%

In this fairly simplistic model, changes in upcoming demand levels are forecasted based on the change observed the day before. This allows the ARMA (1,1) forecasting model to produce a forecasted time series of variable demand levels with coincident fluctuations to real time demand, as illustrated in Figure 3.12. The results show that the ARMA (1,1) model has a stronger correlation to real time demand levels than persistence. For the purposes of control scheduling with the RHOPF routine this was the desired result.

A similar result can be seen in Figure 3.13 for tidal production. Again, using a simple logic oriented ARMA (1,1) model, this time with a 6 hour backshift, forecasted values of tidal production can be produced that fluctuate in tandem with the real time tidal resource. Figure 3.13 and Table V again compare the results of the forecasting technique with the half-hourly persistence forecast.

$$Y_t = \phi Y_{t-1} + \theta(Y_{t-12} - Y_{t-13}) \tag{54}$$

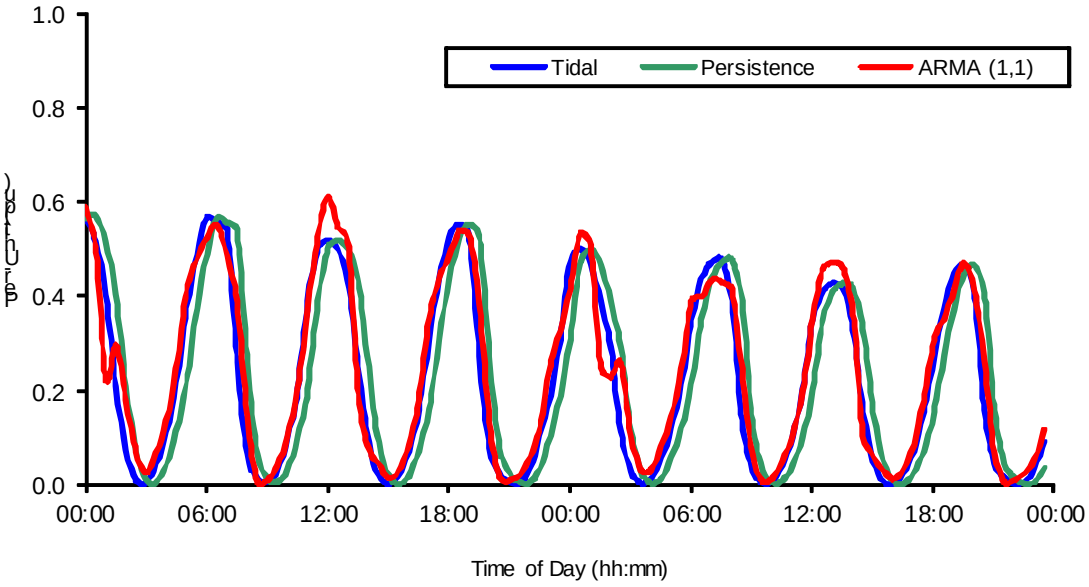

Figure 3.13: Illustration of tidal power forecasting

Table V: Statistics of tidal power forecasting

	Persistence	ARMA(1,1)
Mean Squared Error	0.177	0.182
Mean Absolute Deviation	0.306	0.319
Correlation Coefficient	0.814	0.971
R	90.2%	98.5%

These results again show a stronger correlation between forecasted and real time tidal power levels observed for the ARMA (1,1) model than persistence forecasting at half hourly intervals, as shown in Table V. It is worth noting that tidal power production is eminently more predictable than the results displayed here through alternative more sophisticated means.

For all manifestations of autoregressive modelling, a satisfactory forecasting methodology which exhibited the desired traits was not found. Autoregressive modelling of time series and differenced time series wind production levels did not, from the short data sample studied, identify any under lying trends or rhythmic changes in the short term fluctuations that could be exploited for the purposes of forecasting.

The depth of work required to research forecasting methodologies for multiple resources and across changing horizons was considered too intensive for the scope of this work. At this point it was clear that a fit-for-purpose solution was not going to be found within the time frame to suit all aspects of the work. Research and development of the necessary forecast models then ceased and synthetic forecast data was generated by a simple Weighted Centre Moving Average (WCMA) smoothing process, which is reviewed here and detailed where appropriate in later chapters. A 3rd order WCMA smoothing process is given by:

$$Y_t = \phi_1 Y_{t-1} + \phi_2 Y_t + \phi_3 Y_{t+1} \tag{55}$$

The 'synthesised' forecast value at time *t* is therefore a weighted average of the real time series value at *t-1*, t, and *t+1*.

3.8 DEFINING THE CASE STUDIES

Sections 3.3 to 3.7 have described the architecture, buildings blocks and input data of the simulation procedure followed in this work. In this section two specific network case studies are introduced that are later used to validate, interpret and evolve the performance of OPF techniques for the real time scheduling of ANM settings.

Two test case networks produced from the U.K. Generic Distribution System (GDS) programme, previously available on the SEDG website [107] were studied. These networks are related but differ significantly with the smaller network stated as a reduced

and much more simplified version of the larger for the purpose of demonstrating and visualising newly proposed ANM concepts. The two networks are discussed below and illustrated in Figure 3.14 and Figure 3.16.

The smaller network, referred to as *'EHV1 – ANM'* was used to firstly demonstrate the actions of the OPF algorithm and verify pragmatically its response to varying system power flows. After this the OPF technique is applied to the larger network, referred to as *'EHV1'*, to examine the results of the proposed scheme in a complex network featuring multiple DG developments from two differing renewable energy resources.

Formal identification of the installed DG capacity in each case was favoured to create a well posed model for the real time OPF formulation. Illogical or ill-posed statements of OPF can lead to unnecessary and additional difficulties in the convergence of non-linear optimisation. Based on preceding studies in these networks, realistic potential capacities of 'spare' network headroom were identified on specific network buses.

3.8.1 UKGDS EHV1 – ANM

The simplified EHV1 – ANM case was first used to demonstrate the potential for real time reconfigurable network control to optimise distribution network operation. The system is a section of a weakly meshed network of parallel feeders supplied by two equivalent 30-MVA 132/33-kV transformers. A subsea cable between buses 7 and 8 connects the network infrastructure on the "mainland" to a small "island." The system also contains a voltage regulator (VR) (i.e. an OLTC transformer with a 1:1 voltage ratio) between buses 8 and 9. Reflecting standard U.K. practice at these voltage levels the voltage envelope is ± 6% of nominal.

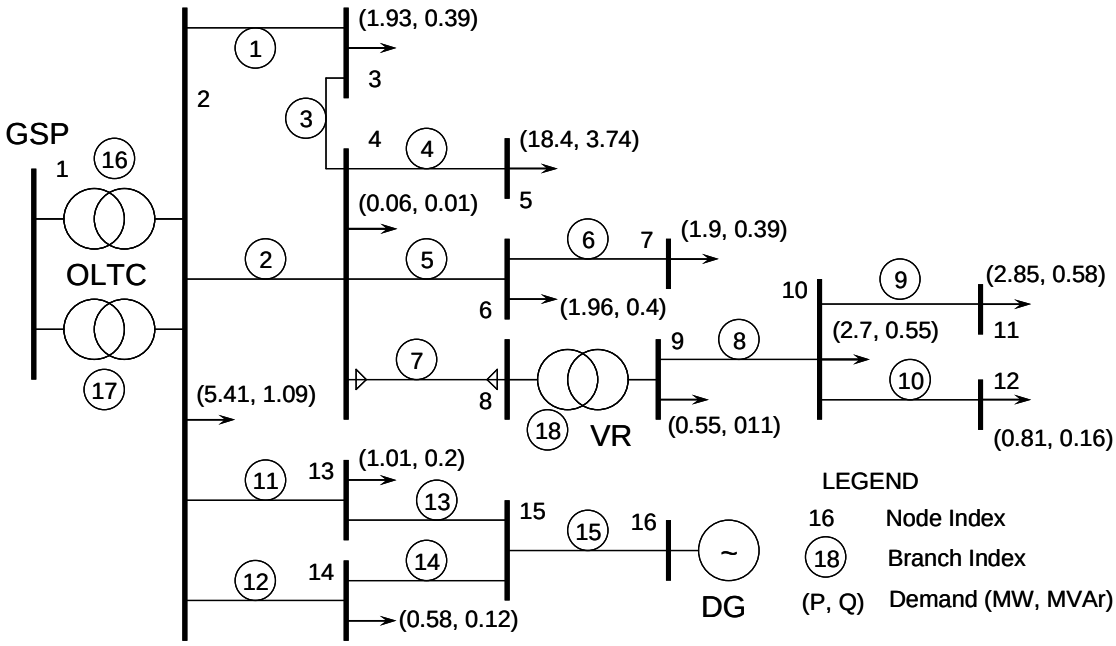

Figure 3.14: U.K. GDS simplified EHV1 – ANM network at maximum load [107]

A single DG development connected at bus 16 is a wind farm. In this analysis, the DG time series output is determined by the wind farm profile and the peak demand of the network (38.2MW) is scaled along the normalised variable demand pattern giving an annual demand of 217 GWh.

In the passive management case, referred to as 'fit-and-forget' the DG development has a firm installed capacity of 3.0MW, as determined by [59], the generator is operated with a constant power factor of 0.98 leading (capacitive) and the substation OLTC and the voltage regulator (VR) have a target voltage of 1.036 pu and 1.03 pu respectively on the secondary windings. The annual output from a 3 MW DG is 10.9 GWh, which is a capacity factor of 41.5%, with annual losses in the network of 7.95 GWh, corresponding to 3.7% of annual demand.

While it is noted that a 3 MW wind farm would, in most situations, not represent significant difficulty for distribution networks at this voltage level, in this particular network the location of the DG in relation to network loads presents significant challenges on the spatial voltage variation and limits network headroom significantly. With the peak demand level at bus 5 (18.4 MW) introducing substantial voltage drops along the upper section of interconnected distribution feeders, a high level of voltage compensation is required at the substation OLTC, and means imposing a high voltage

target at bus 2, which limits the available headroom for DG on the lower feeder section. On the lower section of network with comparatively low levels of demand (1.6 MW), the high voltage level defined at bus 2 is only marginally reduced through to the point of connection for the DG at the end of the feeder. This leaves only a small margin of permissible voltage rise with the export of power from the DG development and a significant restriction on capacity.

The (possibly exaggerated) voltage differential between the upper and lower feeders of this test case network highlights the difficulty of prescribing network control set-points to best suit the needs of all parallel sections of distribution networks with different demographics, making it an excellent demonstration case for the OPF technique proposed for wide-area management of ANM control concepts. The purpose of this network and the test case here, is to demonstrate the potential for new ANM techniques to improve distribution network operation in a clear and concise fashion before extrapolations to large and more complex networks with greater levels of new DG capacity and control, in which it is harder to visualise and interpret all actions of new ANM techniques to the un-informed reader.

For the purposes of this work, existing methods were explored to identify additional network headroom through ANM techniques. The contribution of [59] was to look at the coincident occurrences of generation and demand levels over a one year period and determine the maximum connectable capacity for variable generation under a range of ANM OPF schemes. Aggregation and uncertainty in the representation of generation, demand and network control settings in [59] is likely to incite difficulties in real time. A contribution of the work presented in the thesis, is to minimise the power curtailment of installed renewable DG developments and minimise the impact on real time network operation. The work of [59] was reproduced with a tighter voltage envelope constraint of ±5.5% and maximum annual curtailment limit of 10%. The tighter voltage envelope was chosen to reflect the would-be operating margins of the ANM OPF technique and the curtailment limit was considered to be an acceptable annual curtailment level, based on the balance of additional forced outages to renewable energy developments. An approximation of the results, shown in Figure 3.15, was then used to determine installed renewable DG capacity.

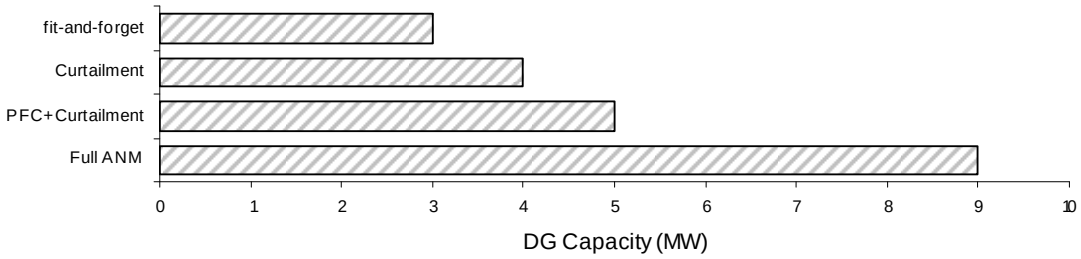

Figure 3.15: EHV1 – ANM network: connectable DG capacity

Figure 3.15 illustrates the potential for ANM techniques to increase the headroom capacity. With the integrated ANM concepts considered, the results show that the network headroom in this case could be as high as 9 MW. This is three times the capacity of the passive management scenario, achieving a penetration level of 563% relative to local feeder demand. Theoretically, annual energy yield could increase to approximately 30 GWh.

The implementation of ANM OPF techniques, specified in this work in real time, to minimise the real power curtailment is presented in this thesis.

3.8.2 UKGDS EHV1

Later in this thesis the real time ANM OPF scheme is extended to a larger more complex network. Evaluation of the real time system consequences from the proposed OPF techniques was conducted on the full EHV1 network under the variability of six DG developments from two renewable energy resources. The network model expands over two tiers of system voltage levels, 33 and 11 kV. The voltage regulation of the full EHV1 network is consistent with that of the simplified network with the added measure of OLTCs at the 33/11-kV distribution transformers. The full network also contains a 15-MVA rated interconnector, which is treated as a constant voltage source at 1.00pu. Prior to the connection of DG, the target voltage on the substation transformers secondary was 1.045 pu, while a consistent target voltage of 1.03pu was applied on all of the lower level distribution transformers.

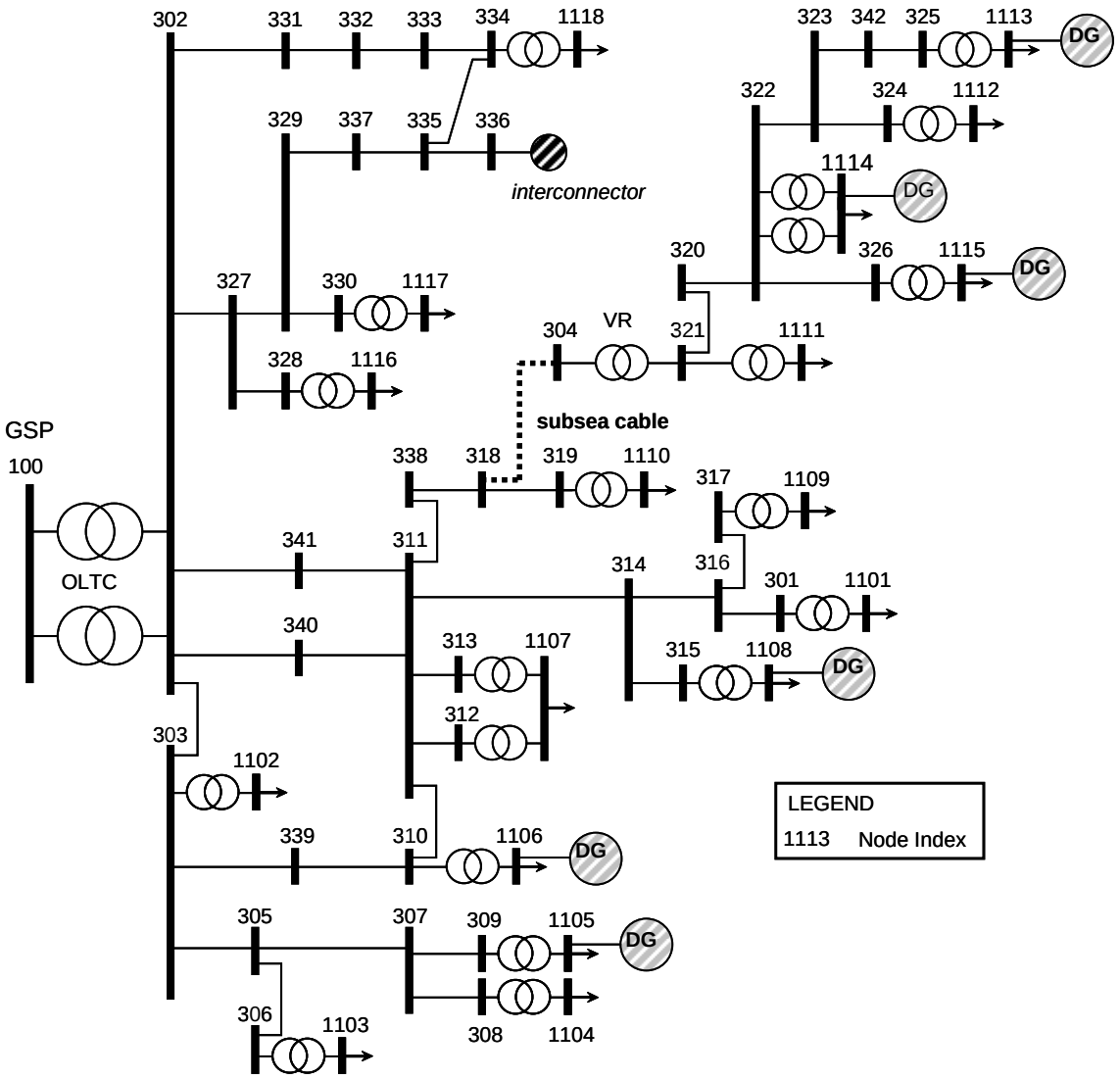

Figure 3.16: UKGDS EHV1 network [59]

Six DG locations were adopted, with two renewable energy technologies considered in two geographically chosen sectors. On the "mainland", wind farm developments were connected on buses 1105, 1106, and 1108. All three of these DG locations were considered to be in sufficient proximity to each other such that they follow the same generation output profile. A subsea cable (line 318-304) connects the "mainland" to an "island" on which three tidal generation sites were connected at buses 1113, 1114, and 1115. These were again considered in close enough proximity to enjoy the same resource pattern and follow the same generation output. Network profiles for load, wind and tidal energy resources are detailed in section 3.6.

Steady-state power flow studies at maximum and minimum (0.36 p.u.) demand conditions were performed to assess the state of the network prior to the integration of DG. Without any DG connected to the network, the steady-state simulations showed the voltage profile on the network to be low but within limits of supply quality. For the maximum demand case the voltage level on the network fell to 0.9433 pu at bus 304, the connection point of the island area to the mainland. On the 11 kV sections of the network, voltage level is held consistently at 1.03 pu by the OLTC capabilities of the 33/11-kV distribution transformers. With the same annual demand profile as the smaller EHV1 – ANM network, the losses in the demand-only case are 4.9%, which is again comparable with typical U.K. rural networks.

The maximum headroom for DG capacity at the adopted locations was again evaluated using the method of [59], with a tighter voltage envelope constraint and two different resources of renewable generation technologies and a variable demand pattern.

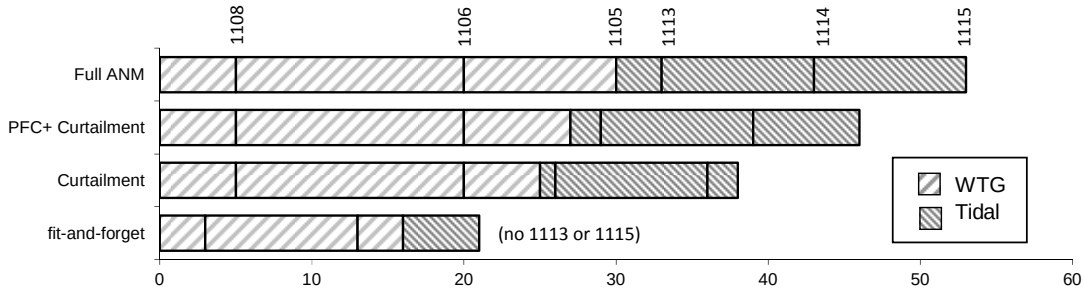

Figure 3.17: DG headroom capacity assessment of the EHV1 network

Given the higher number and large geographical spread of potential DG developments, high DG penetration levels were identified within this case study. For the BAU, 'fit-and-forget' approach, the analysis found that the DG penetration level was limited to 20.5 MW, 55% of system demand. With this approach, the active constraint on further DG capacity is voltage rise on the primary winding of the 33/11-kV distribution transformers connecting to the DG developments, with voltage differential between parallel distribution feeders being less of an issue as DG is present on the majority of network feeders and automatic voltage regulation measures in the form of OLTC, exist at the 33/11-kV distribution transformers on the remainder of the network extremes.

As illustrated by Figure 3.17, the implementation of progressively more liberal ANM strategies once again steadily increased the potential headroom for DG capacity. The initial provision of real power curtailment signified that for an anticipated annual curtailment limit of 10% headroom capacity of DG can be increased by 80% from the fit-and-forget level reaching 38 MW; 100% penetration relative to peak demand. With the addition of variable PFC and CVC strategies, the potential penetration level reached 53 MW, 139% of peak demand levels.

In the full ANM scenario, sections of the distribution system experience a widespread reversal of network power flows depending upon the prevailing supply and demand levels. The active constraint of further DG penetration was a combination of voltage rise and the thermal capacity limit on the 33/11-kV distribution transformers, at the point of DG connection, again depending on the prevailing supply and demand combination.

3.9 TESTING THE OPF ALGORITHM

Extensive testing of the OPF algorithm was conducted using figurative 'open-loop' trials for both test case networks. Studies were performed to determine the robustness of the ANM OPF techniques and their reliability for application in a real time closed loop environment.

In this subsection only the successive convergence properties of the advanced OPF formulations were tested. Therefore, only the time series of full ANM OPF solutions were simulated and not the specific power flow solutions. Validation of the OPF results and interpretation of the network impact is addressed in detail in the following chapters. Figure 3.18 illustrates the different time frames of the preliminary test simulations.

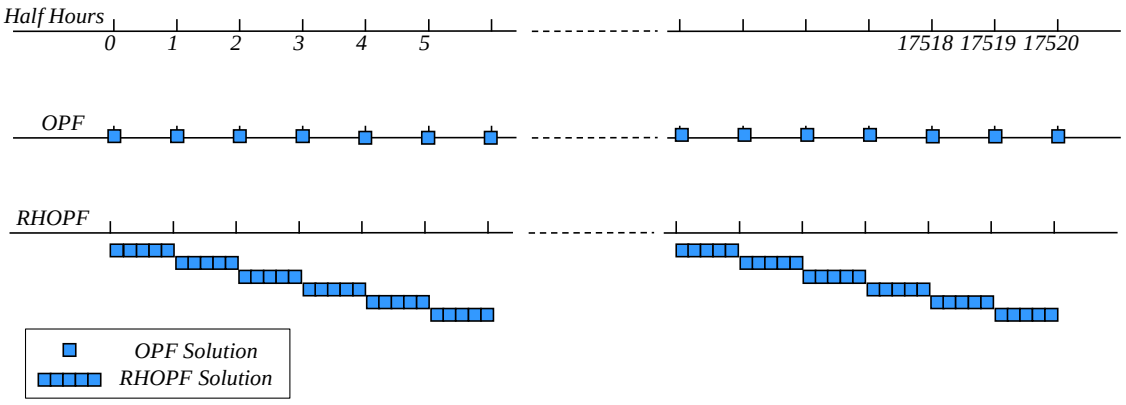

Figure 3.18: Time frame of OPF and RHOPF test simulations

Preliminary test runs of the OPF algorithm were conducted over a one year period at half-hourly intervals using the original time series of variable demand, wind power and tidal power production. Except for the initial solution, which begins from flat start conditions (i.e. global 1.00 pu voltage level at 0° phase angle and 'fit-and-forget' control settings), each successive OPF solution begins from the network control and state variables at the previous solution. The capacity of DG in each network case was the maximum penetration level at the adopted sites under all three considered ANM concepts (curtailment, variable PFC and CVC) as identified in section 3.8 (i.e. 9 MW in the simplified EHV1 – ANM demonstration network and 52 MW in the full EHV1 network). Like the capacity analysis in section 3.8, the real time ANM OPF is formulated with a tighter voltage envelope (±5.5%) than required by statutory regulation dictates (±6%). The OPF test runs were conducted for the full year with current network conditions at each time interval inferred from the last OPF solution. Successful convergence was observed for all formulations at each half-hourly time interval within a satisfactory short period of time. The speed of convergence is shown in Table VI and Table VII. The total time to complete each solution of the OPF algorithm includes the 'generation time' which is the time taken for AIMMS to generate the mathematical optimisation problem and the 'solution time', which is the time taken for the CONOPT solver to converge to a locally optimal solution. The simulations were conducted on a laptop computer with an Intel ® Core(TM) i5 processer and 3.42GB of RAM running a 32-bit version of the software packages.

Table VI: Convergence time for the simplified EHV1 – ANM network

Simplified EHV1-ANM	Generation Time (s)		Solution Time (s)		Total Time (s)	
	Mean	Max	Mean	Max	Mean	Max
OPF1	0.006	0.031	0.039	0.344	0.044	0.375
OPF2	0.004	0.047	0.031	1.203	0.035	1.250
RHOPF1	0.015	0.281	0.111	7.281	0.126	7.562
RHOPF2	0.015	0.266	0.109	10.907	0.124	11.173

Table VII: Convergence time for the EHV1 network

Full EHV1	Generation Time (s)		Solution Time (s)		Total Time (s)	
	Mean	Max	Mean	Max	Mean	Max
OPF1	0.018	0.047	0.115	1.109	0.133	1.156
OPF2	0.014	0.281	0.279	3.016	0.292	3.297
RHOPF1	0.056	0.344	0.471	10.000	0.527	10.344
RHOPF2	0.015	0.047	0.377	23.656	0.392	23.703

Convergence of the OPF over a finite control horizon, composed of multiple discrete time intervals, was conducted to assume convergence of the RHOPF formulation. In this much simplified analysis of the RHOPF algorithm was solved along a horizon of six successive 5 minute intervals, as illustrated in Figure 3.18, determined by linear interpolation across 17520 half-hours in the year. As each RHOPF solution returns new network set-points for six, 5 minute intervals, convergence was tested for 105,120 control cycles over the year.

Testing of the receding-horizon application, where successive multiple interval RHOPF solutions covering a half-hourly period were formulated every 5 minutes, as illustrated in Figure 3.19, would generate results for around 630,720 repeating control cycles, which was beyond the available memory in the distribution management element, MATLAB and therefore not conducted.

Results showed that the RHOPF algorithm successfully converges to an optimal state at nearly all 17520 half-hourly time horizons in the year and the total time taken to solve each solution is appropriate for application in a real time closed environment.

In the full EHV1 network the RHOPF1 formulation returned one instance where the OPF failed to converge and terminated in an intermediate non-optimal solution. In the RHOPF2 formulation the OPF terminated in this state on three occasions. On these occasions, successive iterations in the OPF solution returned a negligible change in objective function for a significant number of steps before terminating. This phenomenon resulted from poorly defined warm start conditions and was not apparent when repeating the OPF solution from flat start network conditions.

Solution time in the RHOPF formulations was expected to decrease significantly and is evident when applied properly in real time, where successive OPF solutions at 5-minute intervals have warm start conditions much closer to the previous solution, due to the smaller changes in generation and demand levels experienced between shorter time steps. Real time application of the RHOPF is shown in Figure 3.19 as an illustration of how successive solutions are much closer to the previous.

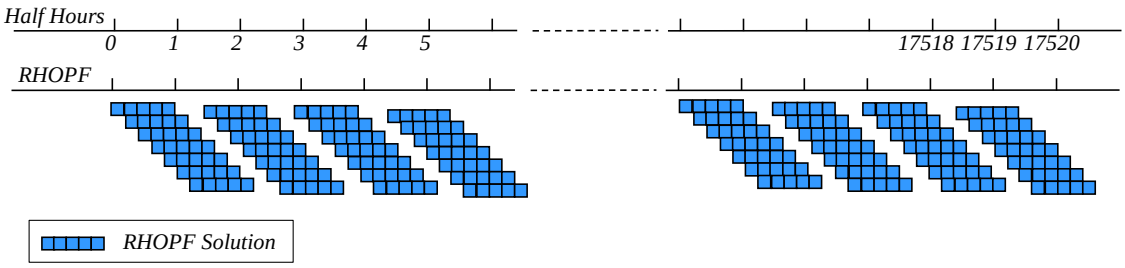

Figure 3.19: Time frame of full Receding-Horizon application test simulations

3.10 CHAPTER SUMMARY

This chapter presents the philosophy, formulation and implementation of a centralised ANM OPF technique to provide real-time, system control targets that better integrate DG from temporal and spatially variant renewable energy resource in the face of significant technical challenges and capacity limitations.

The scheme has been adapted here to function online as an ‘in-the-loop’ decision engine for prescribing active distribution network control set-points. A standard power systems OPF algorithm is customised to approximate new system functionality, based on active regulation of OLTC transformers, DG reactive power control and DG real power curtailment. The scheme provides a basis for the coordination of the real-time ANM options.

The OPF is formulated, externally to the power systems simulation, in the AIMMS optimisation environment. Solution architecture and a software environment have been developed to perform time-sequential power flow resolution simulating ‘real time’ network operation across progressive steady state intervals. The software environment is a suite of interconnected model elements used to emulate ‘real time’ network operation and the consequences of active network controls operating via commands from a distribution management system (DMS). Plug-and play of the OPF into the

software environment via the COM interface allows the OPF to be implemented ‘online’. The system provides the functionality required to assess the pseudo-real time implications and predict system consequences of varying power flow with active control strategies to manage the overall network response whilst continually optimising yield, asset and system response.

To proper formulate and successfully the ANM OPF model for each distribution network, requires accurate information on network topology, such as transmission line and transformer resistance, reactance and thermal capacity. Real time sampling of generation and demand levels is also critical. In order to implement a real time ANM OPF strategy of this type, greater levels of network sampling and higher resolution communication protocols than was previously available through existing standard SCADA systems is necessary.

For the purposes of short term forecasting, a stream of generation and demand forecast data is required. The advantage to the receding-horizon application, is that the resolution of this forecast data does not half to be as high or detailed as the real time sampling measurements.

In addition, this work only considers optimal network control set points based on technical grounds. However, the flexibility of the approach means alternative commercial arrangements and principles of access can be addressed in the same system models.

Chapter 4

Validation and Testing

4.1 INTRODUCTION

This chapter describes the simulation of distribution network behaviour, emulating the effects of the network operating and control practices in response to time-varying demands. It also investigates the system consequences of connecting larger volumes of intermittent and highly variable renewable energy generation to lower voltage networks. The effects of applying the proposed real time OPF techniques to various operating scenarios are explored.

In the previous chapter, the development of a simulation architecture and software environment was described with the ability to perform time-sequential power flow solutions simulating time series of network operation. The system demonstrated an ability to assess the real time implications and predict system consequences of varying power flow with active control strategies to manage the overall network response whilst continually optimising energy yield, through asset and system response. The ANM strategies, discussed in Chapter 2, are strongly recognised by the sector as an immediate and feasible part of the future distribution network operating principles. This chapter presents the results of testing and analysis of the real time network response to a set of progressively more active network control measures on the simplified EHV1 - ANM distribution network.

To validate the simulation environment and measure the network impact of DG subject to conventional passive control practices the network operation was first simulated; (i) without DG and, (ii) with a 3 MW fit-and-forget firm capacity DG added to a passive network.

Next, an increased level of DG capacity was connected with non-firm generation connections allowing the optimisation algorithm to dictate how much, or how little, real power curtailment was required to maintain statutory supply quality under differing power flow conditions. Active regulation of the DG power factor (PFC) and real time coordination of the existing network voltage regulation (CVC) were then introduced, with the OPF algorithm defining appropriate control settings in response to changing power flow. Operation of the ANM practices is described individually and collectively. For each additional ANM control variable, settings of the actual control mechanism were identified by the OPF and applied in the power flow solution of the distribution network.

Finally this chapter investigates the potential for new formulations of the ANM OPF methodology to improve the asset and system response, whilst continually optimising for energy yield. In total three formulations of the objective function were investigated and a new forecasting philosophy for determining control actions was tested.

4.2 POWER FLOW SIMULATIONS OF THE PASSIVE MANAGEMENT CASE

As a means of validating the simulation procedure and providing an assessment of the fit-and-forget approach, simulations were performed emulating normal passive management operation of the network prior to and after connection of the maximum possible level of firm DG. Steady state time sequential power flow solutions at five second intervals were performed as the 'proxy' distribution network in the software element, OpenDSS, illustrated by Figure 4.1, to demonstrate the control functions of the DG and OLTC, including time delays, deadbands and ramp rates. The resulting voltage levels and control operations are discussed.

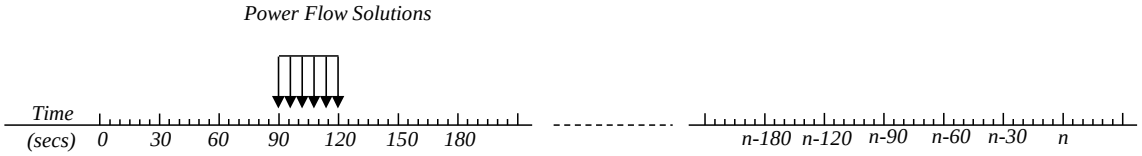

Figure 4.1: Power flow solutions time interval

4.2.1 *Simple Load Variation Without DG*

The network operation over two one-day simulation periods was simulated using the normalised load curves shown in Figure 4.2. The high resolution power flow analyses were conducted by linearly interpolating between the half-hourly intervals of the original time series data. The daily demand profiles depicted in Figure 4.2 correspond to load variation in central Scotland for a winter weekday, Wednesday 17 February 2003 (Case 1) and a summer weekend, Sunday 17 August 2003 (Case 2). The loads applied at each time-step are the values of this normalised load curve multiplied by the maximum value of the real and reactive power demand at each bus as discussed in section 3.6. The power factor of each network load was 0.98 lagging.

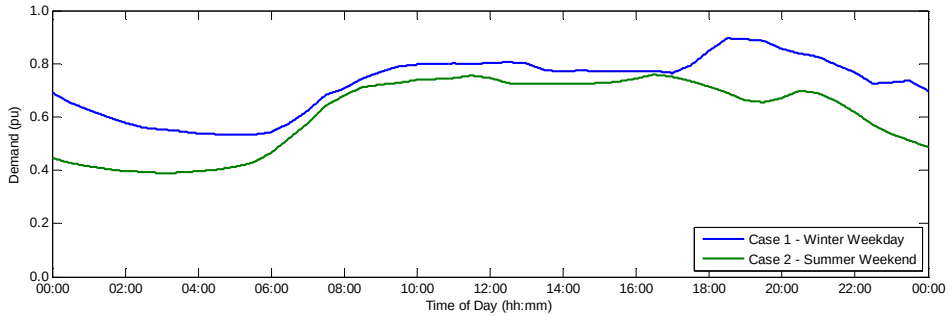

Figure 4.2: Daily demand patterns

The network cases were initialised with the pre-existing control settings at the first time step of all simulations. The passive management simulations were executed with the pre-existing voltage targets of 1.036 pu and 1.03 pu on the substation and voltage regulating transformers respectively. The deadband of each transformer's voltage regulating system was not supplied with the network data, therefore appropriate values were chosen to simulate coordinated network operation. The time delay for the substation OLTC was set at 45 seconds, while the time delay for the VR tap-changing was set at 90 seconds [70]. This staggered actuation of transformer tap operations, reflecting standard network practice, ensures that control actions occur at the first instance of voltage excursion arising from the injection of power to prevent additional unnecessary tap operations. In addition, the OLTC capabilities of the substation and voltage regulating transformers were modelled with a deadband around the target voltage where no action is taken. In this case, there is a 0.625% voltage change per tap

for each transformer and the deadband at the substation and VR transformers was 1.05% and 1.25% respectively; between 1.7 and 2 times the tap increment. This range of no action prevents hunting, where the transformer oscillates between two tap settings that both result in a voltage excursion on either side of the voltage target.

For Case 1, the 24 hour Winter Weekday simulation, the network demand was recorded at 662.9 MWh, 134.5 MVArh where the network experienced losses of 27.1 MWh and 44.2 MVArh. This resulted in an experienced system load at the GSP of 690.0 MWh and 178.7 MVArh, with real power losses accounting for 3.93%. The maximum and minimum observed voltage levels were 1.045 pu and 0.9488 pu.

For the Summer Weekend simulation, the network demand was lower at 561.7 MWh, 113.9 MVArh with losses of 19.6 MWh and 26.6 MVArh, resulting in a detectable system load at the GSP of 581.3 MWh and 140.6 MVArh. Here, real power losses account for 3.37% of the total real power supplied by the GSP. This is broadly as expected as losses are proportional to the P^2+Q^2 and have changed accordingly.

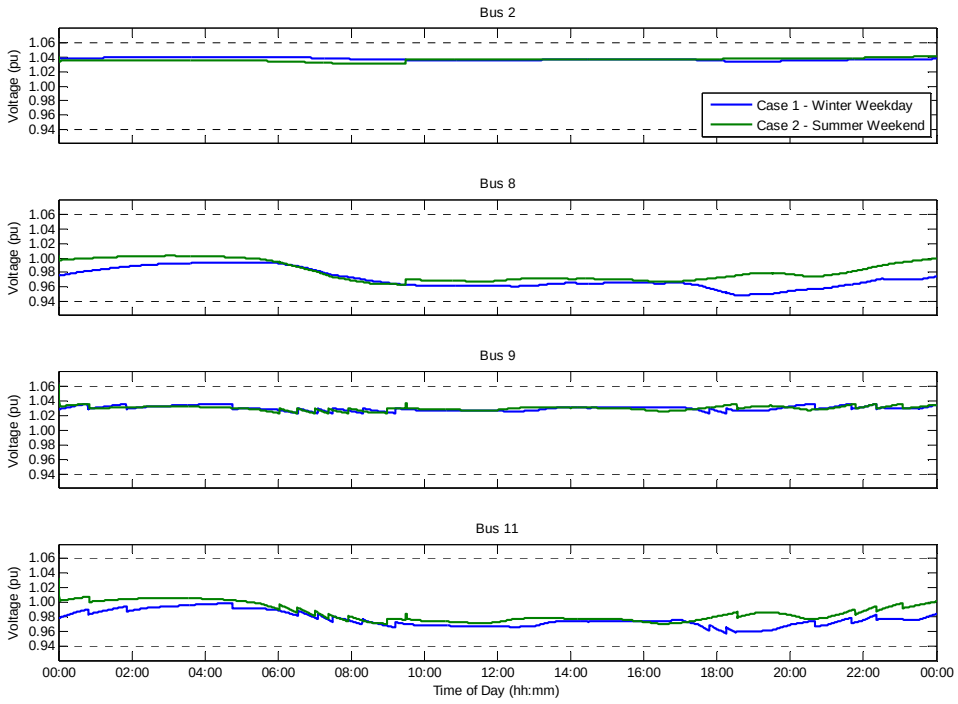

Figure 4.3: Voltage profiles for simple load variation with no DG

The voltage level at each bus in the network was observed over time. Figure 4.3 shows the voltage level variation at strategically important system buses; chosen to demonstrate the network control settings and those whose variation leads to greatest constraint on network operation. Utilising a fixed power factor load model, as expected, it is shown that increasing loading levels results in a steadily increasing voltage drop between the substation transformer and the far end of the distribution feeders. In the demand-only network state, the voltage profiles shown illustrate that the system remains within the ±6% statutory limits of regulation.

At buses 13 and 14 very little voltage variation was observed due to the relatively small magnitude of peak demand (1.6 MW) and close electrical proximity to the substation transformer. With no DG connected at bus 16, buses 15 and 16 (also having no load connected) were disconnected, in this simulation.

A large variation in the recorded voltage was observed throughout the test case observation period for the rest of the network. The relatively large power demand at Bus 5 (18.4 MW) brings about a substantial transfer of power between the GSP and bus 5. This causes a significant drop in system voltage level across the intervening network infrastructure. The large voltage drop between Bus 2 and Bus 4 makes the relatively high pre-set voltage setting of 1.036 on the OLTC, regulating at Bus 2, necessary to ensure the voltage level remains above the minimum statutory limit along all distribution feeders. The lowest point in the network voltage profile occurs at Bus 8, just prior to the voltage regulating transformer at the end of the subsea cable.

Between the secondary winding of the voltage regulating transformer and the distribution feeder ends the long line lengths and relatively large impedances of the lines and transformers result in a further significant voltage drop. Although not as severe as the preceding voltage drop, a high target voltage on the voltage regulating transformer secondary is still necessary.

Inspection of the recorded voltages in Figure 4.3, shows that the voltage at Bus 2 experiences little variation from the target and, from inspection of the tap position trace in Figure 4.4 confirms little intervention from the OLTC capabilities to maintain the pre-set voltage level. At buses 9 and 11, the sharp changes in the voltage level correspond to the tap operations shown in Figure 4.4. Here the voltage regulator is

performing tap operations to maintain pre-set voltage targets as the real time voltage levels vary with changing demand.

In Figure 4.4 the tap position on the primary winding of the network transformers are plotted against time. Because the tap operations occur on the primary winding of the transformers, voltage modification is achieved through inverse modulation of the tap positions. For example, a primary winding tap position of 1.00 would not perform any modulation of the per-unit voltage level across the transformer. Primary winding tap positions of less than 1.00 would, in effect, 'tap-up' the per-unit voltage level across the transformer resulting in a proportionally greater per-unit voltage level on the secondary than the primary winding, with the opposite occurring for primary winding tap positions greater than 1.00.

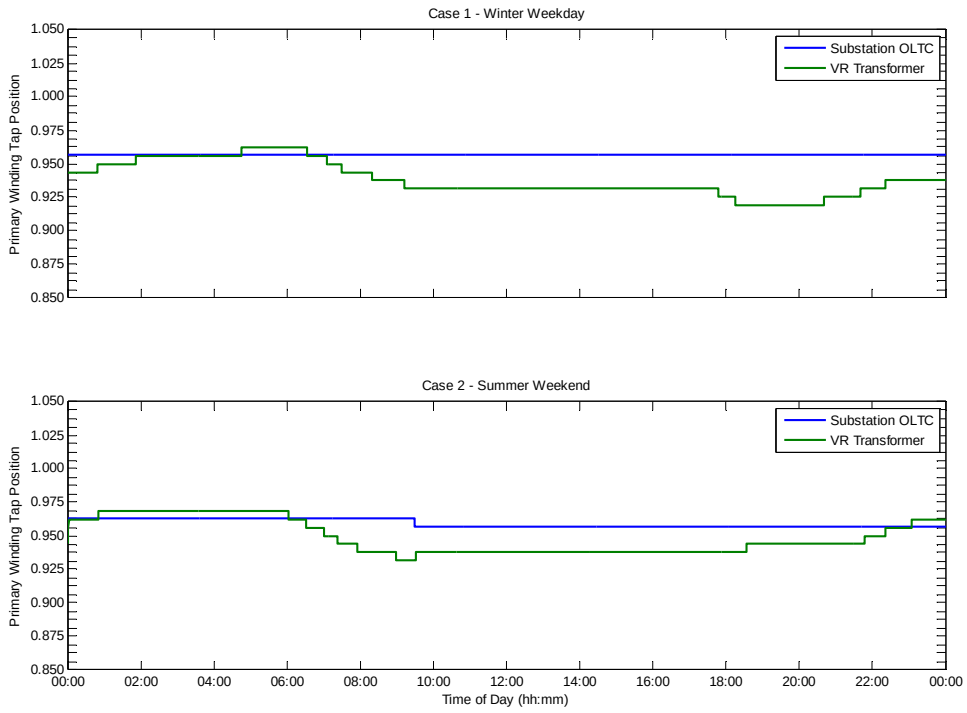

Figure 4.4: Tap positions for the no DG case

Figure 4.4 shows tap operations of the voltage regulator following a pattern that reflects the change in system demand throughout the day. Minimum demand in the early of hours of the morning corresponds to the period of lowest tap deviation from nominal (1.00) and minimum voltage correction, whereas peak demand in the evening of the

Winter Weekday simulation corresponds to maximum voltage support and the lowest primary winding tap position.

4.2.2 FIT-AND-FORGET DG

With the fit-and-forget approach, DG connected to the network at Bus 16 has a maximum installed firm capacity of 3.0 MW, as determined in section 3.8.1, which is approximately twice the peak local demand level (1.6 MW) on the connecting feeder. Standard UK practice when connecting renewable DG to distribution networks normally means DNOs will stipulate that the DG development is operated with the generator at a fixed power factor (or within a specific narrow range). In this manner, the network continues to operate as previously simulated with the substation and voltage regulator tap changing transformers maintaining voltage targets of 1.036 pu and 1.03 pu respectively on the secondary windings. The generator is connected and operated with a fixed power factor of 0.98 leading (capacitive). This power factor was chosen to reflect the power factor of the adjacent network loads, such that there is a proportional variation of both real and reactive power evident in the network and does not upset greatly the circulation of reactive power. In this scenario, the underlying principle of the DG connection is that the DG is considered to operate as negative load and does not alter or degrade any of the existing network control settings.

The simulations were repeated utilising the same daily load profiles of the case 1 (Winter Weekday) and case 2 (Summer Weekend). Concurrent levels of DG production at each time step were determined by the normalised wind power output profile, introduced in section 3.6, multiplied by the firm DG capacity. Again, high resolution power flow solutions were conducted by linearly interpolating between the half-hourly intervals of the original time series data. Normalised DG production levels for the test case periods are illustrated in Figure 4.5.

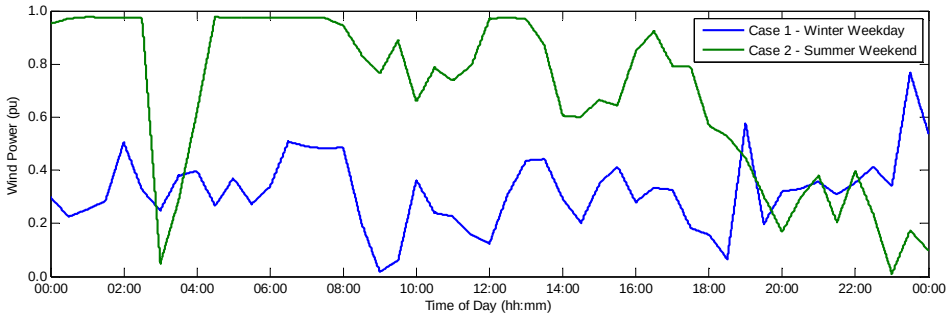

Figure 4.5: Daily wind power generation patterns (normalised)

In this scenario, buses 15 and 16 were no longer disconnected, and experience a high injection of real and reactive power from the DG at the far end of the feeder resulting in an inverted voltage gradient. With the high substation target voltage, and negligible voltage drop between buses 13 and 14, the window available for voltage rise around the DG was severely limited, as illustrated by the variation in voltage profiles observed in Figure 4.6 and Figure 4.7. The peak voltage level, which is the active constraint on the hosting capacity of the DG development, was recorded at 1.0588 pu. In this instance, at the beginning of the Summer Weekend test case period (Case 2), the low demand level occurs simultaneously with near maximum DG production, illustrating well that the operating margin for voltage rise has been fully exploited in the fit-and-forget approach to DG connections.

The addition of the DG had next to no effect on either the voltage profile of the remainder of the network and no adverse impact on the network control operation. Figure 4.8 shows the tap position trace for the fit-and-forget connection.

For the fit-and-forget arrangement, the 3 MW DG produces 23.1 MWh (4.7 MVArh) of energy during a representative period of average production depicted by the Winter Weekday case (Case 1), and 49.4 MWh (10.0 MVArh) over the period of high DG production (Case 2); Summer Weekend. This transpires to capacity factors of 32% and 68% respectively.

The total percentage of perceived network losses, that is the ratio of measured losses to the energy sourced through and detectable at the GSP, increased to 4.1% and 3.8% in case 1 and case 2 respectively. One criticism of recording network losses in this manner

is DG production displaces detectable demand at the GSP and inflates the perceived system losses. Energy losses increased by 0.1 MWh in the moderate DG, high demand scenario of case 1 and by 0.8 MWh in the high DG, low demand scenario of case 2.

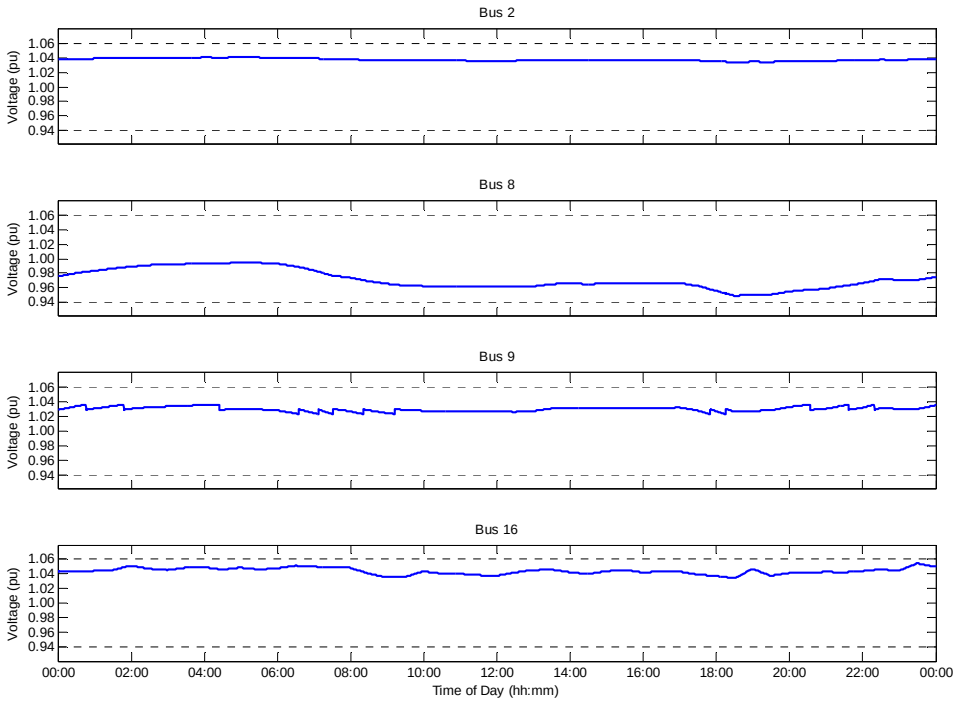

Figure 4.6: Voltage profiles for the fit-and-forget 3 MW DG case 1

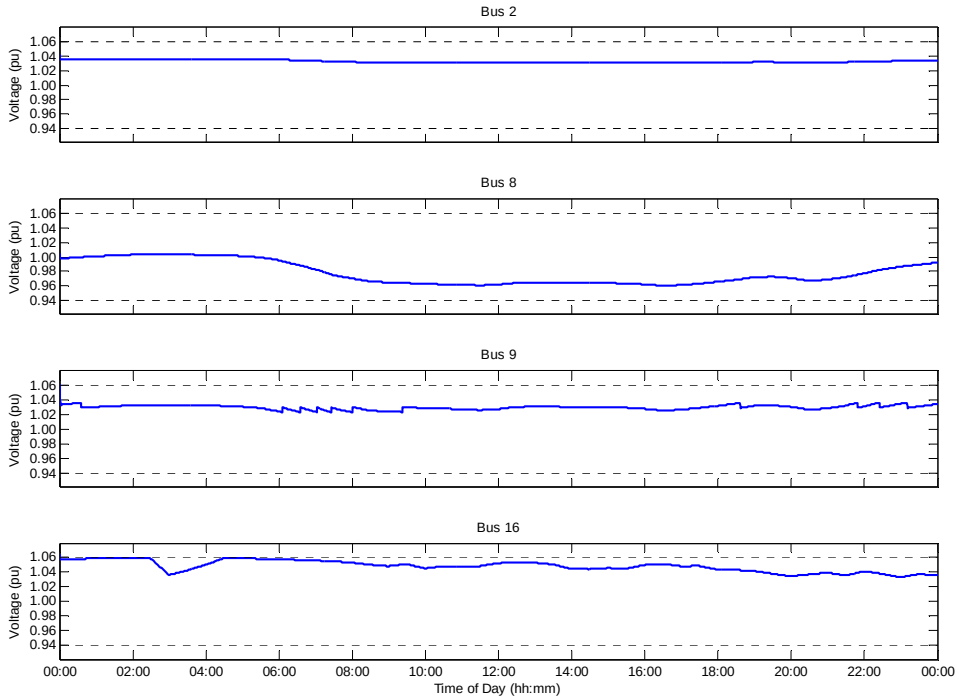

Figure 4.7: Voltage profiles for the fit-and-forget 3 MW DG case 2

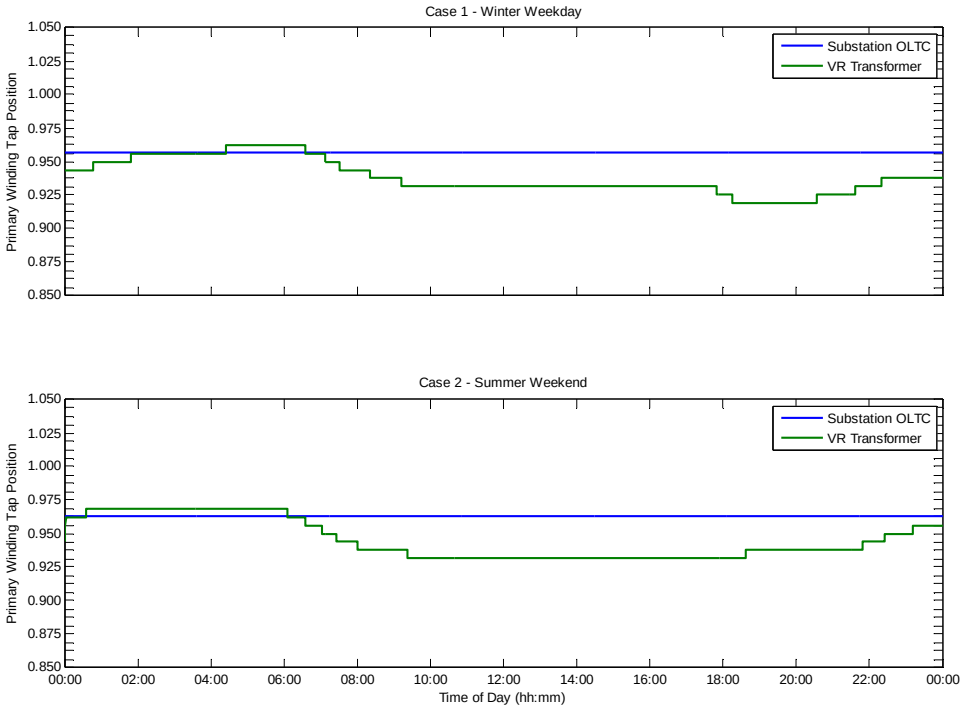

Figure 4.8: Tap positions for the fit-and-forget 3 MW DG

4.3 POWER FLOW SIMULATIONS WITH ENERGY CURTAILMENT OPTIMAL POWER FLOW

The proposed ANM OPF technique was then investigated on the network to assess its effectiveness for improving the network hosting capacity and renewable energy capture by alleviating network constraints. Results allow examination of the behaviour of a real time centralised ANM scheme with variable load and generation patterns. The optimisation algorithm was set up to assume, progressively, control of the wind farm DG set-points as well as pre-set voltage targets of the tap changing transformers. The initial simulation and performance assessment was conducted for the same 24 hour test periods and 5-second time step as before. The real time OPF technique is now implemented to determine and schedule network set-points at 5 minute intervals in order to increase the hosting capacity and energy yield from the renewable DG development. An illustration of the new OPF control cycle with respect to the time sequential power flow solutions is illustrated in Figure 4.9.

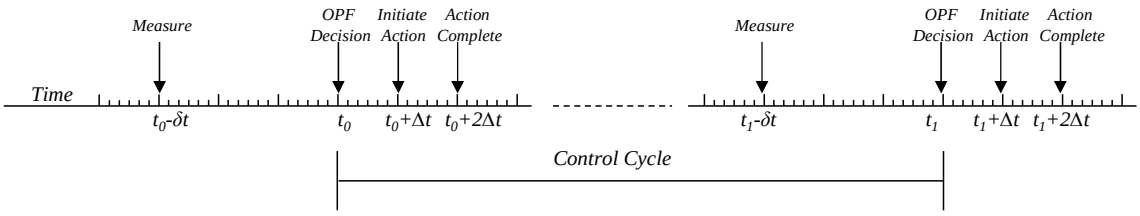

Figure 4.9: ANM OPF control cycle

Figure 4.9 also illustrates the notional network time delays. These include a 90 second (δt) aggregation, communication and processing delay between the real time data measurements, retrieved from the proxy distribution network and the scheduled OPF decision, as well as a 30 second (Δt) communication delay after the OPF decision and a 30 second (Δt) period of generator ramping for changes to the DG power point setting. As discussed in section 3.8, the voltage level constraint in the OPF formulation was restricted to ±5.5%, as opposed to ±6% in the UK legislation, to provide a conservative operational margin and mitigate minor deviations in real time voltage levels.

4.3.1 CURTAILMENT

The primary mechanism of increasing the hosting capacity of distribution networks is for the DG developer to opt-in to an actively managed real power curtailment scheme, where additional generator capacity can be accommodated on the network by accepting the need to curtail generator production during periods of problematic power flows. The OPF techniques were devolved the responsibility for controlling the generator, resource-dependent, real power production level in order to maintain the voltage within statutory limits under differing power flow scenarios. The optimisation was formulated with the minimise energy curtailment objective (OPF1) using the persistence forecasting method discussed in section 3.7, where $j = 1$.

OPF1:
$$Min \sum_{g \in G} p_g^{curt}(k+j|k) \tag{35}$$

With the existing fixed voltage targets on the network tap-changing transformers and the DG continuing to operate at a fixed capacitive power factor, the DG capacity was increased to 9 MW, close to six times the local peak demand level on the connecting feeder. The two 24 hour test cases from above were re-run and the results are discussed below.

With the additional DG capacity, an energy yield of 56.6 MWh, 245% of the fit-and-forget energy yield, was produced over the Winter Weekday observation period (Case 1). A further 12.7 MWh, 18.3% of the possible energy production, was curtailed under the prescription of the OPF technique as shown in Figure 4.10. In Figure 4.10 (top) the normalised control signal is specifying the maximum per-unit production level of the DG, capping in real time the power output from the wind farm to the corresponding value of maximum capacity. This results in the power production profile seen in Figure 4.10 (bottom). Note that in Figure 4.10 (bottom) there is a trend for the optimisation to curtail production above the 3 MW headroom capacity limit identified by the fit-and-forget case.

A similar trend is more clearly evident from the Summer Weekend observation period, with nearly all generation output above the 3 MW limit curtailed by the OPF technique. In this instance, DG production was recorded at 59.2 MWh, a modest increase of 20% from the fit-and-forget energy yield.

With peak localised demand along the distribution feeder containing DG around 1.6 MW, and prolonged periods of generator output at approximately twice that magnitude back up the feeder, increasing network power flows will inevitably lead to higher losses in the system, as observed from the increase in the fit-and-forget approach. Based on the detectable system demand at the GSP the percentage of net system losses increase to 4.4% and 3.9%.The actual increase in network losses from the fit-and-forget cases was 0.6 MWh and 0.2 MWh for each test case. This equates to a 2.16% and a 0.97% increase respectively.

In order to validate the application of the real time OPF technique, a review of the curtailment measures instigated were plotted alongside the binding constraint on power production which, like the fit-and-forget case, was voltage rise at the point of DG connection, Bus 16.

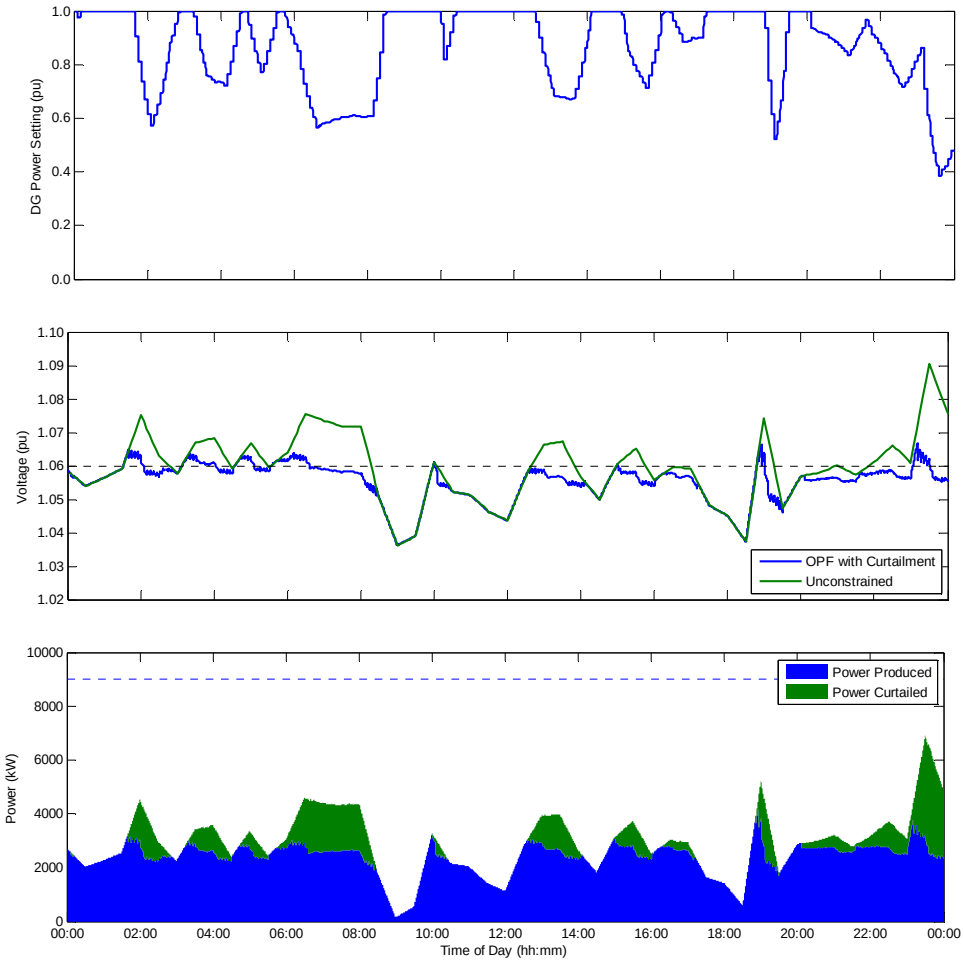

Figure 4.10: Curtailment settings, voltage levels and power output for the OPF technique with curtailment case 1

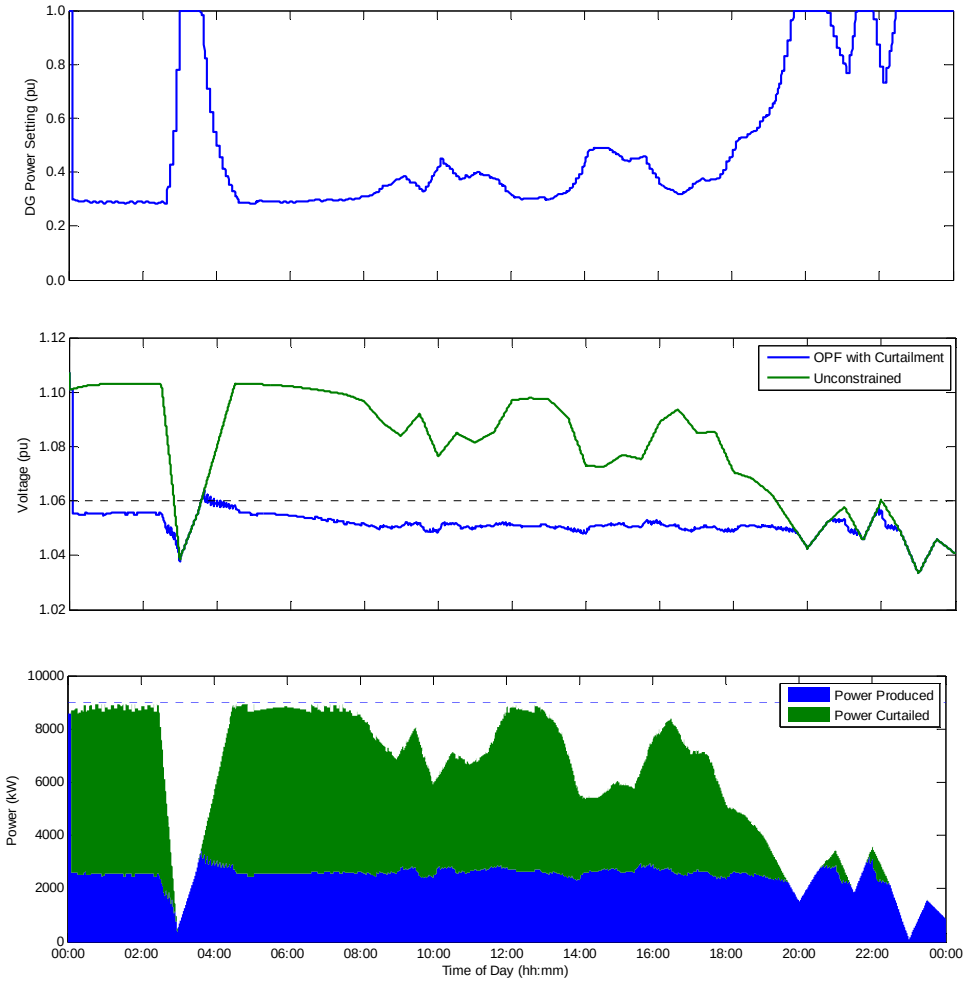

Figure 4.11: Curtailment settings, voltage levels and power output for the OPF technique with curtailment case 2

Figure 4.10 (middle) and Figure 4.11(middle) compare the time-varying voltage level at Bus 16 for the unconstrained case against the optimally prescribed levels of real power curtailment. In both instances it is evident that the OPF technique is actively prescribing maximum power production levels, when required, to curtail power production and prevent violation of the statutory voltage limits.

An interesting effect appeared between the converged OPF solutions and the power flow solutions of the distribution network. In Figure 4.10 (middle) it is possible to see a number of incidents of voltage excursion just above the 1.06 pu upper voltage limit. Also in Figure 4.11(middle), there appears to be levels of curtailment which exceed the

amount required to prevent voltage rise beyond the statutory limit. Closer inspection of the results revealed that fluctuation of the voltage level on Bus 2, critically, within the control deadband of the voltage regulating transformer leaves residual variability in the voltage level in the proxy network simulation not visible to or addressed by the OPF formulation. In Case 1, the voltage level at bus 2 was slightly higher than the target set-point resulting in a situation where DG curtailment was not sufficient to maintain the voltage level at Bus 16 strictly below the 1.06 pu limit at all times. The opposite scenario is witnessed for the majority of the time in Case 2, where the voltage level at Bus 2 is slightly less than the prescribed target voltage and as such the OPF is prescribing levels of curtailment slightly greater than was required to reduce the voltage level at Bus 16 below the threshold. There are a number of measures, such as the collaboration of the OPF with localised distributed automatic control systems, which are reported later in this thesis that can be deployed to resolve this issue.

The peak voltage level observed throughout both 24 hour simulation periods was recorded at 1.0666 pu. This occurred at the end of the (manufactured) 30 second communication delay between the OPF and DG control systems, as discussed in section 3.3, and during the sharp rise in wind resource level at the end of the first test case. In the following 5-second time step the DG control system initiated a corrective control action which reduced the voltage level to 1.0617 pu after the ramping period of the generator. In total for the observation period, the extent of voltage violations was recorded at 15.7% sampled at 5-second time intervals for the Winter Weekday and 1.1% for the Summer Weekend test case. Temporary over-voltage excursions of this magnitude are not in their occurrence a significant problem to DG integration. However, the duration and frequency of minor voltage excursions may be a cause of concern. The European Standard EN 50160 on Voltage Characteristics on Power Distribution Systems [108] recommends that voltage levels measured at 10 minute averages must comply with statutory voltage levels for 95% of a sample observation period, typically one week. In this analysis the total over voltage excursion at bus 16, measured in 10-minute averages, was 15.97% in case 1 and 1.39% in case 2. This averages out to a total overvoltage excursion over a non-continuous 48 hour period of 8.68%, which is not compliant with the EN 50160 recommendation.

In addition to the residual voltage variation, the use of persistence forecasting as a means of determining the real time power flow injections for the OPF formulation, has the potential to increase the imbalance between the OPF solutions and the power flow solutions of the distribution network. In this instance, while the use of persistence forecasting over a 5-minute control cycle shows only small magnitudes of change between time steps, when solving to the tight system boundaries, even small disturbances can introduce measurable negative effects such as moderate voltage excursion as seen in Figure 4.10 (middle) and Figure 4.11(middle).

As expected in this scenario, the remainder of the network was unaffected by the application of the OPF with the pre-existing control regime in the parallel distribution feeders retaining a consistent voltage profile, and the use of on-load tap changers remaining largely unchanged, as illustrated in Figure 4.12.

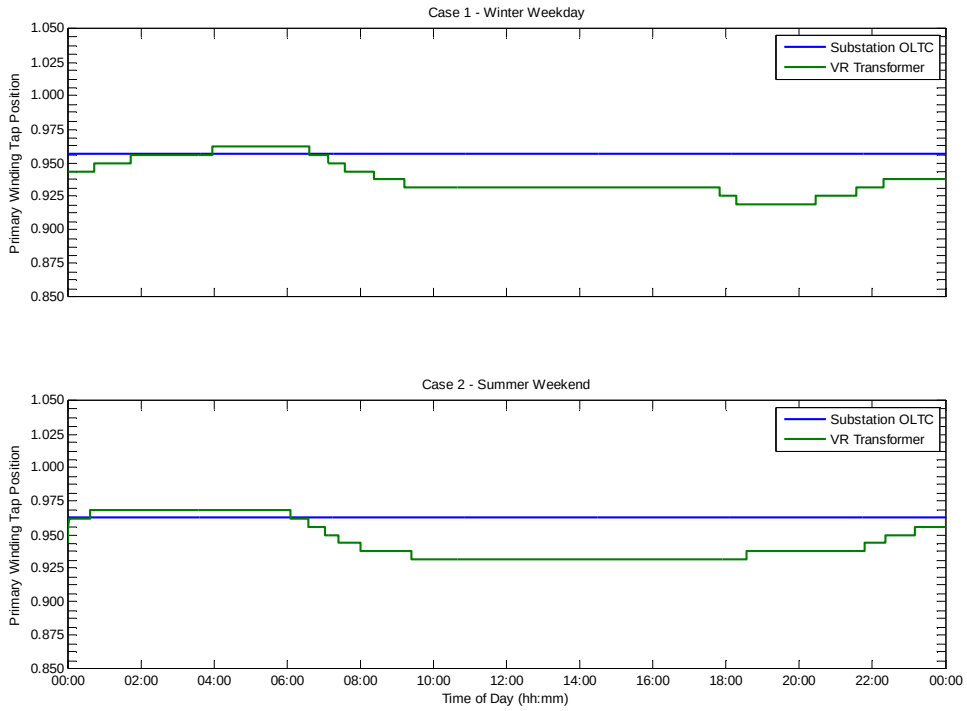

Figure 4.12: Tap positions for the OPF technique with Curtailment

If the capacity of the DG development was better suited to reflect the curtailment only scheme (i.e. significantly reduce the annual levels of prescribed curtailment) then this would pose a very attractive economical and technical alternative to network

reinforcement, although the use of an OPF technique to determine real power curtailment settings for a single feeder with a single DG development could be considered overkill. The added value from the use of a real time OPF technique comes with the ability to determine control configurations for multiple ANM systems that have consequences over a wide network area. In the following sections additional ANM systems are added that justify the use and display the benefit of the OPF techniques presented in this thesis.

4.3.2 Adaptive Power Factor Control And Energy Curtailment

The use of coordinated, real time prescribed power factor or DG voltage control techniques can provide better resolution of network constraints such as voltage rise and thermal capacity limitations than energy curtailment alone; reducing the necessary levels of consequent curtailment and improving the energy yield.

Continuing with the 24 hour example periods utilised before, the simulations were repeated with the OPF able to prescribe a variable PFC set-point in addition to the provision of real power curtailment.

$$\phi_g^- \leq \phi_g(t) \leq \phi_g^+ \tag{42}$$

In the OPF formulation, the generator power factor angle is considered a free variable within bounds. The boundaries of operation were set so that the range of variable power factor control was limited to 0.98 leading and lagging. The optimisation objective and the single scenario, persistence forecast, horizon were continued as before.

In both test cases after the first OPF solution, the generator power factor reverted to a 0.98 inductive power factor, where it remained for the duration of the simulation periods. At the point of connection, the linear relationship between real power production and voltage rise was modified, with occurrences and severity of voltage rise reduced. This resulted in a reduction in the amount of real power curtailment and an increase in energy yield over time.

In Case 1, the energy yield increased 18% from the curtailment only scenario, rising to 66.5 MWh. This was 96% of the available energy, with only 2.8 MWh of energy curtailed. During the high resource availability of the Case 2, energy yield increased 38% from the curtailment only scenario, rising to 81.7 MWh or 55% of the available

energy. Figure 4.13 and Figure 4.14 show the time series profile of wind power production and curtailment over the simulation periods.

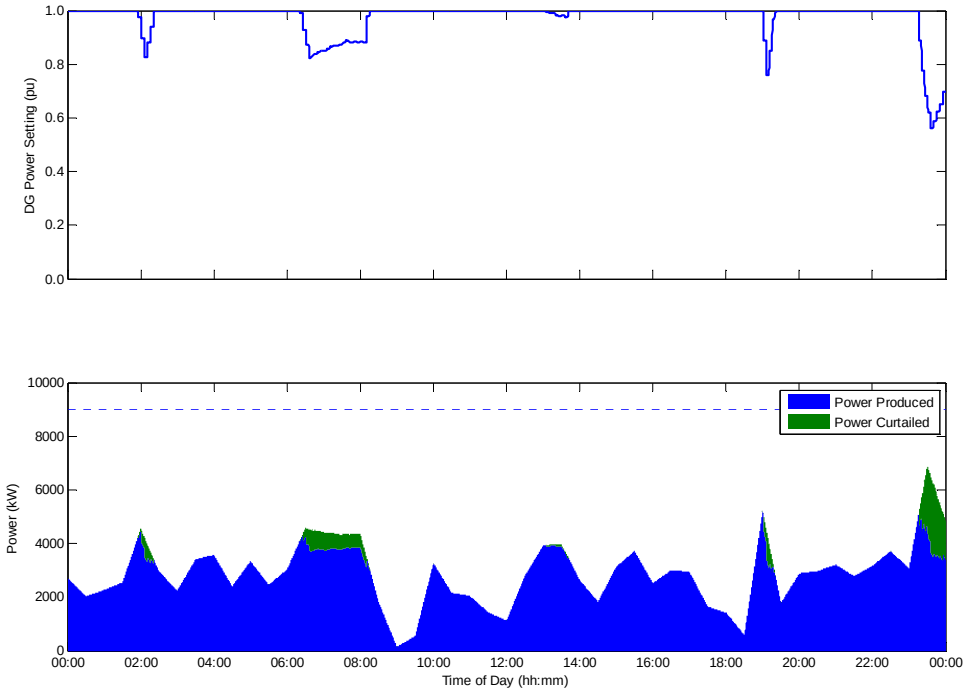

Figure 4.13: Curtailment settings for the OPF technique with PFC + Curtailment case 1

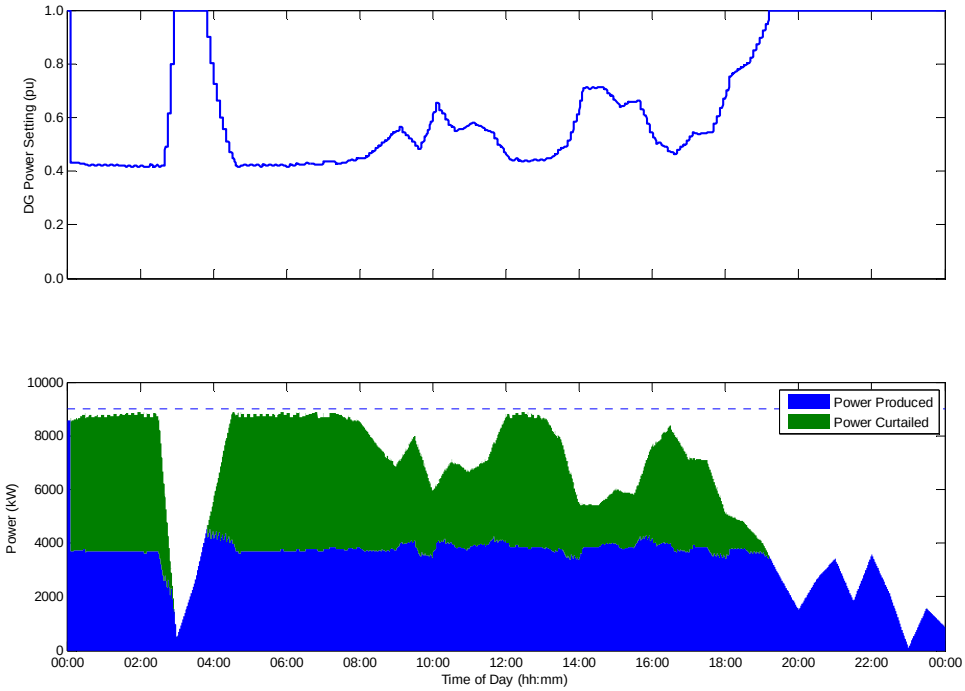

Figure 4.14: Curtailment settings for the OPF technique with PFC + Curtailment case 2

The dominant effect that limited the maximisation of energy yield remained voltage rise at the point of DG connection. One prominent advantage observed with the variable PFC scheme was the significant reduction of minor voltage excursions at the point of connection. Closer inspection of the voltage level at Bus 16 showed most of the simulations settling within the voltage envelope, as demonstrated in Figure 4.15 and Figure 4.16. Excluding the initial state of the Case 2, before the OPF technique was enabled, voltage violations were recorded (in 5 second intervals) for 1.8% of the combined observational period, all occurring during the Winter Weekday Case 1 period and exhibiting a peak recorded voltage of 1.0618, which again occurred at the end of the communication delay prior to the initiation of corrective control measures.

Network losses based on the changing system power flows continued to rise. Due to the additional energy production from the DG, net system demand, as detectable at the GSP, was recorded at 624.7 MWh and 501.4 MWh, network losses were recorded as 4.5% and 4.3%. The actual magnitude of observed system energy losses was 28.3 MWh and 21.4 MWh, which corresponds to a 4% and 5% increase. Based on the original detectable system demand in the fit-and-forget case, the increase in system losses was

only 0.16% and 0.19% respectively in each case. This suggests that the increase in network losses may not be as significant as first thought. The inductive operation of the DG does however increase the reactive power demand on the network. With the generator now consuming 13.4 MVArh in case 1 and 16.3 MVArh in case 2, the reactive energy demand at the GSP was increased to 189.2 MVArh, and 154.3 MVArh respectively, up 9.7% and 19.8% from the fit-and-forget cases. A graphically comparison of the time dependent changes in the reactive power sourced through the GSP for both cases in the no DG, fit-and-forget and PFC + Curtailment analysis is shown in Figure 4.18. The net effect on the overall distribution network power factor was not significant, with GSP power factor dropping just below 0.96 lagging in each test case, this is due partly to narrow range of power factor adopted for the variable PFC control settings.

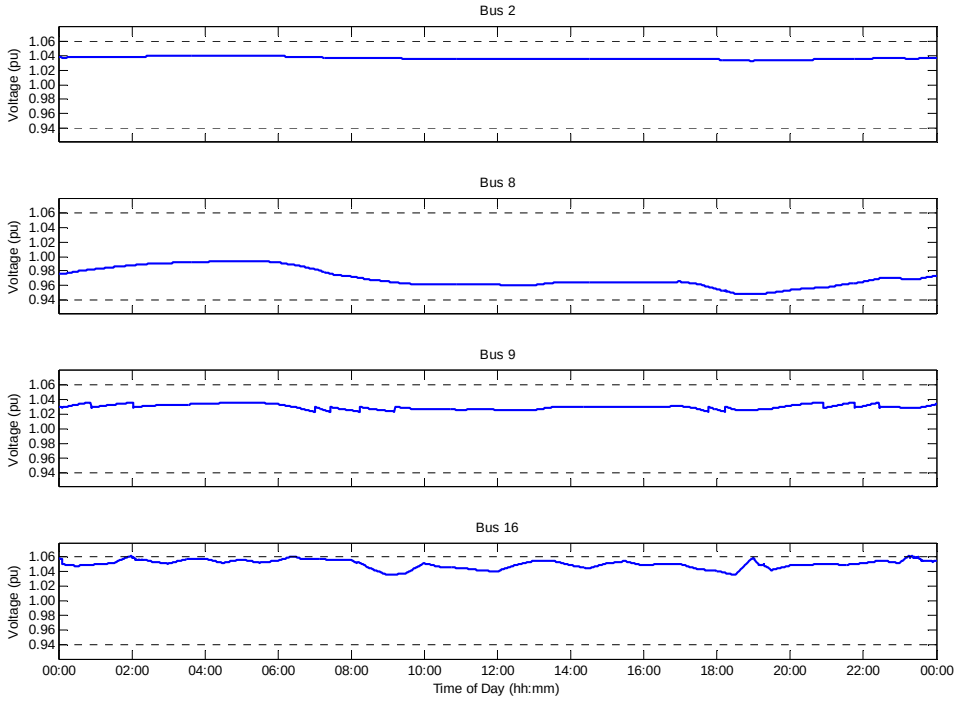

Figure 4.15: Voltage profiles the OPF technique with PFC + Curtailment case 1

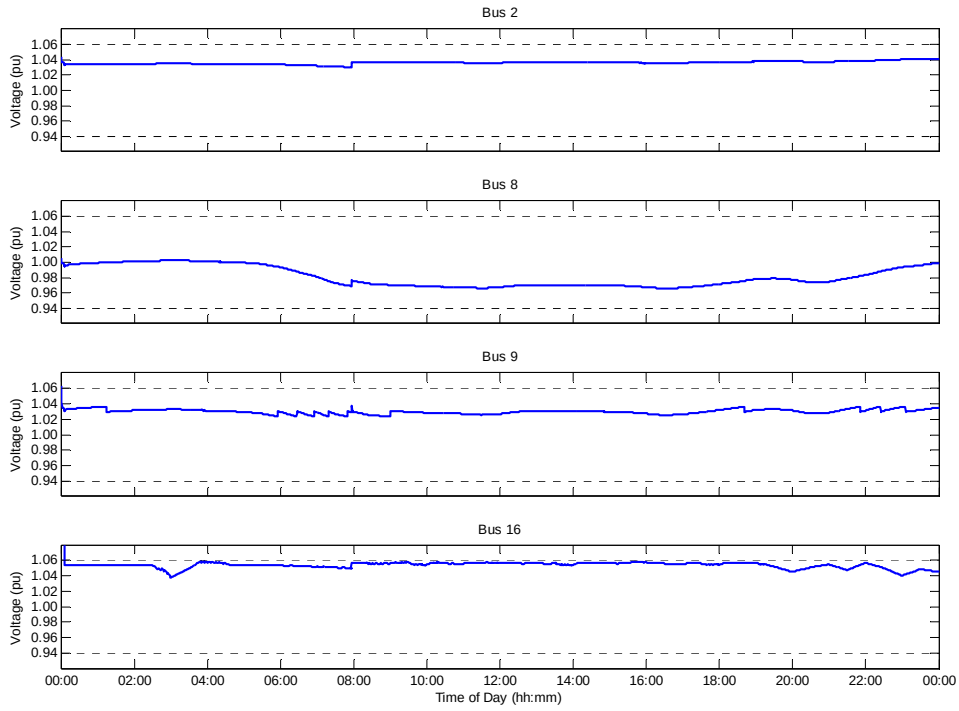

Figure 4.16: Voltage profiles the OPF technique with PFC + Curtailment case 2

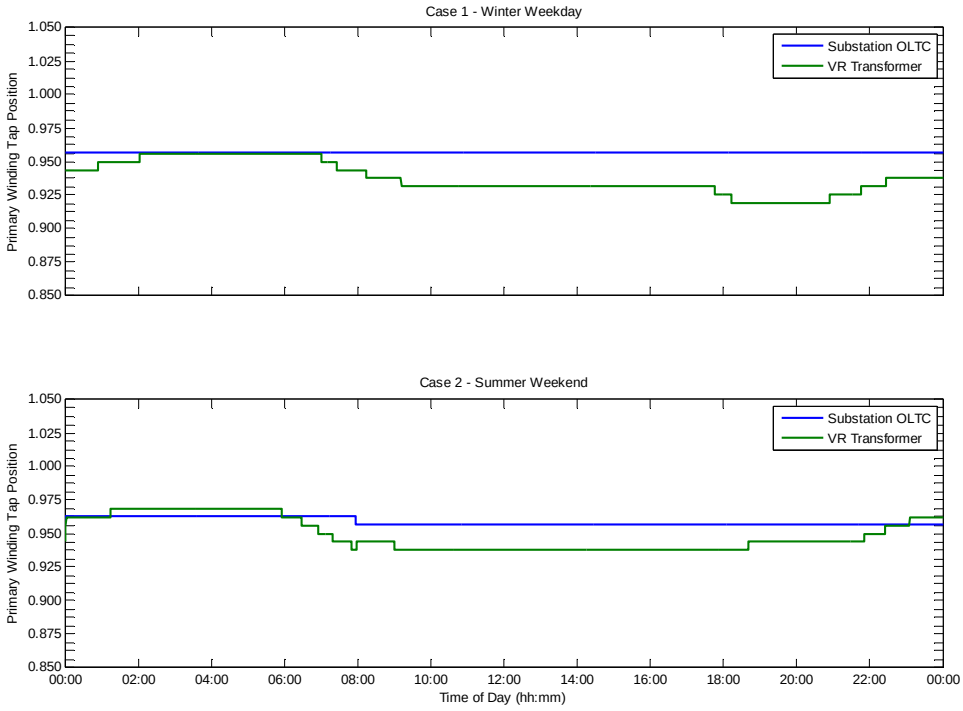

Figure 4.17: Tap positions for the OPF technique with PFC + Curtailment

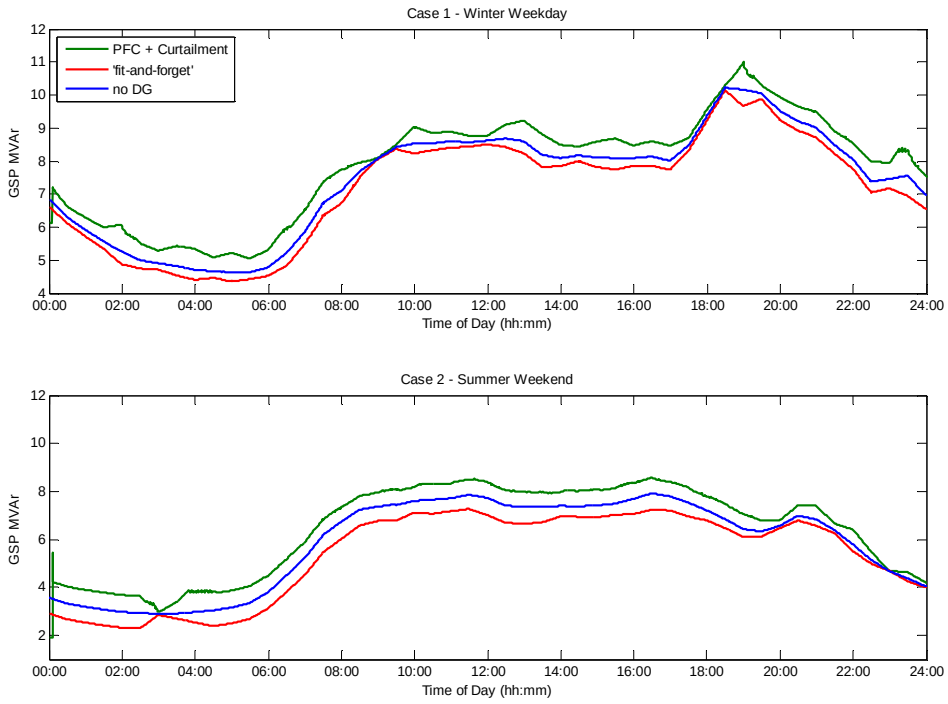

Figure 4.18: Reactive power flow at the GSP

4.3.3 Coordinated Voltage Control And Energy Curtailment

The 24 hour simulations were repeated with variable voltage targets on the network tap changing transformers. The DG power factor control set-point was restored to a fixed setting of 0.98 capacitive (leading) and the voltage set-point on the transformers secondaries was allowed to vary within the range 1.01 to 1.04 pu.

$$V_{OLTC}^{-} \le V_{OLTC}(k+j|k) \le V_{OLTC}^{+} \tag{43}$$

As expected, permitting the voltage level to vary at the upstream distribution network busbars provided more headroom in the voltage envelope for voltage rise at the point of DG connection and greater levels of real power production. Figure 4.19 and Figure 4.20 illustrate the increased generator production pattern, with power curtailment only required under peak load conditions or exceptional power production levels. With reduction of voltage at bus 2 to accommodate enhanced DG production, the constraint on the optimisation became voltage rise at the DG location or voltage drop at Bus 8, the lowest point in the no DG case network voltage profile, depending on the prevailing

generation and supply conditions. The voltage constraint varied with time, with voltage drop becoming the binding effect under peak demand.

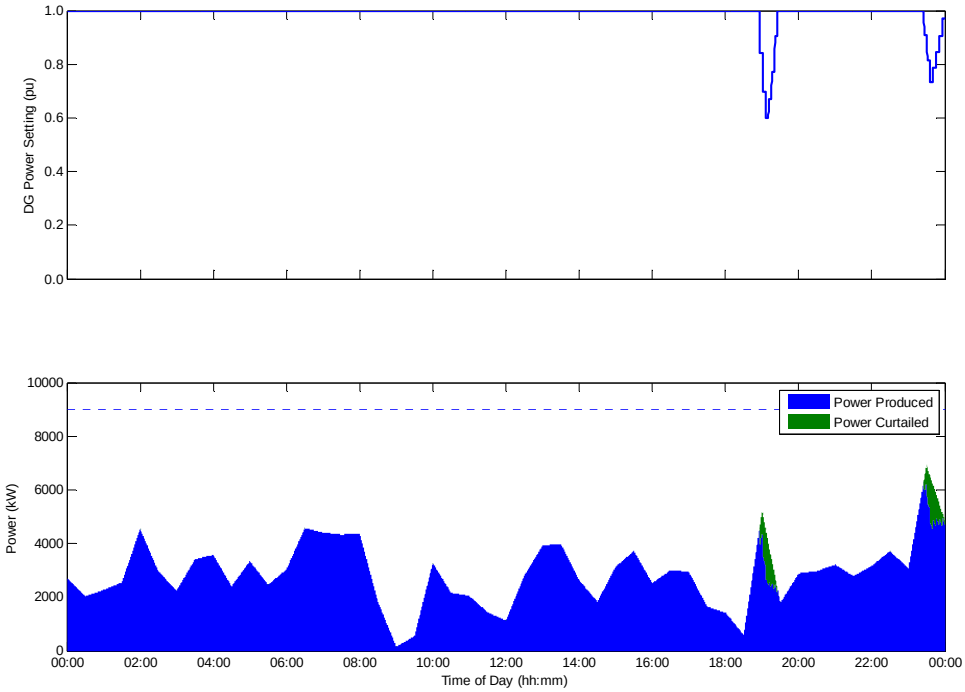

Figure 4.19: Curtailment settings for the OPF technique with CVC + Curtailment case 1

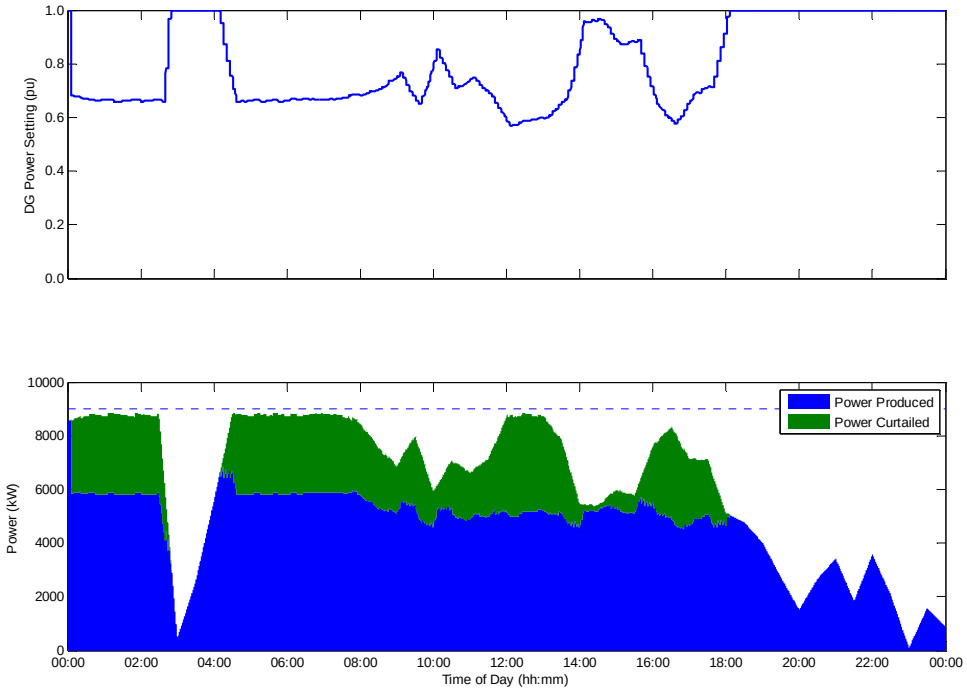

Figure 4.20: Curtailment settings for the OPF technique with CVC + Curtailment case 2

This scenario is now beginning to resemble a more flexible network environment for DG integration. While system demand continues to be prioritised, the network is becoming more responsive to renewable DG. Energy yield is significantly increased to 68.3 MWh and 109.7 MWh (99.3% and 74% of available resource) in the two cases. Network losses also increased, reaching 29.1 MWh and 23.7 MWh respectively. Based on the reduced GSP demands of 623.7 MWh and 475.8 MWh system losses were recorded as 4.7% and 5.0%. The actual increase in the magnitude of energy losses over the curtailment scenario, 1.3 MWh and 3.1 MWh, should not detract from the increased energy capture from the DG (11.7 MWh and 50.5 MWh).

The implementation of the variable voltage control OPF formulation, in its present form, produces poor continuity of the time sequential control configurations derived by the successive solutions of the OPF technique. The issue is illustrated in the time series trace of tap positions shown in Figure 4.21. An example is observed around 08:00 hours on the first Winter Weekday simulation, when prevailing power flows do not require curtailment and there is no binding constraint on the optimisation objective function. In this situation the OPF is not uniquely defined and can converge to any number of

feasible locally optimal solutions. Therefore the time sequential OPF solutions can lack temporal stability and introduce switching of control settings for no apparent need or benefit, as witnessed in Figure 4.21, because the OPF is being utilised in situations where it may not be necessary.

Another situation is witnessed in the late evening of the second Summer Weekend case. Here the OPF formulation performs well until the levels of wind power production drop and the action of the objective function becomes unnecessary as no curtailment is required to maintain voltage levels within statutory limits under these power flows. In addition, the moderate level of demand on the parallel distribution feeder places no specific binding constraint on the system operation or the OPF technique, and as such with successive OPF solutions the substation OLTC and VR transformer control setting and tap position begin to vary without purpose. This introduces a number of spurious and discontinuous (i.e. short lived actions) tap changing operations.

This had a significant adverse impact on the bus voltage levels with tap-changing control actions initiated in discrete time staggered steps. The resultant regulated voltage level is therefore subject to sharp changes which may potentially cause minor short term voltage excursion, as demonstrated on bus 9 between 21:00-22:00 in Figure 4.23.

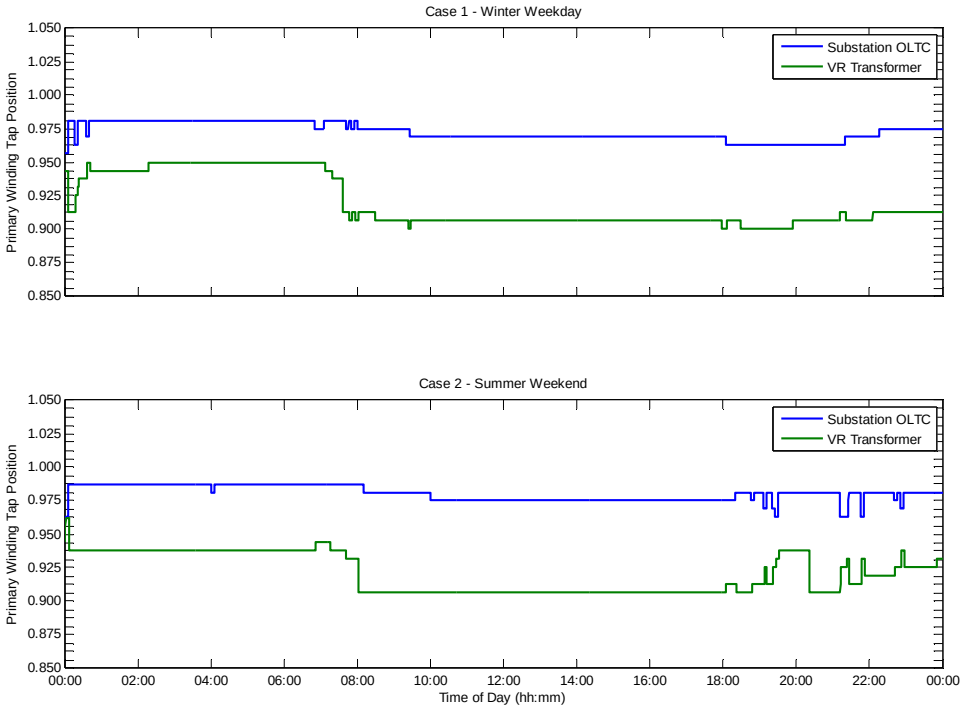

Figure 4.21: Tap positions for the OPF technique with CVC + Curtailment

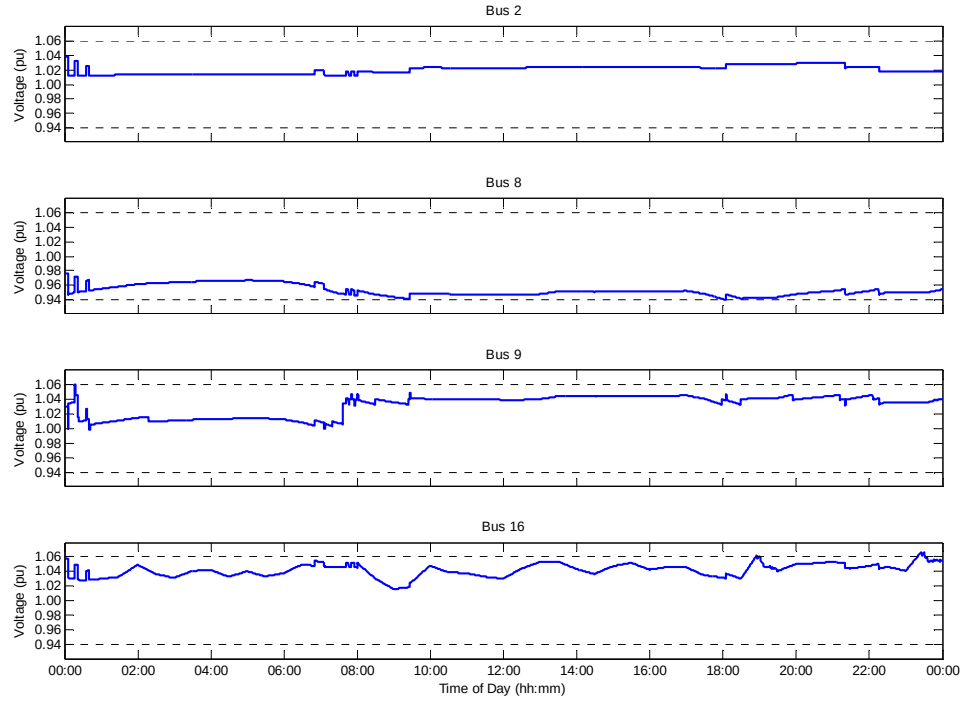

Figure 4.22: Voltage profiles for the OPF technique with CVC + Curtailment case 1

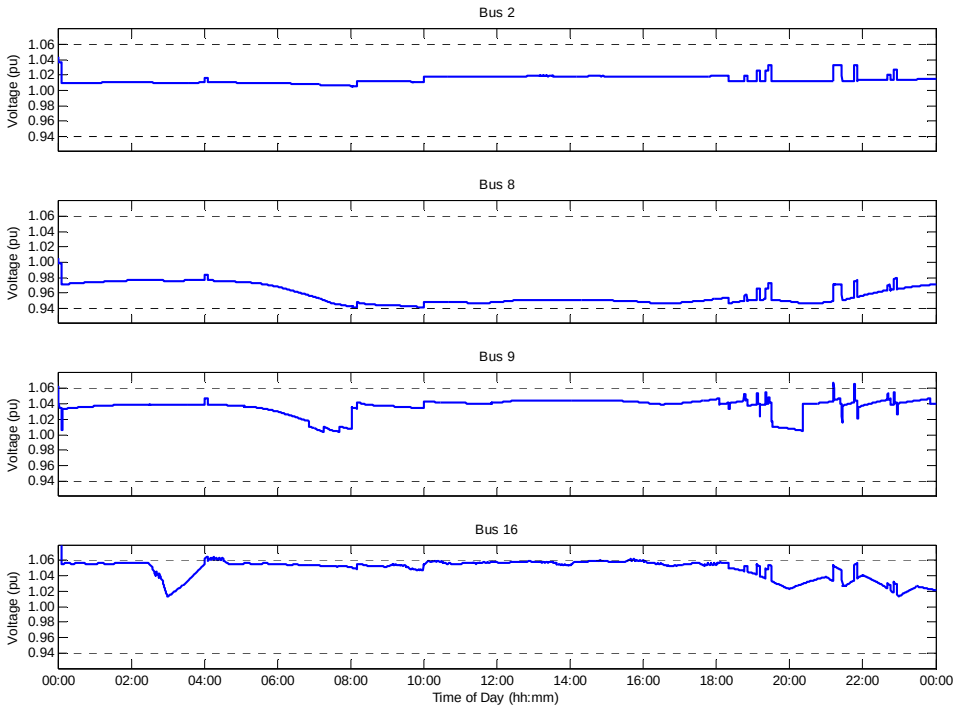

Figure 4.23: Voltage profiles for the OPF technique with CVC + Curtailment case 2

The initial, simple way to alleviate this drawback would be to only deploy the OPF technique to determine new configurations of network control settings during periods of problematic network conditions, where power flows approach or breach system constraints. However, the specific goal and intentions for this work was to research and develop a series of OPF techniques that operate continuously in real time to maximise the future system-wide network benefit from real time ANM techniques, whilst managing power flows against approaching or breaching system constraints. This design ethos was persevered with, as it is believed that in larger, more complex network situations, as well as in the long term future, additional variables of control will coincide with more onerous control scheduling problems that will lead to some of the discontinuity witnessed by the spurious control switching.

In addition, it was preferred that the real time OPF strategy would operate continually, driving new network control settings progressively in order to mitigate against differences in the forecasted and actual power flow injections and better respond to changing system demand and varying power flow injections. The development of

alternative means of forecasting data to enable this, while alleviating the identified issues and providing a pre-emptive network response is reported later in this thesis.

4.3.4 Full Active Network Management OPF1

By combining the variable voltage control strategy with the distributed variable PFC regime, a fully integrated ANM scheme was explored and is now reported. Repeating the same simulations as before, Figure 4.24 and Figure 4.25 illustrate that the real time OPF technique has the potential to avoid nearly all of the previously required instances of power curtailment, achieving 99.9% and 97.9% energy yield in the respective test cases. This is achieved by the OPF technique determining against the time series of power flow appropriate voltage targets for the existing network OLTC transformers, DG power factor set-points and, when curtailment is necessary, a maximum per-unit set-point for the DG real power production.

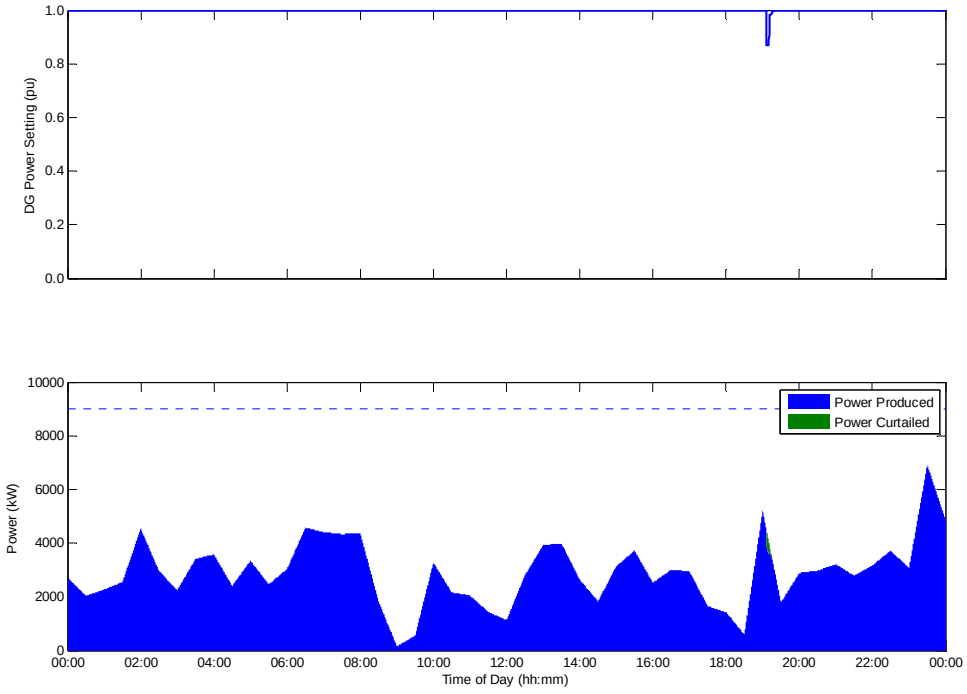

Figure 4.24: Curtailment settings for the full ANM OPF case 1

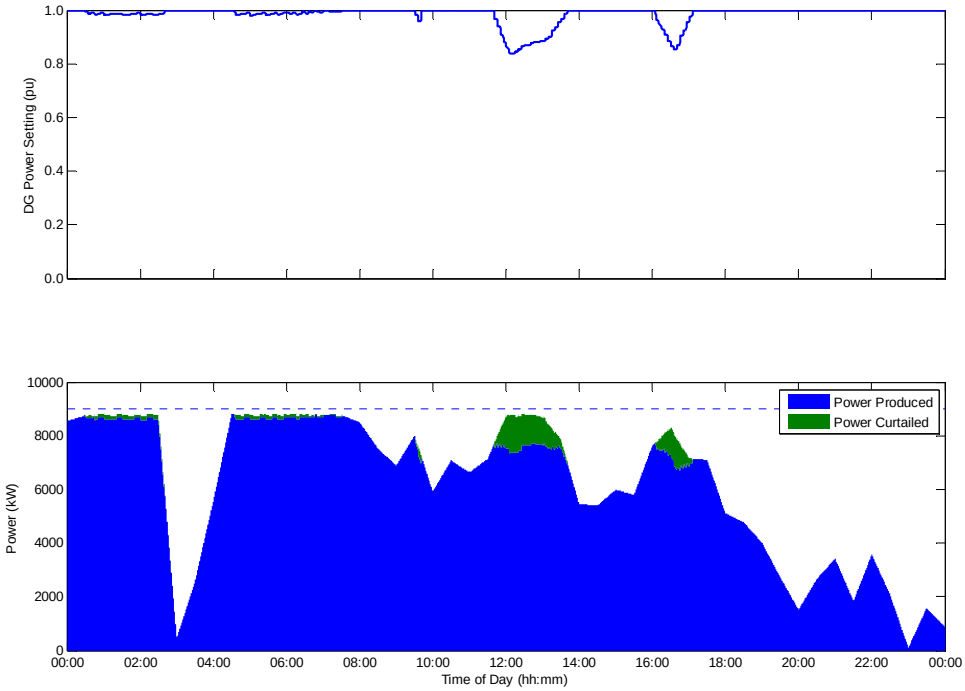

Figure 4.25: Curtailment settings for the full ANM OPF case 2

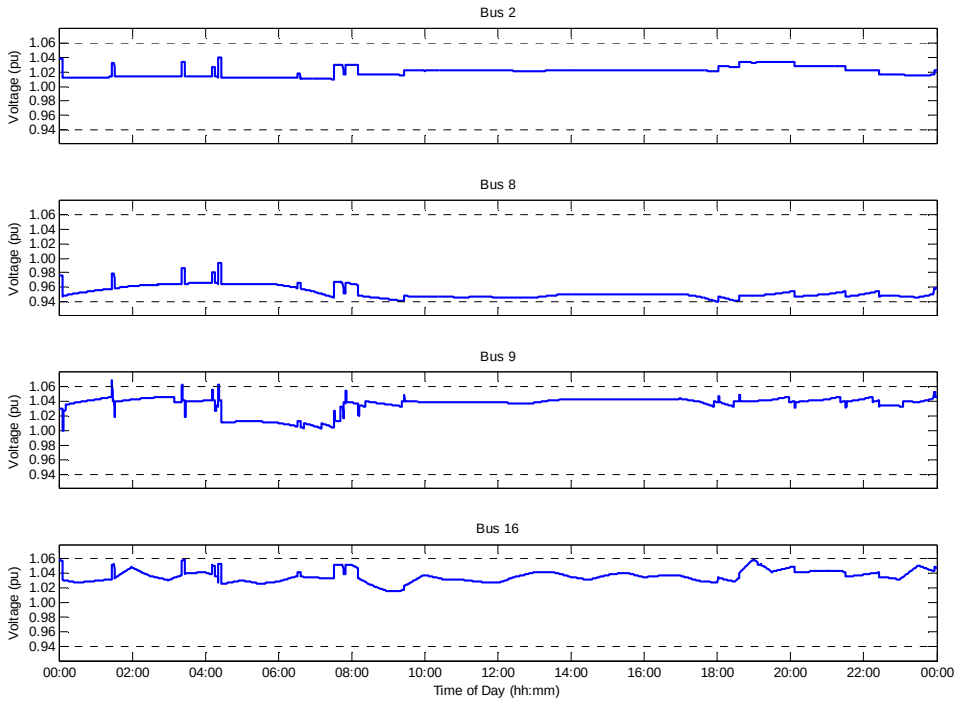

Figure 4.26: Voltage profiles for the full ANM OPF case 1

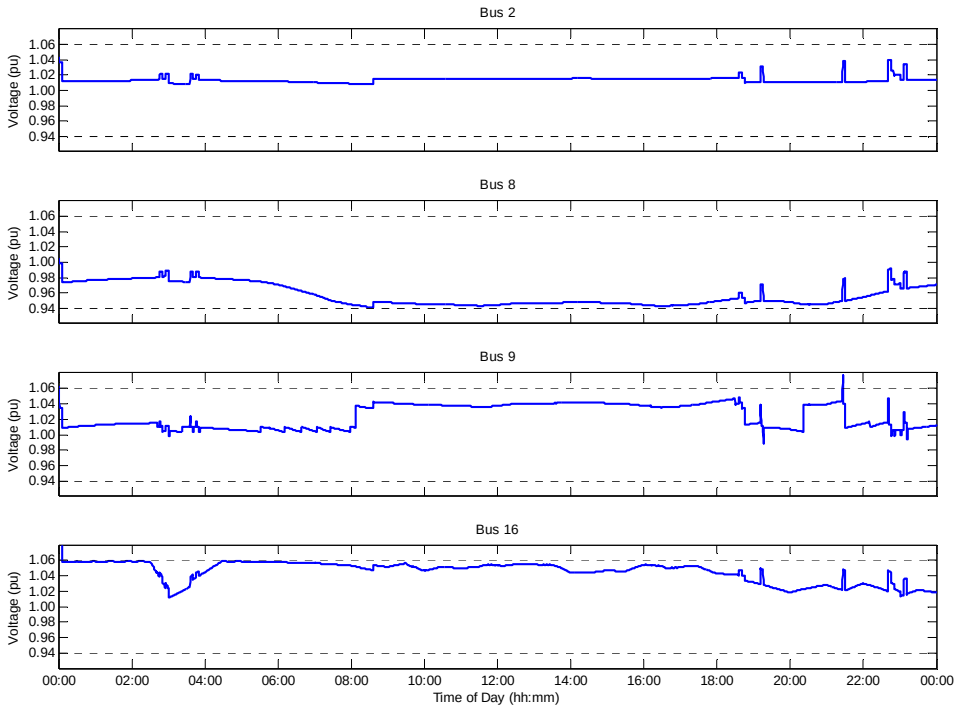

Figure 4.27: Voltage profiles for the full ANM OPF case 2

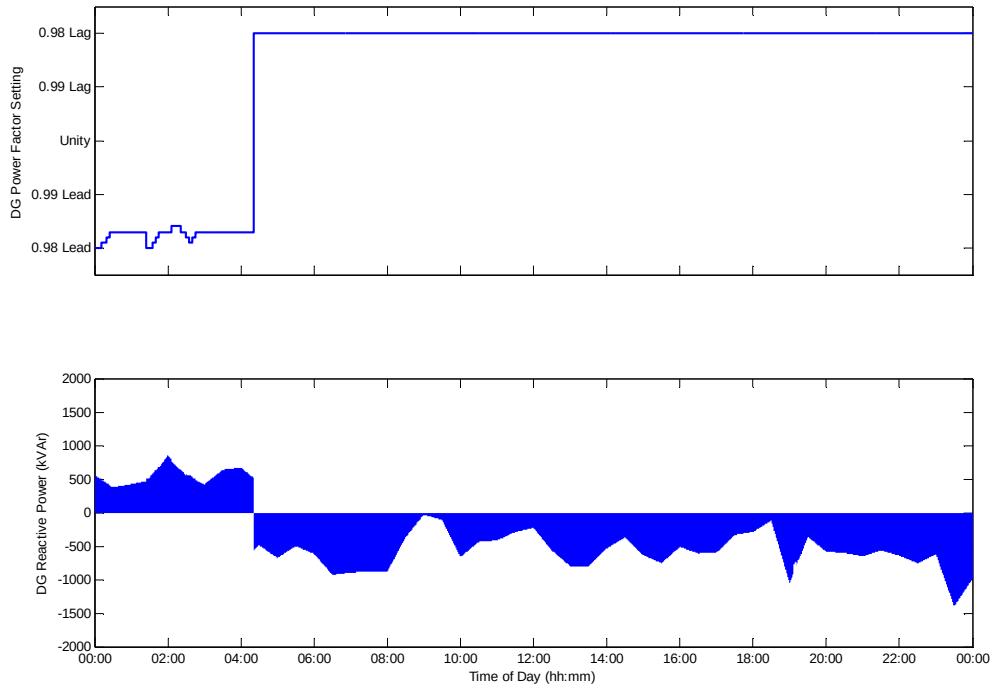

Figure 4.28: Power factor settings for the full ANM OPF case 1

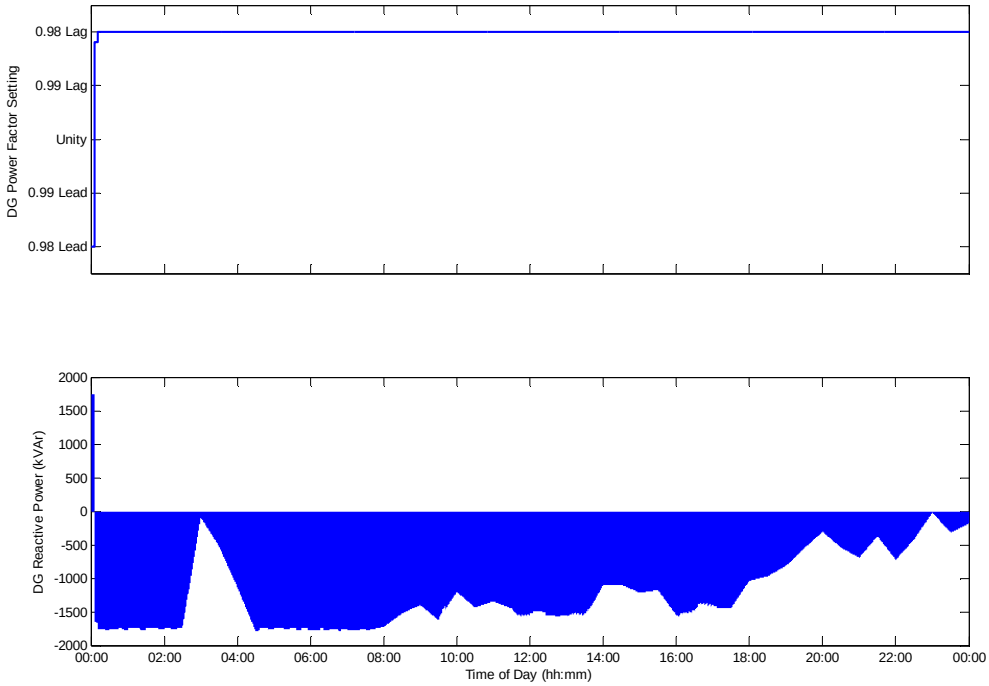

Figure 4.29: Power factor settings for the full ANM OPF case 2

In this scenario, network losses continue to rise, especially in Case 2, due to the heavier loading of feeders and transformers, standing at 4.7% and 6.1% in Case 1 and Case 2 respectively. However in Case 2, the feeder continually experiences reverse power flow of up to 6 or 7 times the no DG case load. Figure 4.26 and Figure 4.27 demonstrate that the combined technique was successful in maintaining the statutory voltage profile for the duration of the simulation periods. The maximum and minimum recorded voltage levels over both simulations periods are 0.9398 pu and 1.0590 pu. Recorded measurements of voltage below the 0.94 level were limited to 0.05% of Case 1 only and would be averaged out to comply with the European Standard EN 50160 [108] regulations.

However, some effects previously observed from the individual ANM practices are still present, and in some situations heightened by the additional freedom inherent in the integrated ANM OPF technique. For example the temporal tap position traces shown in Figure 4.30 highlight more discontinuous and spurious tap switching between the tap changing transformers with time. The response of the variable PFC technique is similar to the PFC + Curtailment case with a tendency for the DG unit to revert from a leading

to a lagging power factor, although in the moderate DG production case, this is less necessary than in the high DG production case 2. This further illustrates the subtleties and potentially counterproductive system consequences of implementing a comprehensive active optimisation routine in sections of previously passive distribution networks.

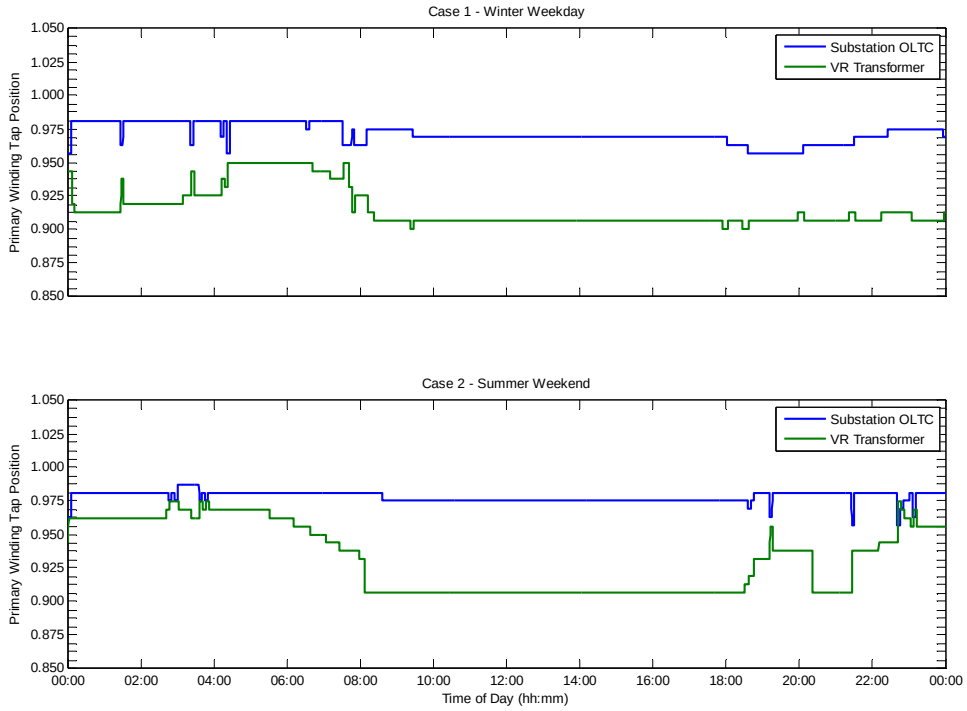

Figure 4.30: Tap positions for the full ANM OPF case 1(top) and case 2(bottom)

4.3.5 SUMMARY AND COMPARISON

Network simulations have illustrated the application of a straight "minimise energy curtailment OPF" objective (OPF1) on the UKGDS EHV1 – ANM test network. Figure 4.31 illustrates how the progressively more coordinated ANM strategies offer the potential to improve the energy yield from renewable energy resources such as wind power by increasing the capacity of DG that can be connected and reducing the levels of energy curtailment (Figure 4.32) necessary to maintain voltage levels within statutory levels under variable power flow regimes. This potential has been identified in earlier work [59]. However, a new formulation of the OPF technique with a capacity for the real time transfer of data was tested with high resolution time sequential simulations to

emulate the system response and assess the network consequences of harvesting these enhanced levels of energy production within the existing network infrastructure.

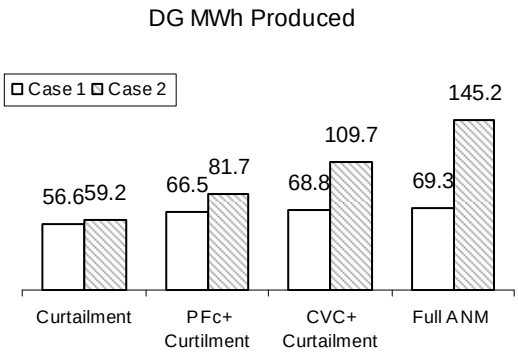

Figure 4.31: DG MWh produced with ANM

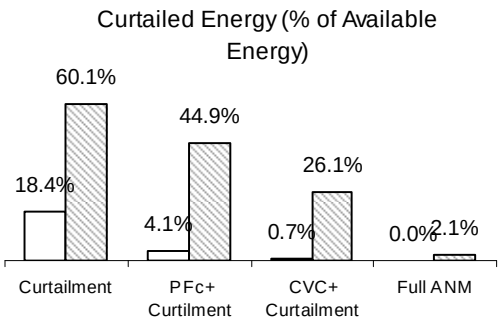

Figure 4.32: Energy curtailed with differing ANM strategies

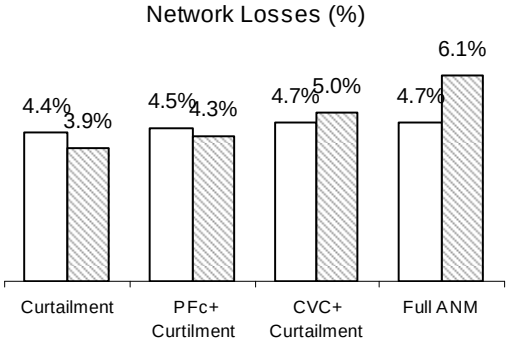

Figure 4.33: Network losses (%) with differing ANM strategies

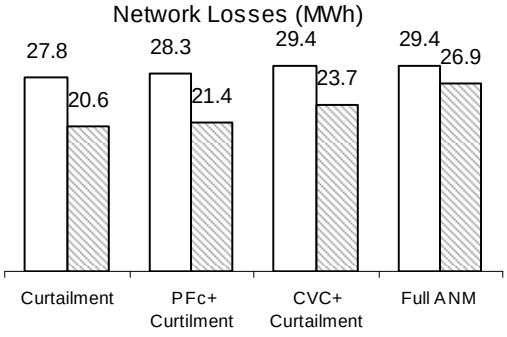

Figure 4.34: Network losses (MWh) with differing ANM strategies

In the work referred to earlier [59], the effect on system losses had been viewed previously as a potential drawback to the integration of high volumes of DG. The reported losses shown in Figure 4.33, as a percentage of the power import at the GSP, are slightly skewed as increased energy from the DG displaces energy transfer from the GSP and artificially inflates the percentage of energy losses. Figure 4.34 demonstrates that overall the actual magnitude of increased losses was not as significant as first thought. However, in this case, losses did rise substantially along the DG connected feeder with increased energy losses in this feeder from 0.7 MWh to 6.3 MW, some 926% higher, between the Curtailment only and full ANM cases.

The high resolution power flow simulations allow detailed investigation and examination of the real time network impacts and system consequences. In this simple demonstration network the binding constraint in the OPF technique was the high voltage level at the point of DG connection. In the examples presented, instances of voltage excursions breaching statutory limits were observed. Figure 4.35 and Figure 4.36 show the minimum and peak recorded voltage levels in each of the OPF formulations tested.

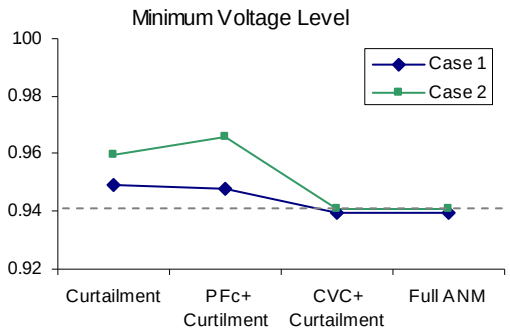

Figure 4.35: Minimum voltage levels with differing ANM strategies

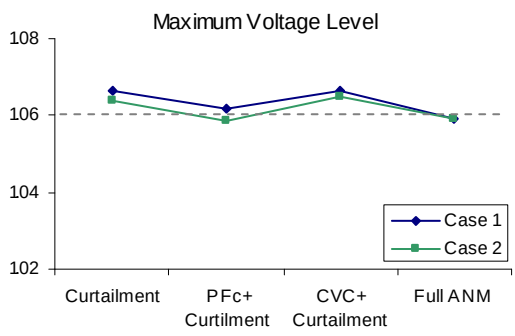

Figure 4.36: Maximum voltage levels with differing ANM strategies

Occurrences of maximum voltage levels out with the voltage envelope are a system response not previously visible through the use of earlier approaches. Instances of voltage violation are only observed at the point of DG connection. There are a few reasons that contribute accumulatively, but the primary cause stems from the deadband of operation around the tap changing transformers and the inception of large scale reverse power flow in the distribution network feeder. With significant reverse power flows in the distribution feeder, small magnitudes of unchecked voltage rise, within the deadband of the transformer tap changing operation, propagate back down the feeder and results in voltage levels above the statutory maximum. This effect was not evident prior to the integration of DG as power flows were uni-directional and the real time impact was not addressed in alternative OPF studies of ANM.

Limited occurrences of minor voltage violations in this manner are not overly problematic as they are not large enough to initiate the operation of protection relays. The European Standard [EN 50160] on the short term breach of statutory voltage envelopes provides a precedent for operating the network close to the regulatory

boundaries provided that the occurrence of voltage violations does not occur for more than 5% (measured in ten minute averages) of an observed time period, usually one week. In all but the curtailment only analysis, the OPF technique was shown to be compliant with the EN 50160 recommendation, with the voltage levels recorded in 10 minute averages breaching the 1.06 pu upper statutory limit a maximum of 3.82% of the total non-continuous 48 hour test period. In any analysis, non-compliance with the EN 50160 was only observed during the curtailment only OPF1 scenario, which had on average a total voltage violation of 8.68% over the total non-continuous 48 hour observational period.

It was also found that localised voltage control techniques lowered residual voltage variation that give rise to these minor voltage violations. This is consistent with [54] where localised PFC measures mitigated the magnitude of permissible voltage excursions.

The additional energy yield resulted in a number of other minor network impacts for the system control settings, as illustrated by the time series profiles discussed earlier. In particular the number of tap changing operations during the two 24-hour analyses was observed to increase dramatically. A count of the tap changing operations over the observation periods is shown in Figure 4.37 and Figure 4.38. It is clear that if the substantial increase in the number of tap actions is repeated continuously, as is suggested by the sharp contrasts in the test case analyses and not just evident during short-term onerous network conditions, this could be considered operationally injurious through accelerated wear and reflects poorly on the performance of the centralised OPF technique. As highlighted earlier, it was clear that the majority of negative consequences observed, given the very short control cycle and continuous scheduling of new control settings from the OPF, stem from a lack of time coordination in the formulation of the OPF control variables. Alterations and improvements to the proposed OPF technique to make it function under all network conditions, not just problematic network conditions were therefore required to address these limitations.

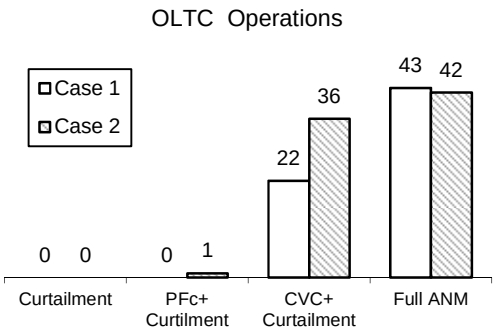

Figure 4.37: No. of OLTC tap operations with differing ANM strategies

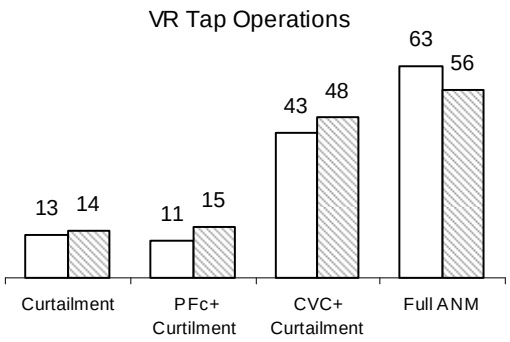

Figure 4.38: No. of VR tap operations with differing ANM strategies

Two techniques to better integrate the ANM concepts in the OPF were further investigated. The first penalises unnecessary voltage variation at the tap changing transformers and is reported in section 4.4, and the second, reported in section 4.5, introduces a measure of look-ahead horizon scanning of future network power injections and demands and produces a planned trajectory of optimal network control configurations.

4.4 POWER FLOW SIMULATIONS WITH MINIMUM DEVIATION OPTIMAL POWER FLOW

The curtailment minimisation objective function (OPF1), while successful in improving the energy yield from the wind farm DG, introduced some discontinuous (or spurious) control actions to the network control systems when operated continuously over a short control cycle, particularly at times when the network power flow conditions did not exert excessive stress on the network. One means of improving the OPF technique, when the network was lightly loaded, to better regulate the network consequences whilst retaining the better energy yield from DG, was to augment the objective function and penalise unnecessary disturbance of network control settings.

OPF2: $$Min \sum_{g \in G} p_g^{curt}(k+j|k) + \sum (V_{OLTC}(k+j|k) - V_{OLTC}^{t\arg et})^2 \quad (36)$$

This second objective function uses a simple least squares method to minimise deviation of the voltage setting on the secondary winding of tap-changing transformer from the pre-existing fit-and-forget targets.

4.4.1 FULL ANM OPF2

Application of the Minimum Deviation objective function (OPF2) was tested with the full ANM strategy. Total energy curtailment required in each sample observation period was 0.05 MWh for Case 1 and 3.1 MWh for Case 2.

With the alternative multi-objective function of OPF2, energy yield remained constant with the straight minimise curtailment objective OPF1 in both cases, showing the multi-objective function had no significant impact on the performance of the OPF technique to increase energy yield. This means that real time OPF technique was able to derive in real time new network control configurations which facilitated energy yield at 300% of the fit-and-forget level in Case 1 and 294% of the fit-and-forget level in Case 2.

Highly promising results from the OPF2 formulation are illustrated in the time series voltage profiles of the system buses and frequency of tap changing operations. For example, the time series voltage profiles shown in Figure 4.41 and Figure 4.42 illustrate a far smoother steady state voltage variation. Inspection of the time series of tap position trace in Figure 4.43 demonstrates a significant improvement in the time-wise progression of tap changing operations and a substantial reduction in the frequency of actions. Finally, Figure 4.44 and Figure 4.45 show a consistency in the absorption of reactive power by the DG, which has been shown to have no adverse impact on network operation thus far.

While a clear improvement is evident with the new multi-objective function, the OPF2 did appear to increase the frequency of residual system voltage excursion with occurrences of 1.9% and 4.5%, recorded at 5-second intervals, in Case 1 and Case 2 respectively.

A further improvement that could have been embedded into the formulation of the real time OPF technique, which would not interfere with the underlying fit-and-forget configuration and improve the response of the OPF2 technique, was to alter the internal Minimum Deviation OPF voltage targets from the fit-and-forget arrangement. Retrospective changes to the existing network infrastructure were intentionally avoided. This was so that the default fail-safe mechanism of any ANM strategy would be to return to the fit-and-forget operating state with pre-set limitations on DGs under such conditions.

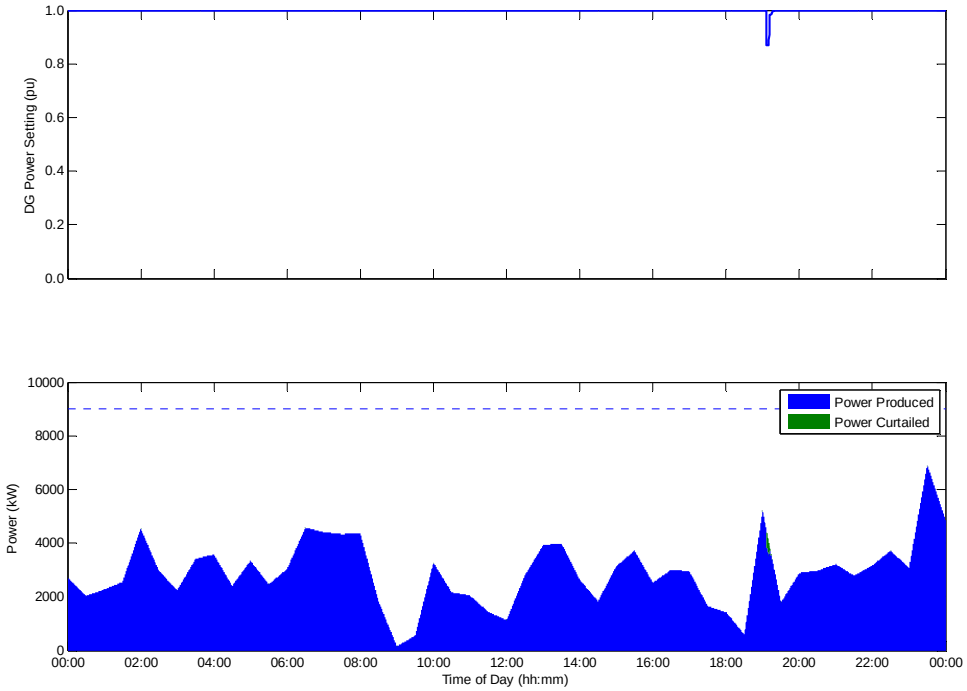

Figure 4.39: Curtailment settings for the full ANM OPF2 case 1

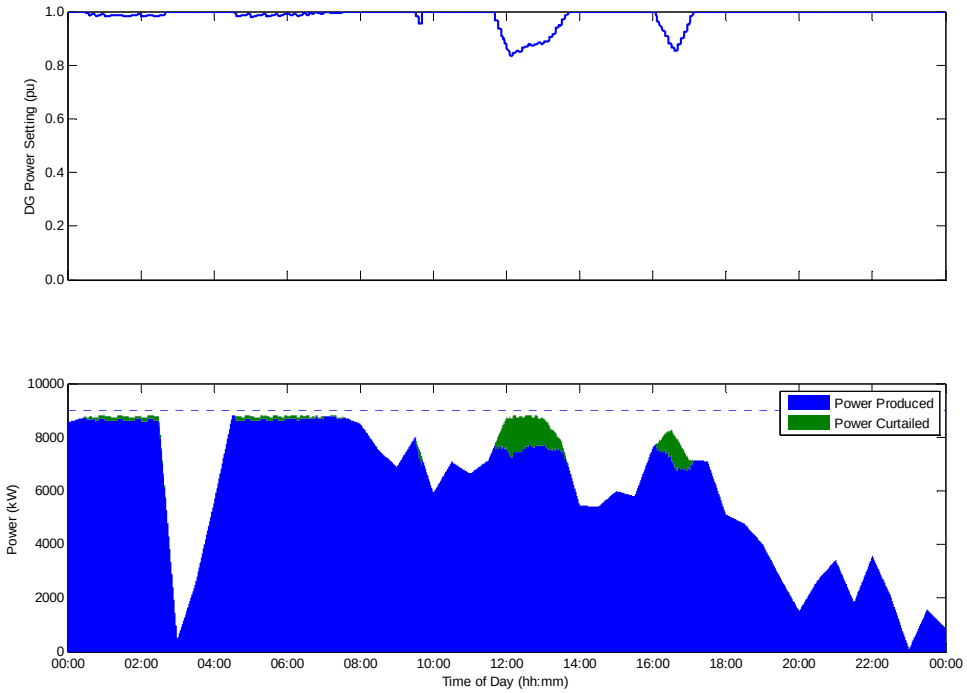

Figure 4.40: Curtailment settings for the full ANM OPF2 case 2

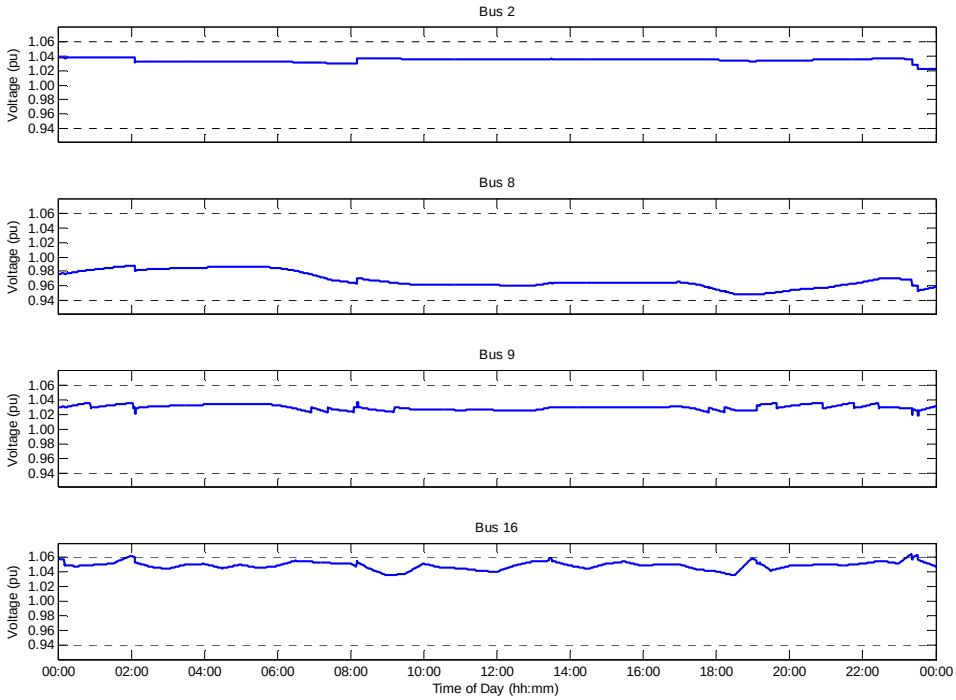

Figure 4.41: Voltage profiles for the full ANM OPF2 case 1

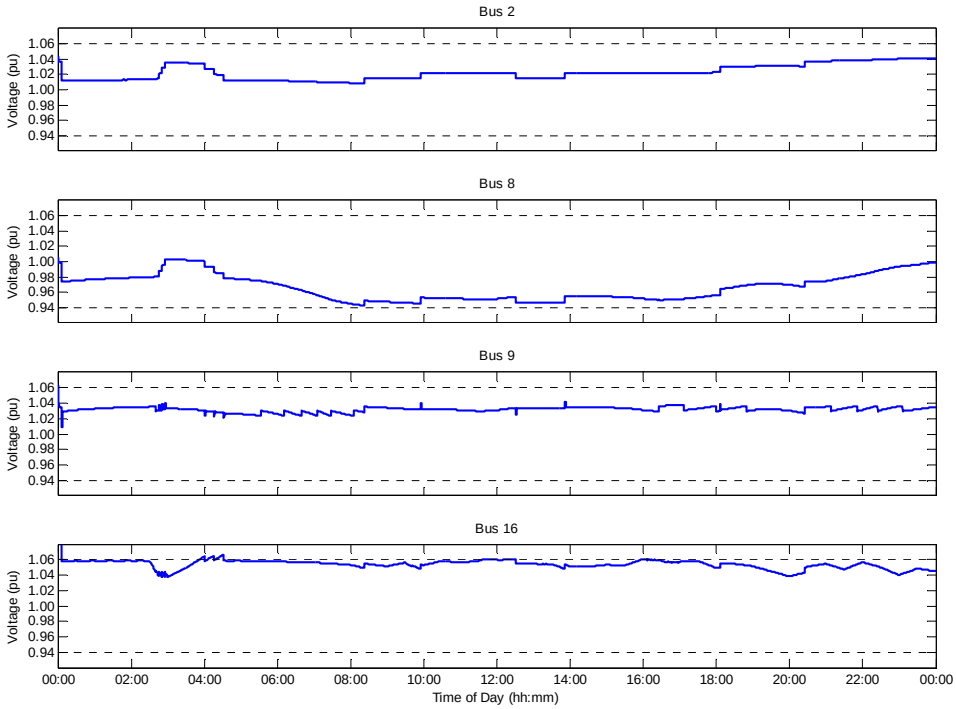

Figure 4.42: Voltage profiles for the full ANM OPF2 Case 2

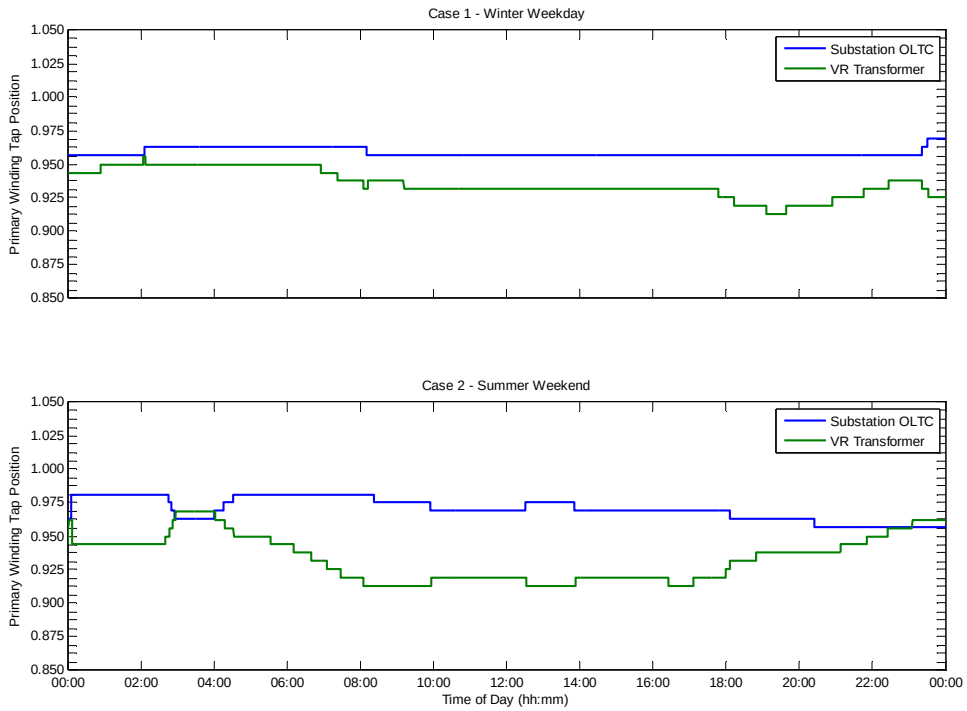

Figure 4.43: Tap positions for the full ANM OPF2 case 1 (top) and case 2 (bottom)

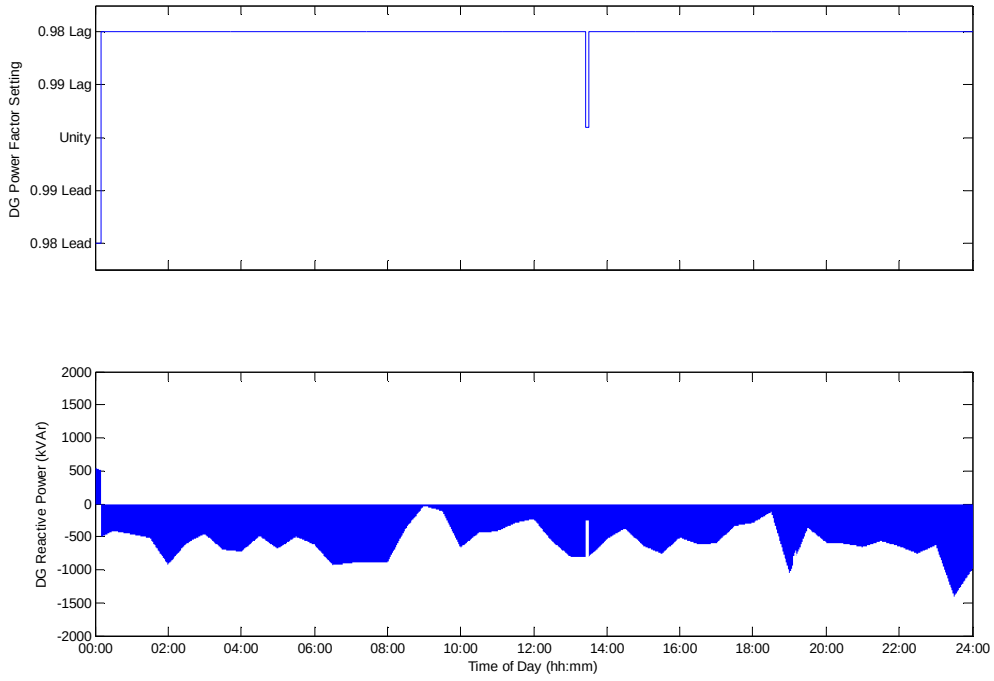

Figure 4.44: Power factor settings for the full ANM OPF2 case 1

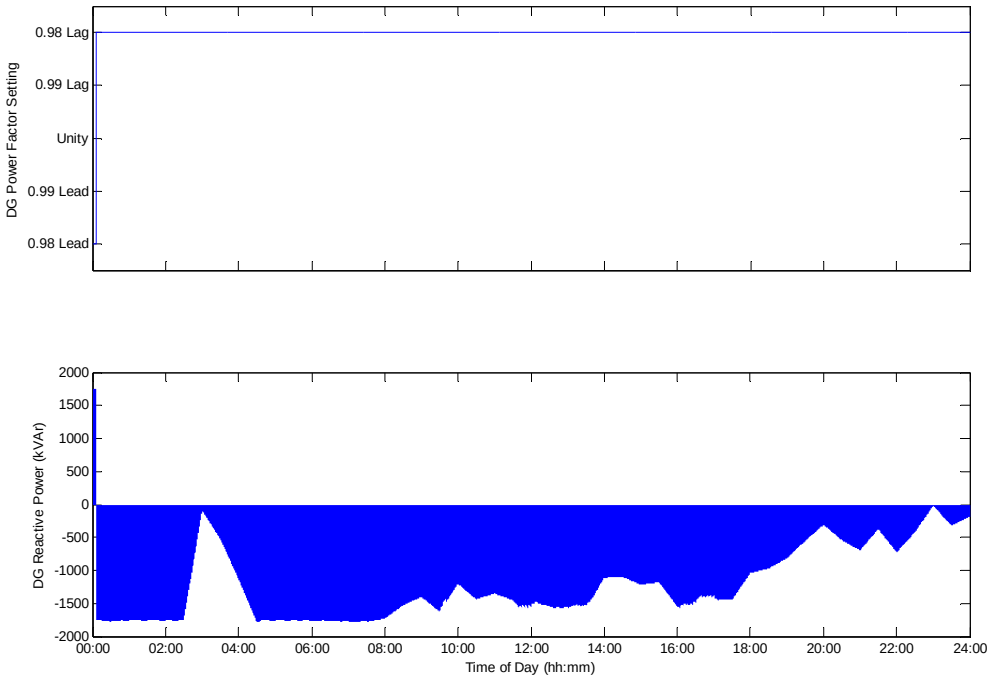

Figure 4.45: Power factor settings for the full ANM OPF2 case 2

4.4.2 FULL ANM OPF3 - FURTHER COORDINATED VOLTAGE CONTROL

An observation from the voltage profile traces in Figure 4.41 and Figure 4.42 was that the majority of system voltage excursion did not occur from a stretching of the system-wide voltage profile beyond the statutory envelope, but as a consequence of the multi-objective OPF2 function operating in an (over-)restrictive voltage configuration that was sticking as closely as possible to the fit-and-forget voltage targets limiting the operational margins for DG.

By slightly altering the pre-determined fit-and-forget voltage targets employed internally in the OPF2 formulation, the standard steady state target of the network can be altered to provide a more conducive hosting regime for DG developments, without altering the fall back, fail-safe fit-and-forget operating conditions of the distribution network. This new formulation of the ANM OPF technique is termed OPF3 and illustrates fine tuning of the proposed OPF solution to specific network requirements.

The simulations were repeated with the pre-set voltage target of the substation transformer OLTC inside the minimum deviation objective function lowered slightly

from 1.036 pu to 1.03 pu, providing more voltage headroom in the network operation for DG real power generation. Results showed further improvement in voltage regulation and better utilisation of the statutory voltage envelope to support the integration of DG. Instances of observed voltage excursions were decreased over the OPF2 formulation with the percentage of overvoltage excursions recorded at 5 second intervals reduced to 0.5% in Case 1 and 3.9% in Case 2. This is without introducing instances of under-voltage anywhere on the network. The peak recorded voltages in each case were 1.0639 pu and 1.0653 pu respectively.

No negative effects were found in either the energy yield or any of the time wise control operations of the network, as shown in Figure 4.46 through Figure 4.50.

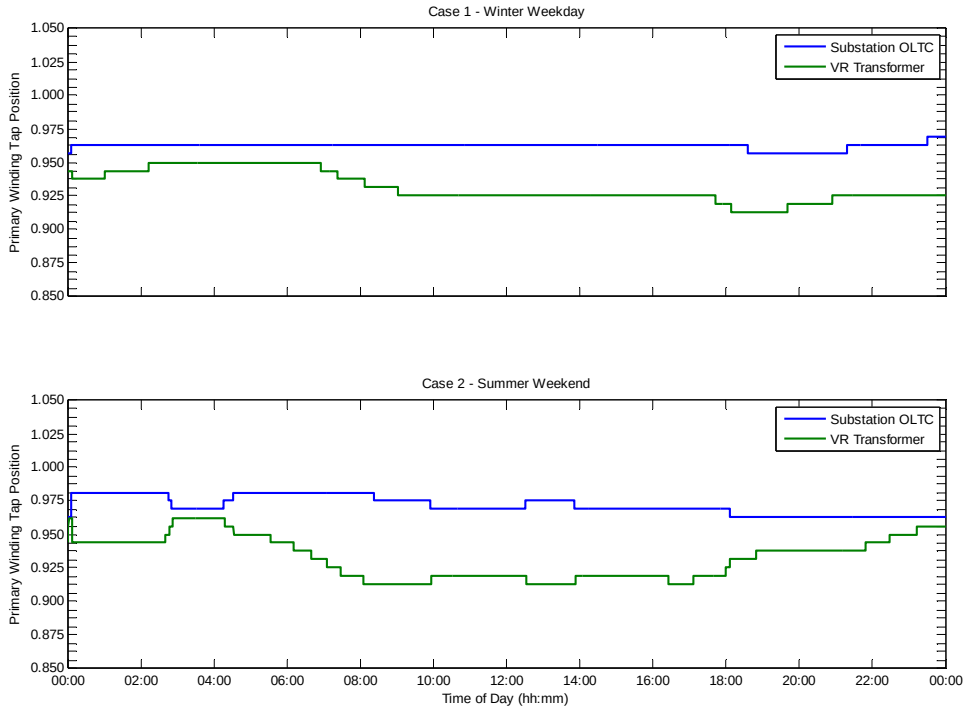

Figure 4.46: Tap positions for the full ANM OPF3 case 1 (top) and case 2 (bottom)

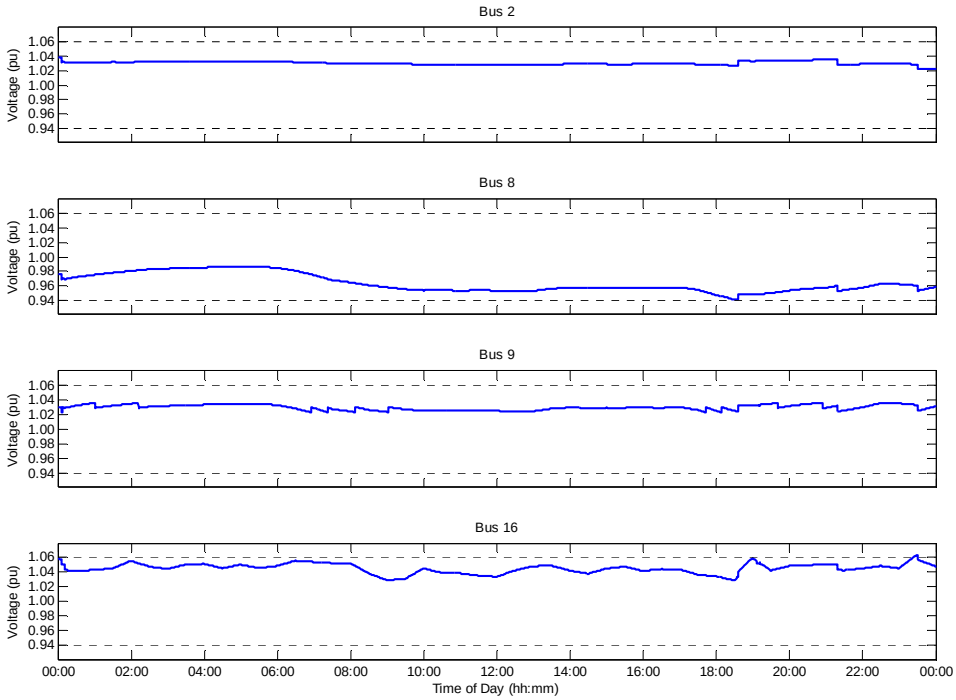

Figure 4.47: Voltage profiles for the full ANM OPF3 case 1

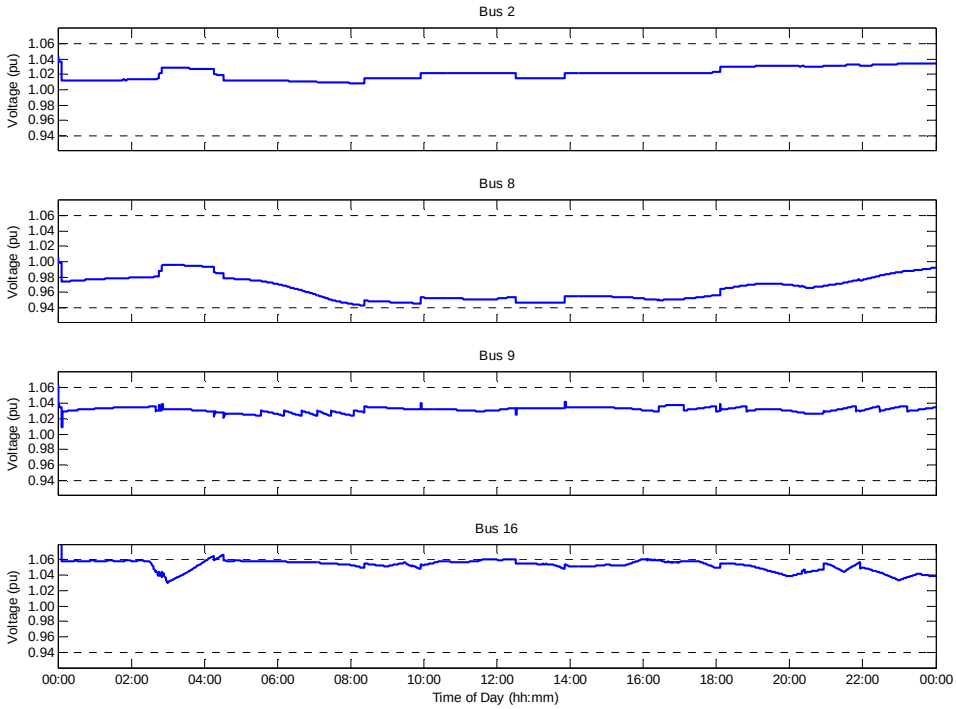

Figure 4.48: Voltage profiles for the full ANM OPF3 case 2

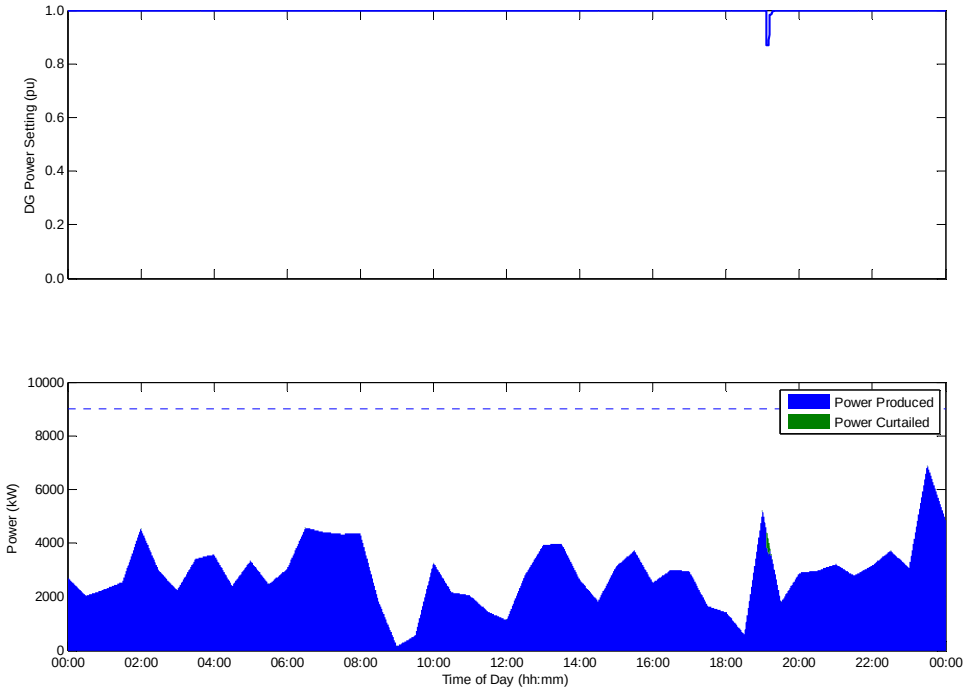

Figure 4.49: Curtailment settings for the full ANM OPF3 case 1

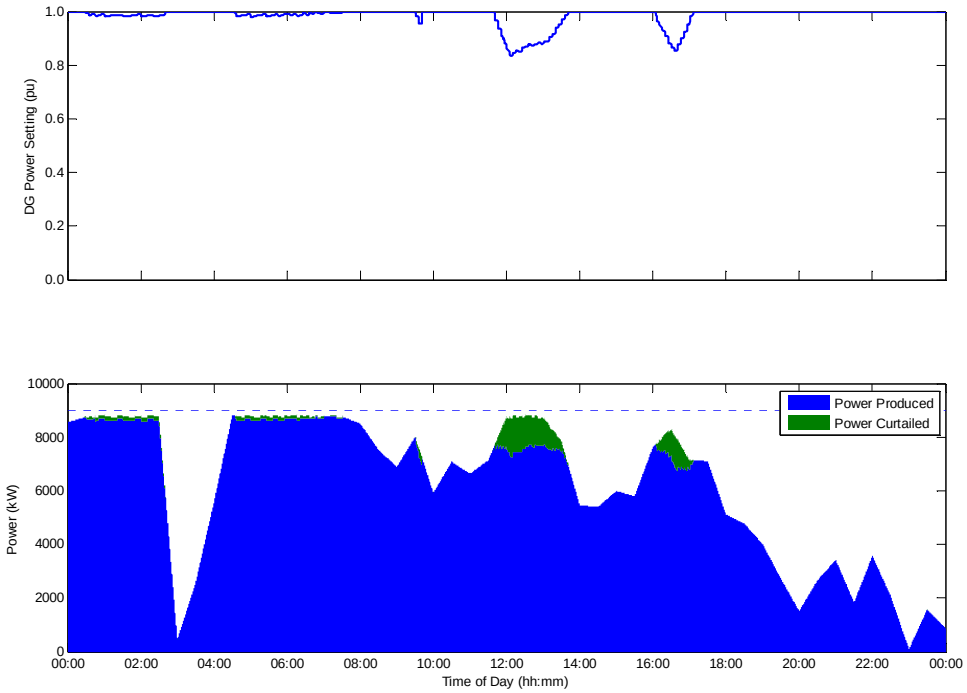

Figure 4.50: Curtailment settings for the full ANM OPF3 case 2

4.4.3 SUMMARY AND COMPARISON

Three formulations of the full ANM OPF technique with persistence forecasting have now been reported:

I. Minimise energy curtailment - OPF1.

II. Minimise curtailment and deviation from fit-and-forget configuration - OPF2.

III. Minimise curtailment and deviation from the new voltage targets - OPF3.

A comparison of each formulation shows a negligible difference in the levels of energy yield as observed in Figure 4.51 and Figure 4.52.

Figure 4.51 to Figure 4.64 compare the statistics of network operation showing the system consequences of each formulation of the OPF objective function for the moderate DG, high demand case 1 and the high DG, low demand case 2.

As expected, the real benefit from the addition of minimum deviation objective to the OPF formulation is that it alleviated the occurrences of unnecessary, random and spurious tap changing operations in the actively pre-scribed control settings as indicated by Figure 4.53 and Figure 4.54.

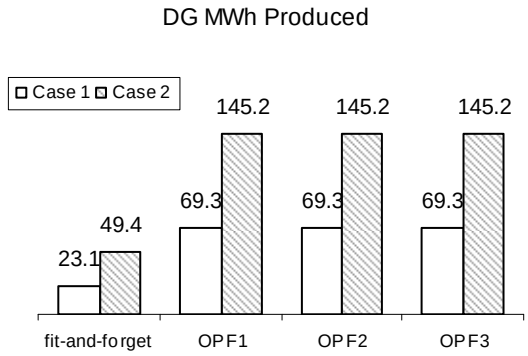

Figure 4.51: DG MWh produced with changing OPF objective function

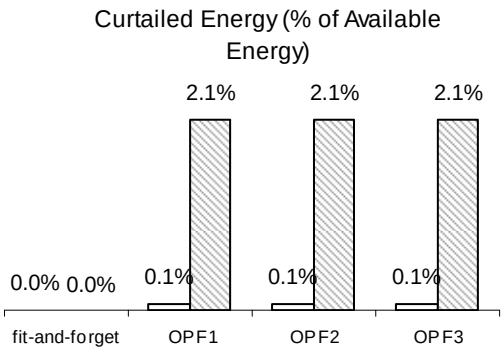

Figure 4.52: Curtailed energy with changing OPF objective function

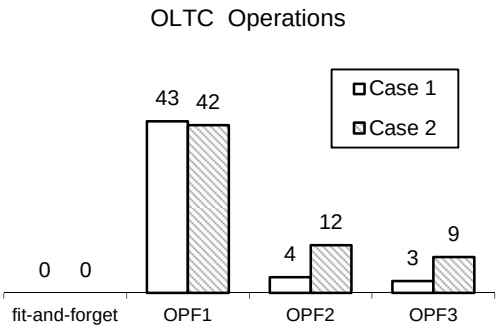

Figure 4.53: No. of OLTC tap operations with changing OPF objective function

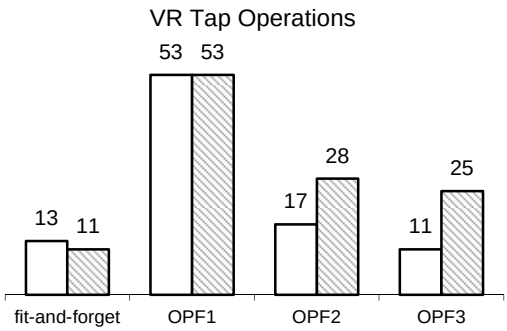

Figure 4.54: No. of VR Tap Operations with changing OPF objective function

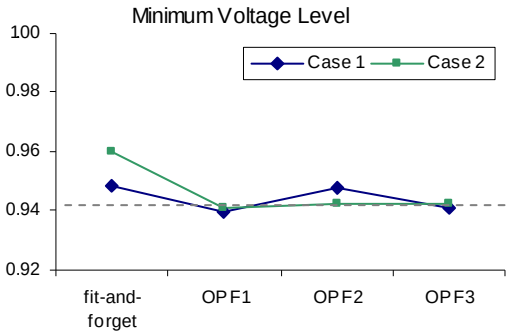

Figure 4.55: Minimum voltage levels with changing OPF objective function

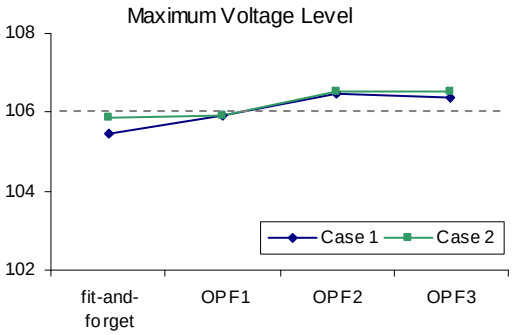

Figure 4.56: Maximum voltage levels with changing OPF objective function

There were however, some negative network impacts and drawbacks to the alternative multi-objective OPF functions, such as instantaneous voltage excursion. Figure 4.55 and Figure 4.56 show the minimum and maximum recorded voltage levels measured in 5 second intervals. As discussed, the magnitude of these momentary breaches are not considered prohibiting and in fact can introduce confidence that the real time system consequences of connecting enhanced levels of DG capacity in this manner are not likely to cause as severe voltage excursions as may have been first feared. Where concern may lie is in the possibility that these voltage excursions occur frequently and for prolonged periods of time. Figure 4.57 and Figure 4.58 show that for the test cases studied, this was not an issue, with voltage levels remaining within the statutory voltage envelope for more than 95% of the sampled periods, when measured in 5 second intervals. To be compliant with the EN 50160 regulations on short term voltage excursions, the voltage level must not exceed the statutory voltage limit for more than

5% of the observation period, measured in 10 minute averages. Table VIII demonstrates that for each objective function in the full ANM scenario, the total number of voltage excursions, measured in 10 minute averages, over the total of the two 24 hour observation periods was within limits.

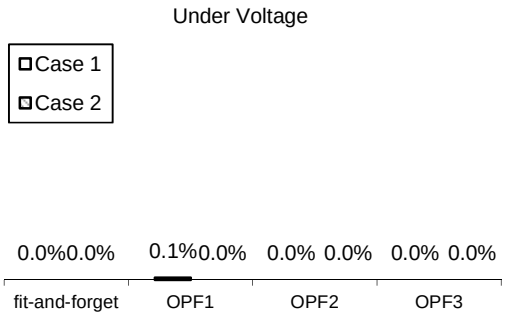

Figure 4.57: Under voltage excursion with changing OPF objective function

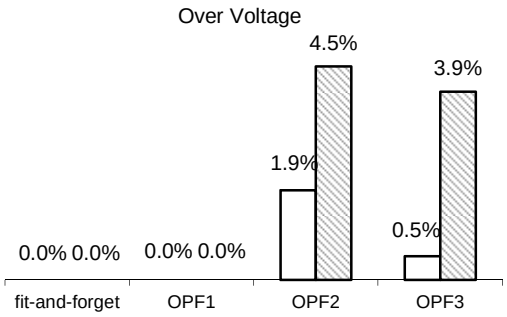

Figure 4.58: Over voltage excursion with changing OPF objective function

Table VIII: EN 50160 compliance with changing objective function

Over Voltage Excursion (%)				
	fit-and-forget	OPF1	OPF2	OPF3
Case 1	0.00%	0.00%	2.08%	0.69%
Case 2	0.00%	0.69%	5.56%	4.86%
Total	0.00%	0.35%	3.82%	2.78%
EN 50160 Compliant	Yes	Yes	Yes	Yes

Further observations of the system consequences highlighted a significant change in measured and detectable system energy losses and the circulation of reactive power. With a significant increase in the DG connected, the distribution feeder, real and reactive power flows and network losses were always going to increase. The change in system losses is proportional to the square of the change in total complex power flow. In the no DG scenario, network losses were 27.1 MWh and 19.6 MWh in case 1 and case 2 respectively. Figure 4.59 shows the magnitude of network losses for each OPF

formulation. Figure 4.60 shows the corresponding percentage of detectable system losses (i.e. losses as a proportion of the respective GSP system demand).

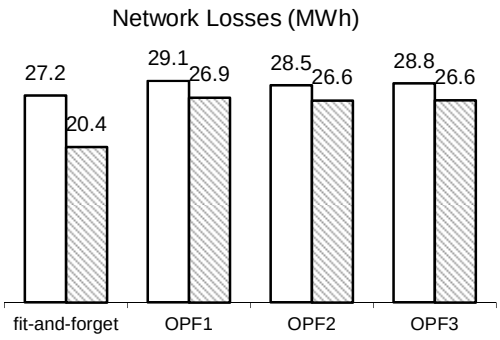

Figure 4.59: Network losses (MWh) with changing OPF objective function

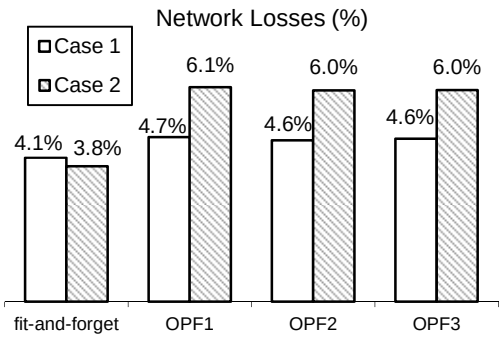

Figure 4.60 Network losses (%) with changing OPF objective function

The numbers illustrate an increase in the overall network losses, particularly for the high DG scenario of case 2. The increase in losses (approximately 8 MWh from the no DG scenario across the two cases) does not detract from the substantial increase in energy yield totalling 214.5 MWh across the two cases.

The circulation of reactive power is also likely to be of significant concern to DNOs. In the test cases studied the voltage rise effect at the point of DG connection was predominantly the limiting factor to DG capacity and energy yield. As such the ANM OPF routine tended to favour operation of the DG at a lagging power factor, where the DG unit absorbs reactive power. This created an increase in reactive power sourced from the GSP, as shown in Figure 4.64 and increased component loading. In this test example the levels of reactive power drawn from the assumed infinite GSP were not restrictive for the network. In the high demand, low DG scenario of case 1, the overall network power factor fell marginally from 0.97 lagging, in the fit-and-forget scenario, to 0.96 lagging in the full ANM scenario for all variations of the objective function. In the low demand, high DG scenario of case 2, this shift was more marked, with an overall network power factor of 0.93 lagging. This was again evident for all variations of the objective function in the Full ANM scenario. In a more complex network environment with multiple and larger DG units this could induce complicated power flows across the distribution network boundaries including the GSP. For example, there is the possibility that, if unchecked, the ANM OPF technique may lead to a situation

where there is a large scale export of real power in conjunction with a large scale import of reactive power. This could place significant stresses on the upstream network and is likely to be restricted by capacity constraints and/or congestion issues.

Should potential power flow regimes introduce complications for the upstream network, the scalable and adaptable approach to the OPF algorithm means that there are numerous adaptations and augmentations to the OPF formulation that can be developed to improve the performance of the OPF technique and implement a bespoke solution to unique system circumstances. For example, the import and export of real and reactive power flows can be restricted by additional (potentially time-dependent) constraints in the OPF formulation to make the external boundary flows compatible with the upstream network limitations. Otherwise, new multi-objective functions can be defined to minimise the real power curtailment and a weighted sum of the reactive power import.

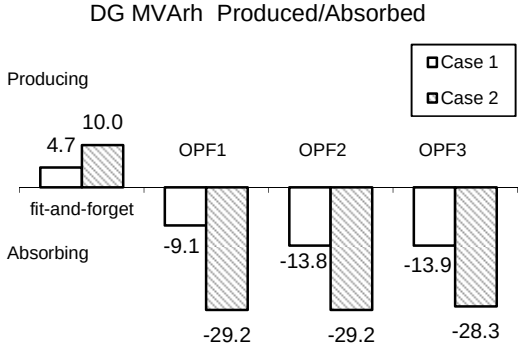

Figure 4.61: DG reactive power with changing OPF objective function

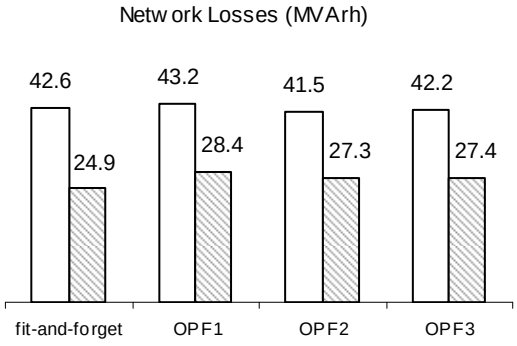

Figure 4.62: Reactive power charge with changing OPF objective function

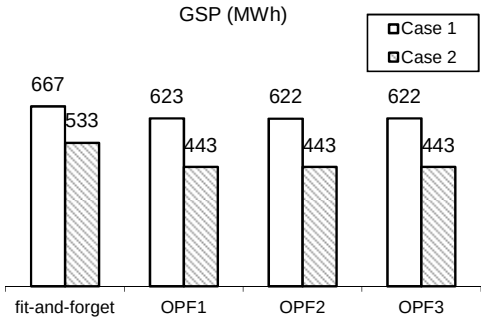

Figure 4.63: GSP real power transfer with changing OPF objective function

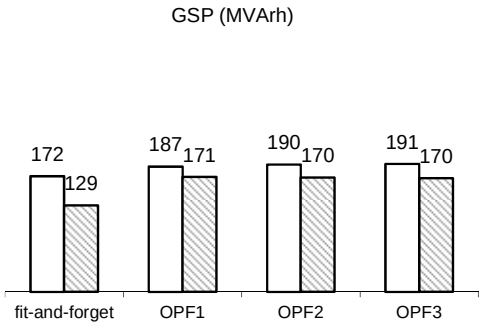

Figure 4.64: GSP reactive power transfer with changing OPF objective function

4.5 POWER FLOW SIMULATIONS WITH RECEDING-HORIZON OPF

The Receding-Horizon principle was also tested as a means of improving the application and implementation of the ANM OPF technique. The RHOPF formulation operates on the same 5 minute control cycle as before but extends the number of successive intervals that the optimisation routine is solved over, producing a sequence of upcoming optimally prescribed control actions for each control cycle. In that respect, the tap changing actions of the network transformers are not prescribed or acted on randomly or discontinuously. In theory, the extended time horizon of the optimisation, driven by forward looking forecasts of generation and demand, provides a longer term view of the required control actions with the potential to avoid unnecessary and short term control actions.

This did, however, require a more progressive and forward looking means of forecasting network power flow injections and demands in order to drive the network settings in anticipation of changing network power flows. As discussed earlier, it is well acknowledged that the best means of forecasting data within the short term operational time frame is persistence forecasting. However, from the literature study and discussions in Section 3.7, it was determined that more intelligent methods of data forecasting than persistence may be possible over the time scales concerned and that a reasonable assimilation of likely forecast data could be approximated by a simple weighted centred moving average (WCMA) smoothing process of the eventual time series variations. In this technique, a stream of half-hourly forecast data was generated based on a third order moving average smoothing process. Forecast data was used to remove irregularities from the perfect load demand and wind production data sets and reflect the likely make up of statistically processed forecast data. Initial trials of a real-time receding-horizon OPF technique with smoothed WCMA *'forecast'* data were conducted to investigate and assess the possible benefits.

4.5.1 FULL ANM

Studies of the fully integrated ANM scheme were tested for the RHOPF routine with the standard minimise curtailment objective function, OPF1. Here the forecast horizon was extended to 30 minutes and comprised of six intervals of 5 minutes in length that had

upcoming power flow injections linearly interpolated from a projected half-hourly forecast.

RHOPF1: $$Min \sum_{g \in G} p_g^{curt}(k+j|k) \qquad j = 1...6 \tag{35}$$

Warm start conditions across the horizon for each successive RHOPF solution were inferred from the last converged solution of the RHOPF.

In this analysis, the proxy distribution network continues to operate independently as before, performing power flow solutions at 5 second intervals and with the OLTC control practices operating autonomously as and when required. Prior to the beginning of each 5 minute control cycle, the distribution management system, samples network state information which, along with a projected forecast level for the half hour ahead is used to generate a control horizon for the RHOPF problem. At the beginning of each 5 minute control cycle the RHOPF analysis computes a trajectory of network control settings in 5 minute intervals for the half hour ahead. At the beginning of the next control cycle the process is repeated. This analysis is illustrated in Figure 4.65. All notional communication delays and DG ramping were the same as above.

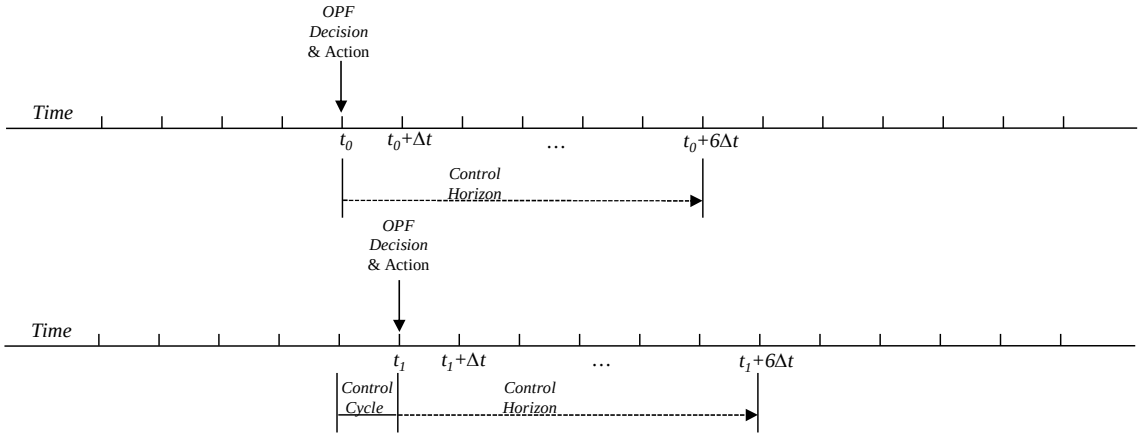

Figure 4.65: Receding-Horizon control cycle

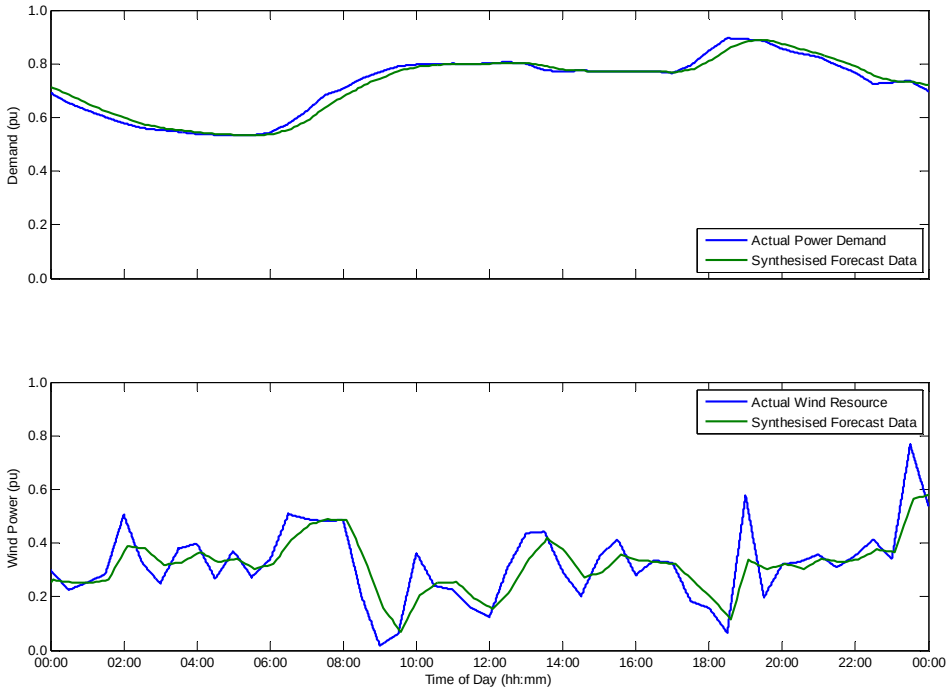

Figure 4.66: Synthesised forecast data case 1 – Winter Weekday

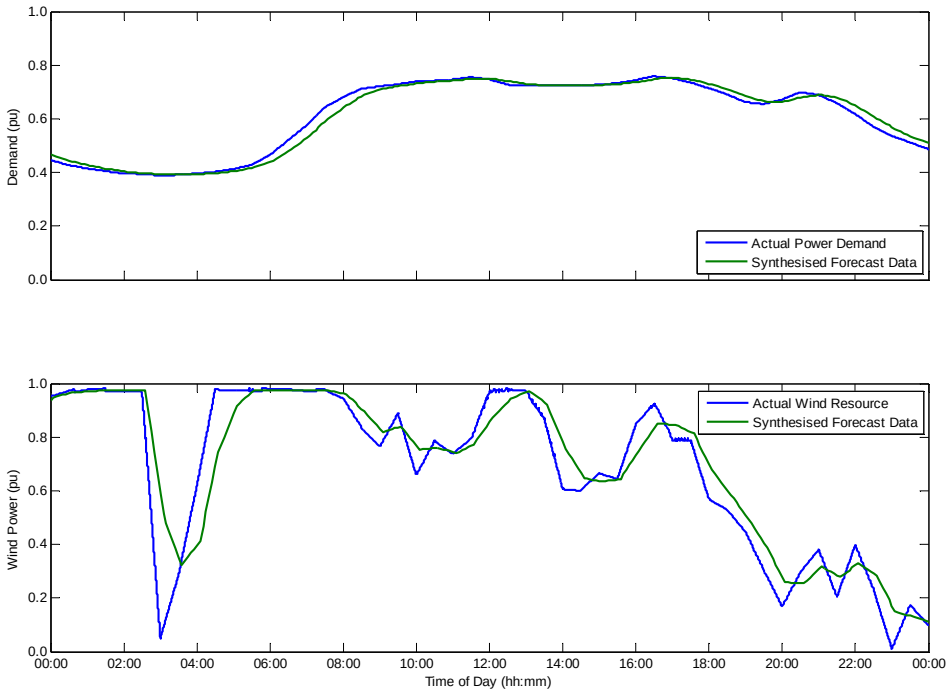

Figure 4.67: Synthesised forecast data case 2 – Summer Weekend

In this section two analyses of the forecast data are investigated. Firstly the RHOPF technique is studied with the time series input data following the pre-processed stream of forecast data. This is referred to as RHOPF-A. In the second analysis, the input data to the RHOPF solution, was a linearly interpolated trajectory between the last measured network data and the linearly interpolated half hourly forecasted value. In this instance the point forecast value at each 5 minute control cycle, for which new network control set-points were scheduled, is close to the persistence value but less susceptible to high frequency deviations in the real time measurement data from the distribution network. This is referred to as RHOPF-B. An example of both RHOPF input data sets is illustrated in Figure 4.68. RHOPF-A has a single input analysis consisting of the Forecast Data (in green), for which the RHOPF formulation is solved repeatedly. RHOPF-B has a double input analysis consisting of the forecast data and the distribution network measurement. The RHOPF formulation in this case is the Horizon Forecast (black dotted line), which changes with each successive solution.

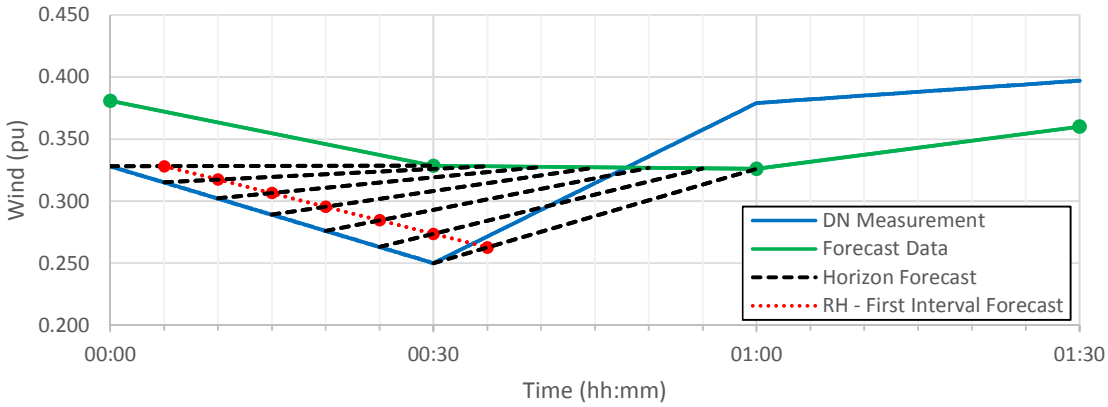

Figure 4.68: Illustration of the receding-horizon forecasting technique

Figure 4.66 and Figure 4.67 illustrate the comparisons between the synthesised forecast data against the actual network power injections and demands. As expected, much of the erratic deviation in the wind pattern was removed; the reduced disturbance in the generation profile shows a smoothed transition of the wind production over time. The WCMA was calculated from three half hourly known power flow measurements. The weights were biased such that the previous measurement (persistence) account for half of the final synthesised forecast value, with the present and following values providing a staggered level of minor guidance to the change in power flow injections.

The time series of DG curtailment settings and real power output levels in each case are shown in Figure 4.69 to Figure 4.72, for the RHOPF-A and RHOPF-B forecasting variations.

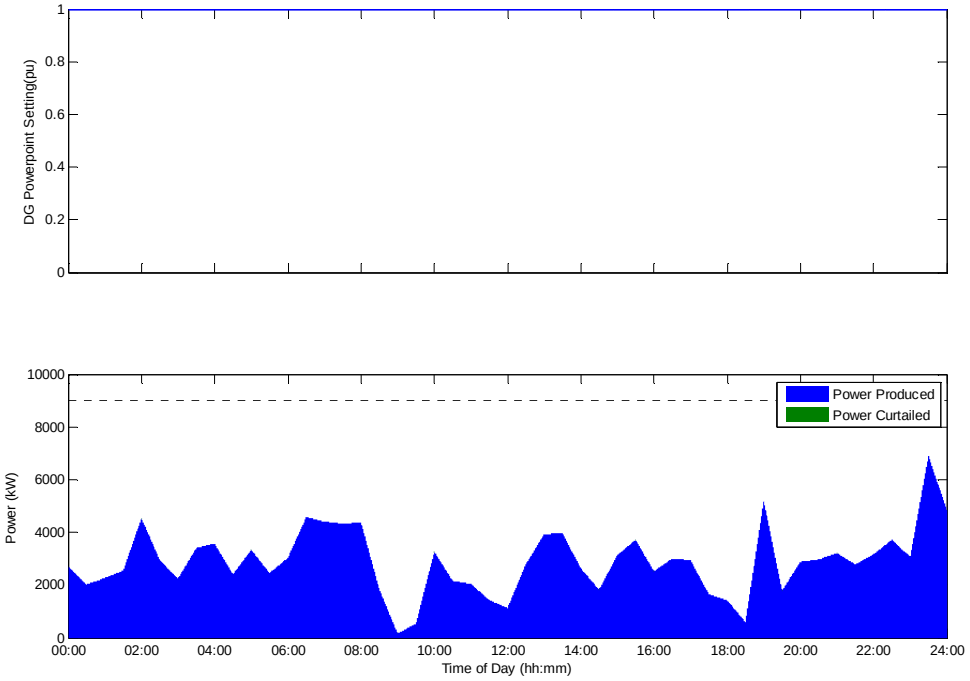

Figure 4.69: Curtailment settings for the full ANM RHOPF-A solution case 1

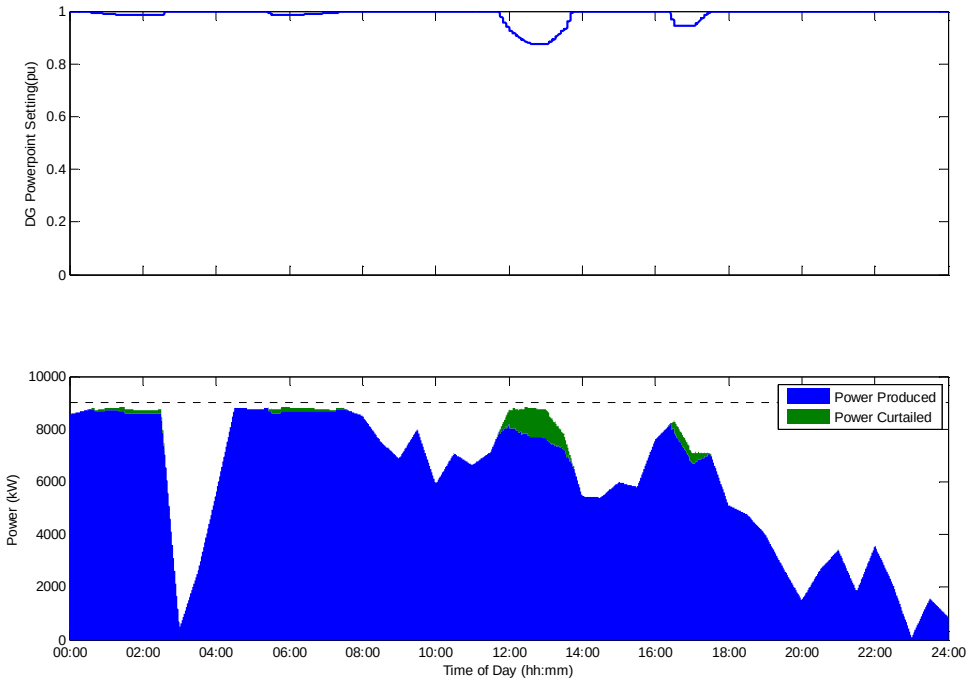

Figure 4.70: Curtailment settings for the full ANM RHOPF-A solution case 2

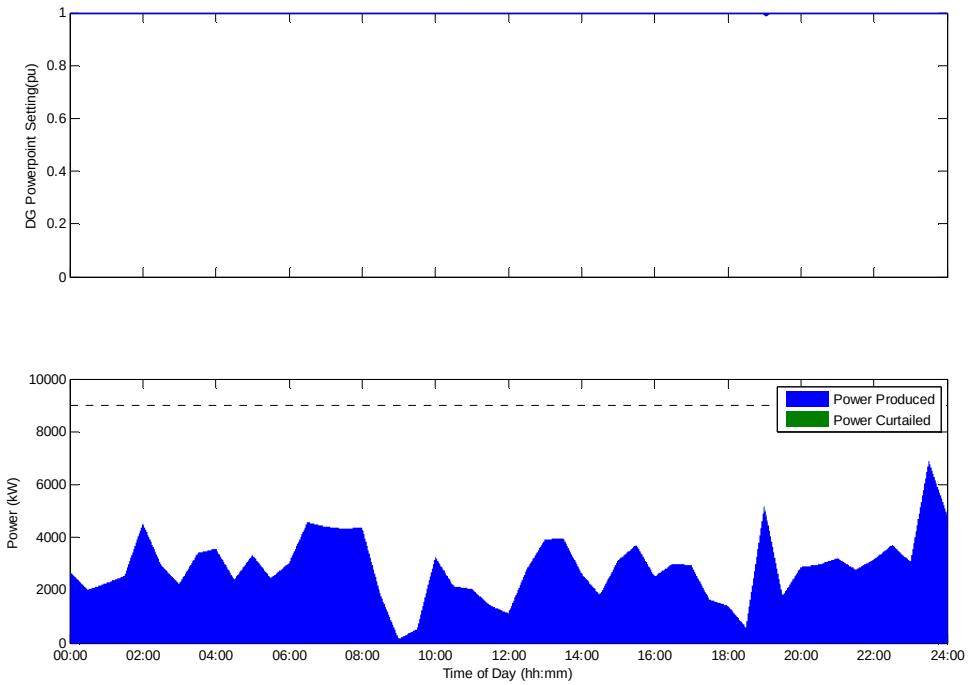

Figure 4.71: Curtailment settings for the full ANM RHOPF-B solution case 1

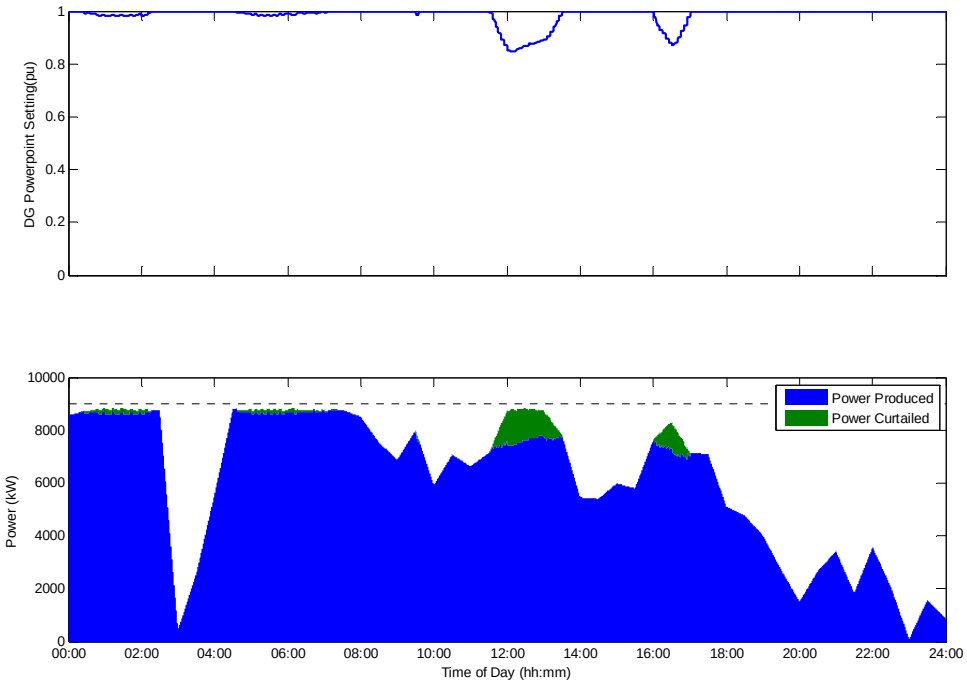

Figure 4.72: Curtailment settings for the full ANM RHOPF-B solution case 2

In case 1 there was no curtailment required in either scenario. In case 2, energy curtailment for both RHOPF analyses was reduced over the OPF analyses. A marginal, 0.6 MWh increase in energy curtailment was evident between the RHOPF-A the RHOPF-B study.

Figure 4.73 shows the time series trace of tap positions over both simulation periods. As expected from the input data, the figure illustrates a pronounced smoothing of the tap variation over time when compared with the standard single scenario minimise curtailment OPF shown in Figure 4.30.

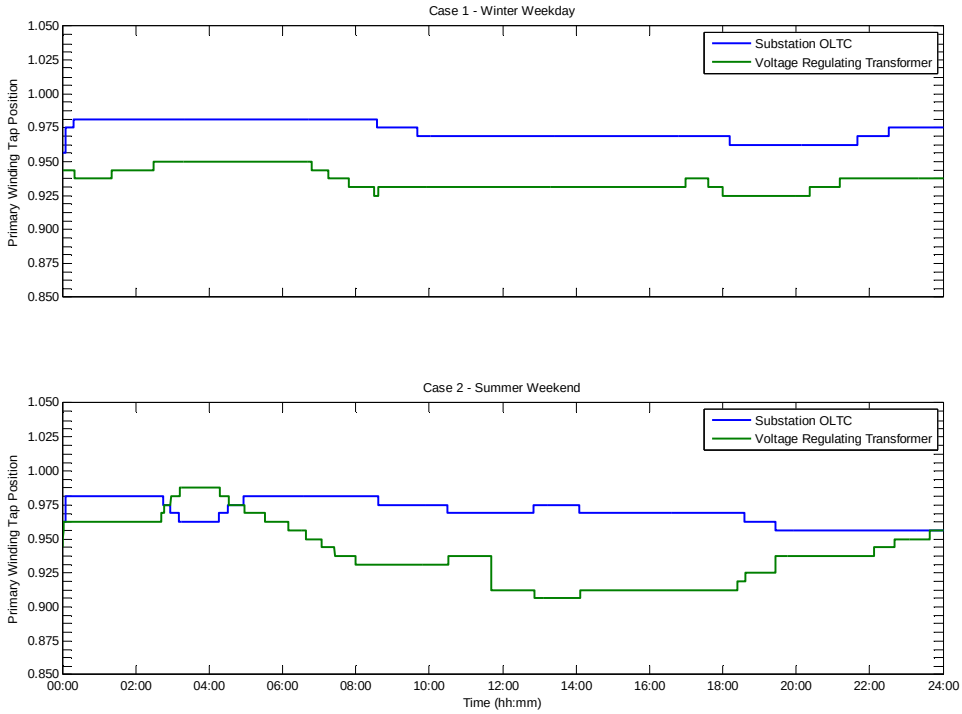

Figure 4.73: Tap positions for the full ANM RHOPF-A

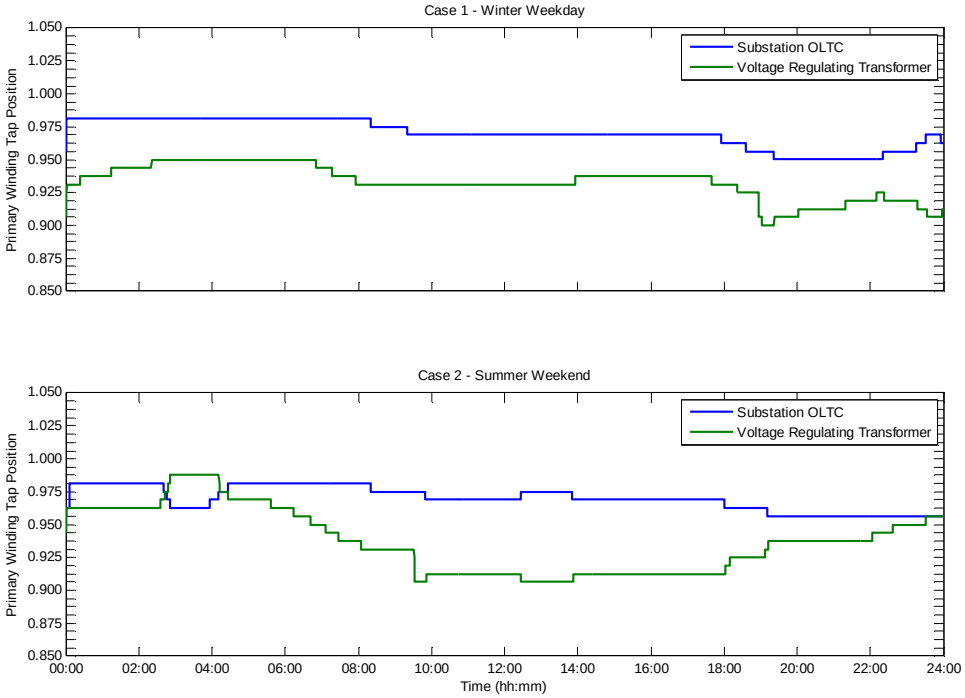

Figure 4.74: Tap positions for the full ANM RHOPF-B

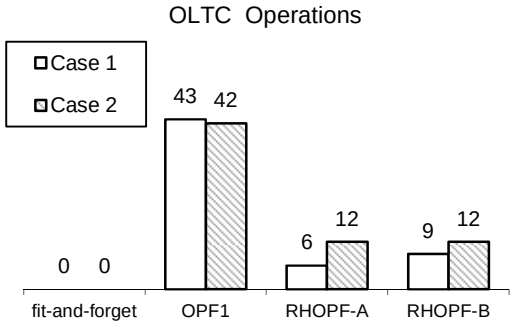

Figure 4.75: No. of OLTC tap operations with changing forecast data

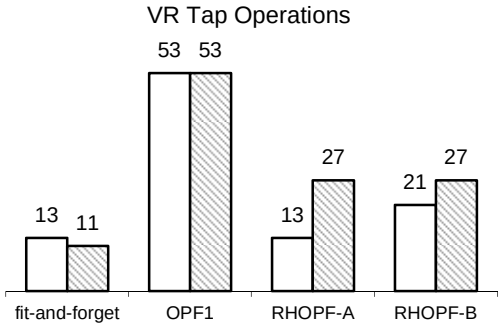

Figure 4.76: No. of VR tap operations with changing forecast data

A key benefit from the Receding-Horizon technique was the significant reduction in the number of tap changing actions. A numeric comparison of the tap changing actions is presented in Figure 4.75 and Figure 4.76. This shows that the repetitive long term optimisation routine can stabilise the temporal variation exhibited for the single scenario OPF formulation.

A drawback to the RHOPF formulation was the potential for differences to occur between the actual and forecast power flow injections to result in excursions from the statutory voltage envelope. This was more significant in the RHOPF-A single stream, forecasting scenario, as a result of errors introduced from the synthesised forecast data. The voltage profile traces are shown in Figure 4.77 and Figure 4.78. As the active constraint on the OPF, voltage rise at the point of connection continued to be a significant concern. Large forecasting errors led to greater levels of voltage violation with a peak of 1.0718 pu and voltage excursions occurring more frequently, when measured in 10 minute averages over the total non-continuous 48 hour period of analysis total overvoltage excursion was 6.25% slightly above the 5% limit.

At this timescale, the synthesised forecast data in RHOPF1-A did not properly reflect upcoming changes in power production. Discrepancies between the forecasted levels of generation and real time output were larger than with the persistence forecasting methodology. The discrepancy between forecasted and real time power production resulted in short term voltage spikes beyond the upper statutory voltage limit. This

occurred consistently with a large rise in DG production before data forecasts were able to respond to sharp changes in production.

From these results it is reasonable to conclude that the Receding-Horizon methodology with the single input RHOPF-A forecasting routine did improve the performance of the real time OPF routine as intended, but was limited at these time scales by the availability of suitable forecasting methodologies for wind power production.

In the RHOPF-B forecasting scenario, residual voltage excursion was limited over the two observational test periods to a maximum value of 1.0635 pu and a percentage occurrence of 3.4%, again measured in 5 second intervals, well within the recommended limits. From these results it was reasonable to conclude that the Receding-Horizon methodology, with the double input RHOPF-B forecasting methodology, significantly improved the performance of the real time OPF routine as intended.

A quantitative comparison between the RHOPF-B and the OPF2 objective function is discussed in the following subsection.

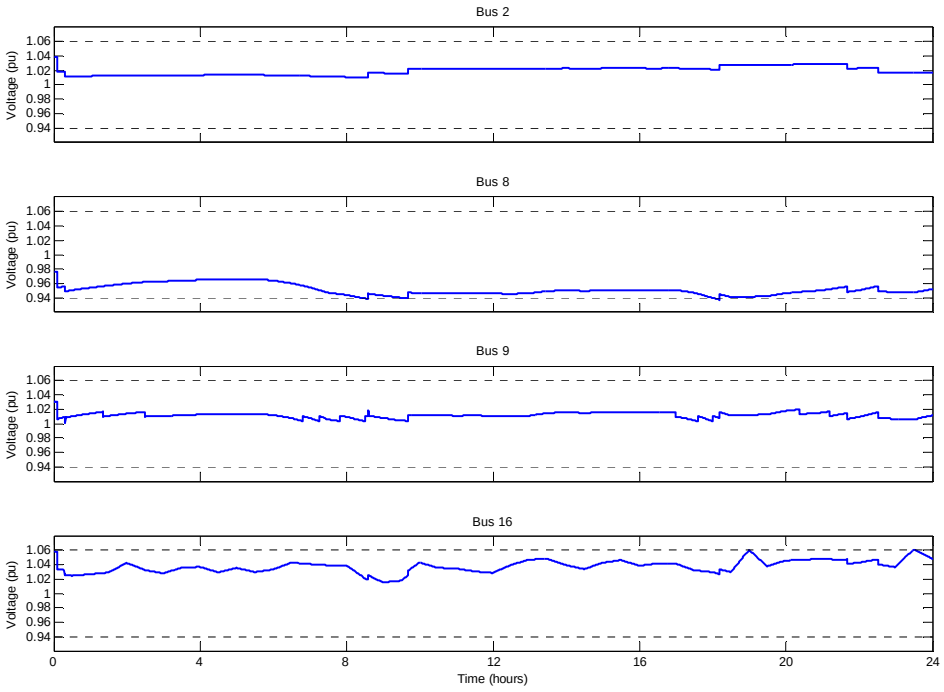

Figure 4.77: Voltage profiles for the full ANM RHOPF-A solution case 1

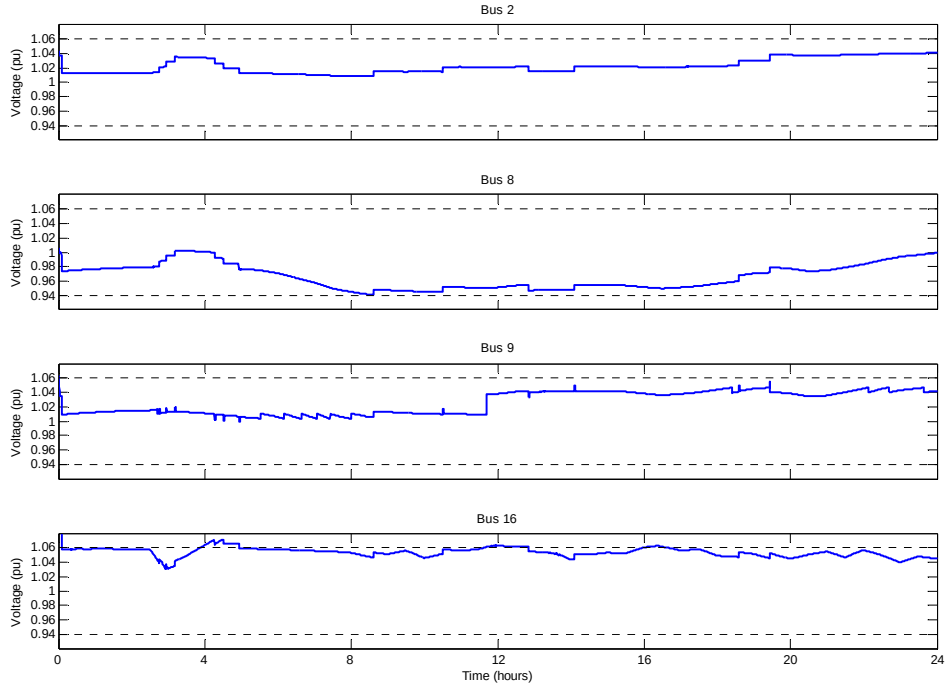

Figure 4.78: Voltage profiles for the full ANM RHOPF-A solution case 2

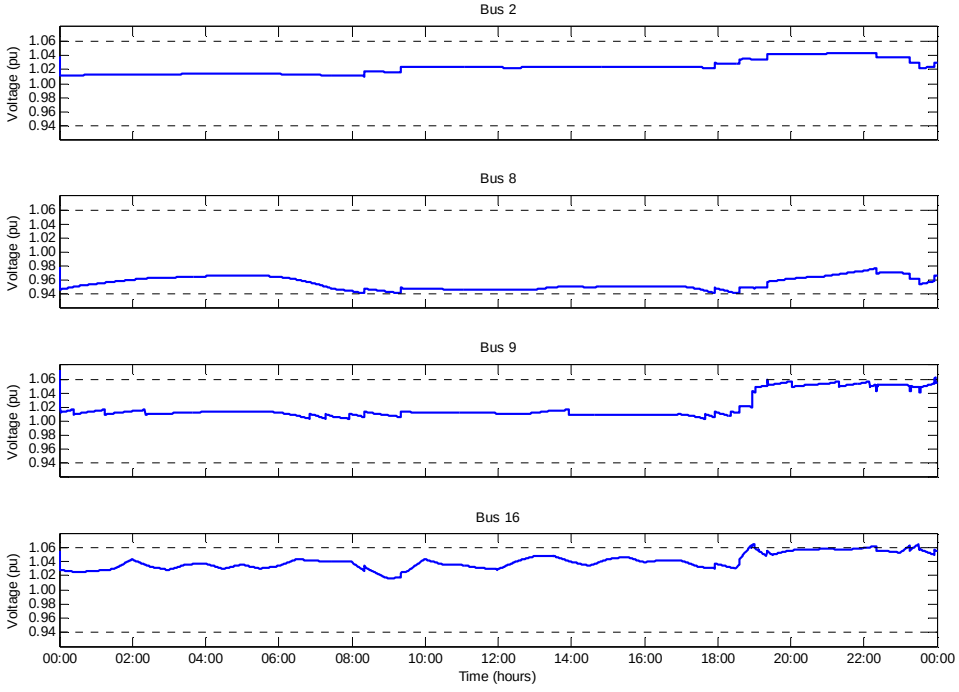

Figure 4.79: Voltage profiles for the full ANM RHOPF-B solution case 1

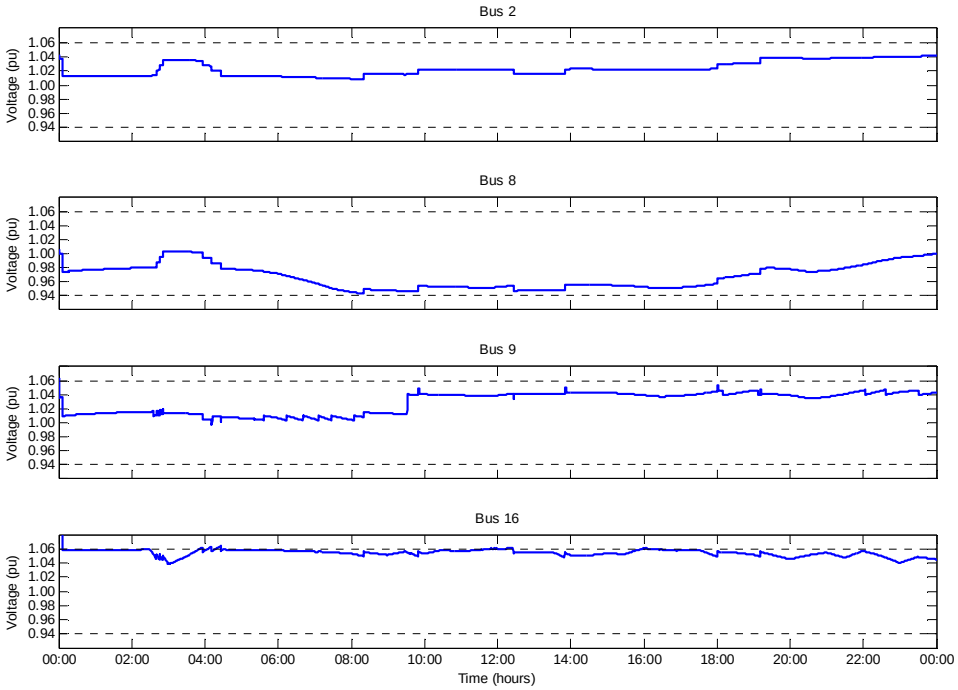

Figure 4.80: Voltage profiles for the full ANM RHOPF-B solution case 2

4.5.2 COMPARISON AND SUMMARY

A comparison of the important g of reactive power in case 1. With a reduction over the OPF1 results in the RHOPF-B and an increase in the OPF2 analysis. This was also evident in the RHOPF-A analysis. In each RHOPF case the ANM OPF favours DG power factor set-point closer to unity, during periods of relatively low wind resource.

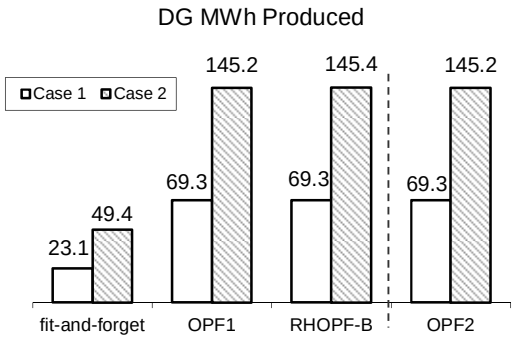

Figure 4.81: DG MWh production with changing forecast data

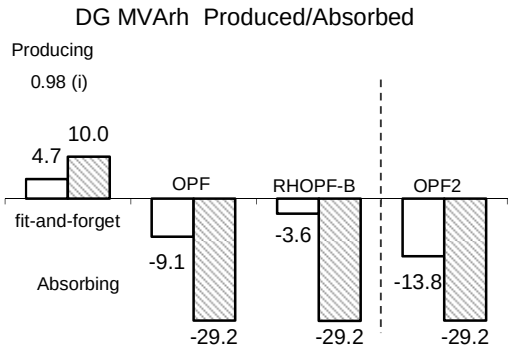

Figure 4.82: DG MVArh production with changing forecast data

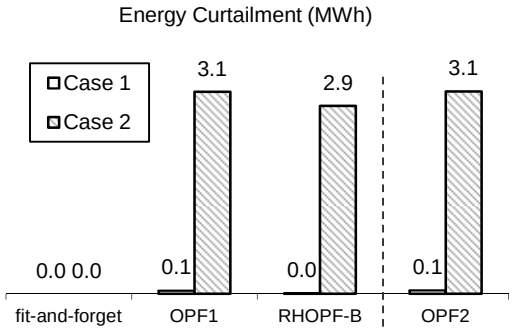

Figure 4.83: Energy curtailment MWh with changing forecast data

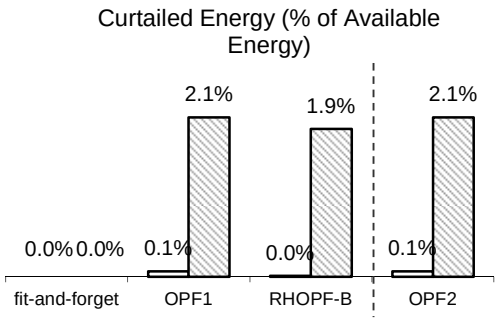

Figure 4.84: Energy curtailment (%) with changing forecast data

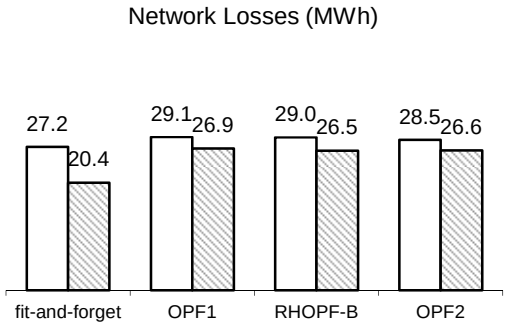

Figure 4.85: Network losses (MWh) with changing forecast data

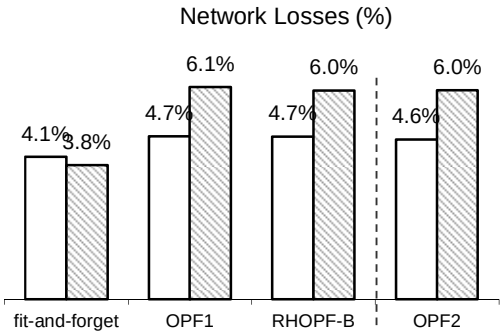

Figure 4.86: Network losses (%) with changing forecast data

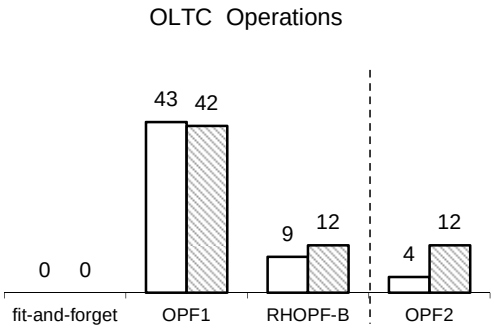

Figure 4.87: No. of OLTC tap operations with changing forecast data

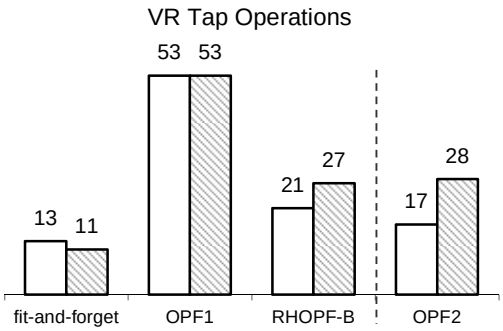

Figure 4.88: No. of VR tap operations with changing forecast data

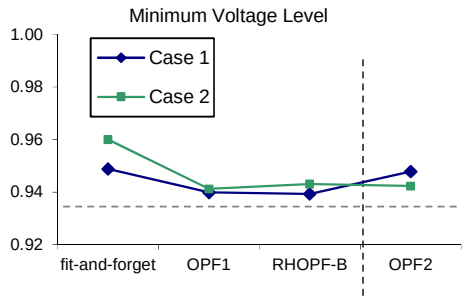

Figure 4.89: Minimum voltage level with changing forecast data

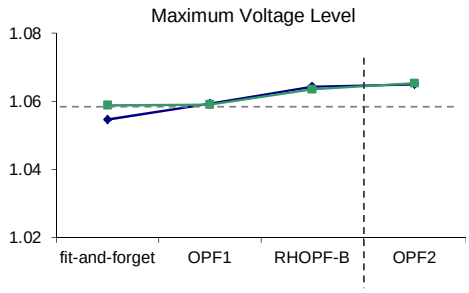

Figure 4.91: Maximum voltage level with changing forecast data

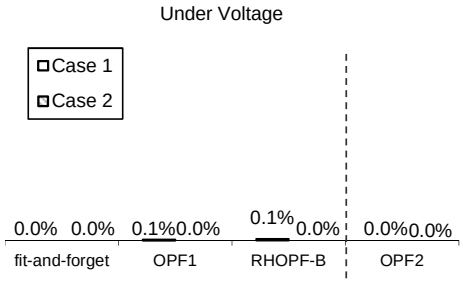

Figure 4.90: Overvoltage occurrences with changing forecast data

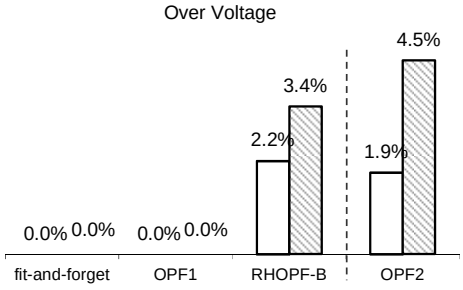

Figure 4.92: Undervoltage occurrences with changing forecast data

From the comparisons, it is evident that both strategies offer a marked improvement over the standard OPF1 technique. It also evident, that the minimum deviation objective function has a marginally reduced network impact for this simple demonstration network. However, at this stage it would not be advantageous to define a better or preferred technique, as each technique may be determined to suit specific network cases. While these analyses are conducted quantatively against each other, it is no the intention that they would be pursued exclusively and that multi-faceted solutions made up of both advanced concepts could harmonise the advantages of both.

Table IX: Results summary case 1 - winter weekend

Case 1 - Winter Weekday	fit-and-forget	OPF1	RHOPF1-A	RHOPF1-B	OPF2
DG MW	3	9	9	9	9
DG MWh	23.1	69.3	69.3	69.3	69.3
DG MVArh	4.7	-9.1	0.0	-3.6	-13.8
EC MWh	0.0	0.1	0.0	0.0	0.1
EC (%)	0.0%	0.1%	0.0%	0.0%	0.1%
Capacity Factor	32.1%	32.1%	32.1%	32.1%	32.1%
GSP MWh	667.0	622.8	623.0	622.7	622.2
GSP MVArh	172.4	186.8	178.3	177.3	189.8
GSP power factor	0.97	0.96	0.96	0.96	0.96
Losses MWh	27.2	29.1	29.4	29.0	28.5
Losses MVArh	42.6	43.2	43.9	39.2	41.5
Losses (%)	4.1%	4.7%	4.7%	4.7%	4.6%
Min Voltage	0.9488	0.9398	0.9376	0.9393	0.9478
Peak Voltage	1.0546	1.0593	1.0609	1.0643	1.0650
UnderVoltage	0.0%	0.1%	1.8%	0.1%	0.0%
OverVoltage	0.0%	0.0%	0.3%	2.2%	1.9%
OLTC Tap changes	0	43	6	9	4
VR Tap changes	13	53	13	21	17

Table X: Results summary case 2 - summer weekend

Case 2 - Summer Weekend	fit-and-forget	OPF1	RHOPF1-A	RHOPF1-B	OPF2
DG MW	3	9	9	9	9
DG MWh	49.4	145.2	146.0	145.4	145.2
DG MVArh	10.0	-29.2	-29.3	-29.2	-29.2
EC MWh	0.0	3.1	2.3	2.9	3.1
EC (%)	0.0%	2.1%	1.6%	1.9%	2.1%
Capacity Factor	68.6%	67.2%	67.6%	67.3%	67.2%
GSP MWh	532.7	443.4	442.3	442.8	443.1
GSP MVArh	128.8	171.4	170.5	166.4	170.3
GSP power factor	0.97	0.93	0.93	0.94	0.93
Losses MWh	20.4	26.9	26.6	26.5	26.6
Losses MVArh	24.9	28.4	27.2	23.3	27.3
Losses (%)	3.8%	6.1%	6.0%	6.0%	6.0%
Min Voltage	0.9600	0.9412	0.9411	0.9430	0.9422
Peak Voltage	1.0588	1.0590	1.0718	1.0635	1.0653
UnderVoltage Excursion	0.0%	0.0%	0.0%	0.0%	0.0%
OverVoltage Excursion	0.0%	0.0%	12.3%	3.4%	4.5%
OLTC Tap changes	0	42	12	12	12
VR Tap changes	11	53	27	27	28

4.6 CHAPTER SUMMARY

The performance of the proposed real time OPF technique from Chapter 3 has been evaluated in this chapter. This entailed the conduction of high resolution, time sequential steady state network simulations to infer and model the 'real time' network characteristics and response.

The OPF technique was employed to coordinate and actively schedule the system control pre-sets under increasingly comprehensive measures of new ANM concepts. It was shown to determine in real time appropriate active DG and responsive network asset controller settings to minimise the real power curtailment at each time step. Over time, this approach led to a maximisation of energy yield from renewable non-firm DG. In the simplified EHV1 – ANM network test case energy yield from a single non firm renewable DG increase by 200%.

Testing of the real time OPF technique identified limitations of the standard OPF formulation, including spurious switching of network controllers and minor voltage excursion due to residual variation between the OPF solution and the power flow solutions of the distribution network.

New approaches to minimise control switching and maximise network benefit were tested. These were a multi-objective function that penalises unnecessary disturbance of network control settings and a receding-horizon OPF to determine a longer term sequence of controlling set points, making control decision based on projected power flow regimes and not purely on current conditions.

Results of the multi-objective formulation showed a significant reduction in spurious tap-changing action, but minor system voltage excursions were still a concern. Further adaptation was tested to favour in the OPF, new target network control settings further away from the statutory system operating boundaries. This was shown to reduce the frequency of observed voltage excursions.

The Receding-Horizon principle was also demonstrated to reduce, against the standard snapshot OPF1 strategy, unnecessary and spurious switching in the active DG and responsive network asset controller actions. Two means of utilising forward-looking forecast data in the receding-horizon methodology were tested. In the first approach

where, the RHOPF technique relied solely on the infeed of forecast data extended the occurrence of voltage excursion close to and potentially beyond the recommended levels. In the second approach, the RHOPF technique was formulated repeatedly using an in-the-loop forecasting application to project real time network data measurements forward against an infeed of higher resolution forecast data. While residual voltage excursion was still observed in this analysis, it was far reduced compared to the first approach and well within the recommended levels.

Results have illustrated that the new advanced formulations of the ANM OPF technique can significantly improve the temporal stability and maximise the network benefit from real time OPF techniques. In the simple demonstration network analysed in this chapter the improvements using all advanced formulations were comparable with the OPF3 analysis demonstrating the best results.

Chapter 5

ANM of Larger Distribution Networks

5.1 INTRODUCTION

Chapter 4 validated the simulation procedure and tested the ANM OPF formulations in a simple network configuration. The results showed that the use of OPF techniques were suitable for determining in real time, active DG and responsive network asset controller settings to minimise real power curtailment from renewable non-firm DG. Advanced formulations were shown to improve the response of time sequential OPF solutions by reducing unnecessary switching actions under varying power flow injections and demand.

This chapter explores the impact of the real-time ANM OPF formulations in large networks with multiple DG developments. The same testing procedures conducted in Chapter 4 were repeated.

In section 5.2 the advanced formulations of the ANM OPF technique were investigated on the simplified EHV1 – ANM network with three DGs from two independent wind resource and one tidal resource pattern. Simulations were conducted using the same time frame of 5 minute OPF control cycles and 5 second power flow solutions deployed in Chapter 4.

In sections 5.3 & 5.4, the advance formulations were extrapolated to the full EHV1 network with 6 renewable non-firm DGs in two clusters of renewable energy resources. Section 5.3 continues with the same operational time frames as analysed previously. Section 5.4 investigates the potential for ANM OPF algorithms on an alternative time

scale. Simulations are conducted over a longer time period, using a 15 minute OPF control cycle and taking data measurements from the proxy distribution network at 5 minute intervals.

Case studies are extended to stress the proposed OPF routine with a variety of supply and demand combinations. The impact of the OPF techniques and the time series of system consequences are discussed. Limitations of the real time OPF techniques are identified and addressed.

An interactive network case study is presented in section 5.4 with the centralised optimal scheduling of active DG and responsive network control assets in combination with local (or decentralised) autonomous DG controllers. This system reflects the ideology and functionality identified in the extensive literature survey discussed in Chapter 2.

5.2 REAL TIME OPF SIMULATIONS WITH MULTIPLE DGS

Having successfully demonstrated the potential for ANM control with advanced real time OPF techniques for a single DG development, the methodology was tested for three different DG developments in the simplified EHV1 – ANM network.

The configuration is shown in Figure 5.1. A second wind farm and a tidal array were considered at buses 7 and 12 respectively. Maximum installed capacity was identified using the same methods as detailed in section 3.8. With the fit-and-forget practices, maximum DG capacity at buses 7 and 12 was constrained at 3.5 and 2 MW respectively due to voltage rise at the point of connection. With the integrated full ANM strategy the network headroom to accommodate DG at these locations was increased to 11 MW for the wind farm at bus 7 and 8MW for the tidal array at bus 12. The wind farm capacity at bus 16 under both the fit-and-forget and full ANM strategies was consistent with Chapter 4. The optimisation was formulated in the full ANM scenario for the OPF1, OPF2, OPF3 and both RHOPF1 analyses, RHOPF-A and RHOPF-B. Simulations were carried out over the same 24 hour observational test cases as before.

In this network configuration the constraint on network headroom for each DG development was voltage rise at the point of connection. Thermal loading of

transmission lines and transformers was not an issue with the maximum loading levels on all network components well below capacity.

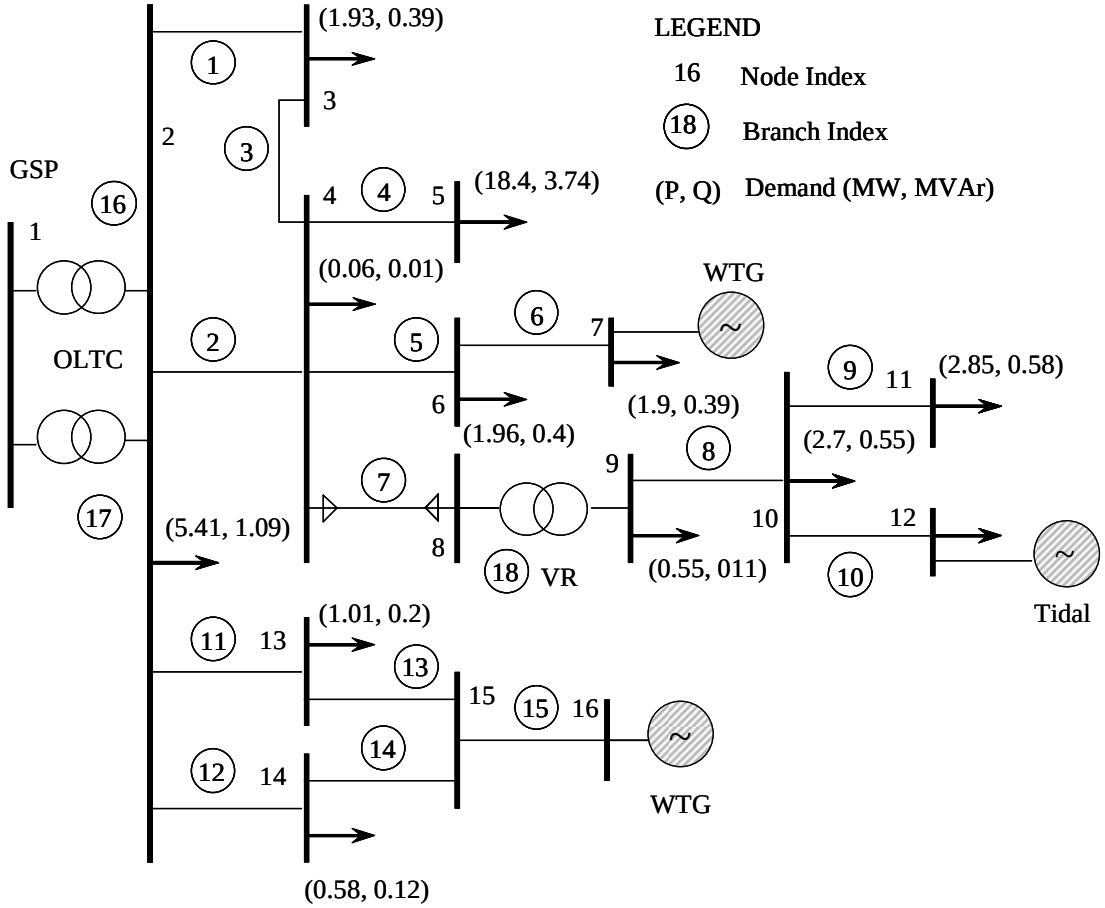

Figure 5.1: Simplified EHV1 - ANM network with three DG developments

The simulations are first presented in the initial OPF1 formulation, with a straight minimise curtailment objective function and persistence forecasting methodology. Here the OPF techniques converged successfully through time and identified based on forecasted levels of generation and demand, variable system control settings to maintain statutory system voltage levels, allowing the high level of DG capacity to remain operating and maximise the system-wide energy yield.

Normalised power production patterns for the two wind farm and tidal array DGs are shown, together with variable demand, for the two observational test cases in Figure 5.2 and Figure 5.3. Case 1 again represents a period of low to moderate DG resource, with a

combined capacity factor of around 22%. Case 2 represents a period of high DG resource with a combined capacity factor of just less than 53%.

A comparison of the energy yield and energy curtailed for both test case observational periods between the fit-and-forget approach, the curtailment only OPF scenario and the full ANM OPF is shown in Figure 5.4 and Figure 5.5.

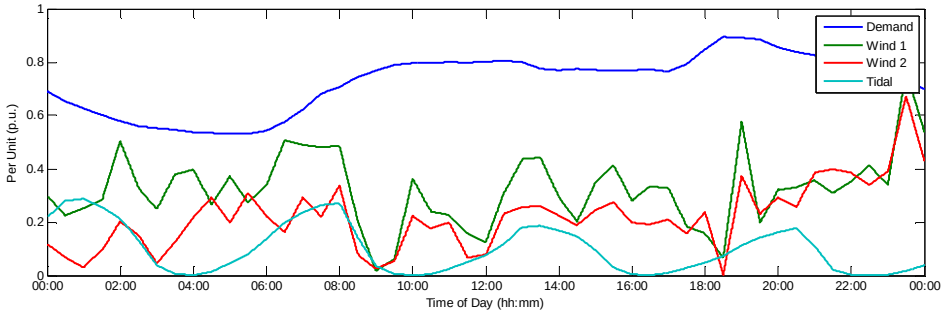

Figure 5.2: Normalised resource and demand profiles for case 1

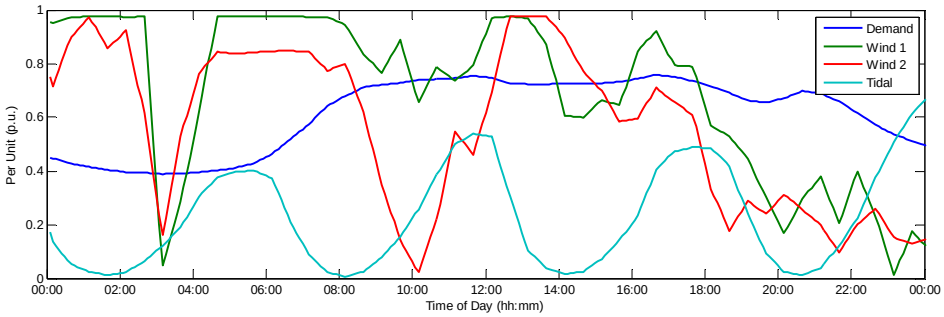

Figure 5.3: Normalised resource and demand profiles for case 2

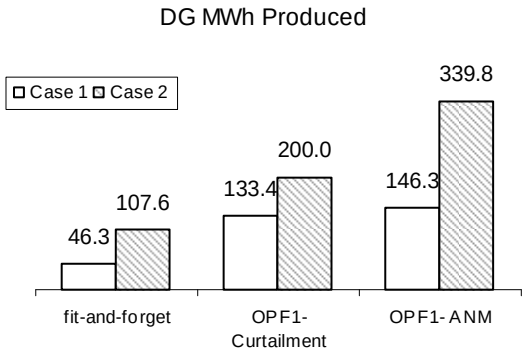

Figure 5.4: Energy yield

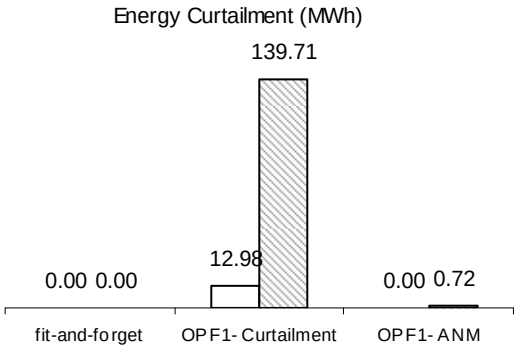

Figure 5.5: Energy curtailment

In each analysis there was a significant increase in energy yield. In the full ANM scenario, no energy curtailment was necessary in case 1, with a very small amount of curtailment required in case 2. The real power production levels for each DG development in the full ANM scenario case 2 is shown in Figure 5.6 to Figure 5.8. In this case study, when system demand was low during the night and wind power output from both wind farms was high, real power flow across the distribution network GSP reverses and the distribution network begins exporting power to the infinite grid. The complex power flow across the distribution network GSP is shown in Figure 5.9.

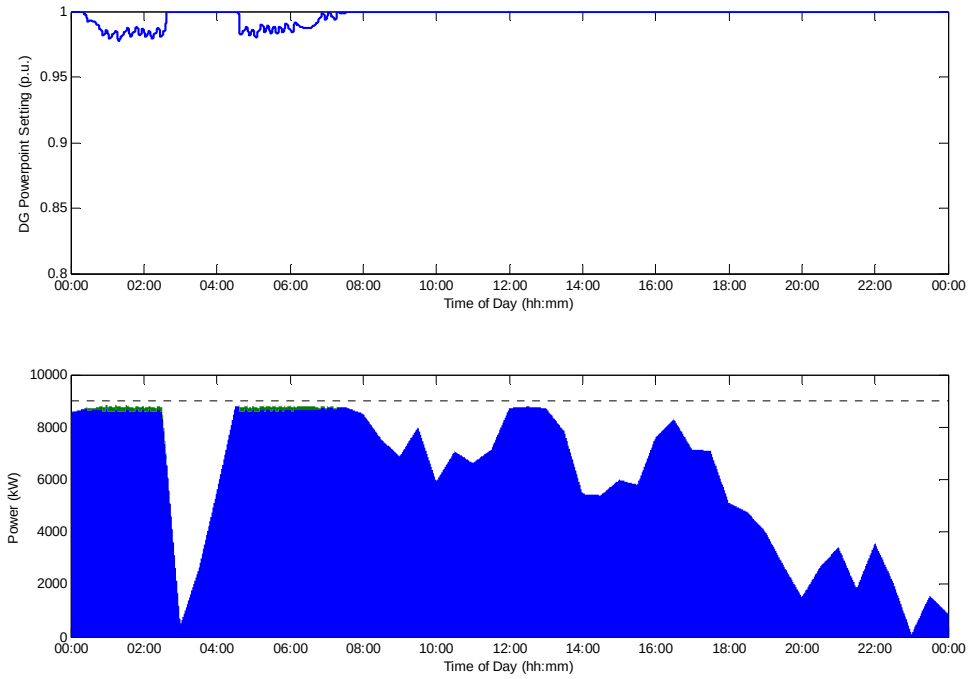

Figure 5.6: Curtailment settings in the OPF1 – full ANM formulation for the DG at Bus 16 case 2

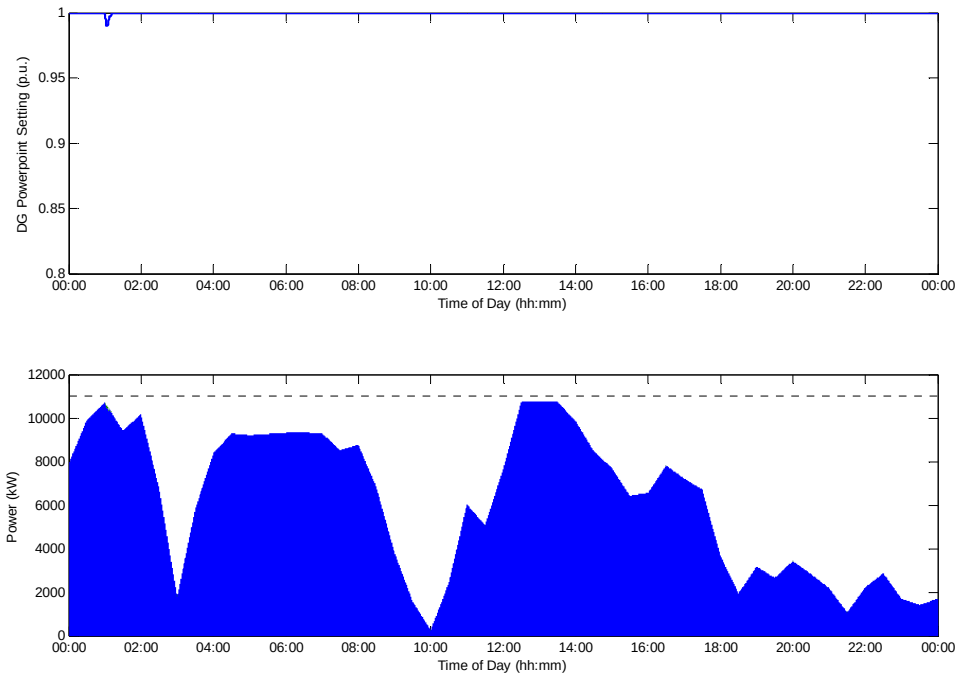

Figure 5.7: Curtailment settings in the OPF1 – full ANM formulation for the DG at Bus 7 case 2

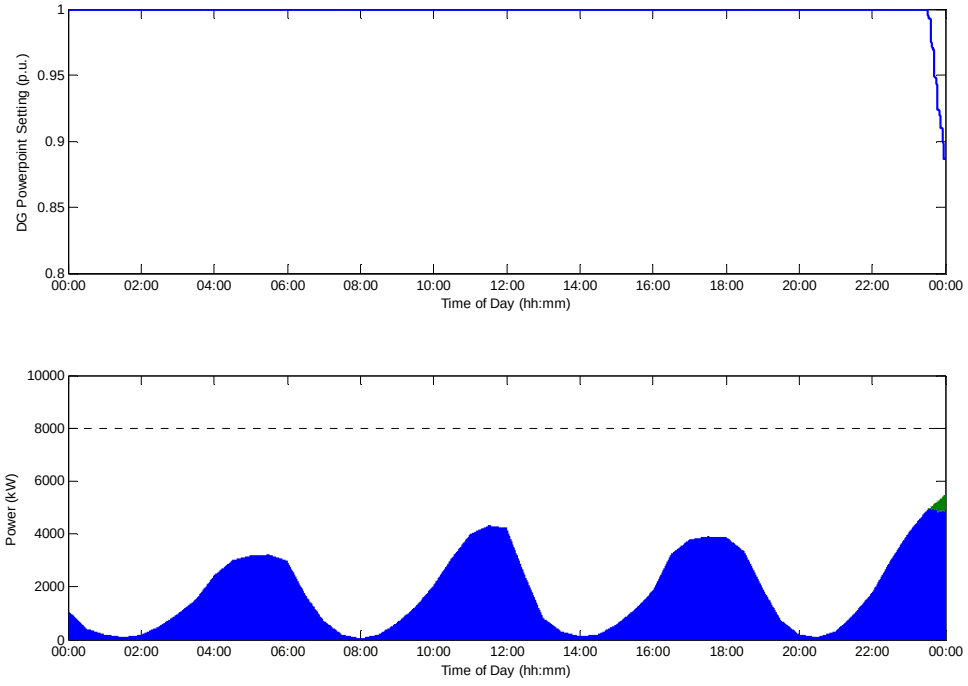

Figure 5.8: Curtailment settings in the OPF1 – full ANM formulation for the DG at Bus 12 case 2

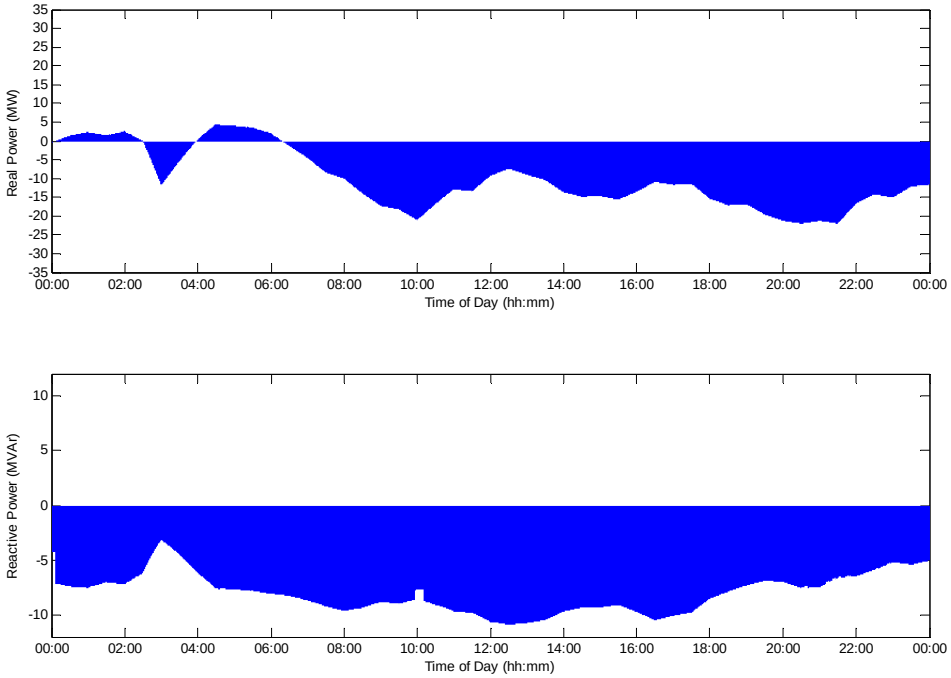

Figure 5.9: GSP real and reactive power flows in the OPF1 – full ANM formulation case 2

The voltage profiles at each of the DG connection points are shown in Figure 5.11 and Figure 5.13, alongside the corresponding traces of tap positions in Figure 5.10 and Figure 5.12. While the OPF1 formulation worked well to determine new network control settings. Spurious switching of tap changing transformers in particular, resulted in network voltage excursion from the statutory voltage envelope, which are likely to trip overvoltage protection relays, as shown in Figure 5.13, particularly at bus 12.

As was seen for the single DG development discussed in Chapter 4, during periods of moderate or low levels of DG production a substantial level of spurious and unnecessary tap changing actions were evident with the continuous automation of the OPF1 formulation. This form of voltage profile would not be acceptable by a DNO as it breached voltage disturbance regulations of the distribution code [109] (in accordance with Engineering Recommendation P28) in terms of the severity and frequency, with frequent voltage disturbances greater than 3% in magnitude.

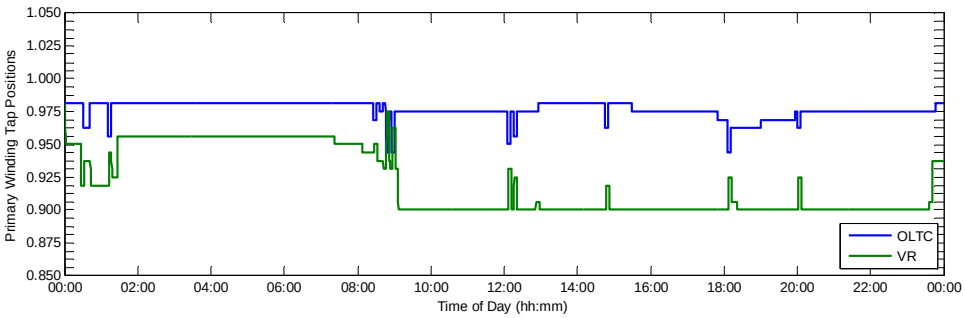

Figure 5.10: Tap positions in the OPF1 – full ANM formulation case 1

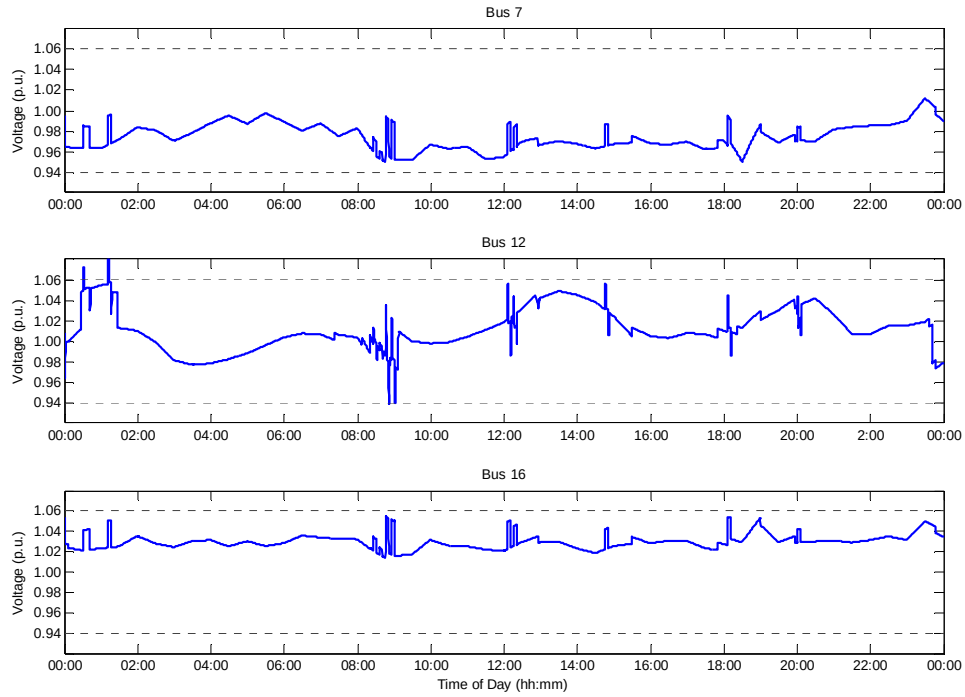

Figure 5.11: Voltage profiles at DG in the OPF1 – full ANM formulation case 1

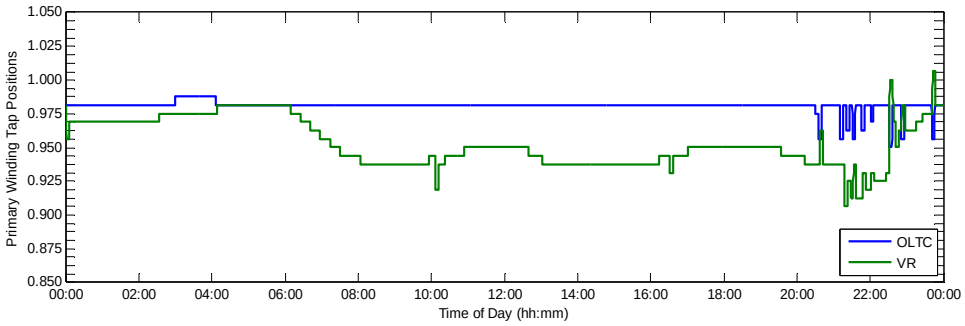

Figure 5.12: Tap positions in the OPF1 – full ANM formulation case 2

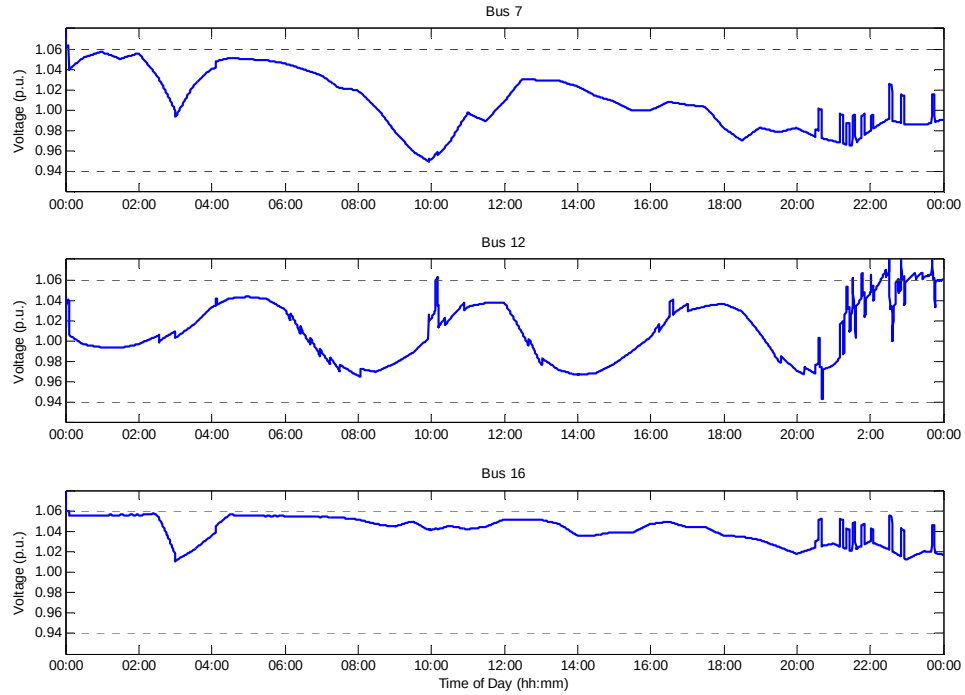

Figure 5.13: Voltage profiles at DG in the OPF1 – full ANM formulation case 2

Simulation of the same system over the same observational periods with the OPF2 formulation is shown in Figure 5.14 through Figure 5.17. Results showed that the OPF technique maintained system voltage levels within or sufficiently close to the statutory envelope for the duration of both test cases. The OPF2 formulation removed much of the spurious disturbances, but still featured a lot of unnecessary tap changing actions during periods of both high and low DG output.

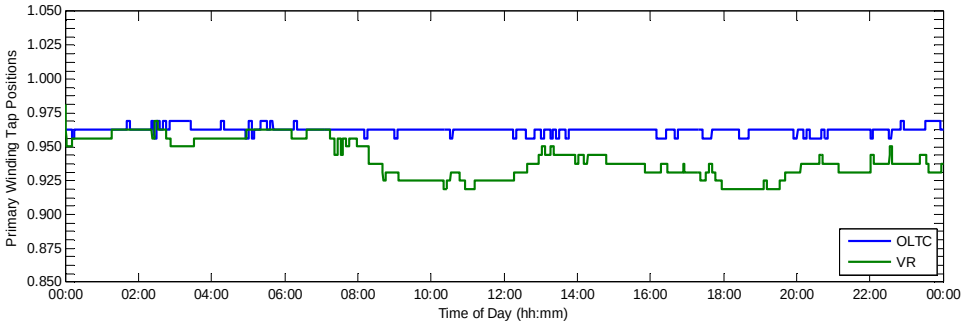

Figure 5.14: Tap positions in the OPF2 formulation case 1

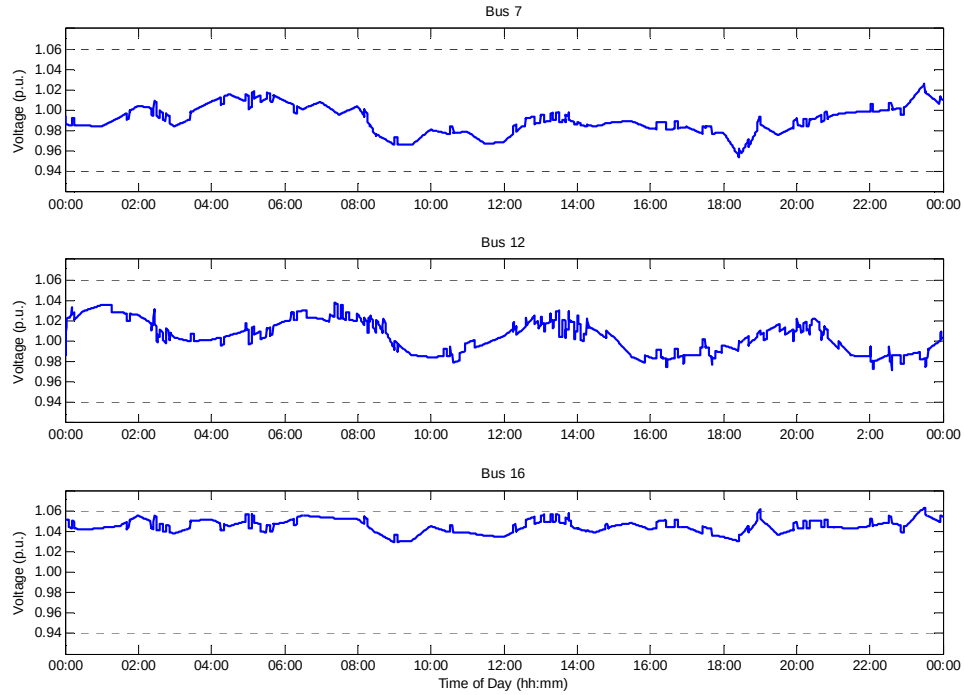

Figure 5.15: Voltage profiles at DG in the OPF2 formulation case 1

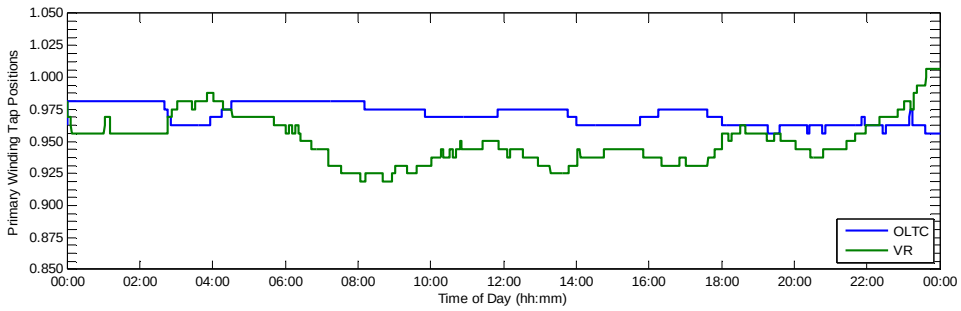

Figure 5.16: Tap positions in the OPF2 formulation case 2

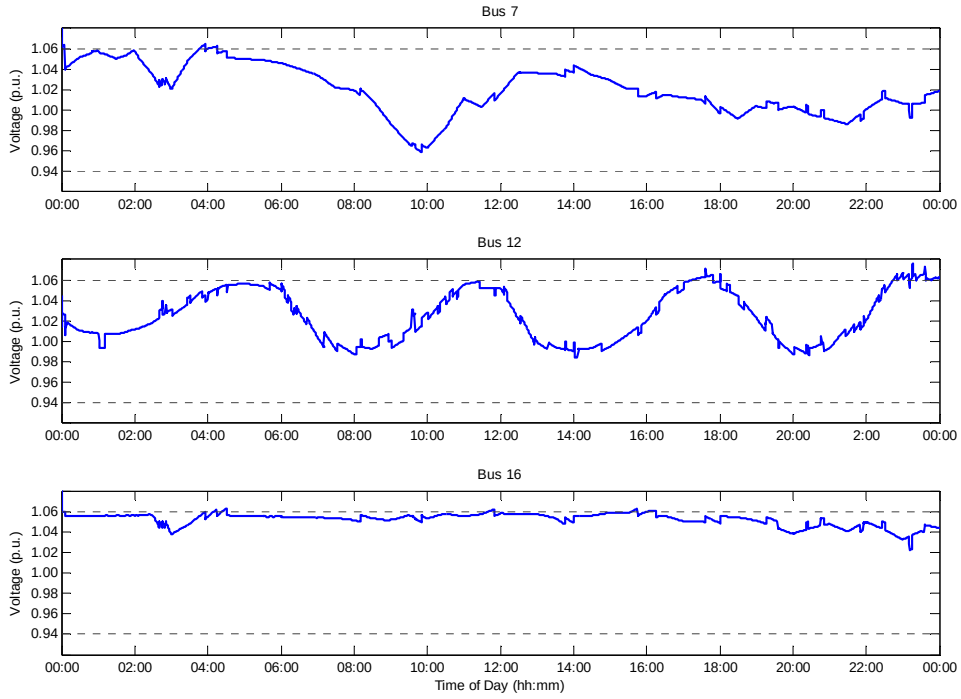

Figure 5.17: Voltage Profiles at the point of DG Connection in the OPF2 formulation case 2

The OPF3 formulation was successful in prescribing control settings that avoided the spurious and unnecessary tap changing actions incurred by the OPF1 and OPF2 formulations during both test case simulations. In the OPF3 formulation, the internal OPF targets for the regulated voltage settings on the OLTC and VR tap changing transformers were both 1.03 pu. The resultant time series of transformer tap positions

and voltage levels at the point of DG connection are shown in Figure 5.18 to Figure 5.21.

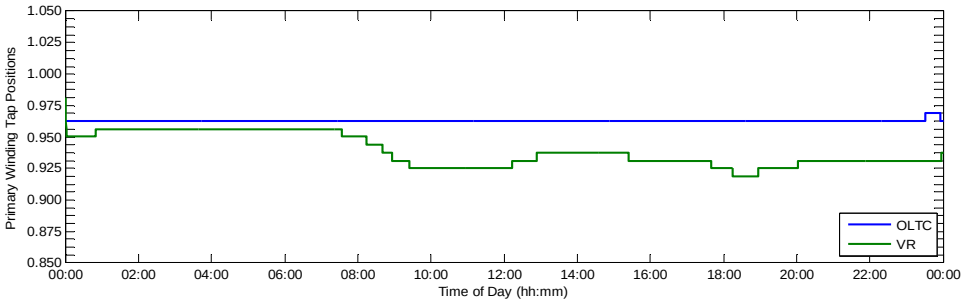

Figure 5.18: Tap positions in the OPF3 formulation case 1

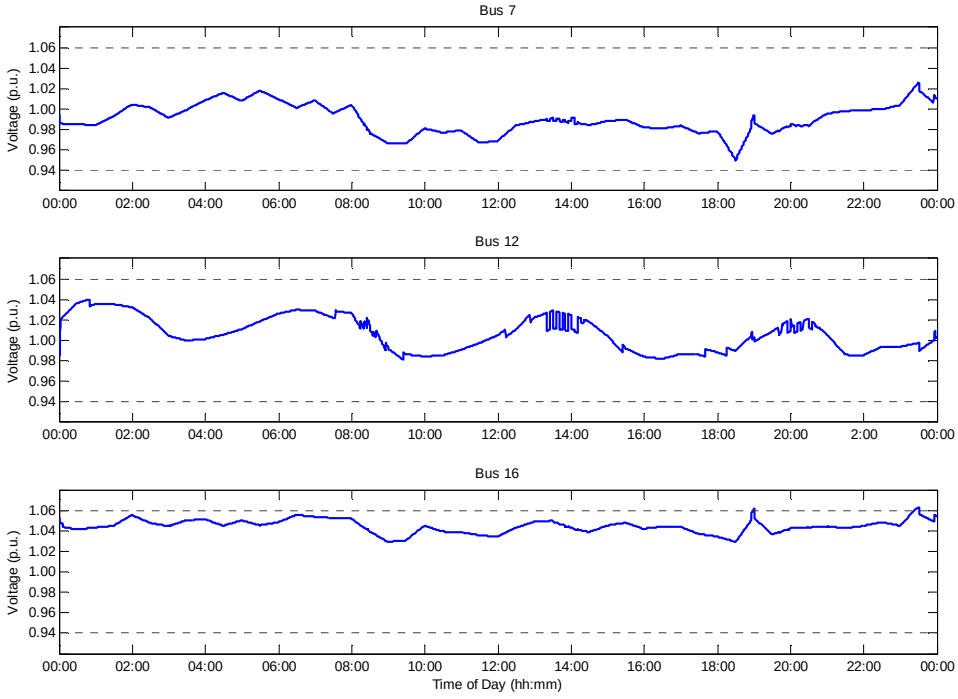

Figure 5.19 Voltage profiles at DG in the OPF3 formulation case 1

Some additional and unnecessary disturbance to the network voltage levels was evident in the OPF3 formulation. This was instigated by spurious switching of the associated DG power factor control setting.

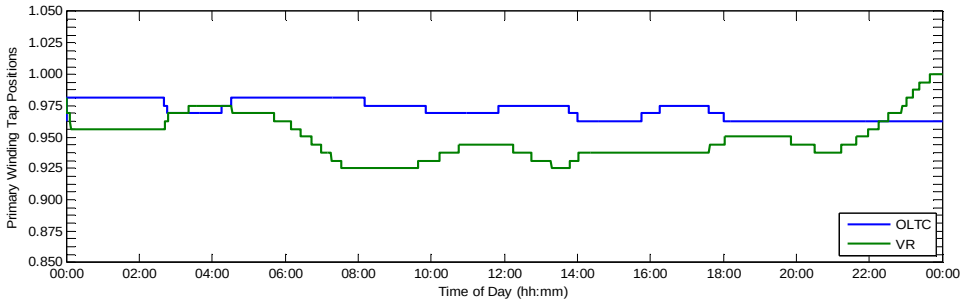

Figure 5.20: Tap positions in the OPF3 formulation case 2

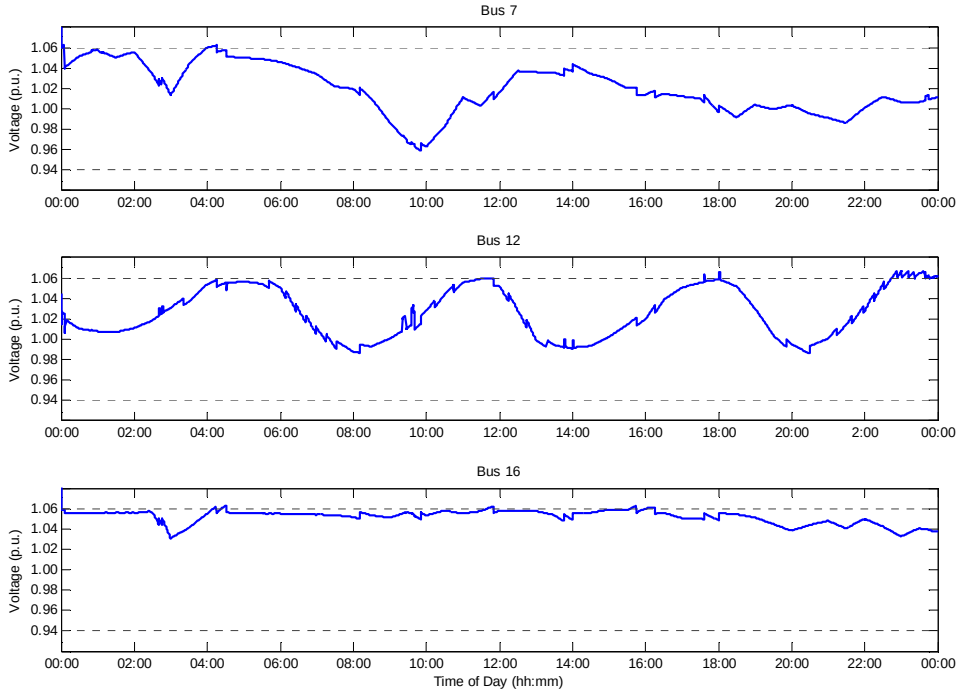

Figure 5.21: Voltage profiles at DG in the OPF3 formulation case 2

The same system configuration was tested with the receding-horizon formulation. Forecast data was synthesised, as before (see section 4.5), by a WCMA smoothing process based on three half-hourly values and is shown in Figure 5.22 and Figure 5.23. In the RHOPF1 simulations, under both variations of forecasting (RHOPF-A and RHOPF-B), spurious tap changing and DG power factor switching actions were removed and the stability of time sequential network control settings was greatly improved. Figure 5.24 and Figure 5.26 show the time series of tap positions on the network tap changing transformers from the RHOPF1-B analysis.

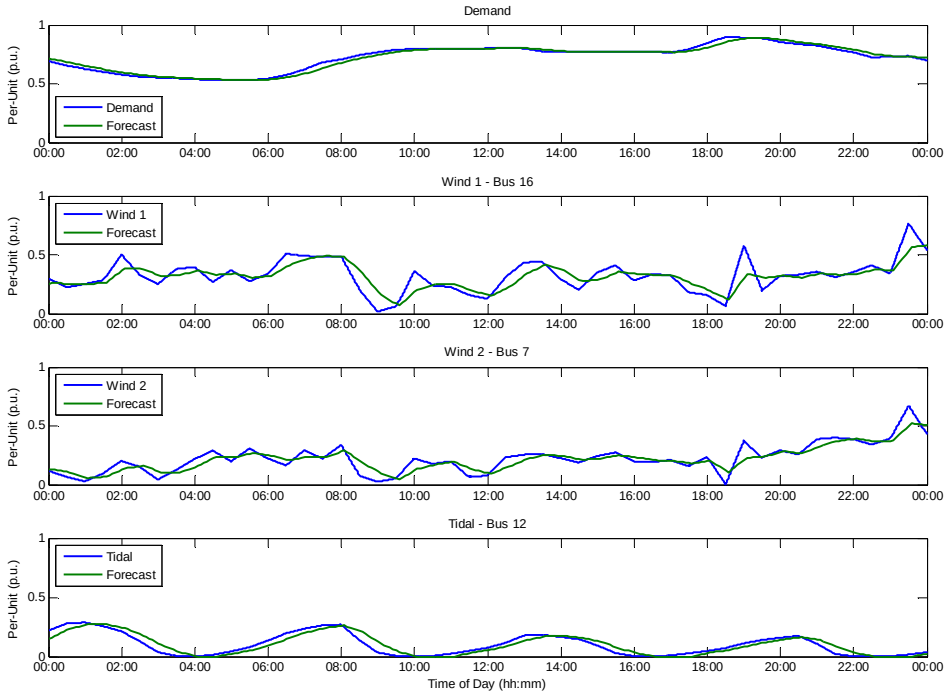

Figure 5.22: Comparison of synthesised forecast and real time resource case 1

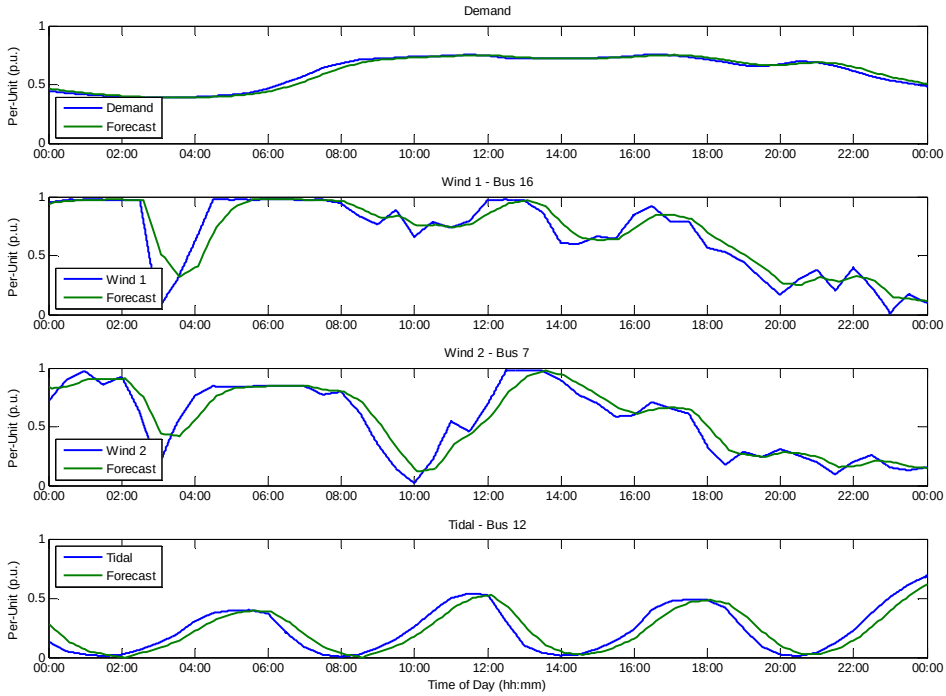

Figure 5.23: Comparison of synthesised forecast and real time resource case 2

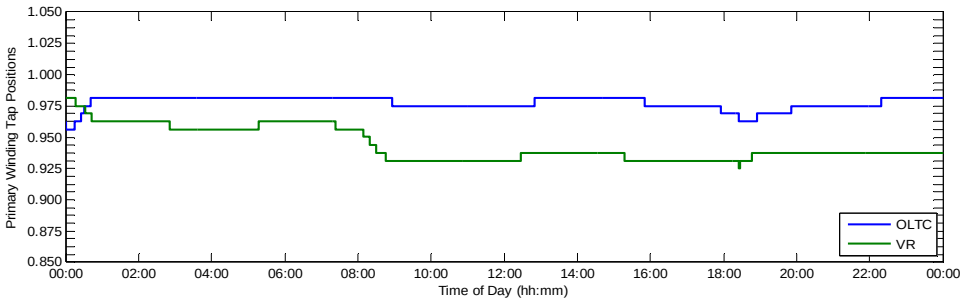

Figure 5.24: Tap positions in the RHOPF1-B formulation case 1

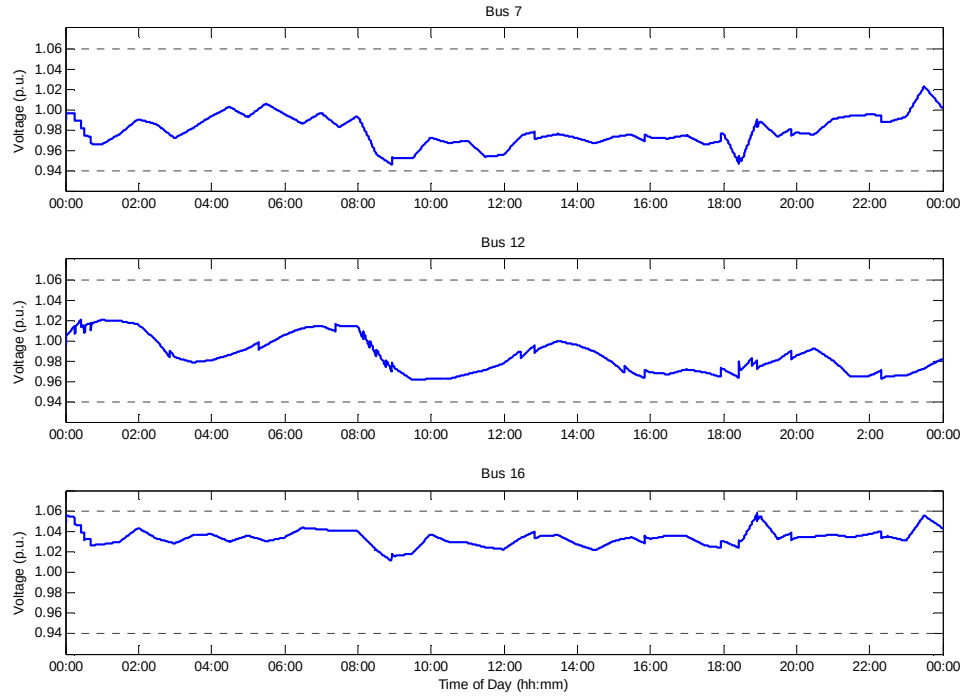

Figure 5.25: Voltage profiles at DG in the RHOPF1-B formulation case 1

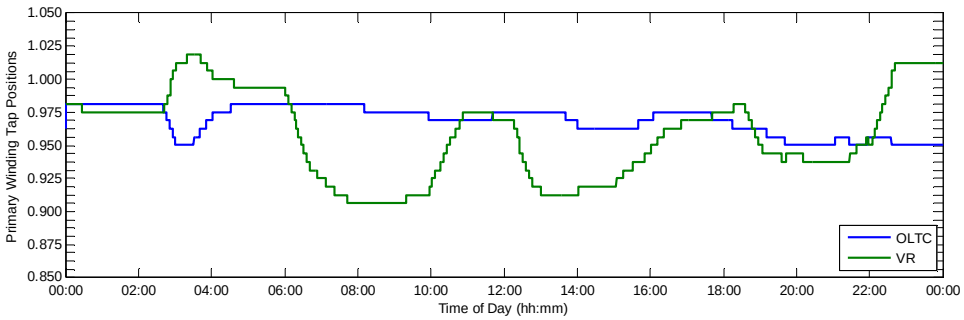

Figure 5.26: Tap position in the RHOPF1-B formulation case 2

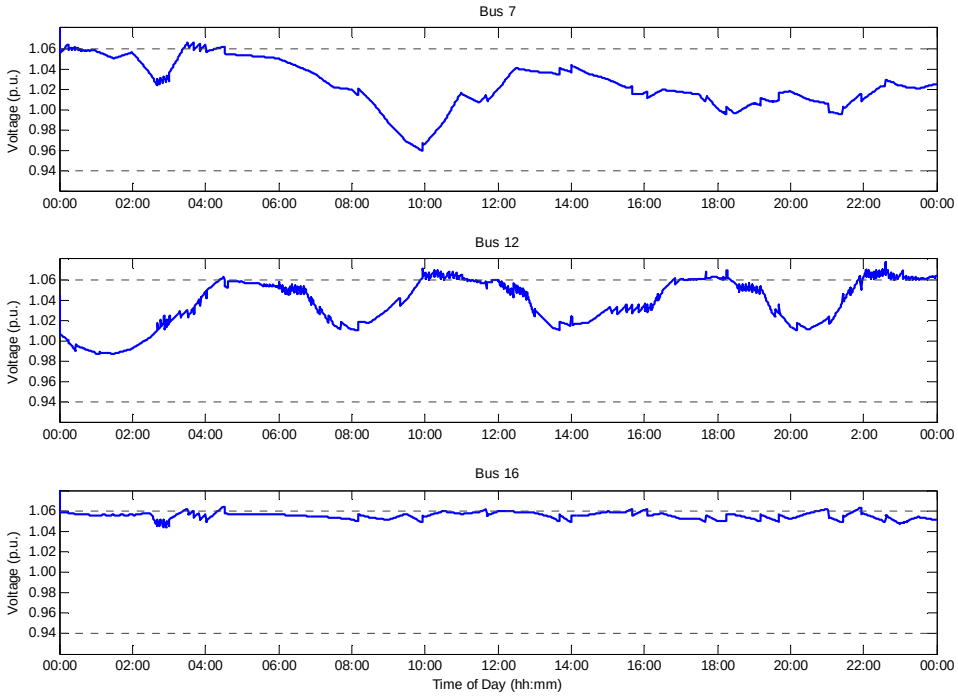

Figure 5.27: Voltage profiles at the point of DG Connection in the RHOPF1-B formulation case 2

In Figure 5.27, minor network overvoltage excursion was observed consistently at bus 12 during the sharp ramp-up of the tidal power output. While the magnitude of voltage excursion was once again within acceptable levels, the frequency during this observational test case would not be compliant with the EN50160 engineering recommendation. One simple solution would be to formulate a multi-faceted real time ANM OPF technique. For example the combination of the multi-objective function with

the receding-horizon methodology, in a RHOPF3-B formulation, produced comparable results to all other formulations, but significantly reduced the frequency of minor overvoltage excursions to 3.4% (measured in 5 second intervals on average over the total non-continuous 48 hour observation period) by tuning the new network control settings in the RHOPF from operating close to the voltage envelope boundaries. A comparison of the network impacts and parameters for the OPF and RHOPF analyses is demonstrated in Figure 5.28 to Figure 5.33. Figure 5.28 demonstrates that the alternative formulations have little impact on the system-wide energy yield. Figure 5.29 illustrates that the impact on network losses was variable, with network losses lower than the 'fit-and-forget' approach during the low to moderate DG production levels of case 1, and increasing substantially during the high DG production of case 2.

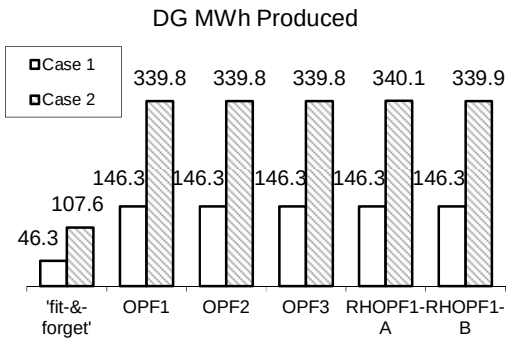

Figure 5.28: Energy yield

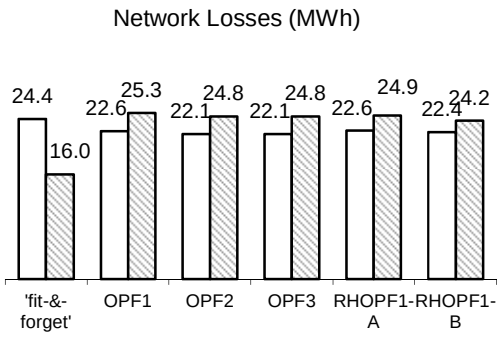

Figure 5.29: Network losses

Figure 5.30 and Figure 5.31 show, that all formulations of the real time OPF technique, the system response to real time scheduling of active controller settings resulted in some form of voltage excursion. The maximum occurrence of overvoltage excursions, measured in 5 second intervals, is shown in Figure 5.32 for each case and each ANM OPF formulation.

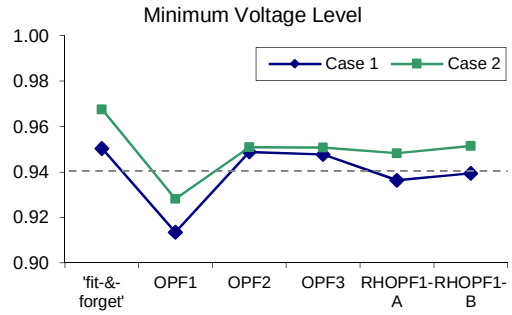

Figure 5.30: Minimum voltage Levels

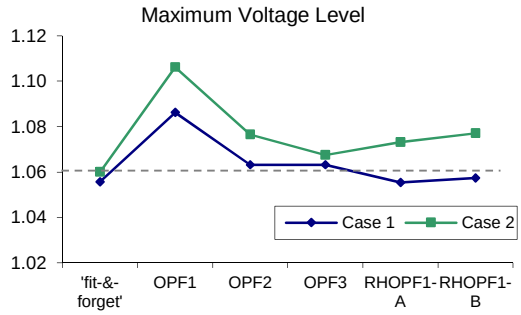

Figure 5.31: Maximum Voltage Levels

In the OPF1 formulation, the spurious switching of transformer settings and the time delay between the tap changing actions of the two network transformers resulted in the occasional but significant under and over voltage excursion on bus 9. Under voltage excursion was only evident for this formulation and occurred for 0.3% of the observational period in case 1.

In the advanced formulations of the real time ANM OPF, minor overvoltage excursions were evident at the connection point of the DGs. This was again caused by a combination of residual voltage variation and the differences in DG output between persistence forecasting sampling intervals and the real time resource level. The combined frequency of overvoltage excursion across both observational test cases was not deemed to be a limiting factor for all but the RHOPF1 formulation regardless of the forecasting routine. Analysis of a multi-faceted RHOPF3-B formulation, which represented tuning of the OPF response to specific network configuration, has proven to bring the frequency of overvoltage excursion within recommended limits.

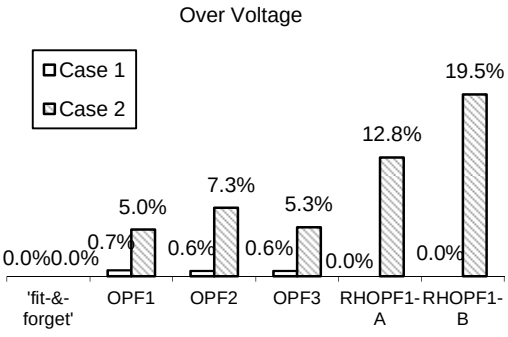

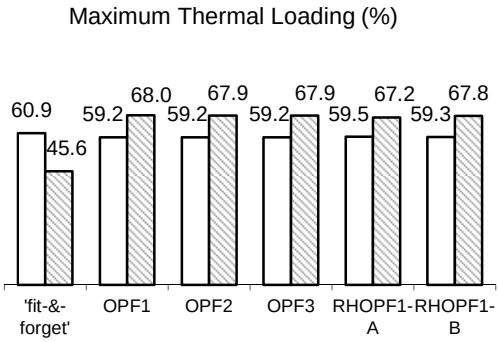

Figure 5.32: Overvoltage Excursion

Figure 5.33: Maximum Thermal Loading

The limitations of the proposed optimisation techniques to hold, at all times, system voltage levels strictly within statutory levels was neither caused by a failure of the OPF technique or the network control practices, but stems from the inevitable variation between the steady mathematical model of the network in the OPF and the physical network response to continuously changing power injections.

One means of mitigating potentially unseen changes in system power flow injections, is to combine the optimal scheduling of active DG control settings with autonomous decentralised control practices that prevent DG power output from exceeding the prescribed level. This philosophy is discussed further and simulated in section 5.4.

5.3 REAL TIME OPF SIMULATIONS IN THE FULL EHV1 NETWORK

Section 5.2 established that OPF techniques could be used to determine appropriate network control settings in distribution networks with multiple DGs from differing renewable energy resources. This section investigates the application of the proposed OPF techniques in a much larger and more complex distribution network. In this subsection the real time ANM OPF technique was tested on the full EHV1 network shown in Figure 5.34, with six DG developments from two clusters of renewable energy resources. Analyses were conducted with the OPF operating on a 5 minute control cycle and intermediate power flow solutions at 5 second intervals.

The network configuration was, as described in section 3.8.2. In the 'fit-and-forget' approach, maximum installed capacity was identified as 20.5 MW, made up of four DGs connecting at buses 1105, 1106, 1108 and 1114 only. With the fully integrated ANM approach maximum installed capacity was identified as 52 MW, which is 137% of peak network demand. The three wind farm developments at buses 1105, 1106 and 1108 had capacities of 10, 15 and 5 MW respectively. On the 'island' the three tidal arrays had capacities of 2, 10 and 10 MW respectively on buses 1113, 1114 and 1115.

In the ANM scenario, voltage settings on the substation OLTC, VR transformer and 33/11-kV distribution transformers, which connect to DGs were all considered variable within the range of 1.01 pu to 1.04 pu.

In this network both voltage envelope and thermal loading constraints restrict the headroom at differing sections of the network. On the 'mainland', next to the wind farm DG developments, thermal loading constraints were more prevalent at two of the DGs, while voltage rise originally constrained further DG capacity on the third wind farm DG on the mainland and all tidal array DGs on the 'island'.

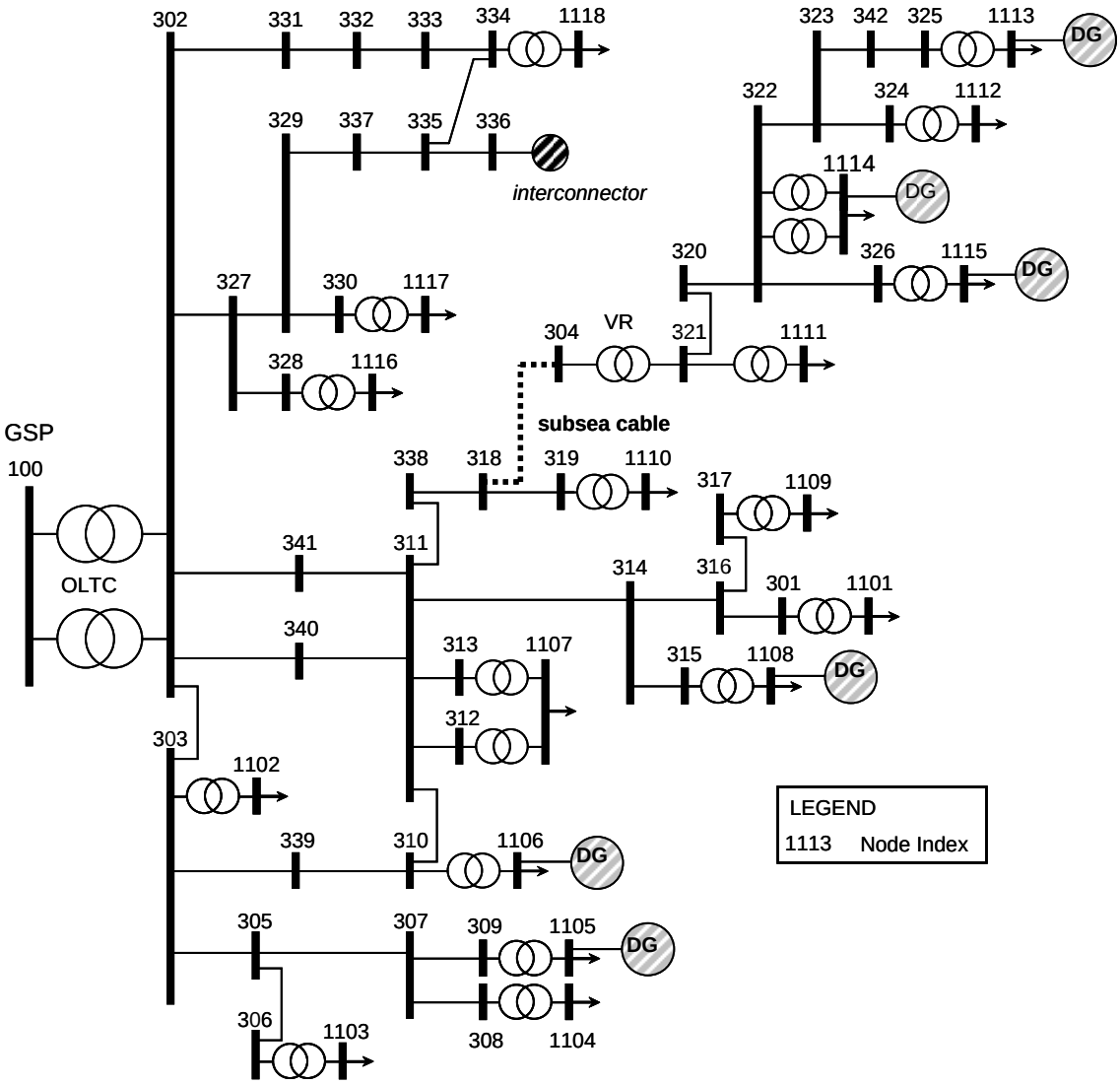

Figure 5.34: UKGDS EHV1 Network [59]

OLTC capabilities were deployed on all distribution network transformers. The substation OLTC has a voltage target of 1.045 pu, whilst the voltage regulator transformer and all 33/11-kV distribution transformers had a regulated voltage target of 1.03 pu.

An observational case study shown in Figure 5.35, which features a variety of supply and demand combinations, was used to investigate the potential for ANM OPF in real time. This was based on the original set of half-hourly generation and demand profiles introduced in section 3.7. For the purposes of short term analysis, generation and demand levels were linearly interpolated between the half-hourly intervals.

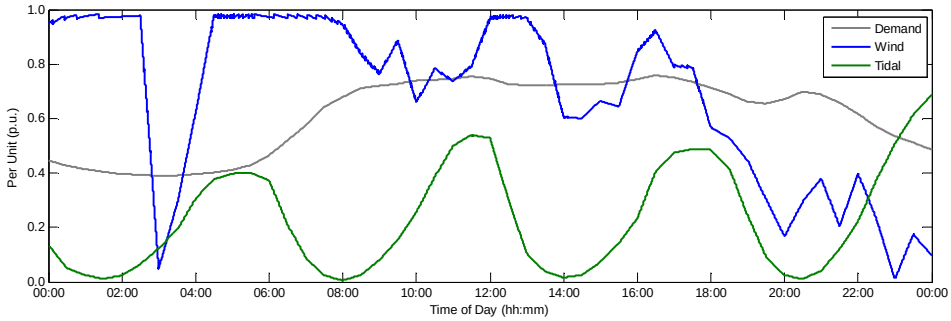

Figure 5.35: Case study resource levels

5.3.1 EHV1 'FIT-AND-FORGET' POWER FLOW SOLUTIONS

Simulations were first performed to analyse and interpret system operation in the fit-and-forget scenario. The total energy yield over the observational test case for each DG in this scenario is shown in Table XI.

Table XI: EHV1 'fit-and-forget' DG energy yield

'fit-and-forget' DG	WTG 1105	WTG 1106	WTG 1108	Tidal 1113	Tidal 1114	Tidal 1115
MW	2.5	10	3	-	5	-
MWh	41.2	164.7	49.4	-	27.5	-
MVArh	8.4	33.5	10.0	-	5.6	-
EC MWh	0.0	0.0	0.0	-	0.0	-
EC (%)	0.0%	0.0%	0.0%	-	0.0%	-
Capacity Factor (%)	68.6%	68.6%	68.6%	-	23.0%	-

Figure 5.36 and Figure 5.37 demonstrated the real power production from each DG. Figure 5.38 shows the corresponding thermal loading on each of 33/11-kV distribution transformers connecting to the wind farm DGs. This illustrates that, as the binding constraint on DG capacity, for the wind farms at buses 1106 and 1108, thermal loading on the distribution transformers reached (or was close to) the rated limit at near full rated power production.

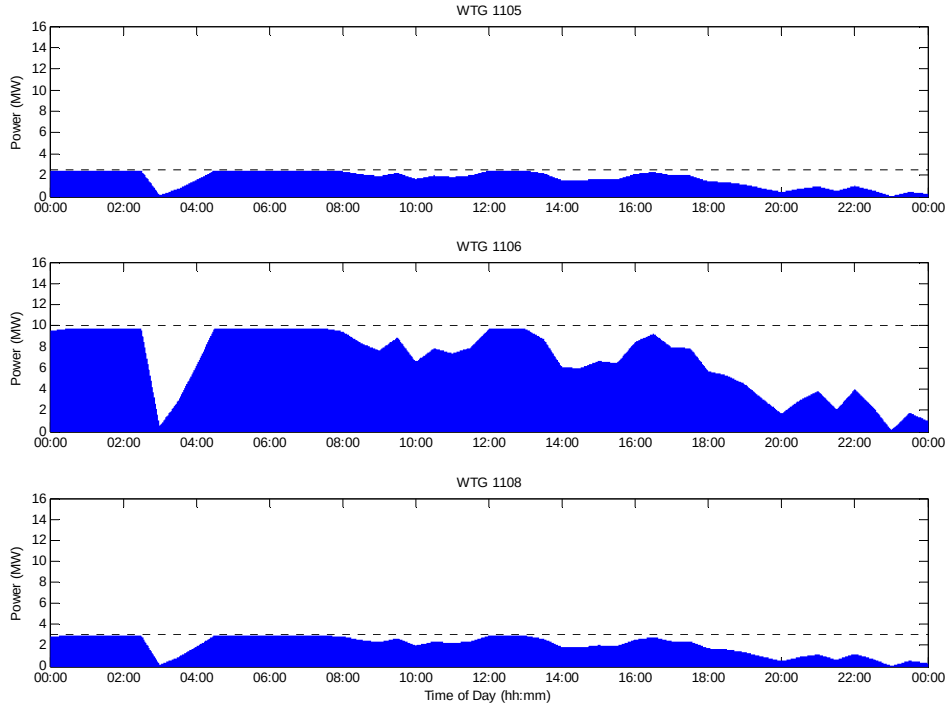

Figure 5.36: Wind farm DGs real power production – 'fit-and-forget'

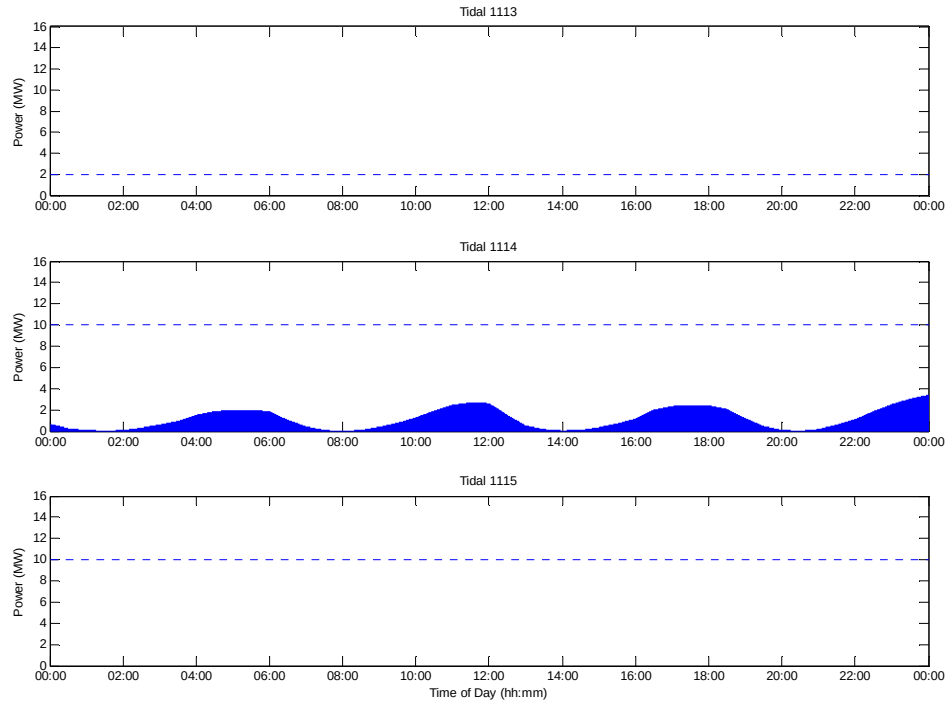

Figure 5.37: Tidal array DGs real power production – 'fit-and-forget'

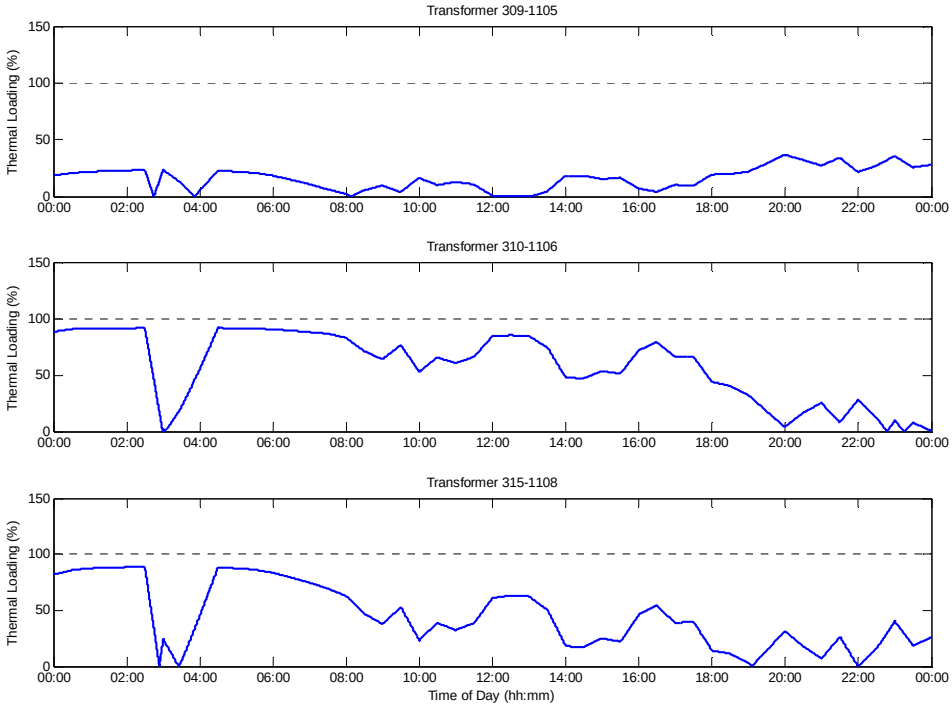

Figure 5.38: Thermal loading of wind farm DG distribution transformers – 'fit-and-forget'

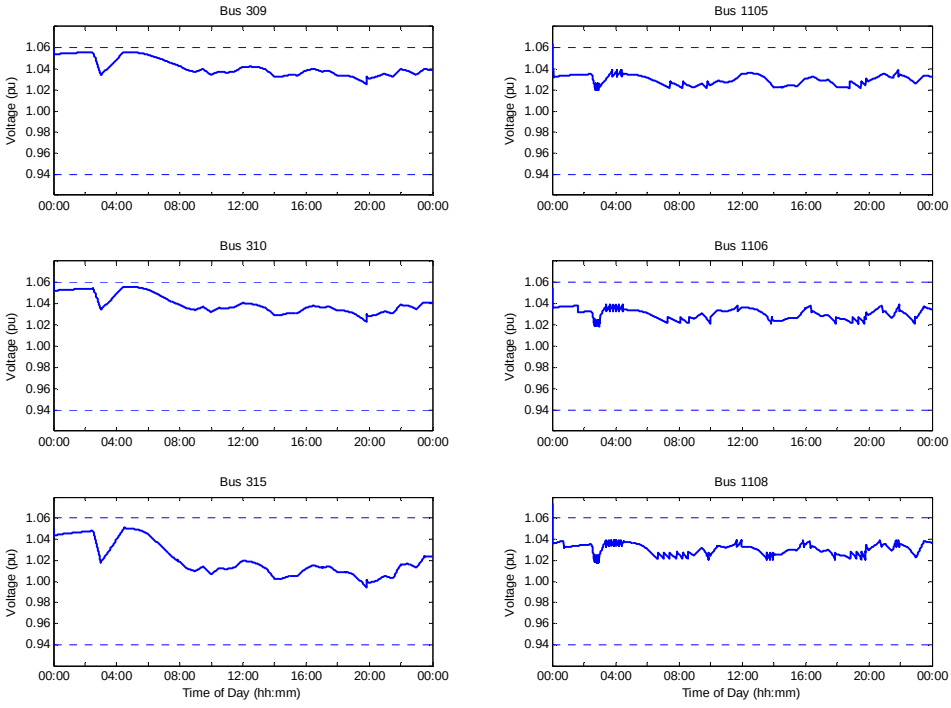

Figure 5.39: Voltage profiles of wind farm DG distribution transformers – 'fit-and-forget'

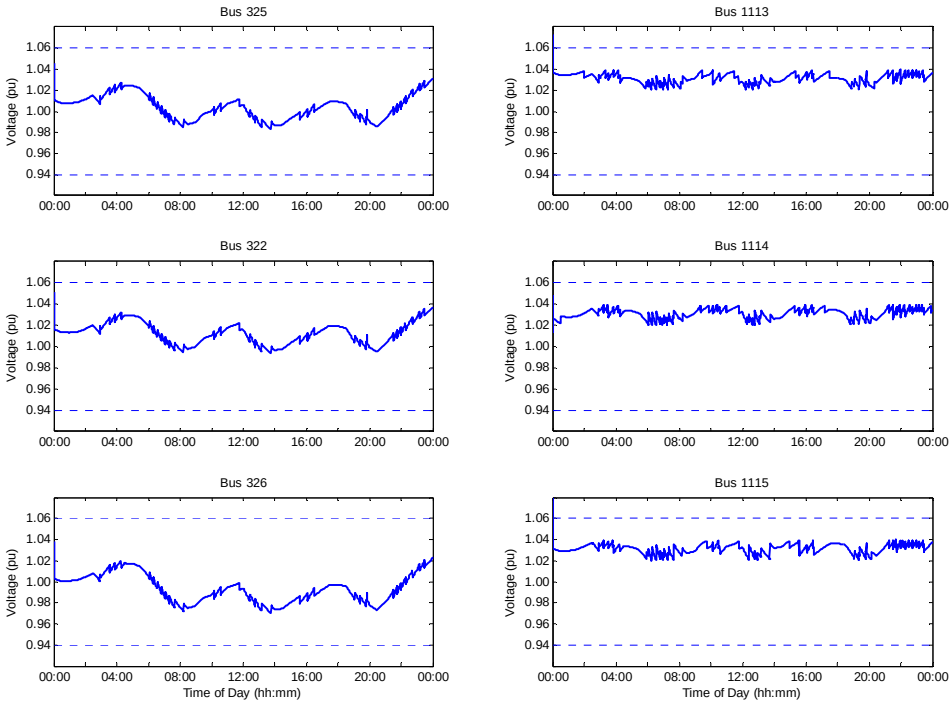

Figure 5.40: Voltage profiles of tidal array DG distribution transformers – 'fit-and-forget'

Voltage level on the wind farm DG distribution transformers are shown in Figure 5.39. It shows that voltage levels on the primary winding of these transformers, buses 309, 310 and 315, were close to the upper statutory limit at peak wind power production. On the island section, voltage levels during the test case did not reach system constraints, as shown in Figure 5.40.

For future reference, the corresponding time series of tap positions on the substation OLTC and VR transformers, the 33/11-kV distribution transformers connecting to the wind farm and tidal array DGs, and the complex power flow exchange between the distribution network and electricity grid at large in the fit-and-forget scenario are shown in Figure 5.41 to Figure 5.45 respectively.

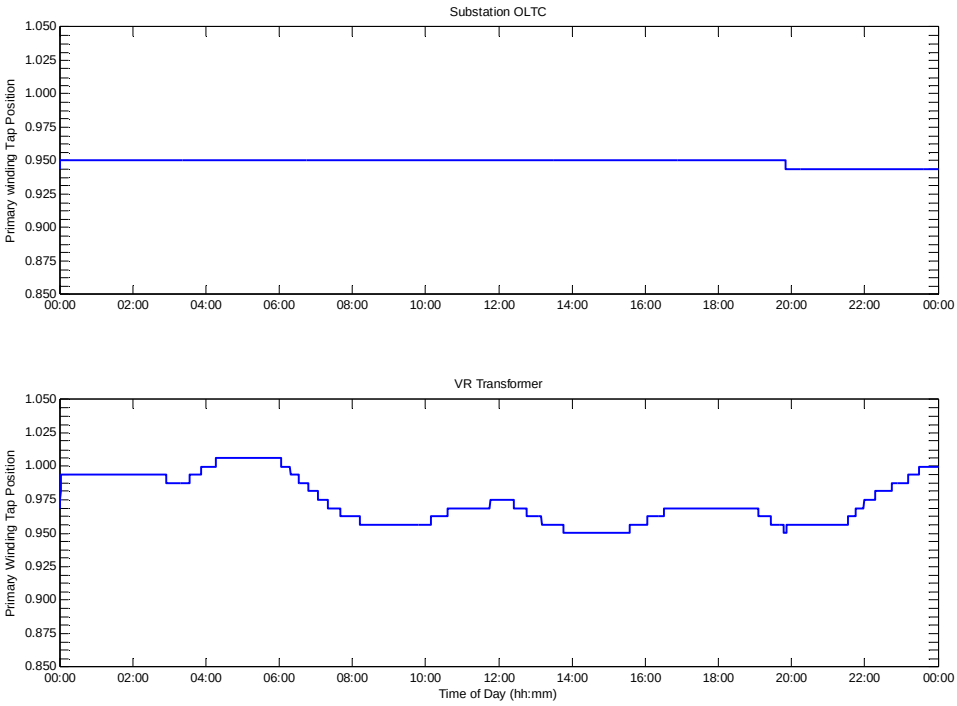

Figure 5.41: Tap positions on network transformers – 'fit-and-forget'

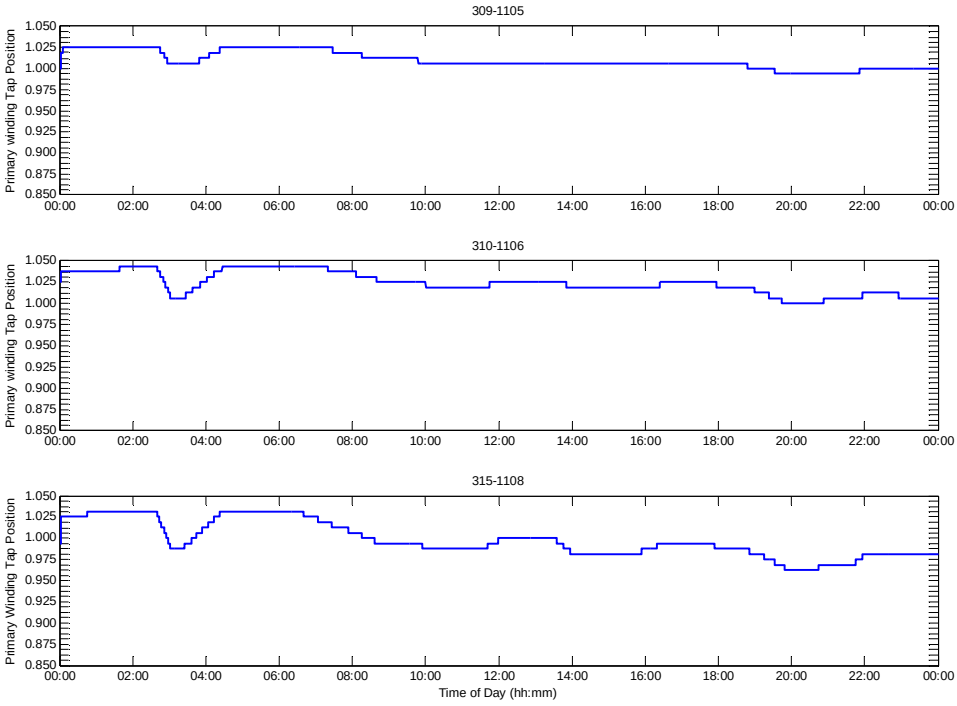

Figure 5.42: Tap positions on wind farm DG distribution transformers – 'fit-and-forget'

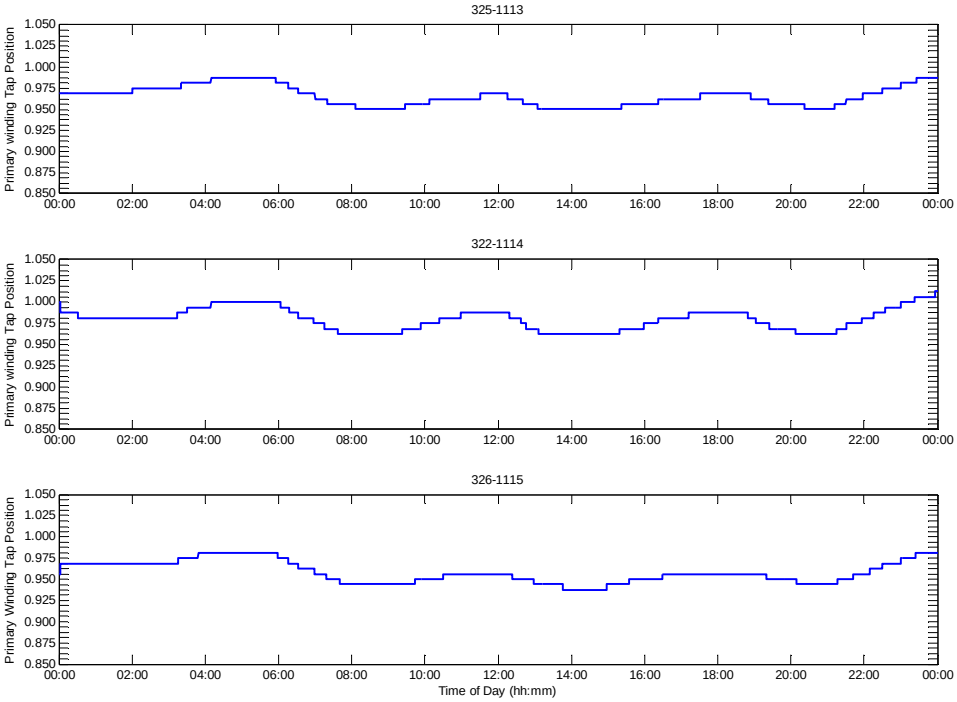

Figure 5.43: Tap positions on tidal array DG distribution transformers – 'fit-and-forget'

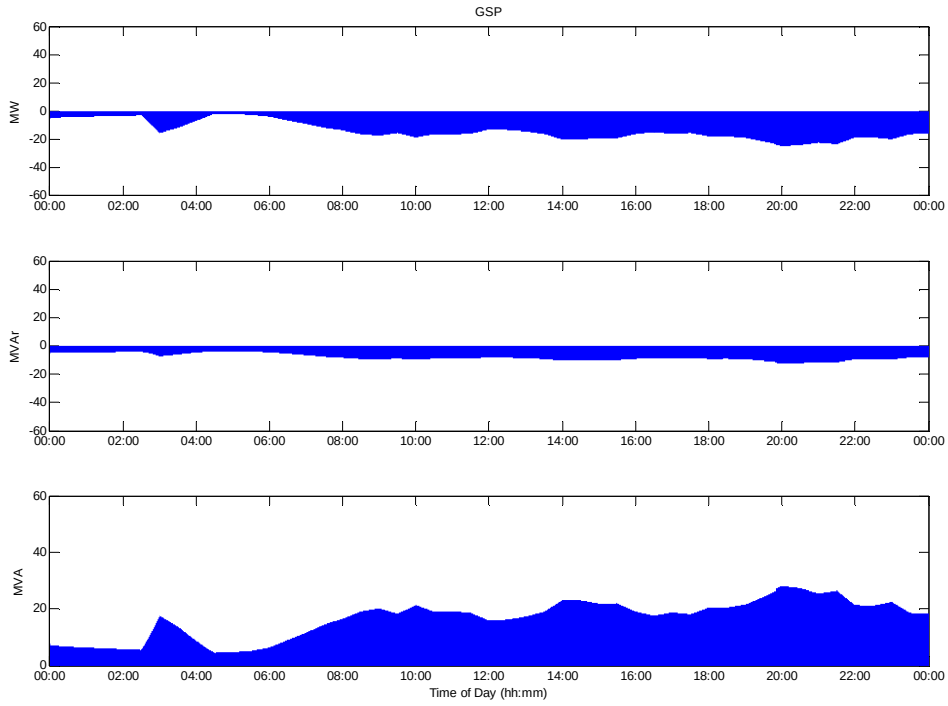

Figure 5.44: EHV1 GSP power flow – 'fit-and-forget'

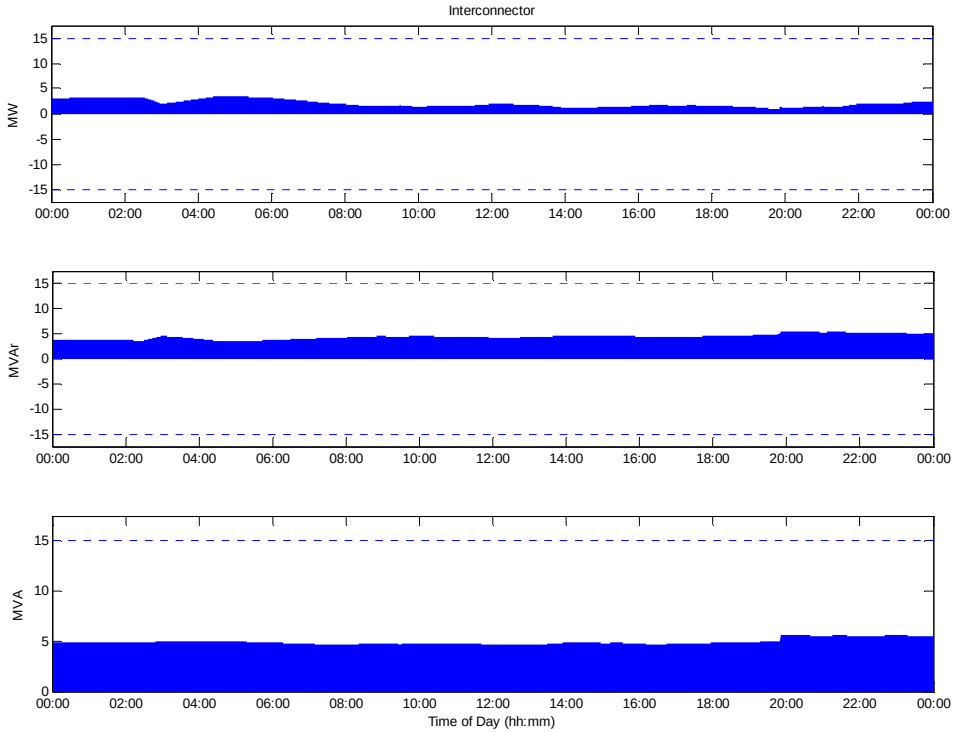

Figure 5.45: EHV1 Interconnector power flow – 'fit-and-forget'

5.3.2 EHV1 POWER FLOW SOLUTIONS WITH OPF

Real time application of the ANM OPF technique was then studied on this network with an installed DG capacity of 52 MW. Energy yield from each DG is shown in Table XII. In this scenario, installed capacity was increased by 153%; system-wide energy yield over the observational test case increased by 92%. The analyses were conducted on the same timescales as before, with power flow solutions monitoring network state and modelling network control interactions at 5 second intervals, while new network control settings were determined on a 5 minute control cycle by the OPF technique.

OPF1	WTG 1105	WTG 1106	WTG 1108	Tidal 1113	Tidal 1114	Tidal 1115
MW	10	15	5	2	10	10
MWh	136.8	214.3	70.3	11.0	54.9	54.8
MVArh	8.7	-4.1	3.0	-2.1	-10.3	-10.2
EC MWh	27.7	32.5	12.0	0.0	0.2	0.3
EC (%)	16.8%	13.2%	14.5%	0.0%	0.3%	0.5%
Capacity Factor (%)	57.0%	59.5%	58.6%	22.9%	22.9%	22.8%

Table XII: EHV1 DG energy yield - OPF1

The increase in energy yield over the fit-and-forget scenario for the wind farms at buses 1106 and 1108 was 30% and 42% respectively. Conversely, energy yield from the third

wind farm DG at bus 1105, where voltage rise previously restricted real power production, increased by 232%. Further increases to energy yield from this DG were now restricted by the thermal loading of the connecting distribution transformer.

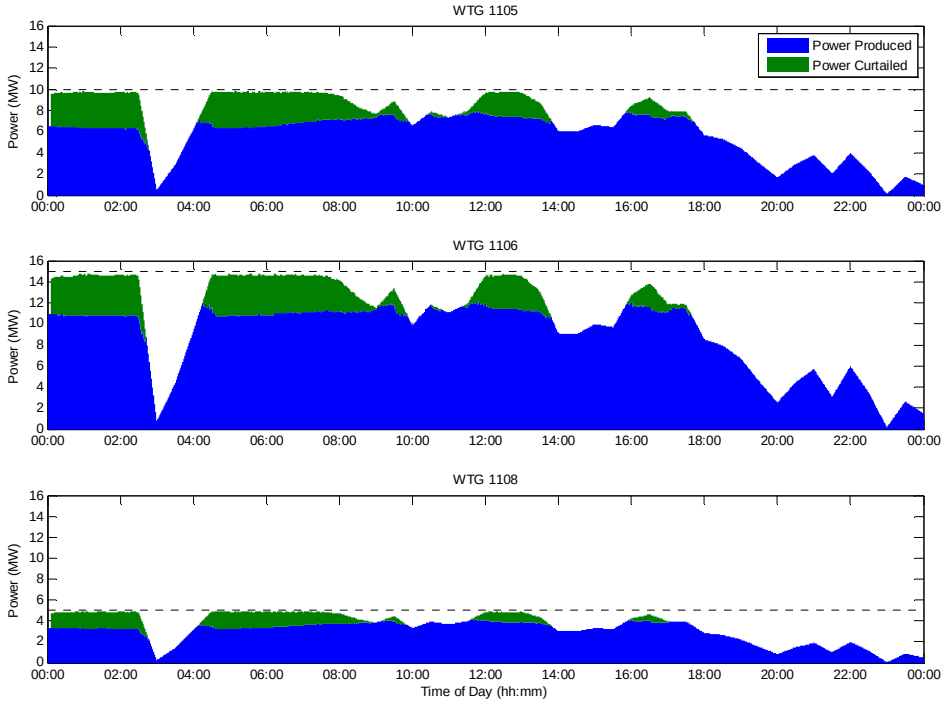

Figure 5.46: EHV1 wind farm DGs real power production – OPF1

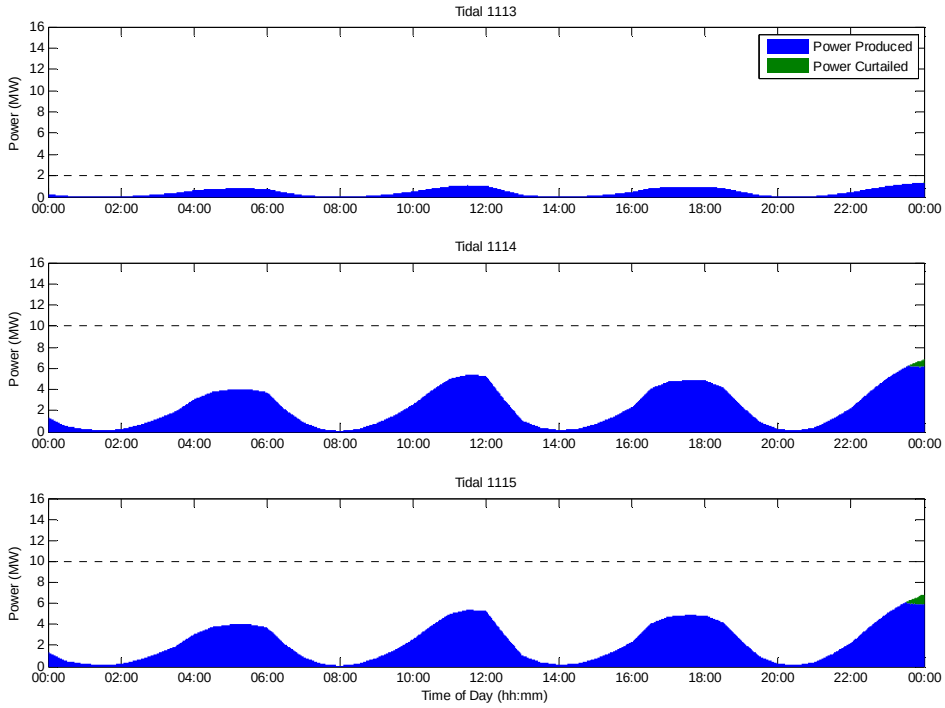

Figure 5.47: EHV1 tidal array DGs real power production – OPF1

Figure 5.46 and Figure 5.47 show the real power production levels for each DG. The application of ANM strategies, including variable PFC and CVC, have little flexibility to alleviate thermal loading constraints therefore, as expected, real power production above the level of maximum fit-and-forget capacity was curtailed by the OPF algorithm, for the three wind farm DGs.

Energy yield from the original tidal array DG increased by 99% while the new tidal array DGs at buses 1113 and 1115 had a combined energy yield of 65.8 MWh, which was 115% of the total system-wide energy yield in the fit-and-forget scenario.

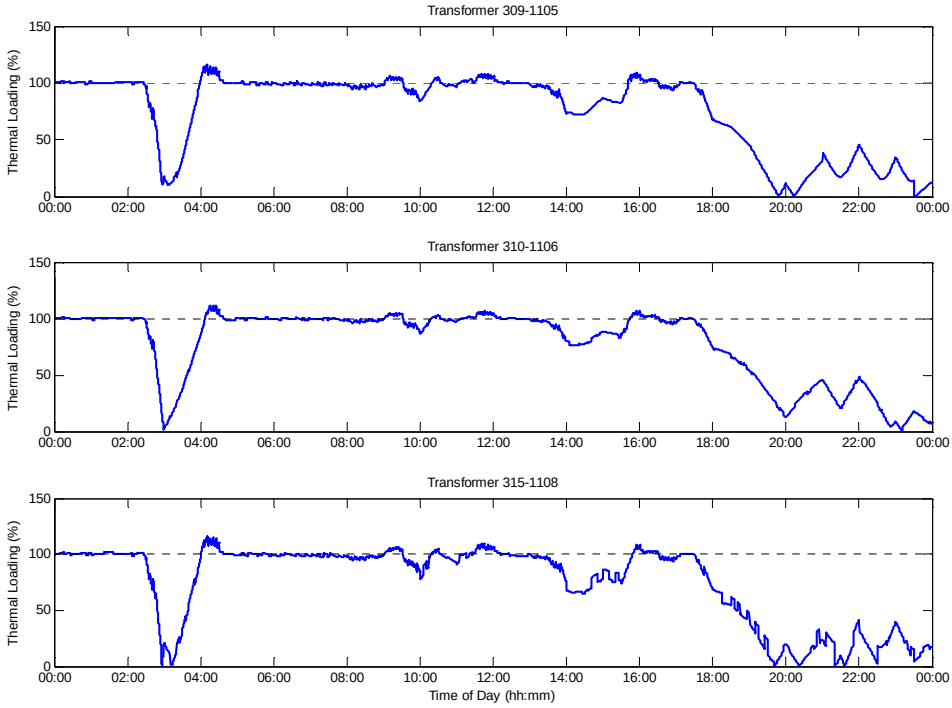

Figure 5.48: Thermal loading of wind farm DG distribution transformers - OPF1

One drawback to the real time ANM of network power flows was overloading in the wind farm DG distribution transformers in the network power flow solutions, as shown in Figure 5.48. Thermal overloading was caused by imbalances and fluctuation of the wind power resource between the persistence forecasting level in successive OPF solutions and the real time resource levels in the power flow solutions. The maximum instantaneous thermal loading on any network component was 116.6% and the frequency of thermal overloading in the observational test case for the worst affected transformer was 27.4%. However, for more than 95% of the observational period, thermal loading of the distribution transformers was below 105% of the respective transformer thermal rating. This is demonstrated by the box plot diagrams in Figure 5.49, which extend to the 5^{th} and 95^{th} percentile of the instantaneous transformer loading measurements over the observational test case.

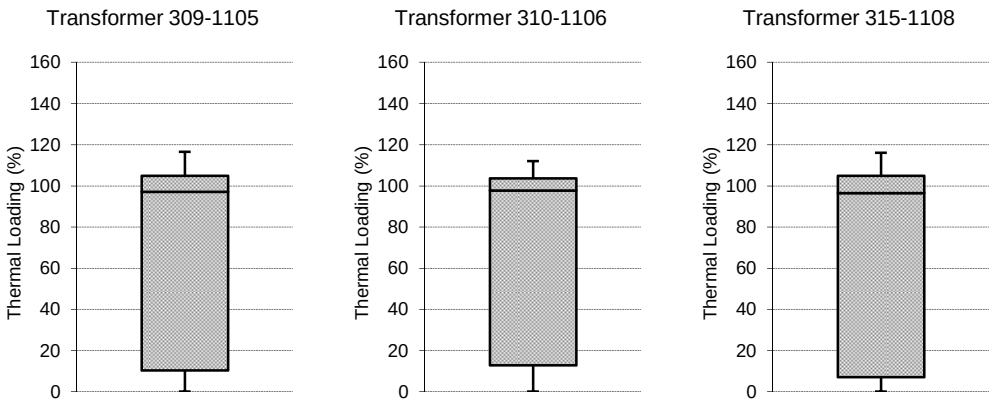

Figure 5.49: Box plots of wind farm distribution transformer loading levels – OPF1

As identified in the preceding studies, spurious and unnecessary tap changing actions was a consistent boundary to the performance of the OPF1 formulation for implementation with the very short control cycle in this continuous and autonomous fashion. Figure 5.50 shows a recurrence of this in the EHV1 network on a 5 minute OPF control cycle over a single 24 hour observational period, with unrealistic use of the network OLTC and VR transformers.

Spurious switching of transformer tap positions was repeated in the downstream 33/11-kV distribution transformers, as demonstrated in Figure 5.51, by the time series of tap positions for the three distribution transformers which connect to the tidal array DGs, and by Figure 5.52, the bar chart of accumulative tap changing actions for all tap changing transformers in the full EHV1 network.

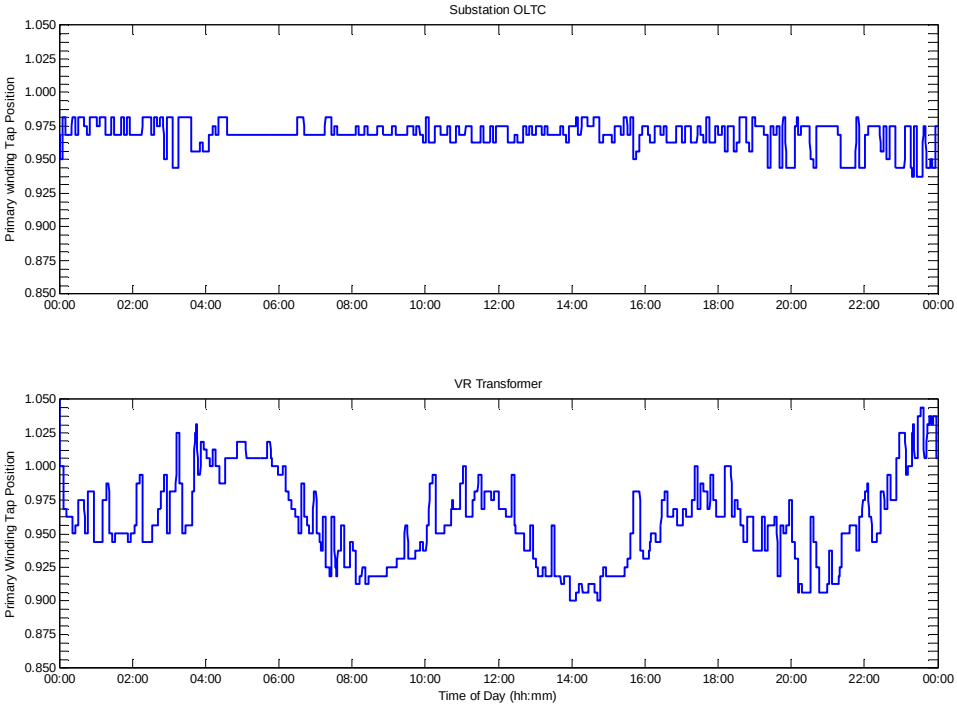

Figure 5.50: Tap Positions for the network transformers - OPF1

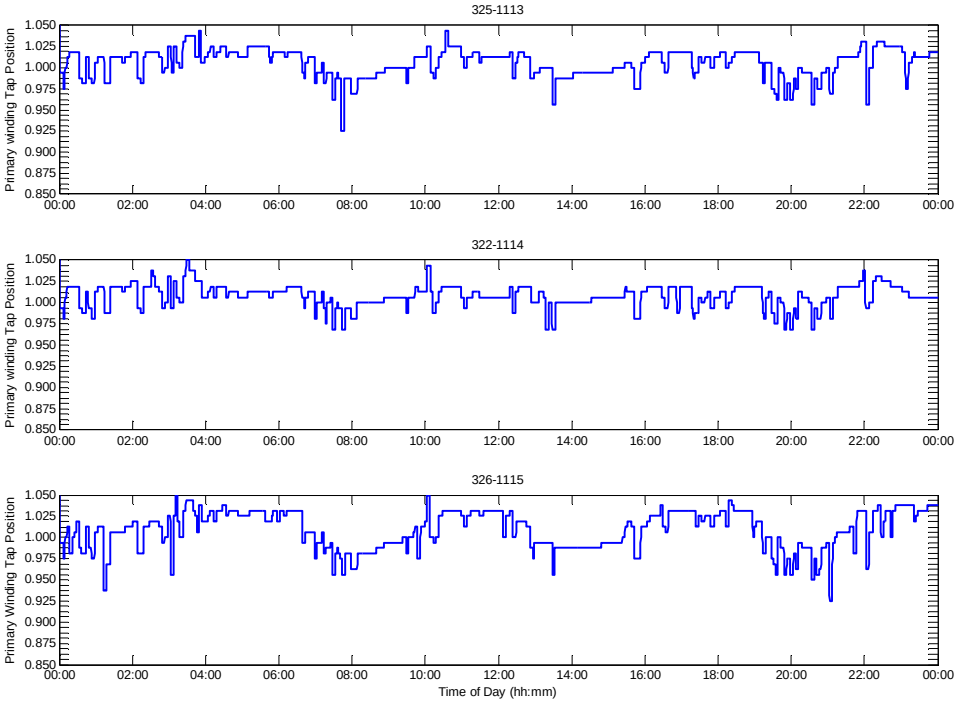

Figure 5.51: Tap Positions for the tidal array distribution transformers - OPF1

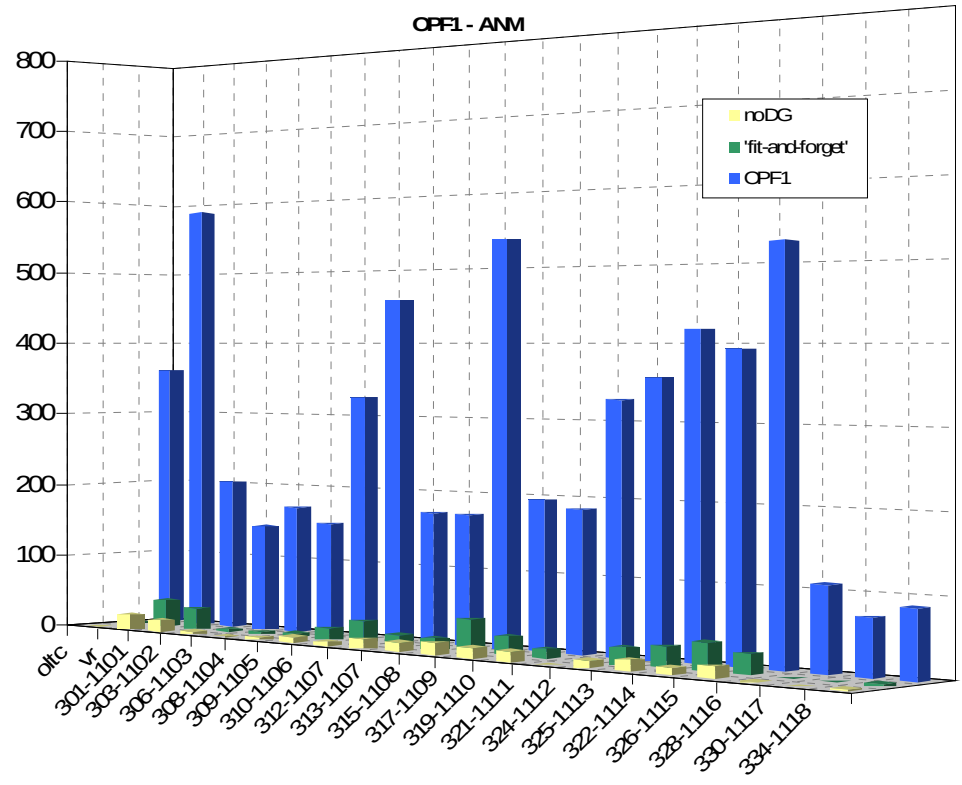

Figure 5.52: Total tap changing actions for all network transformers - OPF1

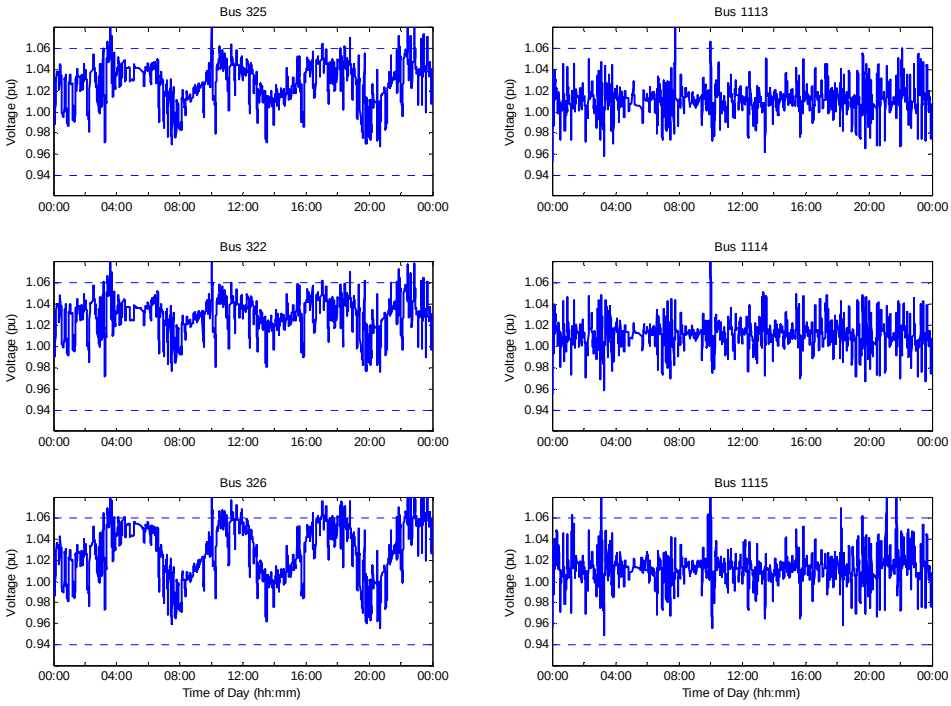

Figure 5.53: Voltage profiles for the tidal array distribution transformers - OPF1

This has a significant adverse effect on network voltage levels which frequently breach the statutory voltage envelope and distribution code on voltage disturbance due to the voltage step differences in consecutive control actions, as demonstrated in Figure 5.53, which depicts the voltage levels on the three 33/11-kV distribution transformers which connect to the tidal array DGs. The disturbance to network voltage levels, caused by the spurious switching with staggered time delays, would then trip over voltage protection relays. In the larger EHV1 network with greater magnitudes of power flow injections from DG, the severity of voltage steps induced between tap changing actions was significantly higher.

As before, the multi-objective formulations of the ANM OPF technique, OPF2 and OPF3, were investigated to minimise the levels of control switching in the network. In the OPF3 case, the internal OPF voltage targets on the substation and VR tap changing transformers were reduced from 1.045 pu and 1.03 pu to 1.03 pu and 1.02 pu respectively. The internal OPF voltage target was unchanged from 1.03 pu for all actively regulated distribution transformers. The energy yield from each DG in these studies is shown in Table XIII and Table XIV. Once again there was no more than a negligible change in the energy yield of the OPF1 formulation in these cases.

Table XIII: EHV1 DG energy yield - OPF2

OPF2	WTG 1105	WTG 1106	WTG 1108	Tidal 1113	Tidal 1114	Tidal 1115
MW	10	15	5	2	10	10
MWh	136.7	214.2	70.3	11.0	54.9	54.8
MVArh	-1.6	6.1	6.0	-2.0	-10.5	-10.2
EC MWh	27.7	32.6	12.0	0.0	0.2	0.3
EC (%)	16.9%	13.2%	14.6%	0.0%	0.3%	0.5%
Capacity Factor (%)	57.0%	59.5%	58.6%	22.9%	22.9%	22.8%

Table XIV: EHV1 DG energy yield – OPF3

OPF3	WTG 1105	WTG 1106	WTG 1108	Tidal 1113	Tidal 1114	Tidal 1115
MW	10	15	5	2	10	10
MWh	136.8	214.2	70.3	11.0	54.9	54.8
MVArh	7.7	3.6	5.6	-2.0	-10.2	-10.4
EC MWh	27.7	32.5	12.0	0.0	0.2	0.3
EC (%)	16.8%	13.2%	14.5%	0.0%	0.3%	0.5%
Capacity Factor (%)	57.0%	59.5%	58.6%	22.9%	22.9%	22.8%

A significant reduction in the tap changing actions was brought about by applying the minimum deviation objective functions, as demonstrated by the count of tap changing actions illustrated in Figure 5.54 and Figure 5.55.

In contradiction to the findings in the simplified EHV1 – ANM network, the multi-objective formulations of OPF2 and OPF3 did not mitigate all instances of spurious network control switching. These formulations penalised unnecessary deviation of the voltage settings on tap-changing controlled buses and not the number of tap changing actions explicitly. In the simplified EHV1 – ANM, where voltage level constraints restricted DG real power production and the DG was forced to operate at a specific power factor, this formulation was sufficient to remove the spurious actions. However, in the full EHV1 network, where thermal loading constraints were more prominent in some sections of the network, spurious and unnecessary switching of the DG power factor set-point was also evident.

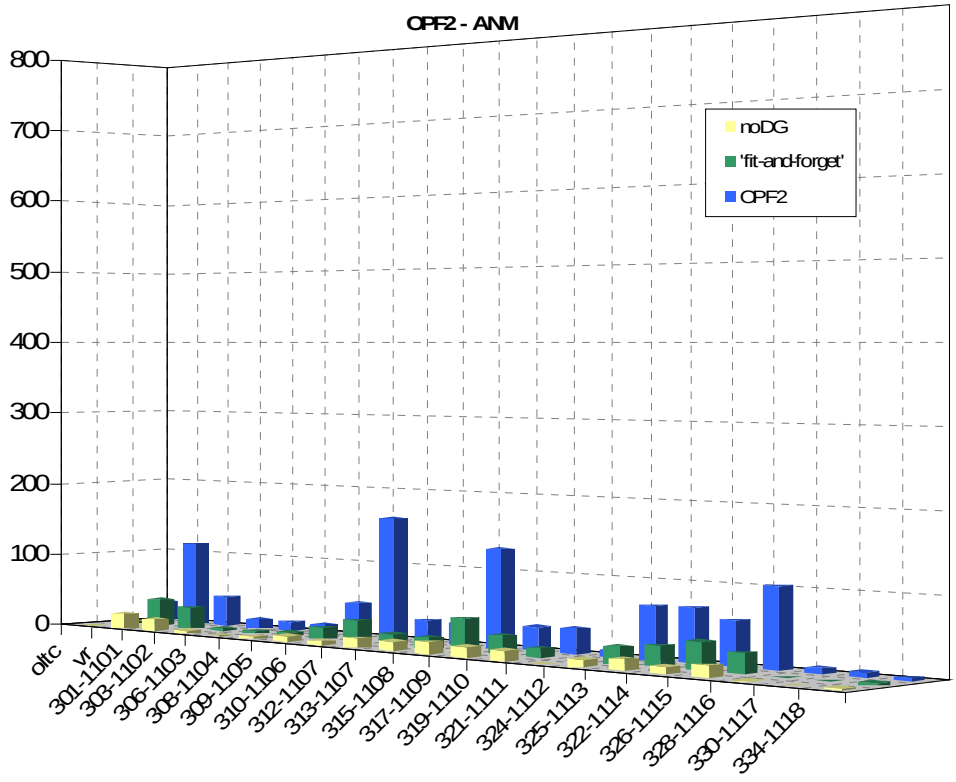

Figure 5.54: Total tap changing actions for all network transformers – OPF2

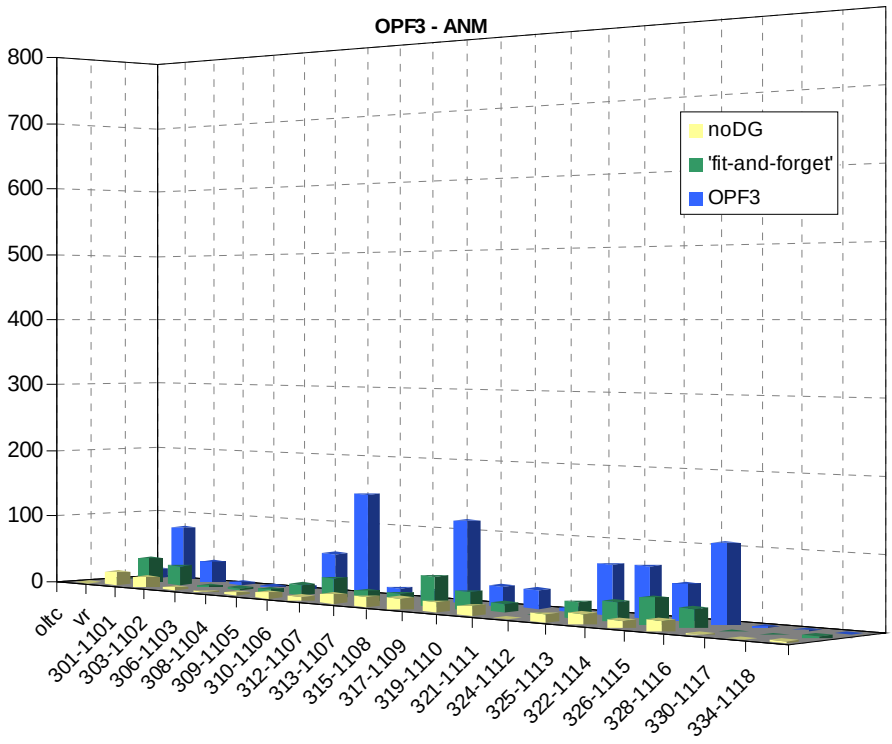

Figure 5.55: Total tap changing actions for all network transformers – OPF3

This is demonstrated by the reactive power production on each of the wind farm DGs in the OPF3 formulation, illustrated in Figure 5.56. The effect of the unnecessary switching of the DG power factor settings invoked additional tap-changing actions as observed in Figure 5.57 and Figure 5.58. Figure 5.57 illustrates the time series of tap positions for the OLTC and VR transformers and Figure 5.58 illustrates the time series of tap positions for the 33/11-kV distribution transformers connected to the wind farm DGs.

The impact of this switching of network control settings in the OPF3 formulation is demonstrated by the corresponding voltage levels on either side of the 33/11-kV distribution transformers connecting to the wind farm DGs, shown in Figure 5.59.

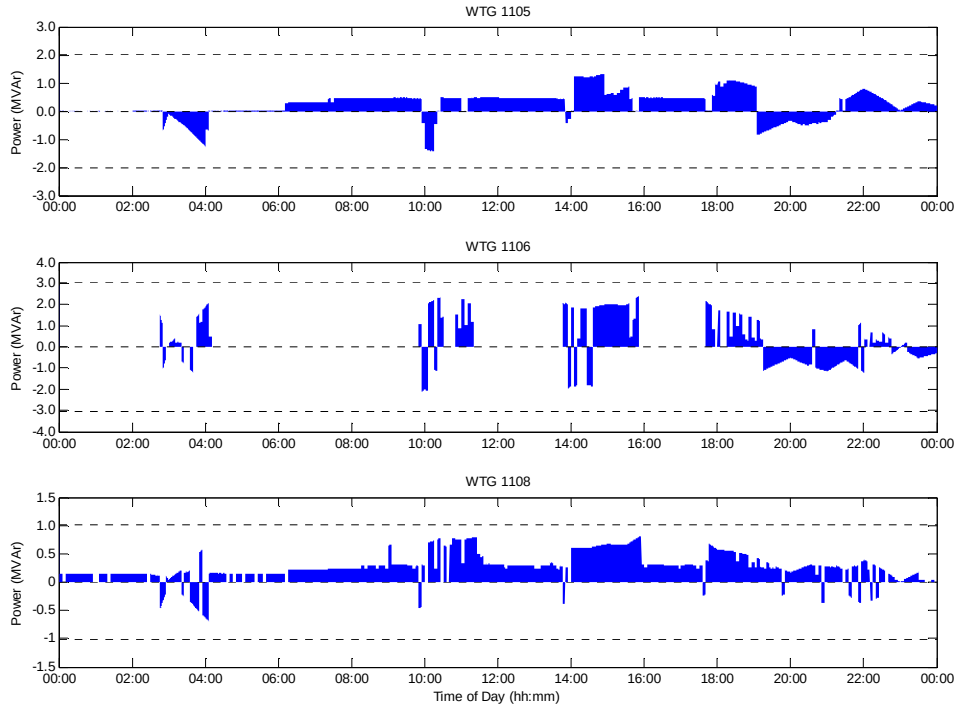

Figure 5.56: Reactive power output from the wind farm DGs - OPF3

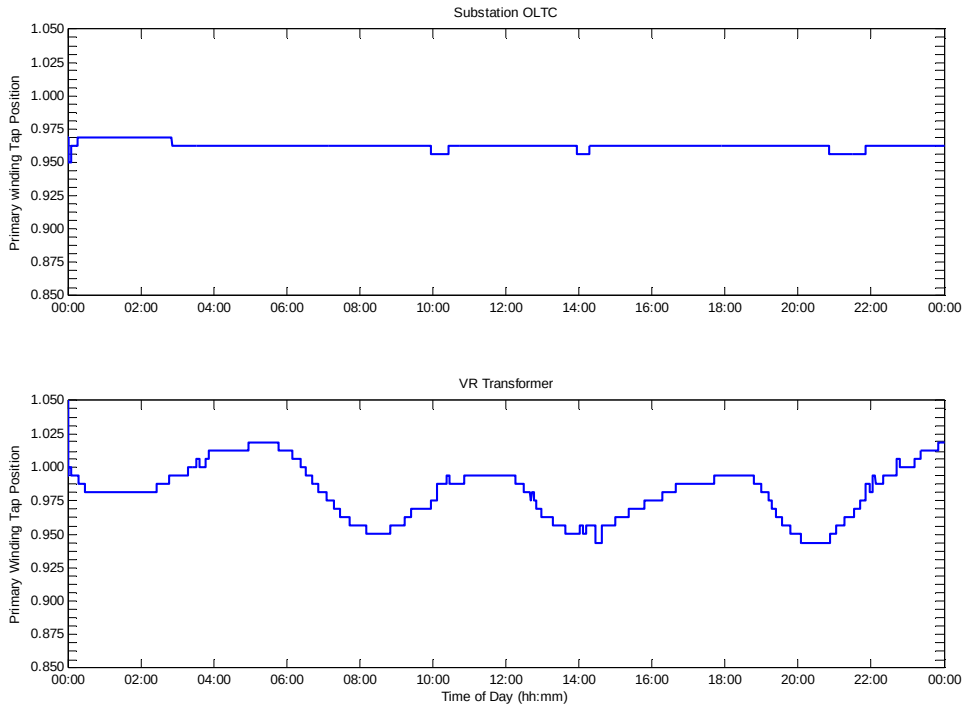

Figure 5.57: Tap positions for the network transformers - OPF3

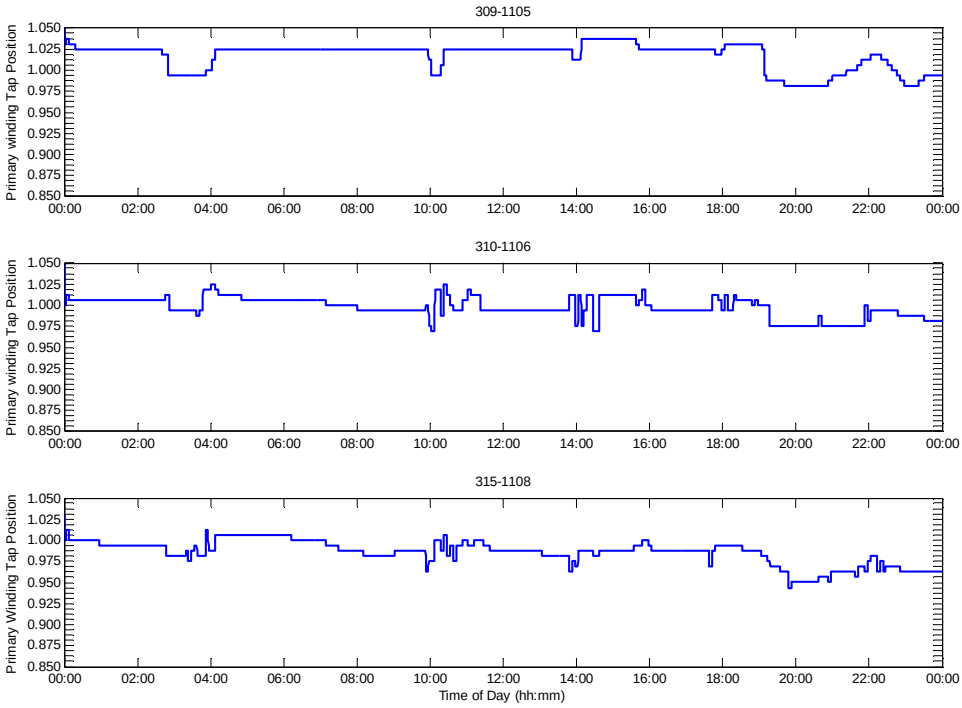

Figure 5.58: Tap positions for the wind farm DG distribution transformers – OPF3

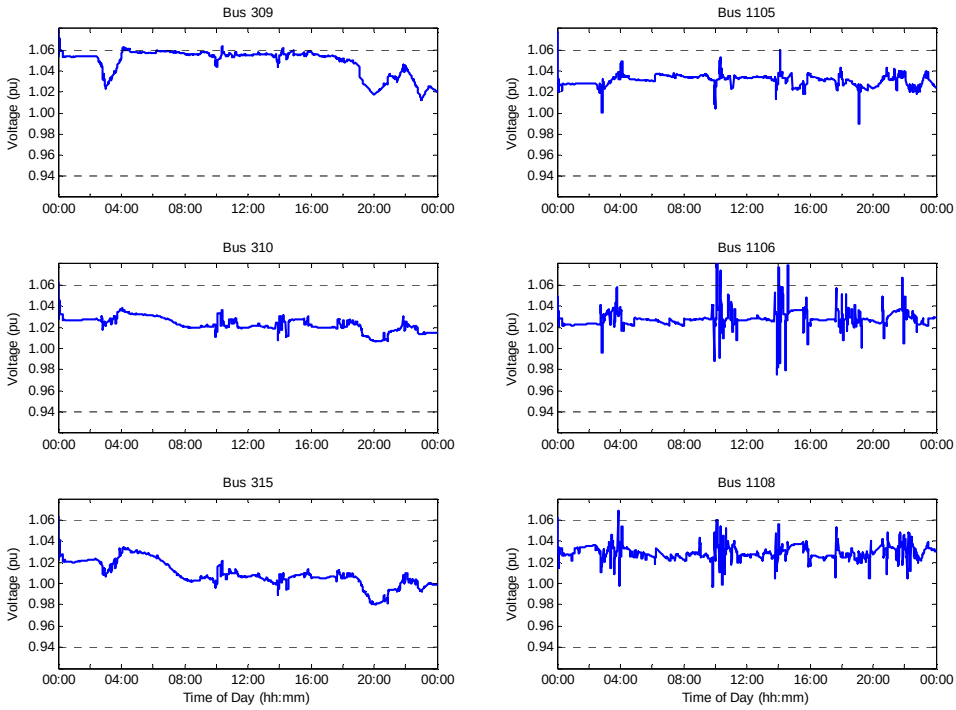

Figure 5.59: Voltage profiles for the wind farm DG distribution transformers - OPF3

5.3.3 EHV1 POWER FLOW SOLUTIONS WITH RHOPF

Simulations were conducted using the RHOPF formulation, with both the single input (RHOPF-A) and double-input short-term forecasting technique (RHOPF-B), as detailed in section 4.5.1. In this analysis, the RHOPF formulation operates continuously on a 5 minute control cycle. As before, the RHOPF technique determines a sequence of new network control settings for the upcoming half-hour, based on six 5 minute intervals. After the first 5 minute control cycle, the process is repeated. The control cycle is illustrated in Figure 5.60.

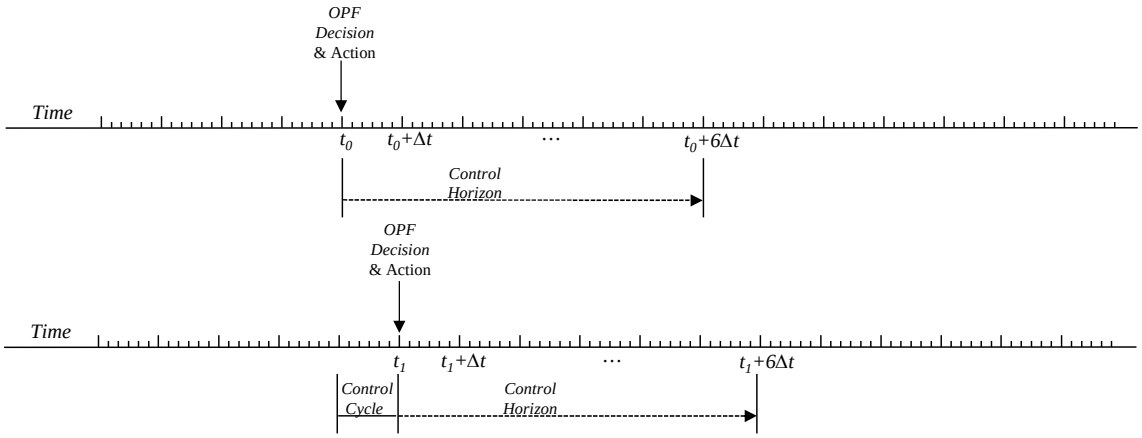

Figure 5.60: Time series event chart for the RHOPF analysis

In this scenario all unnecessary switching of active control settings was removed with a further reduction in the number of tap changing actions system-wide, as shown in Figure 5.63. To emphasise the impact of the RHOPF formulation, Figure 5.61 shows a summation of all tap changing actions in this network for each of the real time ANM OPF formulations.

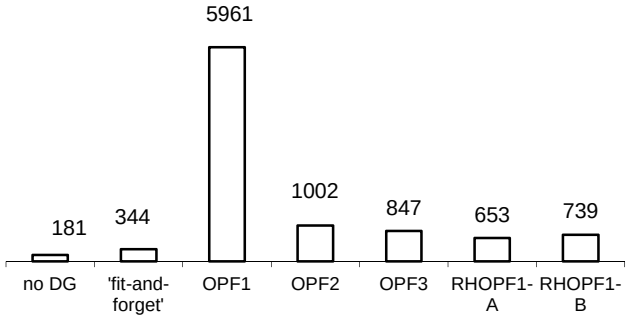

Figure 5.61: EHV1 Total tap changing actions

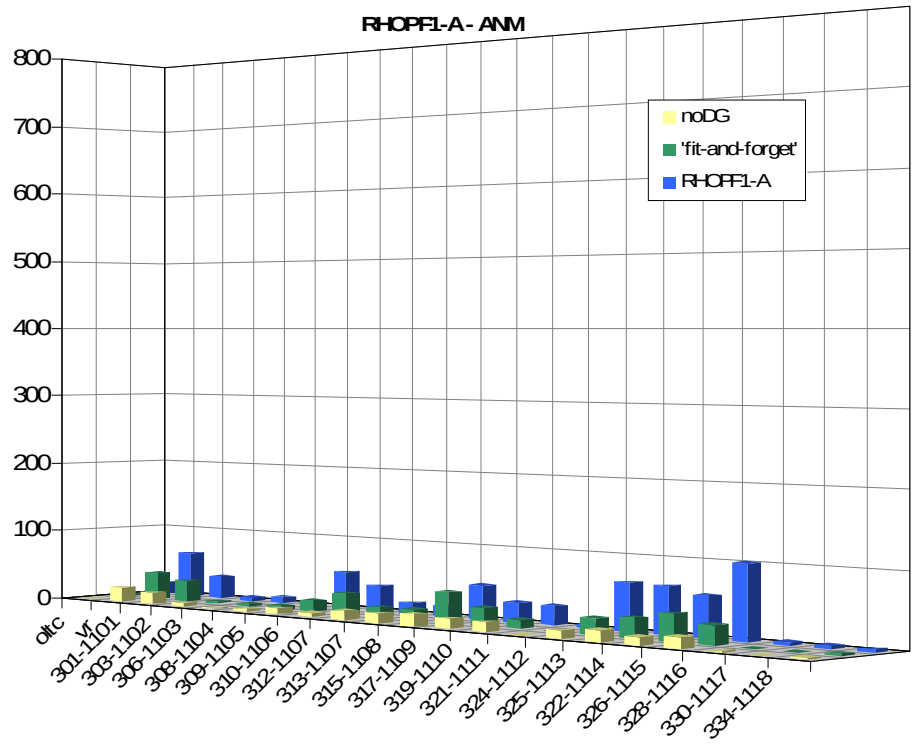

Figure 5.62: Total tap changing actions for all network transformers – RHOPF1-A

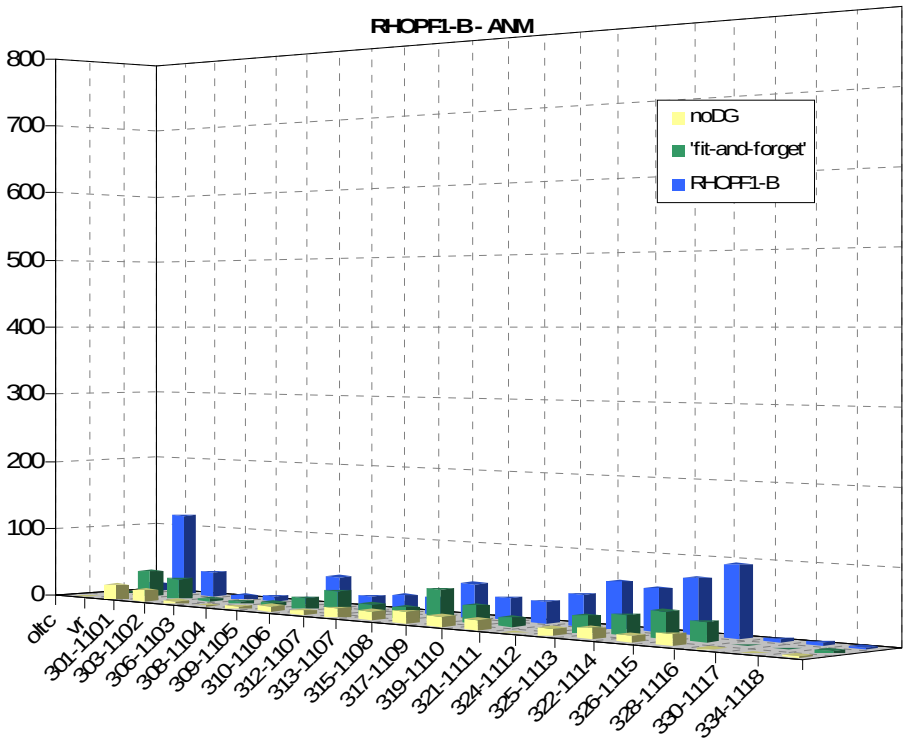

Figure 5.63: Total tap changing actions for all network transformers – RHOPF1-B

The resulting active network control settings and system operation under the action of the ANM OPF technique are demonstrated in the following series of figures for the RHOPF1-B scenario. The real power production for each of the wind farm and tidal array DGs are shown in Figure 5.64 and Figure 5.65. Respective reactive power production or absorption is shown in Figure 5.66 and Figure 5.67. The time series of tap positions in the OLTC and VR transformers and all the 33/11-kV distribution transformers directly connected to DGs is illustrated in Figure 5.68 through Figure 5.70.

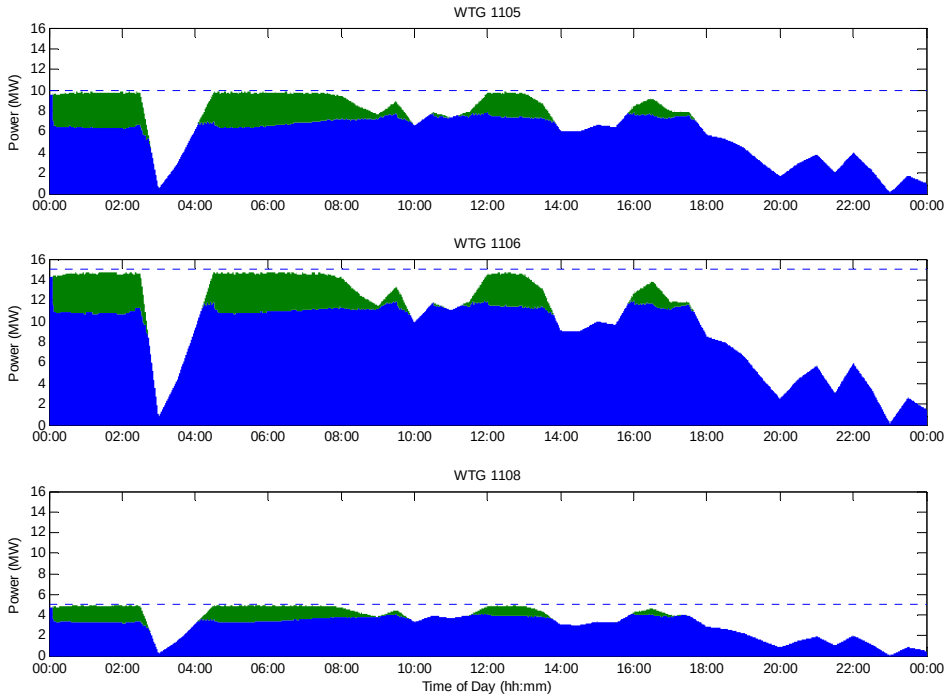

Figure 5.64: EHV1 wind farm DGs real power production – RHOPF1-B

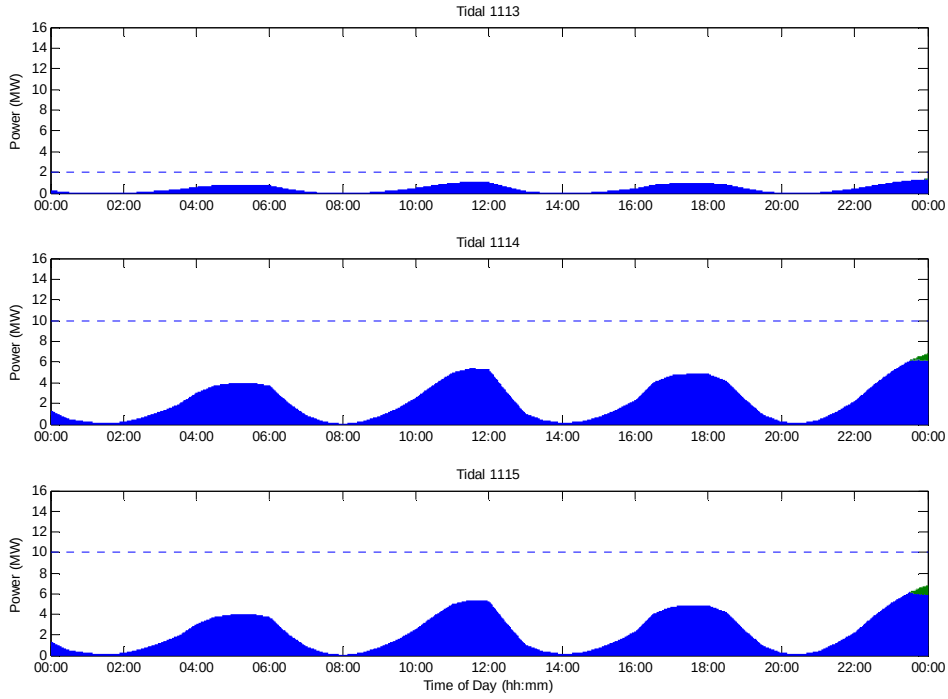

Figure 5.65: EHV1 tidal array DGs real power production – RHOPF1-B

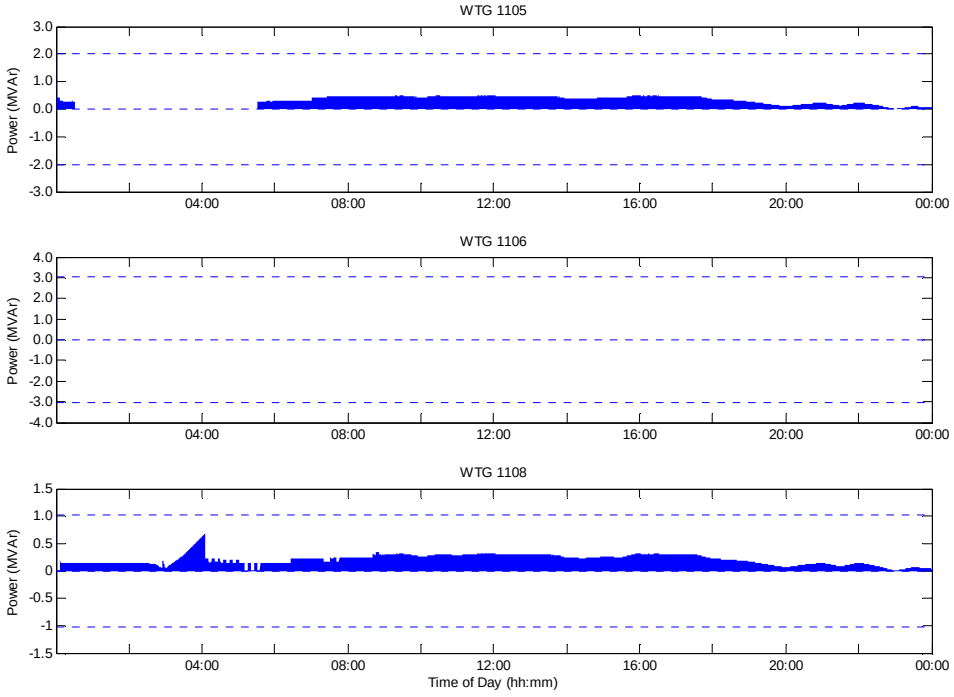

Figure 5.66: EHV1 wind farm DGs reactive power production – RHOPF1-B

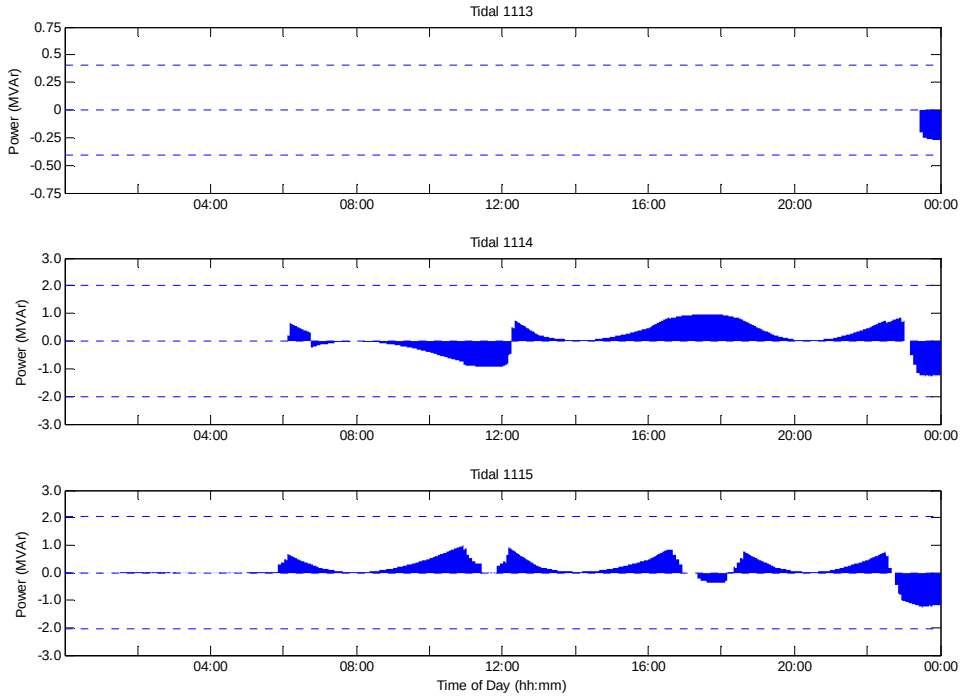

Figure 5.67: EHV1 tidal array DGs reactive power production – RHOPF1-B

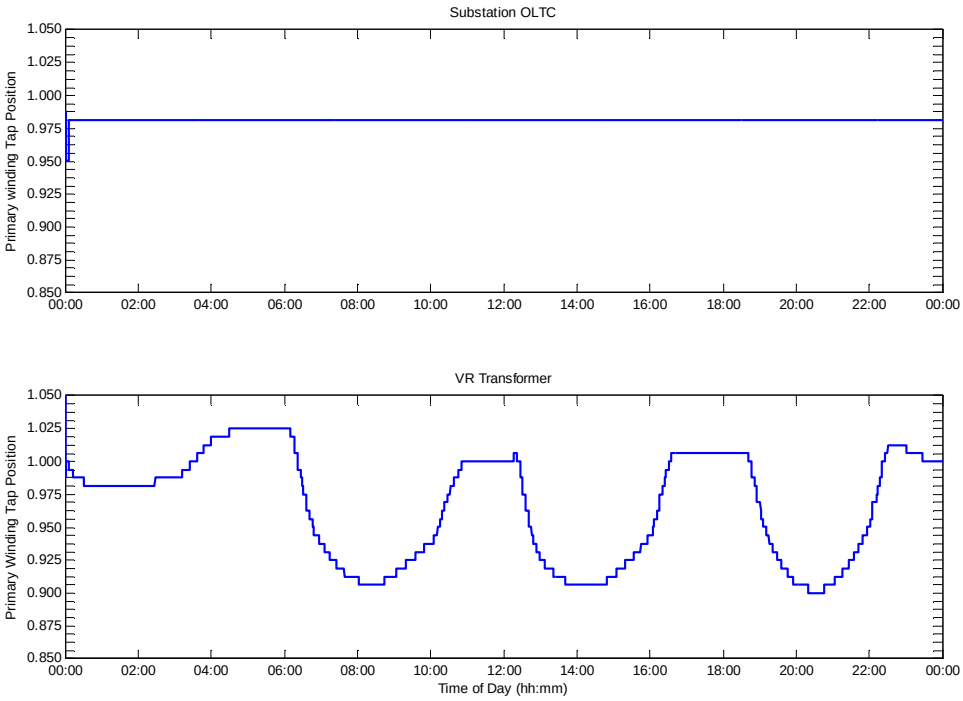

Figure 5.68: Tap positions for the network transformers – RHOPF1-B

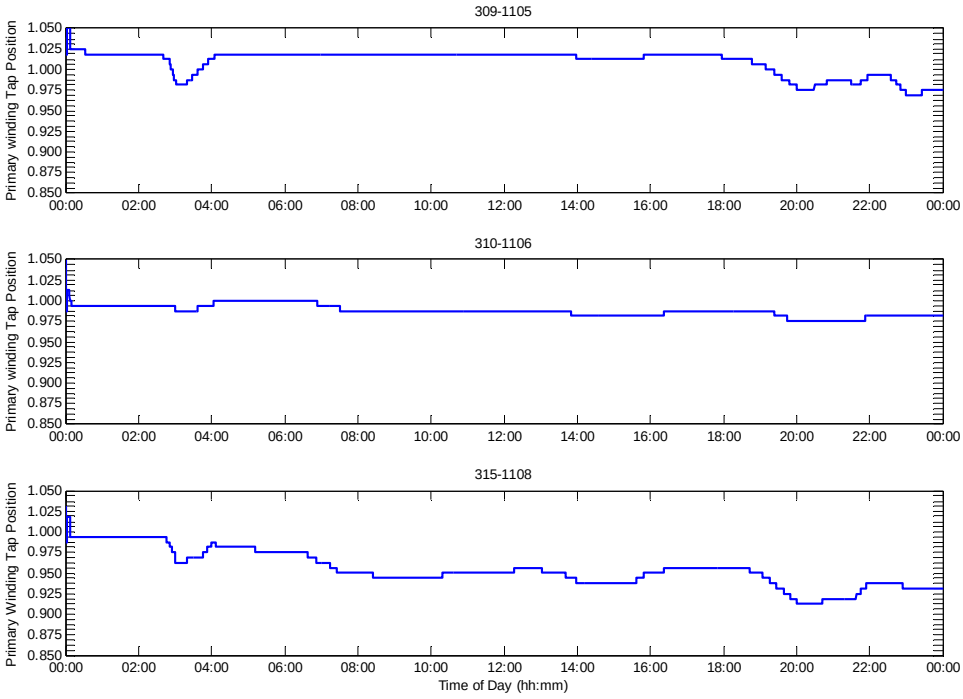

Figure 5.69: Tap positions for the wind farm distribution transformers – RHOPF1-B

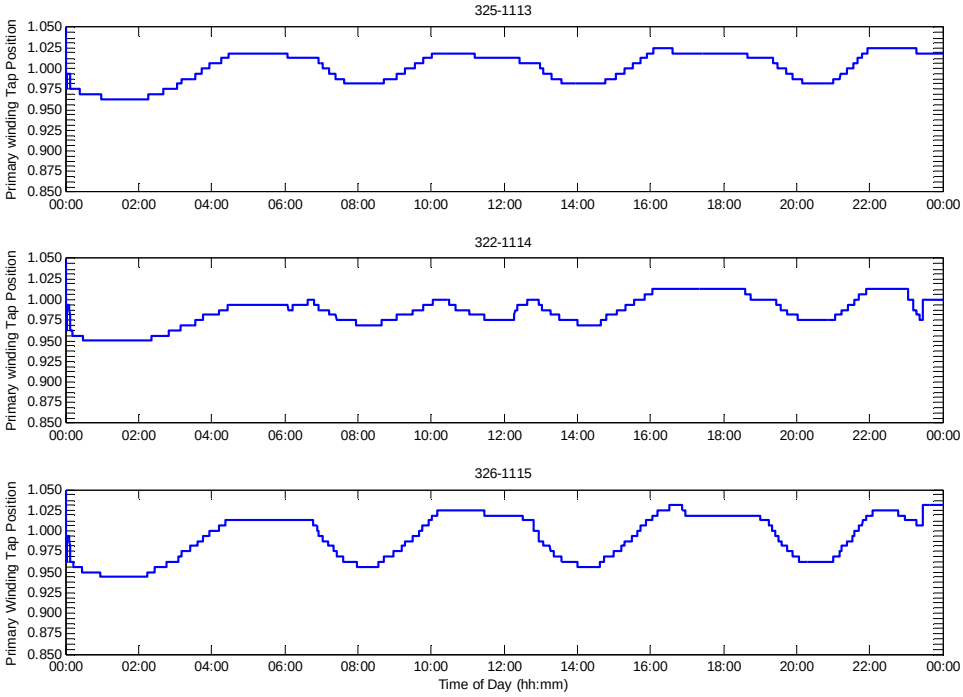

Figure 5.70: Tap positions for the tidal arrays distribution transformers – RHOPF1-B

Figure 5.64 to Figure 5.70 illustrate and confirm that solving the OPF over a longer time horizon and updating the procedure at an intermediate step, beginning from the previously derived plan of action, effectively guides the time sequential solutions of the OPF technique and prevents spurious switching of network control settings bringing temporal stability to successive OPF solutions. A similar pattern of results was evident for the RHOPF1-A analysis.

Energy yield in the RHOPF analysis is shown in Table XV and Table XVI. The total system wide energy yield from each DG development increased slightly, with a marginal reduction in the levels of prescribed energy curtailment.

RHOPF	WTG 1105	WTG 1106	WTG 1108	Tidal 1113	Tidal 1114	Tidal 1115
MW	10	15	5	2	10	10
MWh	138.3	216.6	71.0	11.0	55.1	55.1
MVArh	6.8	-1.7	4.7	-2.2	-11.0	-11.0
EC MWh	26.5	30.6	11.4	0.0	0.0	0.0
EC (%)	16.1%	12.4%	13.8%	0.0%	0.0%	0.1%
Capacity Factor (%)	57.6%	60.2%	59.2%	23.0%	23.0%	22.9%

Table XV: EHV1 DG energy yield – RHOPF1-A

RHOPF1	WTG 1105	WTG 1106	WTG 1108	Tidal 1113	Tidal 1114	Tidal 1115
MW	10	15	5	2	10	10
MWh	137.4	215.2	70.6	11.0	54.9	54.8
MVArh	6.7	0.0	5.0	-0.1	1.8	3.2
EC MWh	27.3	32.0	11.8	0.0	0.2	0.3
EC (%)	16.6%	12.9%	14.3%	0.0%	0.3%	0.5%
Capacity Factor (%)	57.3%	59.8%	58.8%	23.0%	22.9%	22.8%

Table XVI: EHV1 DG energy yield – RHOPF1-B

The synthesised forecast data employed in the full EHV1 network observational case study are shown in Figure 5.71 against the real time demand and resource levels. This was generated in same manner as before, taking a weighted central moving average of the real time resource levels from the original half-hourly time series data introduced in section 3.6. Much of the problematic impacts experienced on the network occur during instances of sharp rises in resource level. This is particularly evident for the wind farm developments where forecasted resource levels differ significantly during the sharp drop and quick rise in resource.

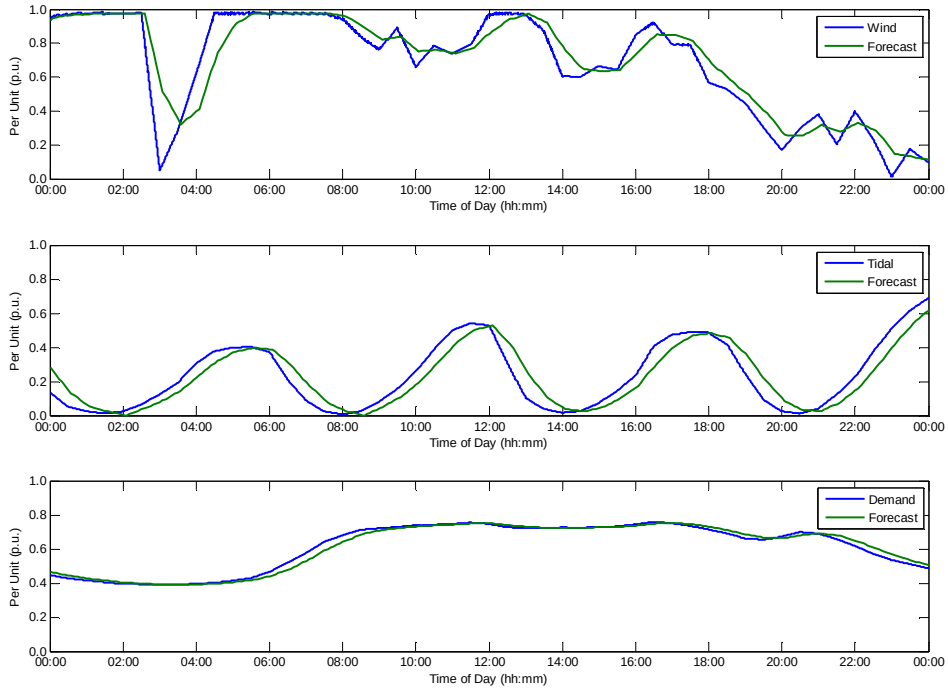

Figure 5.71: Comparison of synthesised forecast data – RHOPF

With the single input forecasting analysis, RHOPF1-A, the use of low resolution forward-looking forecast data to predict upcoming power flow injections left the potential for the network to stray significantly and perhaps detrimentally from the optimally prescribed state, as was seen in the simplified EHV1 – ANM network. In this observational test case, imbalances in the forecasted and real time availability of power from renewable energy DGs led to severe thermal overloading of certain system components and minor system voltage excursion.

For the wind farm developments, the substantial imbalance in the level of resource between 02:00 and 05:00 hours led to a significant thermal overload experienced by the connecting infrastructure. Thermal loading peaked at more than 150% on the 33/11-kV distribution transformer connecting to the 15 MW wind farm at bus 1106.

Figure 5.72 (bottom) illustrates the discrepancy in power production from the wind farm at bus 1105 between the RHOPF1-A solutions (AIMMS) with synthesised forecast data and the power flow solutions of the distribution network (OpenDSS). A comparison of the thermal loading of the connecting distribution network transformer between the

RHOPF1-A solutions and the network power flow solutions is shown in Figure 5.72 (top).

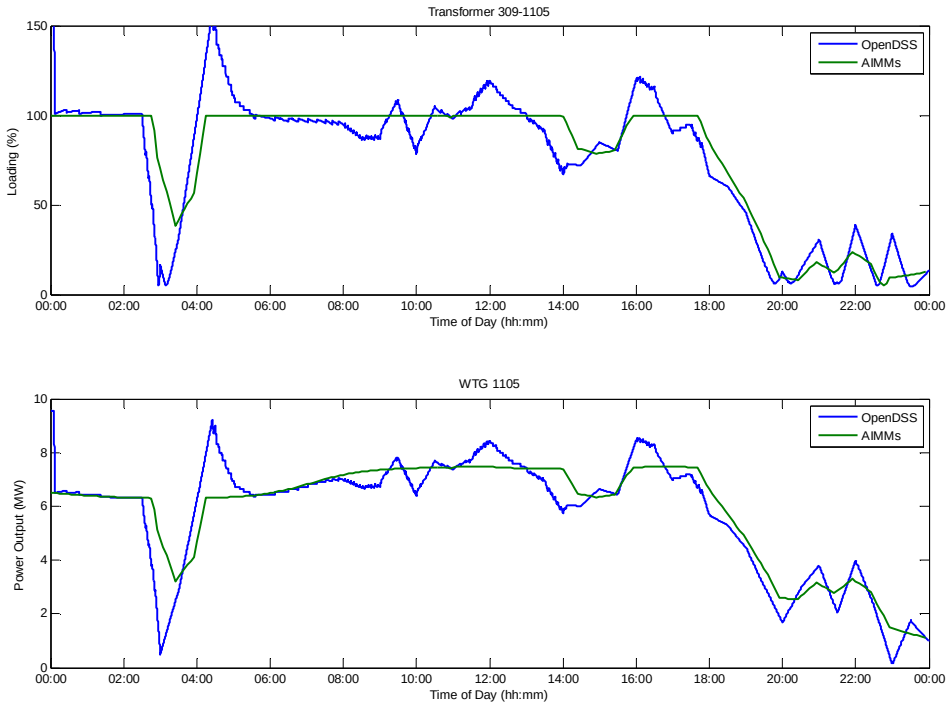

Figure 5.72: Real power output and transformer loading for the 10 MW wind farm – RHOPF1-A

Figure 5.72 shows that network thermal overloading was a direct consequence of those large errors in the forecast data and actual real time resource level. Box plots, extending to the 5^{th} and 95^{th} percentile of the thermal loading levels on the overloaded wind farm distribution transformers are shown in Figure 5.73. These demonstrate that large errors in the forecast data can initiate higher levels of component overloading, which can trigger thermal protection relays.

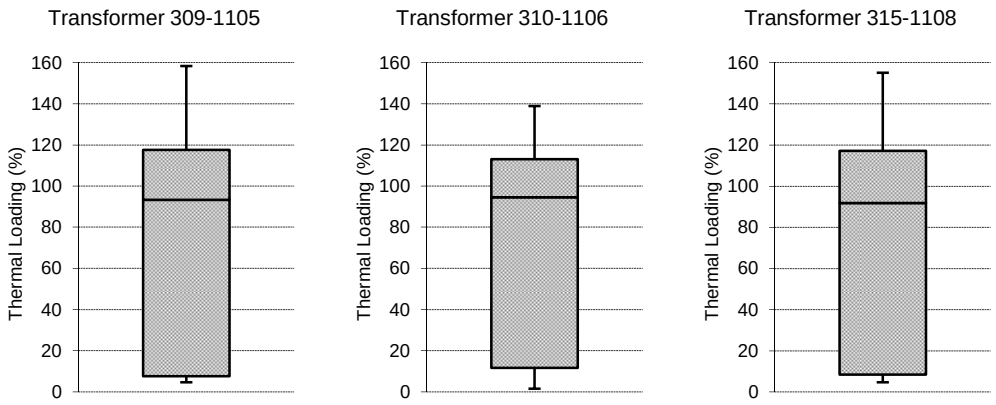

Figure 5.73: Box plots of wind farms distribution transformer loading – RHOPF1-A

With the more short term, double input forecasting routine in the RHOPF1-B analysis, the worst impacts of the single input forecast data were mitigated against. Maximum short-term thermal loading on all overloaded transformers was below 115% of rated capacity and the short term thermal overloading of the network components was below 105% of the rated thermal capacity for more than 95% of the observational test case.

Short term overloading of network components can be tolerated at the discretion of DNOs, partly due to the conservative estimates of environmental and atmospheric conditions made during the thermal capacity assessment.

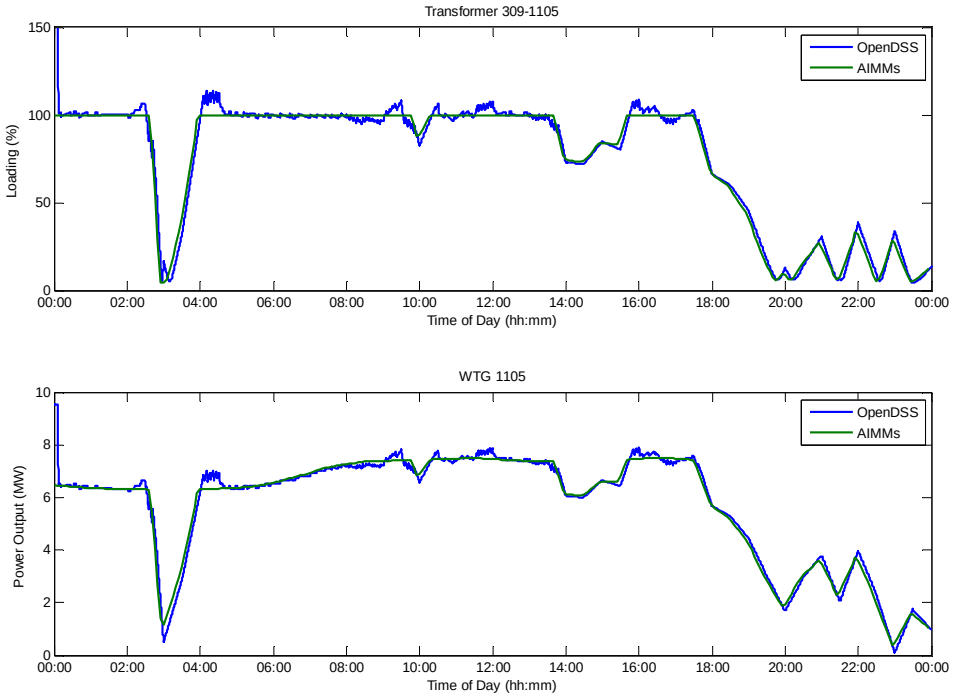

Figure 5.74: Real power output and transformer loading for the 10 MW wind farm – RHOPF1-B

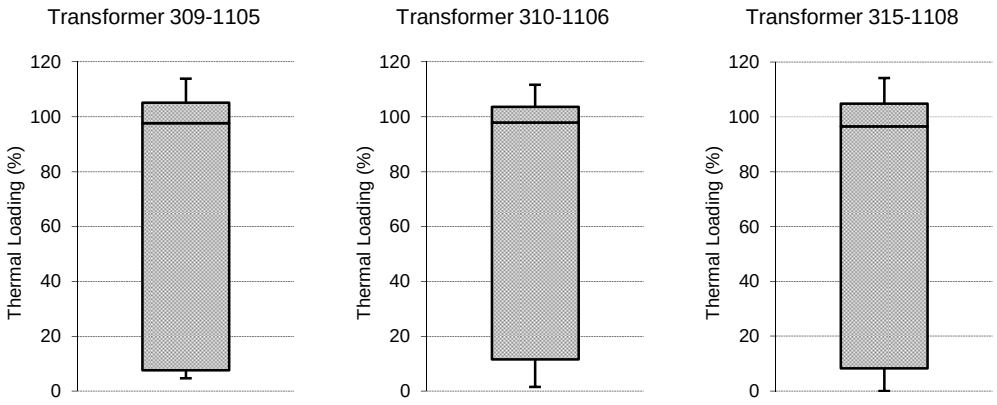

Figure 5.75: Box plots of wind farms distribution transformer loading– RHOPF1-B

Network voltage levels in the RHOPF1-A analysis were, despite minor short term excursions, within the recommended limits of the statutory voltage envelope, as demonstrated by the voltage levels on the 33/11-kV distribution transformers connecting to the DGs, shown in Figure 5.76 and Figure 5.77

In the RHOPF1-B analysis, residual voltage variation at bus 326 did continuously push the voltage level above the statutory envelope for more than 5% of the case study.

Multi-faceted formulations of the advanced ANM OPF technique were determined to reduce this within the recommended limits. In the RHOPF1-B analysis overvoltage excursion at bus 326 was observed for 21.3% of the 24-hour time period, as shown in Figure 5.79. With the RHOPF2-B and RHOPF3-B formulations this was reduced to 4.8% and 2.1% respectively, without incurring any network undervoltage excursion and whilst further reducing the number of tap changing actions.

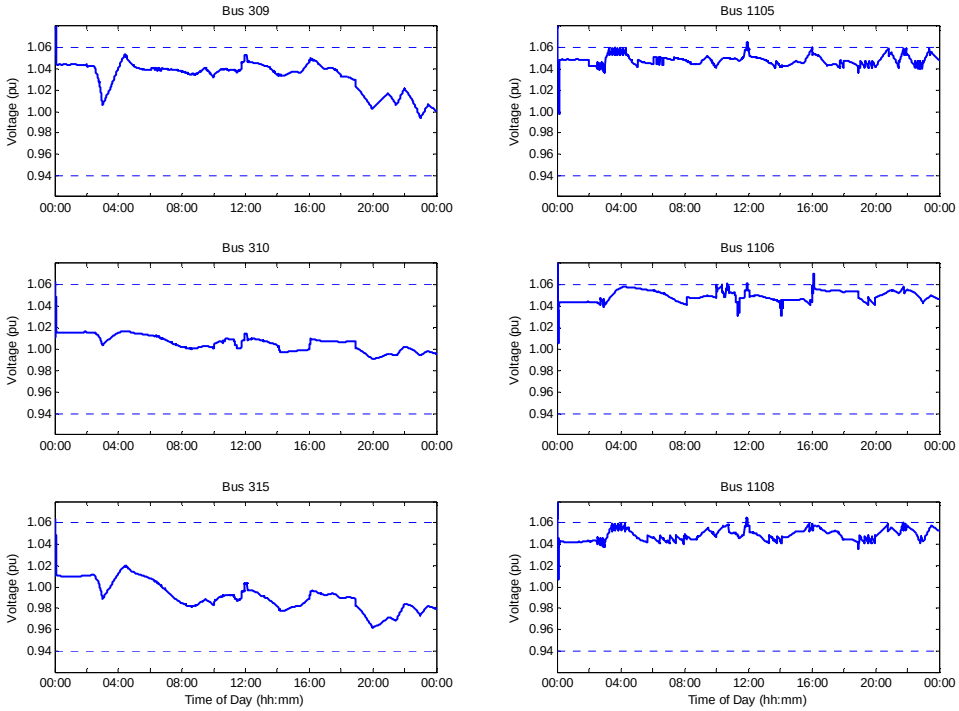

Figure 5.76: Voltage Levels on the wind farms distribution transformers – RHOPF1-A

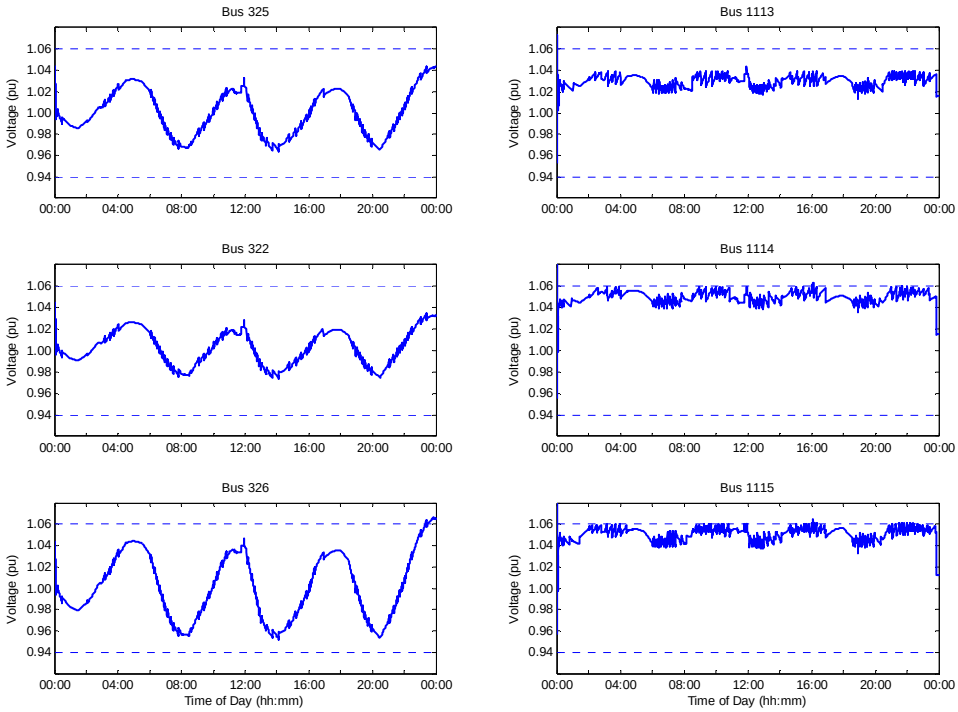

Figure 5.77: Voltage levels on the tidal arrays distribution transformers - RHOPF1-A

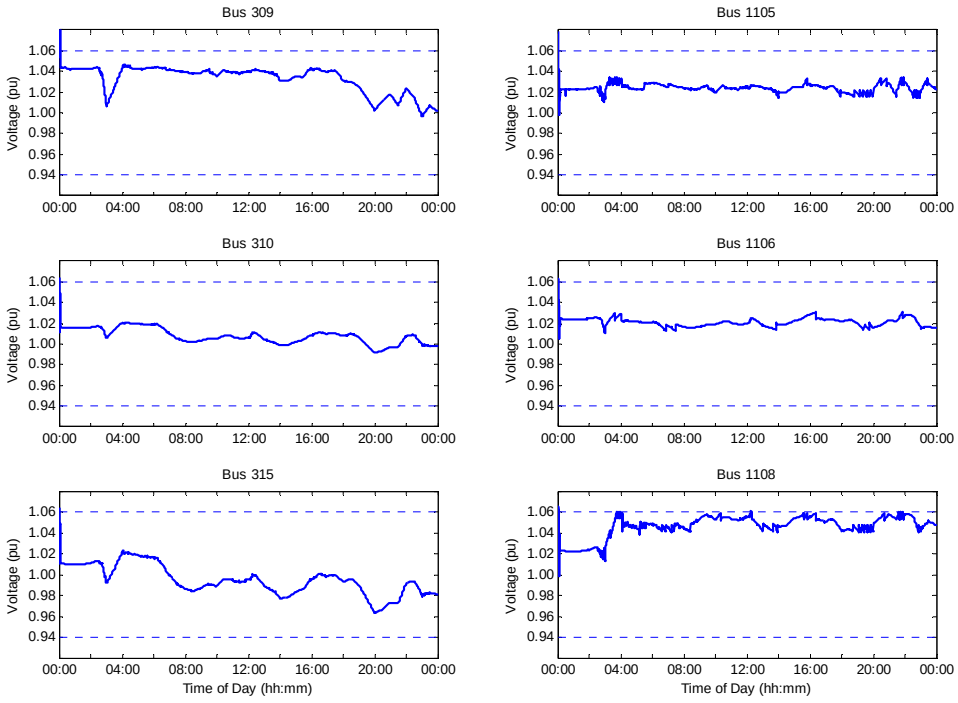

Figure 5.78: Voltage Levels on the wind farms distribution transformers – RHOPF1-B

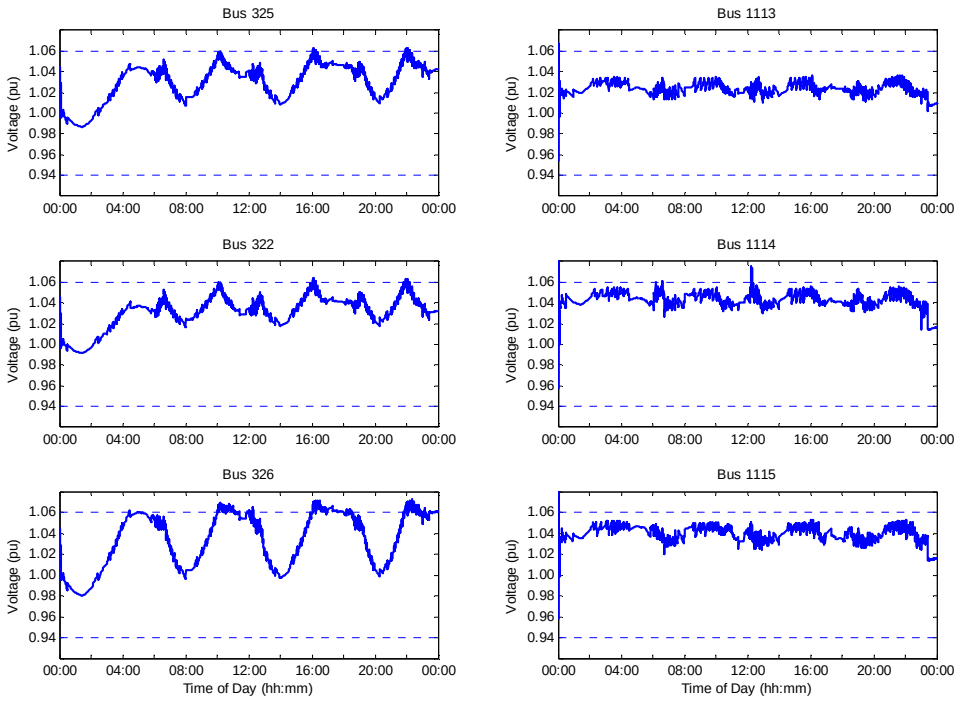

Figure 5.79: Voltage levels on the tidal arrays distribution transformers – RHOPF1-B

In the network configuration studied, the installed capacity of DG was greater than the peak network demand. During the period of high DG production in the observational test case, power flow between the distribution network and electricity grid at large was exchanged in both directions. Figure 5.80 and Figure 5.81 show the import and export of complex power over time. This was comparable for both the RHOPF1-A and RHOPF1-B analyses.

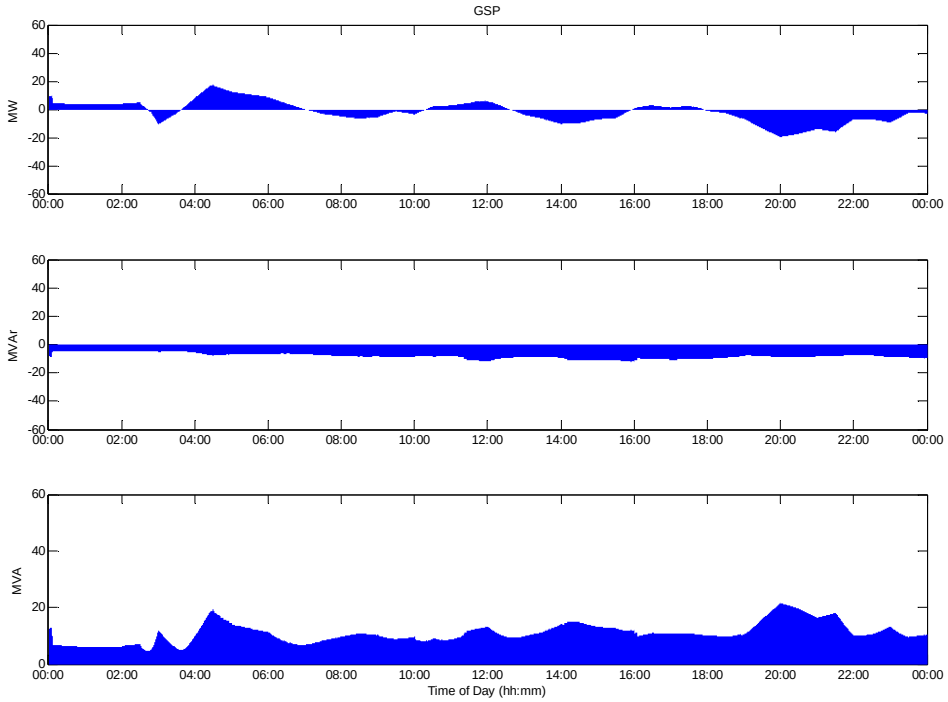

Figure 5.80: EHV1 GSP power flow – RHOPF1-A

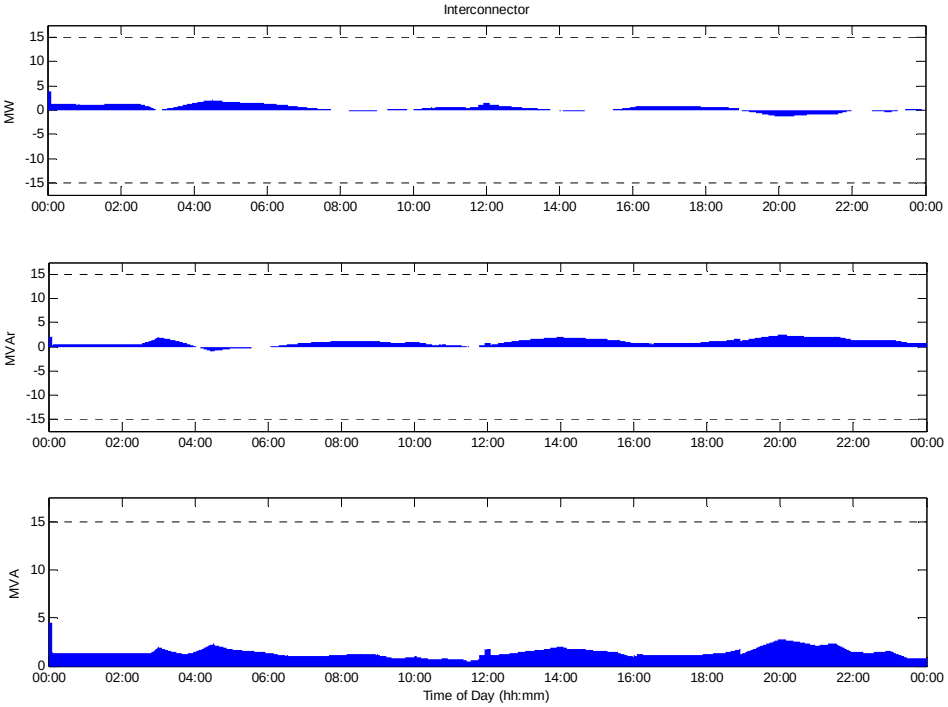

Figure 5.81: EHV1 Interconnector power flow – RHOPF1-A

Figure 5.82 shows the change of network losses across different configurations and operating philosophies. Network losses in the full ANM scenario with 52 MW of installed DG capacity was comparable to the 'fit-and-forget' scenario with 20.5 MW of installed DG and only slightly increased from the network operation with no DG.

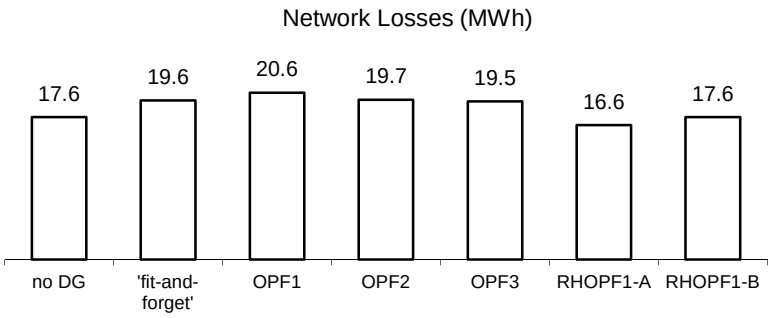

Figure 5.82: EHV1 network losses

5.3.4 SUMMARY

This section has studied and interpreted the application of the advanced ANM OPF techniques in the full EHV1 network. This confirms that the OPF technique can be implemented in real time to larger and more complex distribution networks.

Investigations have shown that spurious and unnecessary control actions was a consistent barrier to the continuous single scenario snapshot formulations of OPF in real time. Once again, the receding-horizon principle provided temporal stability to real time OPF solutions and eliminated all instances of unnecessary control switching.

Large errors between the forecast data and actual real time resource levels were a boundary to the RHOPF1-A technique. The potential for DG power production to far exceed the predicted power output was shown to have severe consequences for the network. In the RHOPF1-B analysis, the real time, short term forecasting technique, which linearly interpolates a trajectory between the measured network power injections and the longer term forecast level, mitigated the severe system impacts, but was still hindered by the residual variation in network parameters. Multi-faceted formulations of the real-time ANM OPF technique were investigated and determined to improve the network response and avoid the most severe network consequences from residual variations in network power flows.

A more abrupt method of preventing excessive DG production was to infer additional (load limiting) control settings on secondary, self-regulating, control measures of regulated non-firm DGs. Subsection 5.4 explores decentralised or distributed automation (DA) control techniques assigned to work in combination with the real time OPF techniques to mitigate errors in data forecasts and deviations in power output from the optimally prescribed state.

5.4 COMBINING OPF WITH LOCAL CONTROL

In Chapter 5 so far, the boundaries and reality of using OPF techniques in real time to schedule active DG and responsive network asset control settings in larger distribution networks were identified. Two phenomena which exhibit a significant influence on this potential application were: spurious network switching actions and errors in the short-term fluctuations of renewable DG resource. Advanced formulations of the ANM OPF technique have been explored to improve the temporal stability of successive OPF solutions on a very short, 5 minute control cycle.

Inevitably, although centralised optimisation of all system control assets is necessary to maximise the system-wide energy yield and network benefits, secondary localised control infrastructure will have to assume more responsibility for final power output at each DG to account for short term fluctuations and forecast errors.

In this section more responsive control practices at the DGs were included in the power flow solutions of the distribution network. Further details of these schemes are presented in section 5.4.1.

In previous examples, due to the volume of data produced, the investigation and network observations were only conducted over relatively short periods of time (24 hours). With the adoption of more authoritative DG control practices to regulate and maintain the OPF prescribed network set-points between OPF intervals, the length of the study was extended to model wider variation and more progressive changes in supply and demand variations. This was achieved by using a longer, coarser time interval, for both the successive OPF solutions and the time series of power flow solutions which represent the real network response.

In this section only, time series power flow analysis was simulated through successive steady state solutions at 5 minute intervals. Optimised scheduling of the system pre-sets was performed on a 15 minute control cycle, the time series of control cycles are shown in Figure 5.83. In the case of persistence forecasting, the lag time for OPF scheduling was 5 minutes. The simulations in this section were conducted on the larger and more complex full EHV1 network.

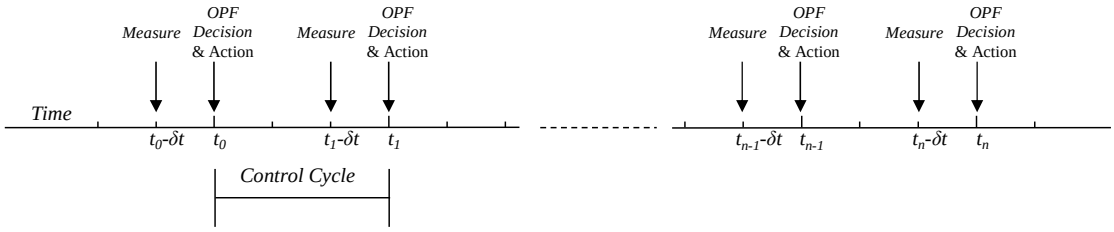

Figure 5.83: ANM OPF control cycle

5.4.1 DESCRIPTION OF LOCAL CONTROL PRACTICES

In the preceding analysis, the production of more DG real power than was prescribed by the OPF solutions was facilitated by the 'active' control practices applied to the DGs. The per-unit production setting applied to the power flow solutions was a proportion of the maximum power output divided by the forecast of respective resources. This ensured that active control settings were reflective of the prevailing resource levels and only curtailing real power production to appropriate levels; and not unnecessarily turning down excess production. Hence, errors and fluctuations in resource patterns meant that the final real time DG output differed from the predicted value.

In the forthcoming analysis, a secondary control loop was included in the power flow solutions representing the actual distribution network, which limited real power production from the renewable non-firm DGs to the power output of the preceding OPF solution. Local controllers were simulated to act with corrective, curtailment of real power output only in the event of power output at the DG point of connection creeping significantly beyond the maximum level identified by the OPF solution. These control practices were termed Distributed Automation (DA)[2] and can be deployed in

[2] DA control practices with this precise functionality were identified in Chapter 2.

combination with the OPF scheduling routine. A flow chart, detailing the control practices is shown in Figure 5.84. At each power flow solution in the proxy distribution network, the DG power output level is monitored. If the observed production level is greater than the steady state tolerance limit of power dispatched plus 1% of installed capacity (P_{limit}) then the local DG controller acts autonomously to curtail DG output until it is constrained within the prescribed level of the OPF solution (P_{set}). This local control cycle occurs on a short term time frame faster than the 5 minute intervals recorded by the distribution management system, as illustrated in Figure 5.85. This interactive approach harmonises the centralised optimal scheduling of system assets with decentralised control intelligence to maximise the network benefit from ANM.

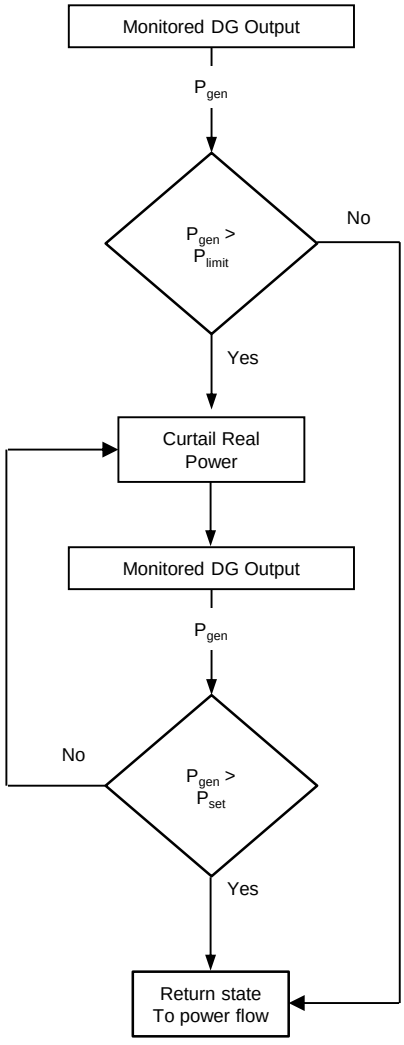

Figure 5.84: DA control practice flow chart

A similar interactive approach, which in the absence of pre-existing voltage control measures at the point of connection, such as the case in the simplified EHV1- ANM network, can operate with the hybrid voltage DA control measures, such as AVPFC.

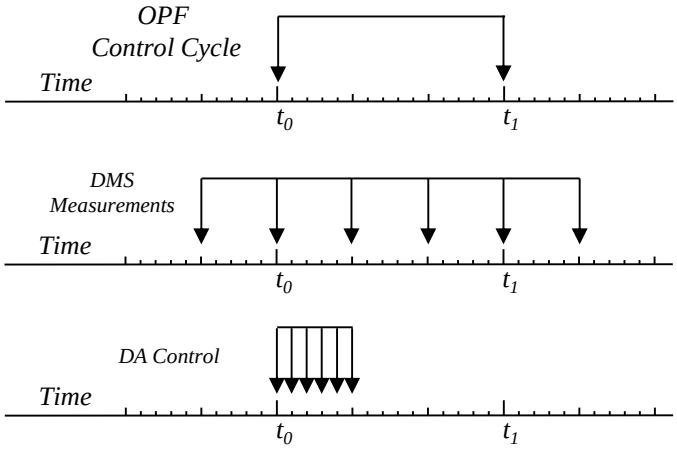

Figure 5.85: Time frame of concurrent elements

5.4.2 OBSERVATIONAL TEST CASES

Two case studies of varying system demand featuring a wide variety of multiple supply and demand combinations were analysed. Testing at the coarser time interval meant simulations could be performed and more easily reviewed over a longer simulation period. The test case simulations were each conducted over a one week observational period.

The intermittent generation profiles and variable demand pattern are illustrated in Figure 5.86 and Figure 5.87. Case 1 had a wind power capacity factor of 64.9% and was considered a period of extremely high wind power resource. Tidal resource in case 1 was very low with a total capacity factor of 9.9%. The availability of each resource was reversed in case 2, with a rising trend in tidal power and a lull in wind power resource. Capacity factors for wind and tidal resources in case 2 were 17.5% and 34.1% respectively. Case 1 covers a winter period of relatively high demand, while case 2 covers a summer period of relatively low demand.

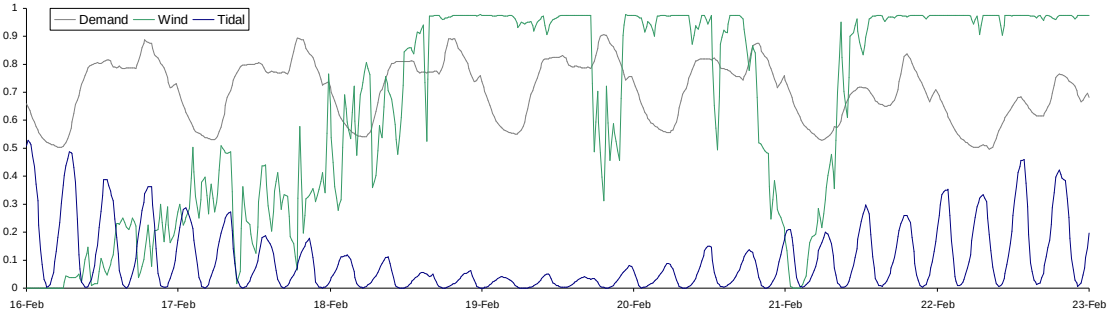

Figure 5.86: Weekly generation and demand patterns for case 1

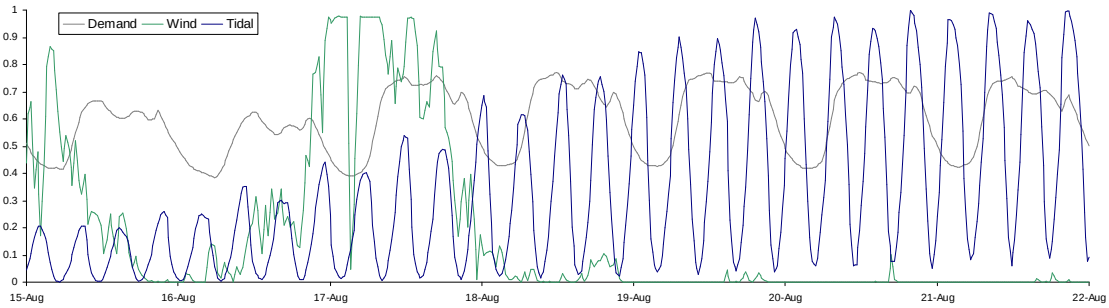

Figure 5.87: Weekly generation and demand patterns for case 2

5.4.3 POWER FLOW NO DG

Network performance was assessed on the system power flow prior to the connection of any DG. The results are included here to provide the back-drop of the pre-existing network response from which to analyse and interpret the changing power flow regimes after the connection of DG.

The network control settings, namely the voltage settings on the substation OLTC transformer, VR transformer and the 33/11-kV distribution transformers, are shown in Figure 5.88 to Figure 5.93. In these illustrations, the continual transition of local and upstream tap changing transformers had a tendency to make the voltage profile appear noisy, when viewed on this protracted time scale. This is particularly evident for the distribution transformers on the ‘island’ where voltage levels are subject to three tiers of tap-changing actions.

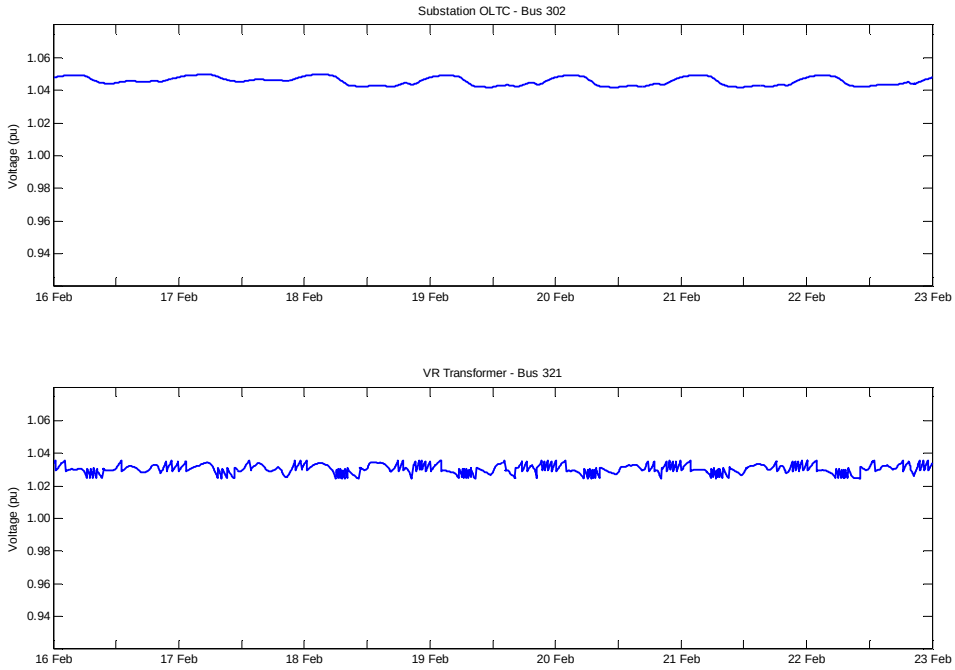

Figure 5.88: no DG network transformer voltages case 1

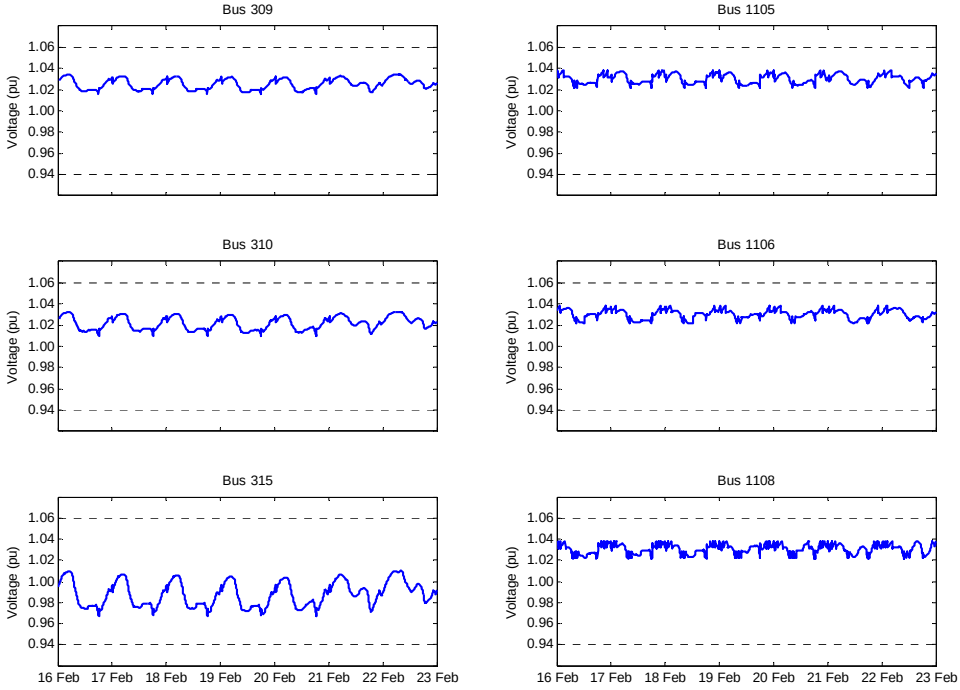

Figure 5.89: no DG wind farm transformer voltages case 1

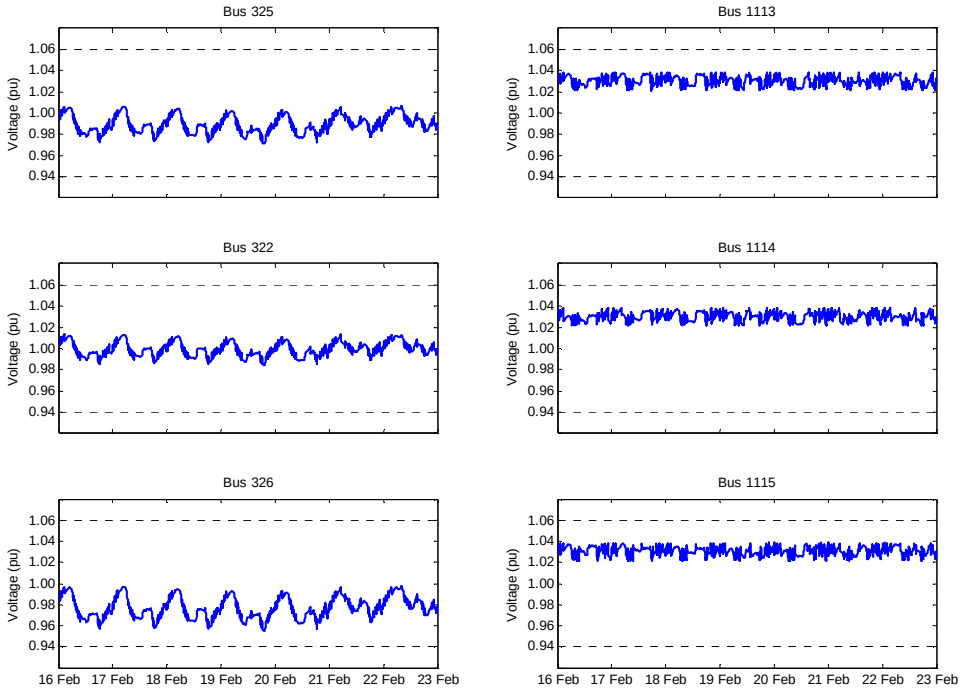

Figure 5.90: no DG tidal transformer voltages case 1

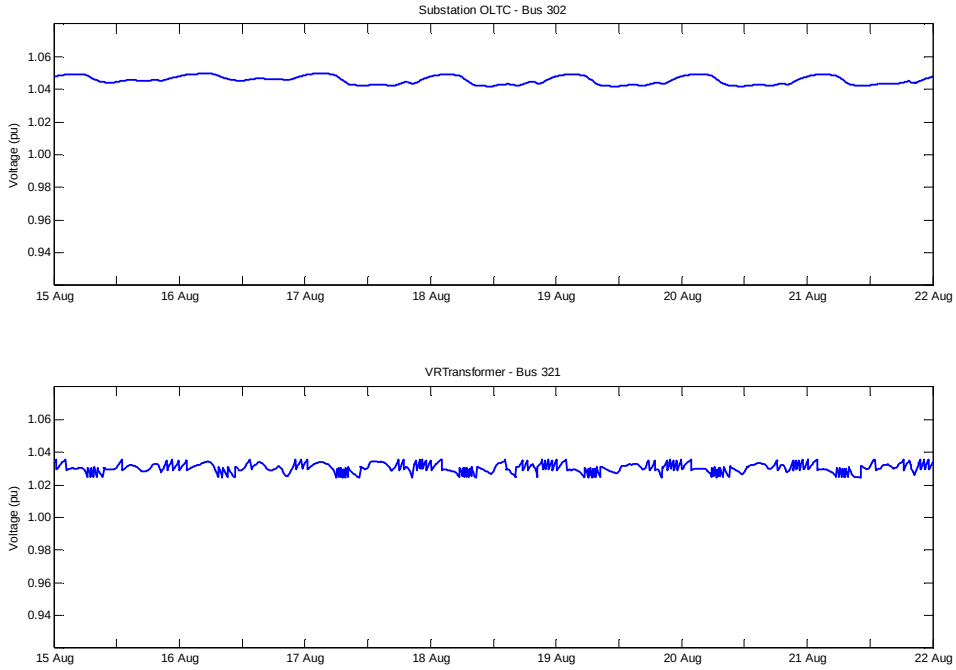

Figure 5.91: no DG network transformer voltages case 2

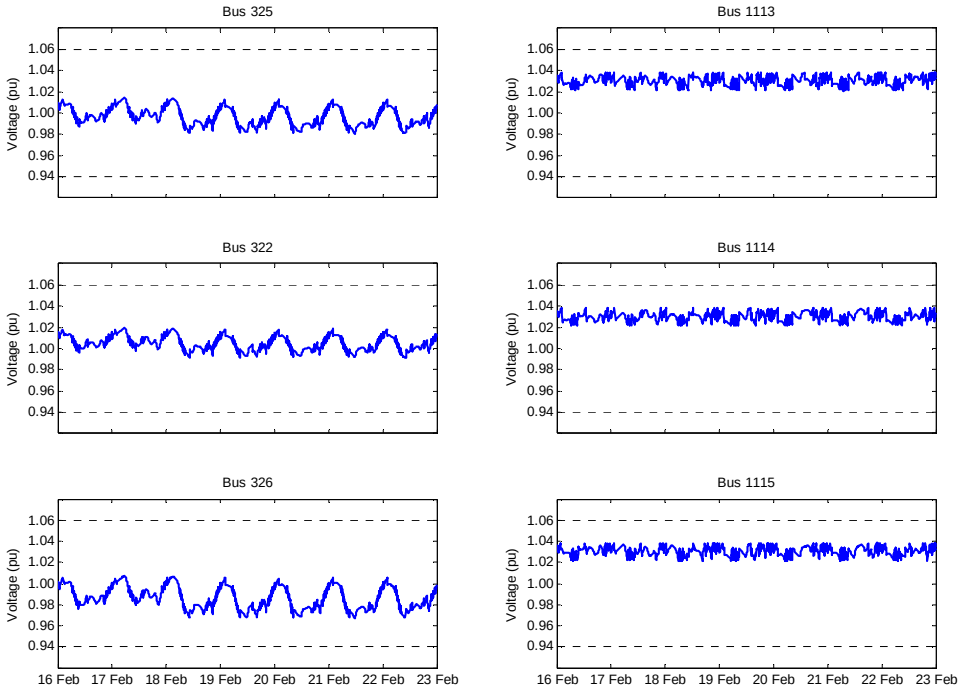

Figure 5.92: no DG tidal transformer voltages case 2

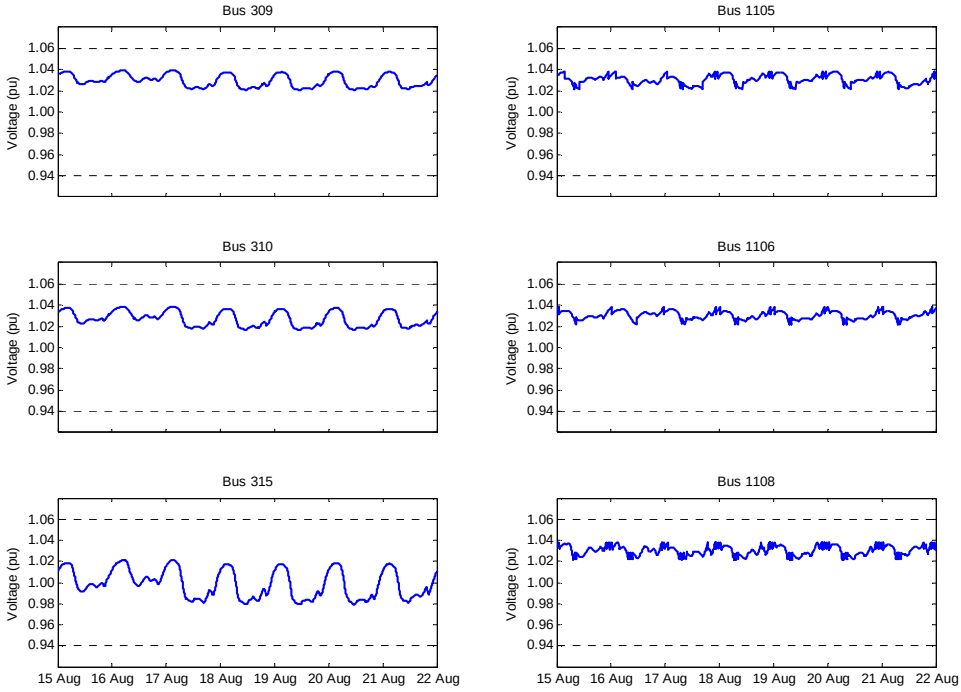

Figure 5.93: no DG wind farm transformer voltages case2

The time series traces of all automatic control actions were consistent and appropriate to network demands. Figure 5.94 and Figure 5.99 show the time series progression of the tap positions on the substation OLTC and VR transformers. On first impression, there appears to be a lot of tap action on the VR transformer. During the observational test cases (1 and 2) tap changing actions were recorded on average once every 103 and 105 minutes respectively.

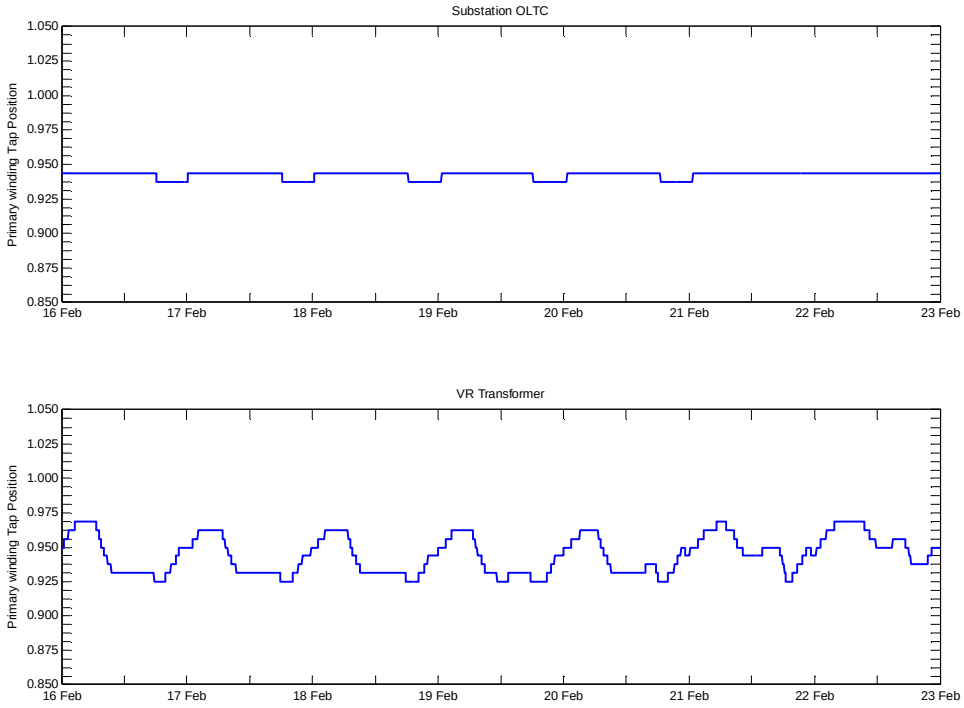

Figure 5.94: EHV1 network transformer tap actions for the No DG case 1

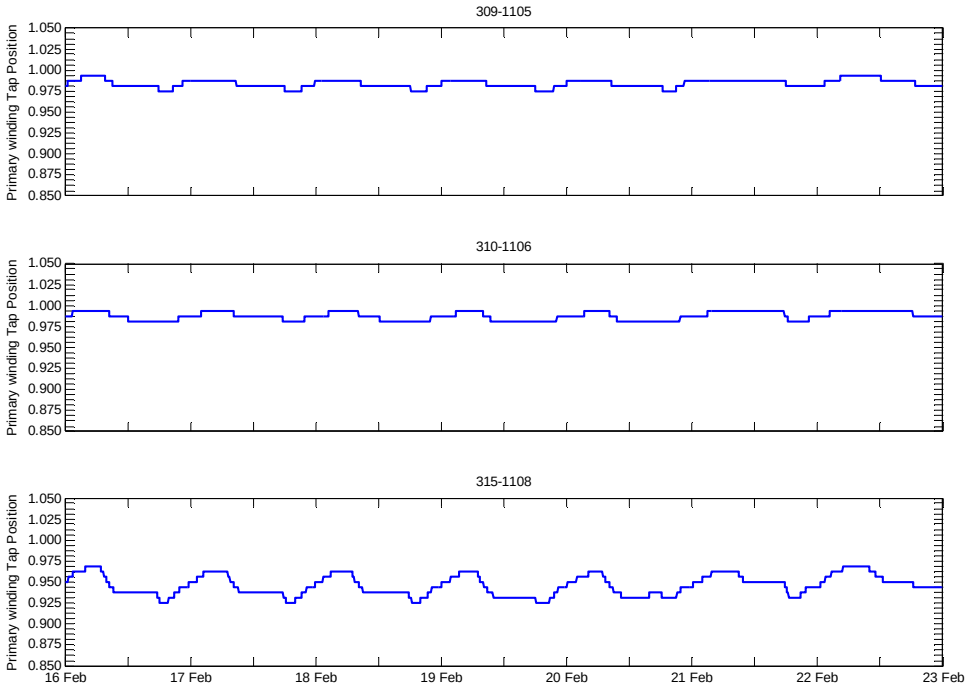

Figure 5.95: EHV1 wind farm distribution transformers tap actions for the No DG case 1

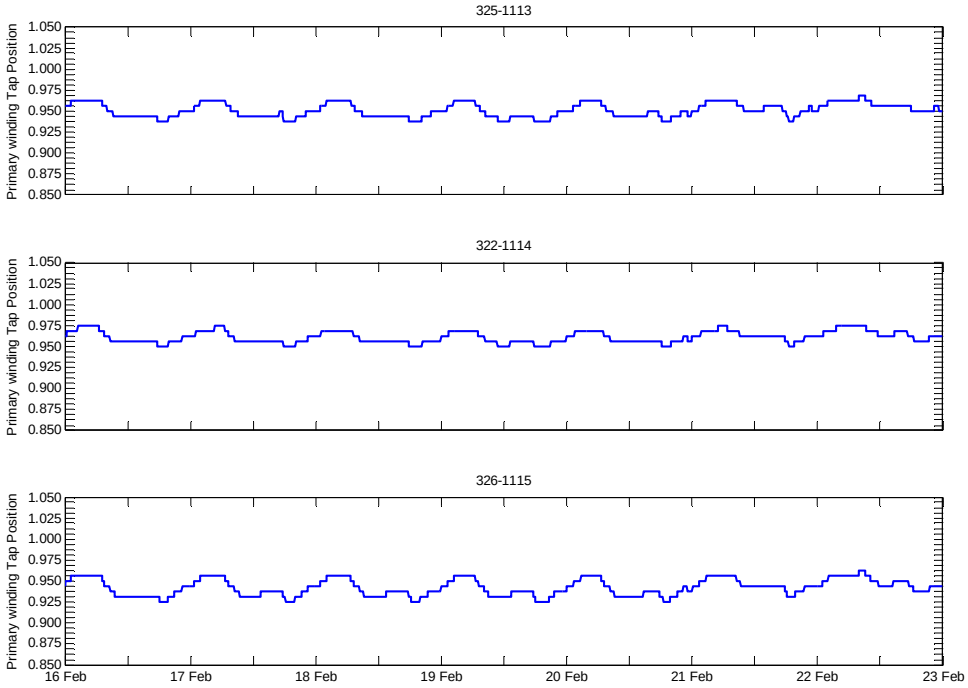

Figure 5.96: EHV1 tidal distribution transformers tap actions for the No DG case 1

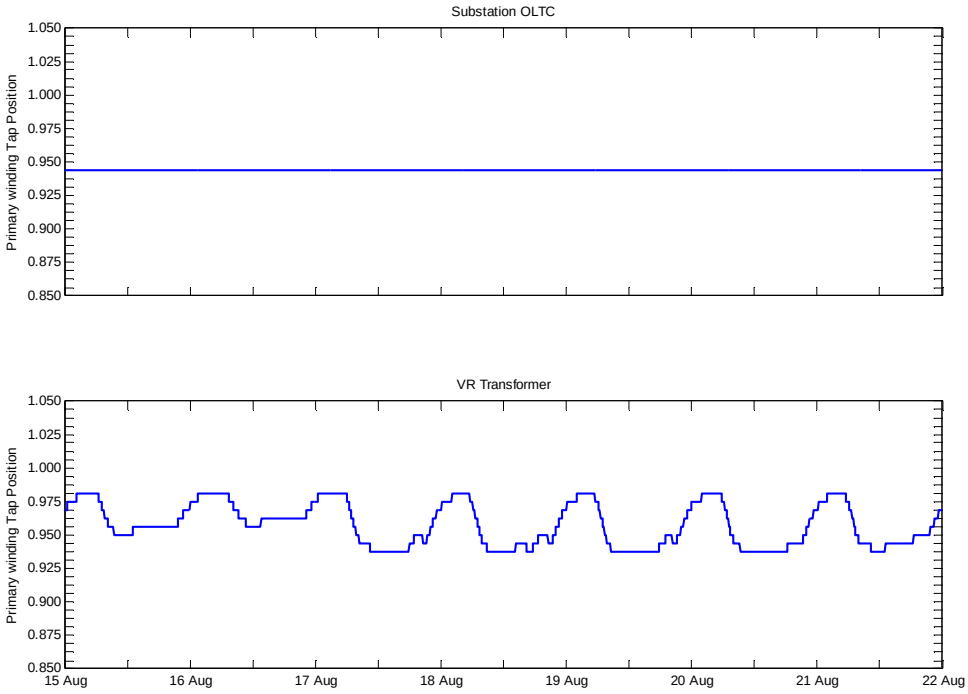

Figure 5.97: EHV1 network transformers tap actions for the No DG case 2

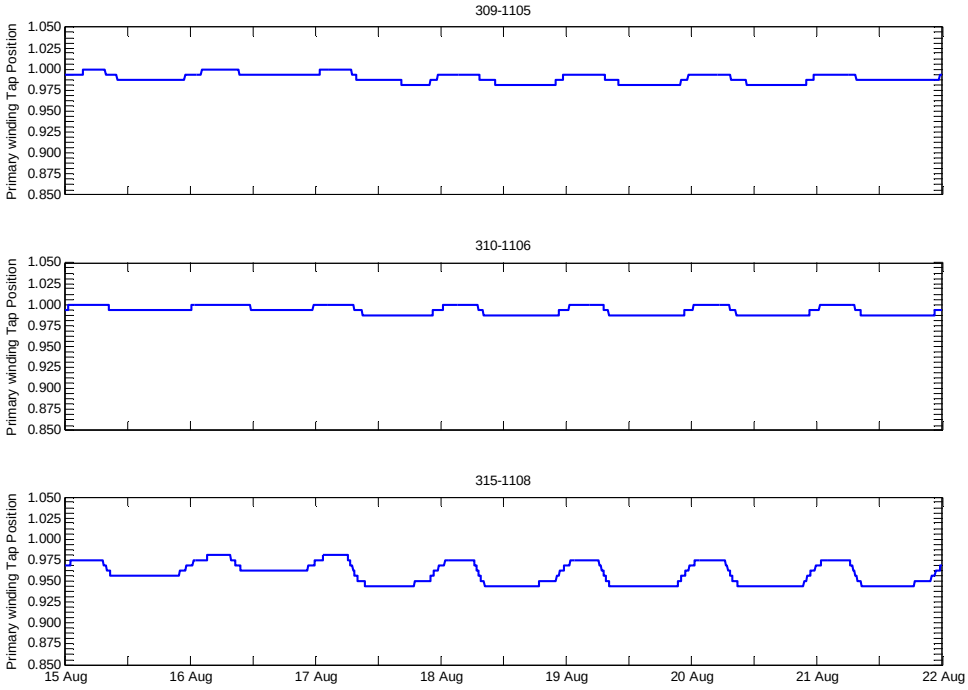

Figure 5.98: EHV1 wind farm distribution transformer tap actions for the No DG case 2

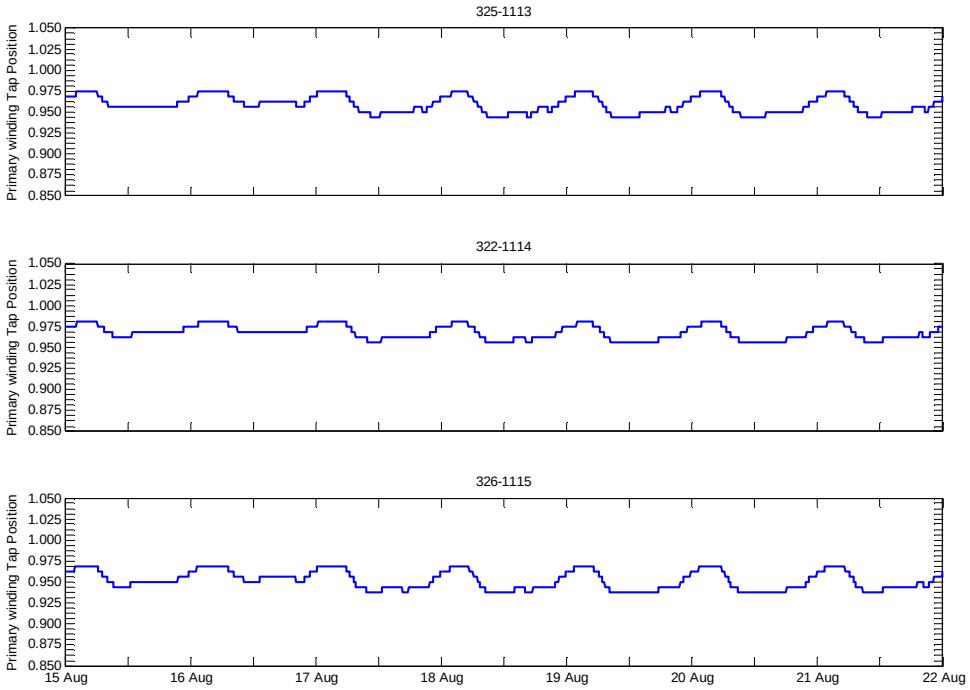

Figure 5.99: EHV1 tidal distribution transformers tap actions for the No DG case 2

5.4.4 FIT-AND-FORGET POWER FLOW

Analysis of the network headroom for DG capacity was presented in section 3.8.2. Under the fit-and-forget connection policy, the installed capacity of DG was 20.5 MW. The three wind farm DGs connected to bus 1105, 1106 and 1108 had an installed capacity of 2.5 MW, 10 MW and 3 MW respectively. DG on the island was restricted to a single development of 5 MW at Bus 1114. All DGs were operated in power factor control mode with a standard power factor setting of 0.98 leading.

Energy yield for each of the observational test cases in the fit-and-forget scenario is detailed in Table XVII and Table XVIII.

Table XVII: EHV1 'fit-and-forget' energy yield case 1

'fit-and-forget'	WTG 1105	WTG 1106	WTG 1108	Tidal 1113	Tidal 1114	Tidal 1115
MW	2.5	10	3	-	5	-
MWh	272.4	1089.6	326.9	-	83.3	-
MVArh	55.3	221.2	66.4	-	16.9	-
EC MWh	0.0	0.0	0.0	-	0.0	-
EC (%)	0.0%	0.0%	0.0%	-	0.0%	-
Capacity Factor	64.9%	64.9%	64.9%	-	9.9%	-

Table XVIII: EHV1 'fit-and-forget' energy yield case 2

'fit-and-forget'	WTG 1105	WTG 1106	WTG 1108	Tidal 1113	Tidal 1114	Tidal 1115
MW	2.5	10	3	-	5	-
MWh	73.5	293.9	88.2	-	286.7	-
MVArh	14.9	59.7	17.9	-	58.2	-
EC MWh	0.0	0.0	0.0	-	0.0	-
EC (%)	0.0%	0.0%	0.0%	-	0.0%	-
Capacity Factor	17.5%	17.5%	17.5%		34.1%	-

The fit-and-forget case studies results show that the network was operating as expected by the original prescription of the system control presets. There were no recorded instances of system voltage excursion or thermal overloading. With the introduction of 20.5 MW of DG from renewable energy resources, the time series of tap settings, illustrated in Figure 5.100 and Figure 5.101, now follow a superimposed pattern of supply and demand. On average, tap changing actions on the VR transformer occurred once every 72.5 minutes in case 1 and once every 42.9 minutes in case 2.

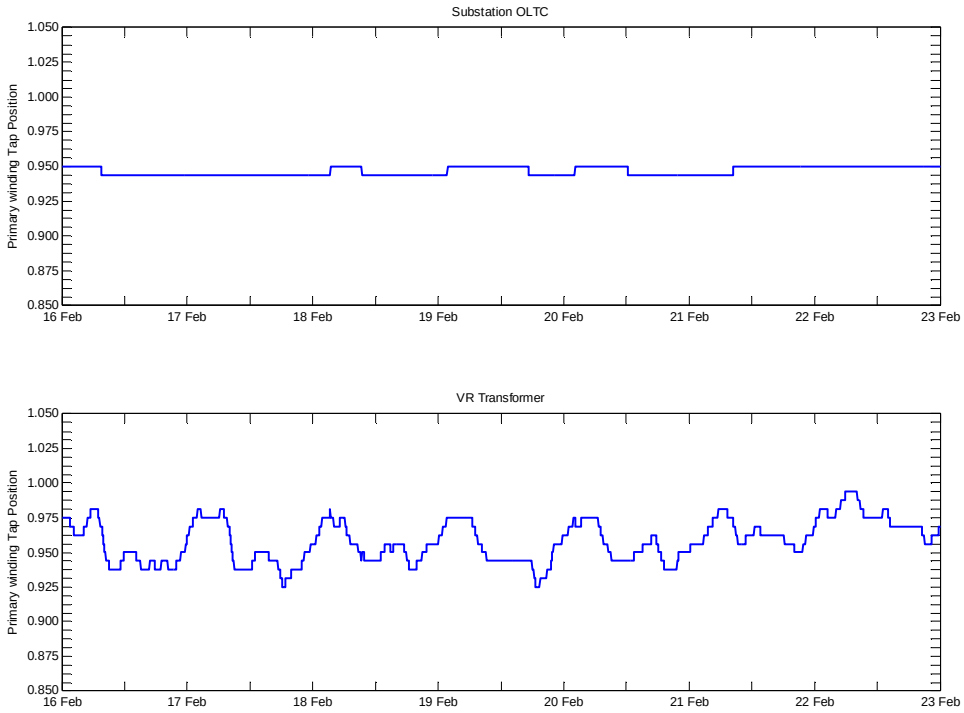

Figure 5.100: EHV1 network transformer tap actions for the 'fit-and-forget' DG case 1

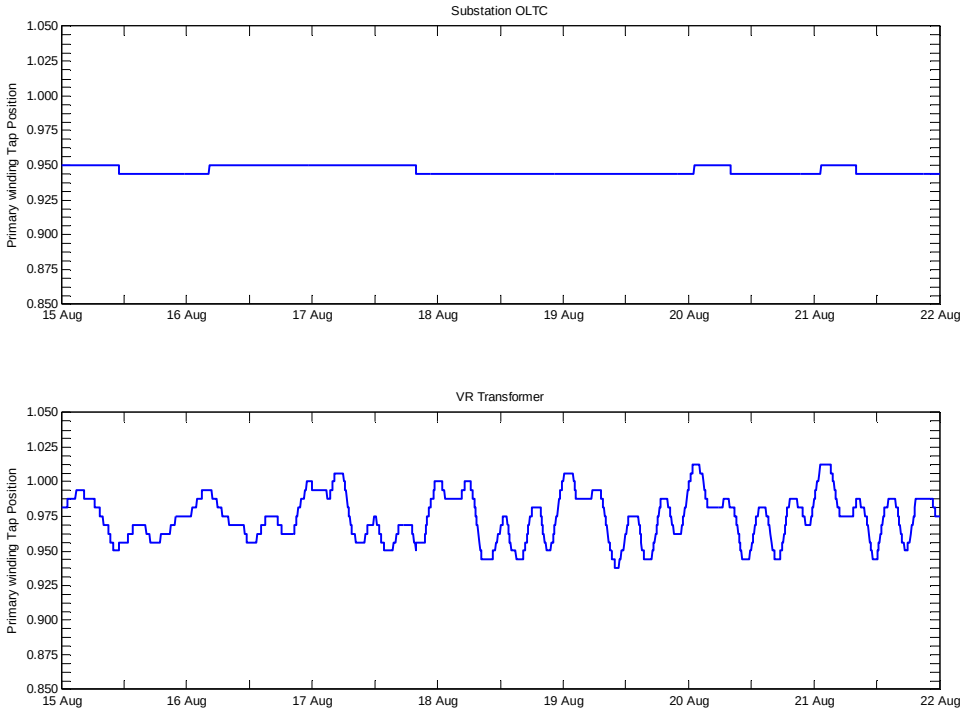

Figure 5.101: EHV1 network transformer tap actions with 'fit-and-forget' DG case 2

The same pattern of change was observed for the 33/11-kV distribution transformers with (or where in future will have) DG connected to the lower voltage secondary. Close inspection of the tap position traces, shown in Figure 5.102 to Figure 5.105, demonstrates that their variation is consistent with the time variation of generation and demand on the network and not in discontinuous, hysteric or spurious tap changing actions. In case 1, the VR transformer had the highest frequency of tap changing, with a tap change occurring on average once every 67.2 minutes. The most frequently used tap changing transformer in case 2 was the 33/11-kV distribution transformer connected to the tidal array at bus 1114. During the higher tidal production period of case 2, tap changing actions occurred on average once every 34.8 minutes. The VR transformer in case 2 had on average a tap change every 42.9 minutes. Therefore results indicate that the addition of 20.5 MW of DG does not affect the functionality or severely impact on the integrity of the infrastructure, despite significant changes to the no DG power flows. A count of tap changing actions in all network transformers is shown in Figure 5.106 and Figure 5.107.

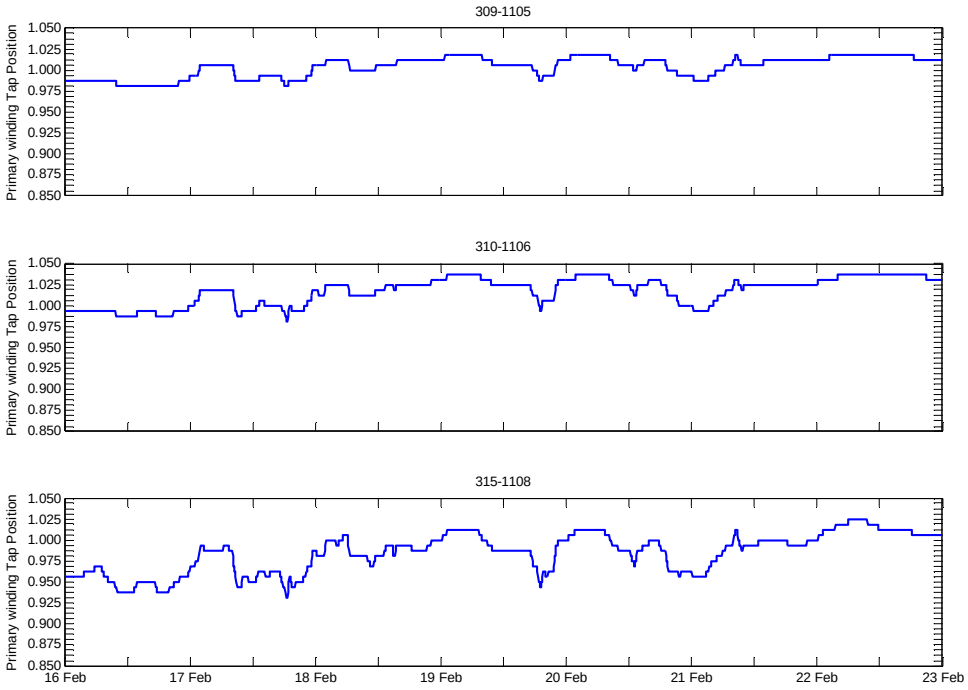

Figure 5.102: Tap positions on wind farm distribution transformers – 'fit-and-forget' case 1

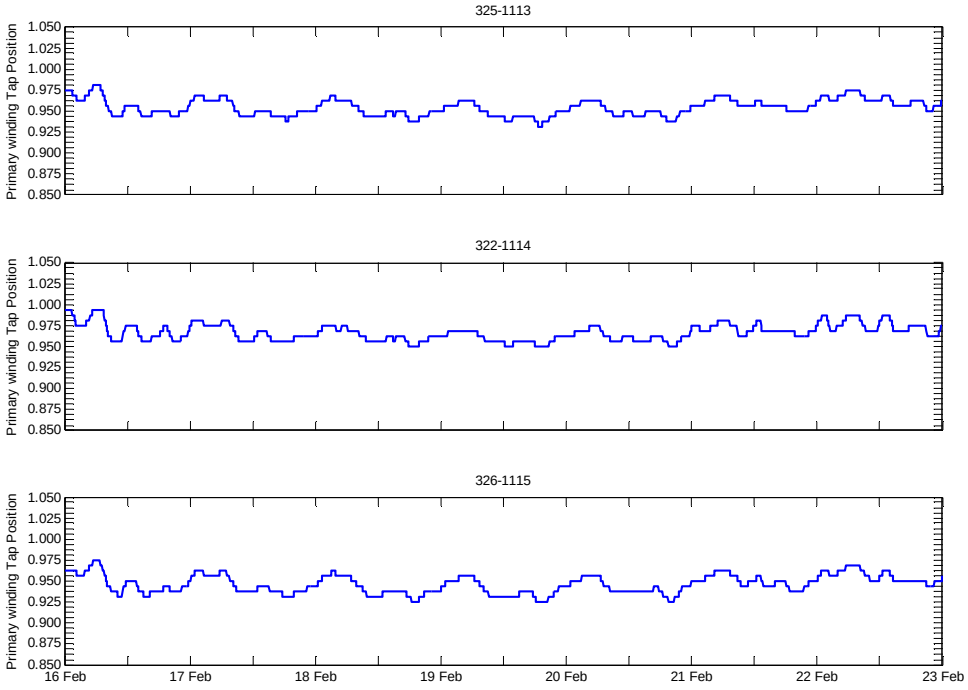

Figure 5.103: Tap positions on tidal array distribution transformers – 'fit-and-forget' case 1

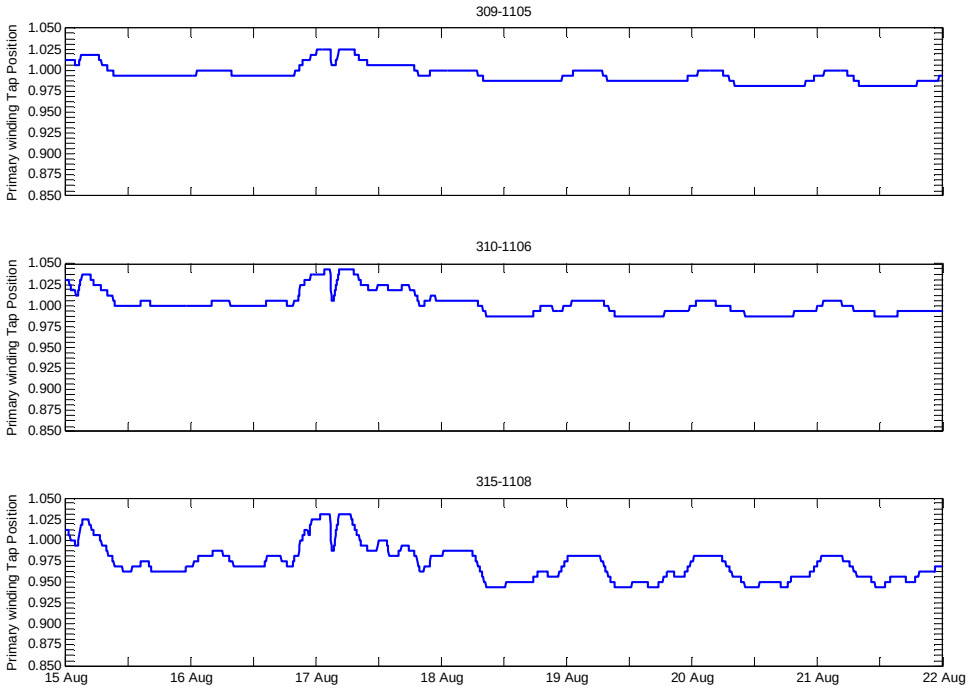

Figure 5.104: Wind farm distribution transformers tap actions for the 'fit-and-forget' case 2

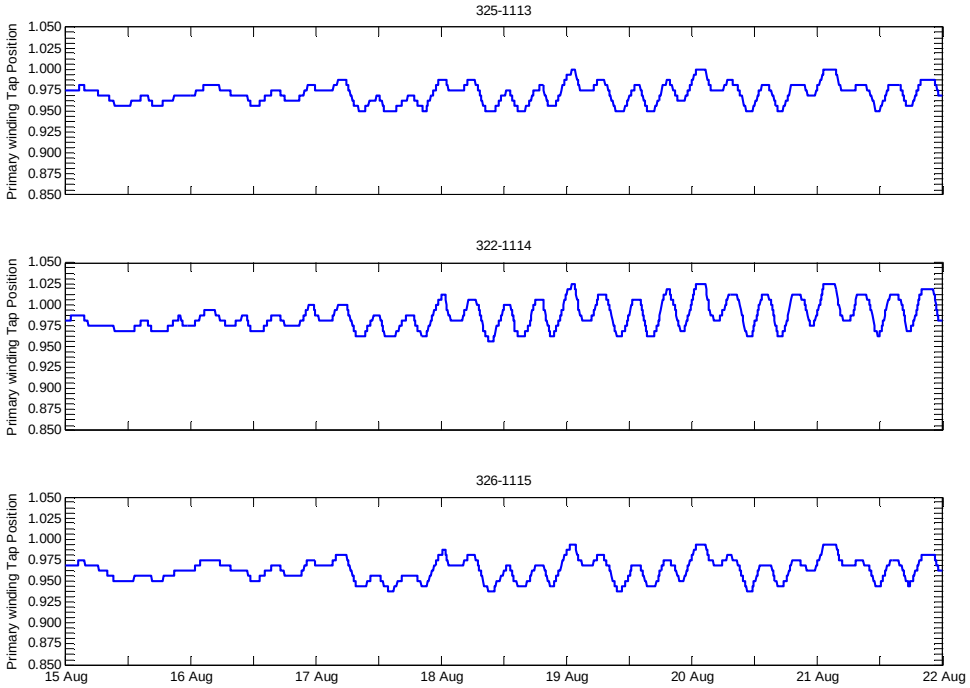

Figure 5.105: Tap positions on wind farm distribution transformers – 'fit-and-forget' case 2

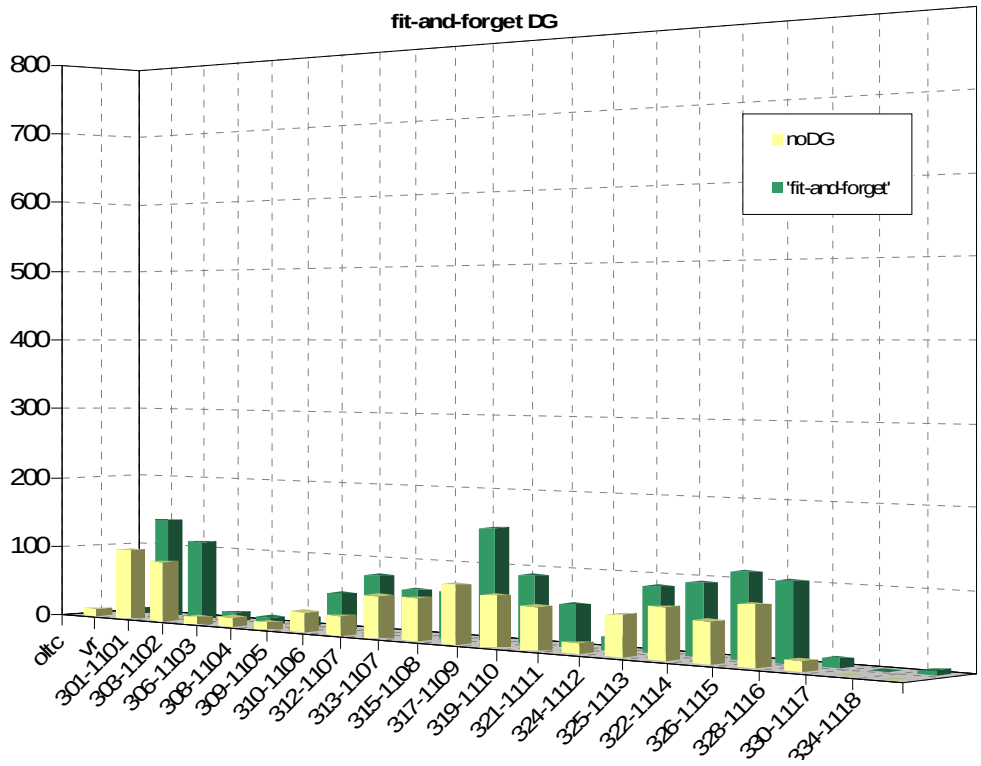

Figure 5.106: Total tap changing actions of all transformers – 'fit-and-forget' case 1

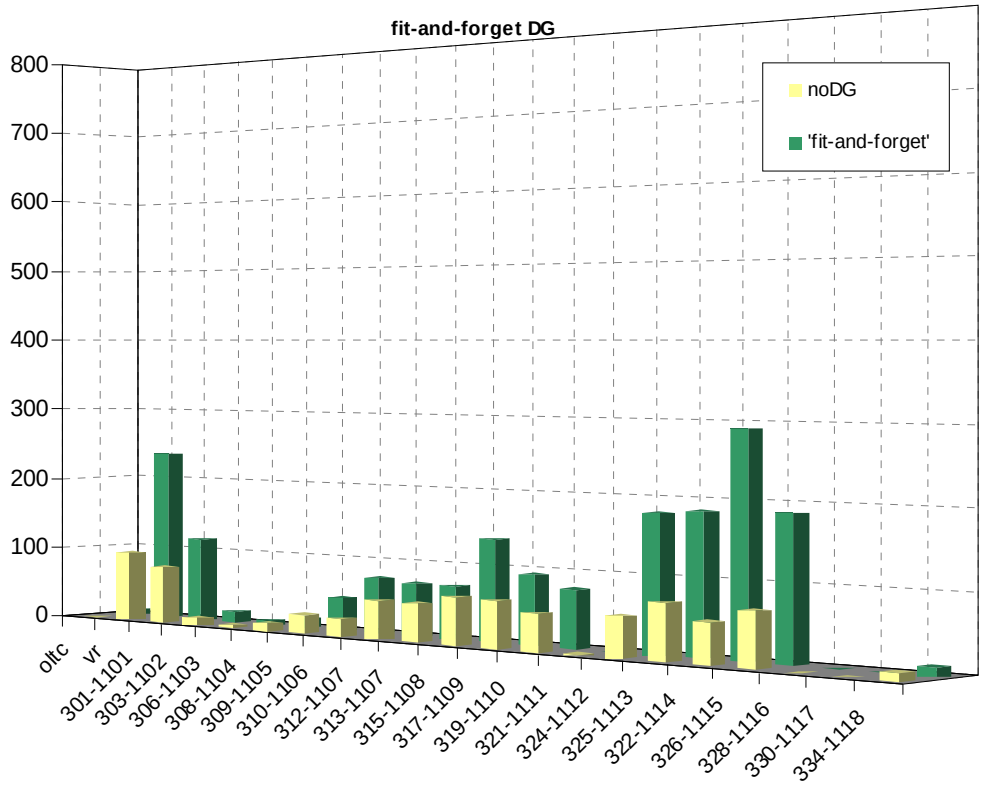

Figure 5.107: Total tap changing actions of all transformers – 'fit-and-forget' case 2

Losses between the no DG and the fit-and-forget DG scenario were reduced in real terms by 27% and 25% in each observational test case, as DG serves load locally and displaces power import through the GSP.

5.4.5 POWER FLOW SOLUTIONS WITH ANM OPF

With the fully integrated ANM strategy operating on a 15 minute control cycle, the installed capacity of DG was increased to 52 MW as before. The three wind farm DGs connected to buses 1105, 1106 and 1108 had an installed capacity of 10 MW, 15 MW and 5 MW respectively. The restriction on further DG capacity and the operational export of real power was the thermal rating of the connecting 33/11-kV distribution transformers. DG on the island was significantly increased. Two further tidal array DGs were able to connect at buses 1113 and 1115, with an installed capacity of 2 MW and 10 MW respectively. The original tidal array DG at bus 1114 was increased to 10 MW.

In the two, one-week simulation periods, energy yield increased over the 'fit-and-forget' approach by 67% and 142% respectively. As a combined total, energy yield in these test cases was increased by 88% from the fit-and-forget scenario. There was very little difference in the energy yield between all formulations of the real time ANM OPF technique. The specific energy yield for each DG in all single scenario formulations of the ANM OPF technique is shown in Table XIX to Table XXIV.

Table XIX: EHV1 DG energy yield - OPF1 case 1

OPF1	WTG 1105	WTG 1106	WTG 1108	Tidal 1113	Tidal 1114	Tidal 1115
MW	10	15	5	2	10	10
MWh	858.3	1321.3	444.3	30.0	149.1	149.1
MVArh	21.8	-31.2	11.0	-5.6	-26.9	-27.3
EC MWh	231.3	313.0	100.5	3.3	17.4	16.8
EC (%)	21.2%	19.2%	18.4%	9.9%	10.5%	10.1%
Capacity Factor	51.1%	52.4%	52.9%	8.9%	8.9%	8.9%

Table XX: EHV1 DG energy yield - OPF2 case 1

OPF2	WTG 1105	WTG 1106	WTG 1108	Tidal 1113	Tidal 1114	Tidal 1115
MW	10	15	5	2	10	10
MWh	858.1	1321.6	444.4	30.0	149.1	149.1
MVArh	-1.0	-25.3	19.6	-5.9	-29.8	-27.1
EC MWh	231.4	313.0	100.4	3.3	17.4	16.8
EC (%)	21.2%	19.1%	18.4%	9.9%	10.5%	10.1%
Capacity Factor	51.1%	52.4%	52.9%	8.9%	8.9%	8.9%

Table XXI: EHV1 DG energy yield - OPF3 case 1

OPF3	WTG 1105	WTG 1106	WTG 1108	Tidal 1113	Tidal 1114	Tidal 1115
MW	10	15	5	2	10	10
MWh	858.3	1321.4	444.3	30.0	149.1	149.1
MVArh	30.0	-14.9	20.7	-5.9	-27.8	-23.0
EC MWh	231.4	313.0	100.5	3.3	17.4	16.8
EC (%)	21.2%	19.2%	18.4%	9.9%	10.5%	10.1%
Capacity Factor	51.1%	52.4%	52.9%	8.9%	8.9%	8.9%

Table XXII: EHV1 DG energy yield - OPF1 case 2

OPF1	WTG 1105	WTG 1106	WTG 1108	Tidal 1113	Tidal 1114	Tidal 1115
MW	10	15	5	2	10	10
MWh	244.3	391.3	128.0	93.9	479.5	455.8
MVArh	-1.2	-5.2	-3.5	-17.5	-92.3	-87.5
EC MWh	49.6	49.7	18.9	20.8	93.9	116.2
EC (%)	16.9%	11.3%	12.9%	18.1%	16.4%	20.3%
Capacity Factor	14.5%	15.5%	15.2%	27.9%	28.5%	27.1%

Table XXIII: EHV1 DG energy yield - OPF2 case 2

OPF2	WTG 1105	WTG 1106	WTG 1108	Tidal 1113	Tidal 1114	Tidal 1115
MW	10	15	5	2	10	10
MWh	244.3	391.2	128.0	93.9	479.4	455.6
MVArh	-9.6	-13.2	0.5	-18.6	-93.7	-90.6
EC MWh	49.7	49.8	18.9	20.8	94.0	116.5
EC (%)	16.9%	11.3%	12.9%	18.1%	16.4%	20.4%
Capacity Factor	14.5%	15.5%	15.2%	27.9%	28.5%	27.1%

Table XXIV: EHV1 DG energy yield - OPF3 case 2

OPF3	WTG 1105	WTG 1106	WTG 1108	Tidal 1113	Tidal 1114	Tidal 1115
MW	10	15	5	2	10	10
MWh	244.3	391.3	128.0	93.9	479.4	455.6
MVArh	-2.2	-21.3	-0.4	-18.6	-95.1	-88.4
EC MWh	49.6	49.7	18.9	20.8	94.0	116.5
EC (%)	16.9%	11.3%	12.9%	18.1%	16.4%	20.4%
Capacity Factor	14.5%	15.5%	15.2%	27.9%	28.5%	27.1%

The added benefit from local active DG controllers was to curtail short spikes in DG real power output, as shown in section 5.3, which were are not visible to the successive OPF solutions and would have otherwise led to a violation of system constraints.

One disadvantage to the local active DG controllers was the continual curtailment of DG real power output on the ramp-up of renewable energy resource, as demonstrated Figure 5.108 to Figure 5.111. In effect, this operation curtails increases in DG real power output until the changing power injections are seen by the ANM OPF technique and the control settings can be adjusted accordingly.

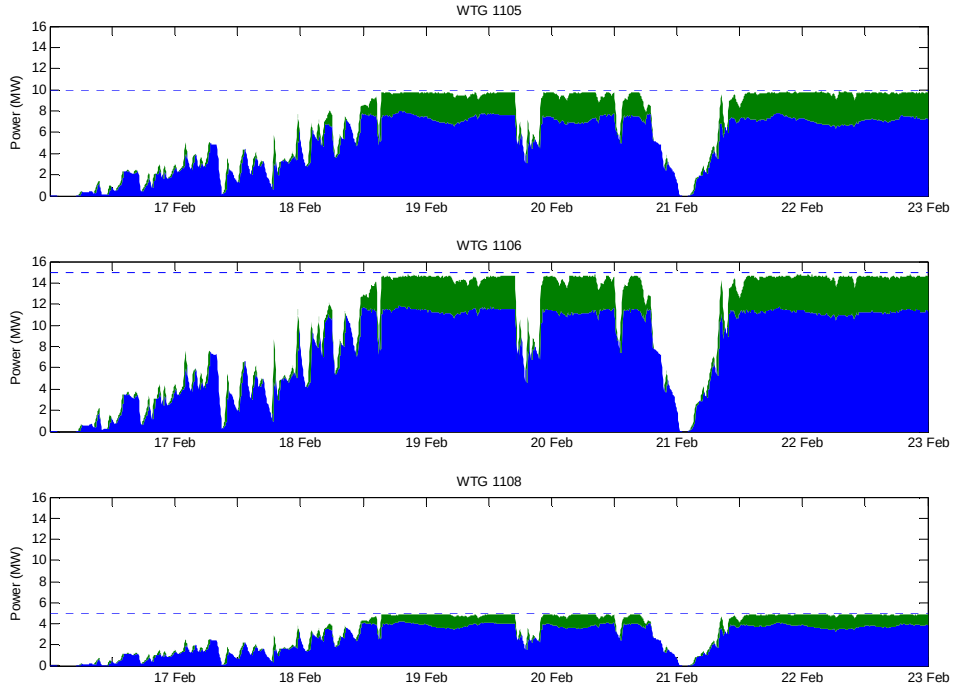

Figure 5.108: Wind farm real power production - OPF2 case 1

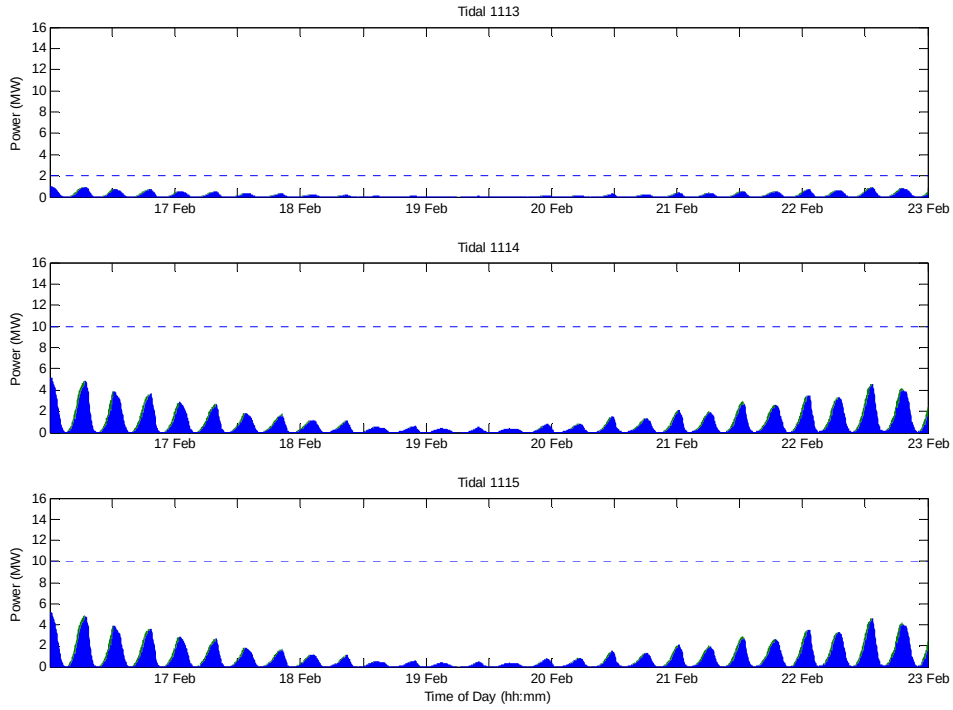

Figure 5.109: Tidal array real power production - OPF2 case 1

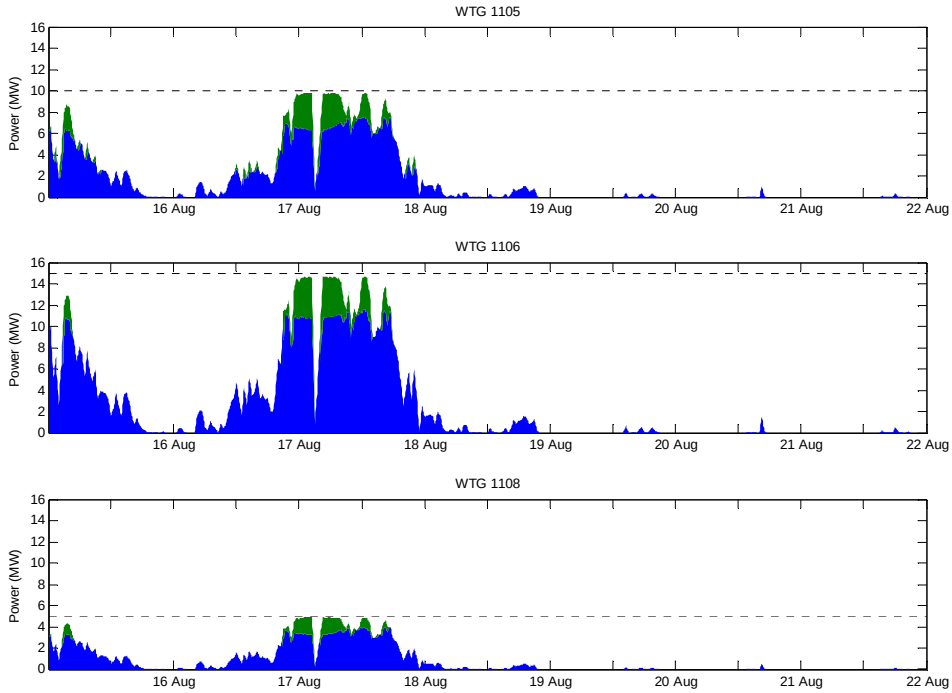

Figure 5.110: Wind farm real power production - OPF2 case 2

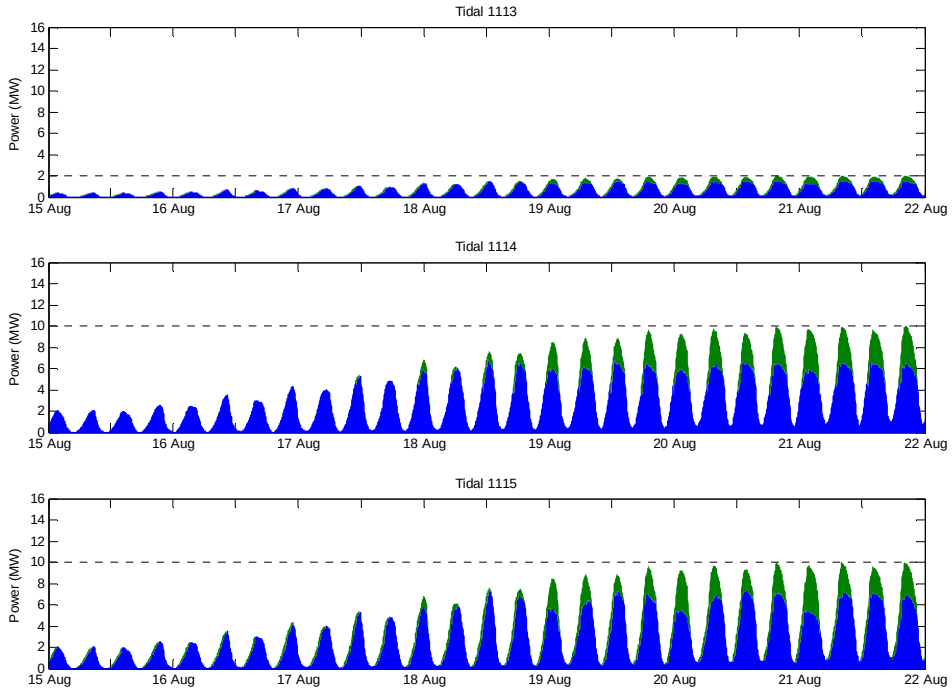

Figure 5.111: Tidal array real power production - OPF2 case 2

5.4.6 POWER FLOW SOLUTIONS WITH ANM RHOPF

The RHOPF technique was formulated in this analysis over a one hour control horizon of four 15 minute intervals. The time series of events in this case is illustrated in Figure 5.112 and Figure 5.113. Time sequential power flow solutions were performed in the proxy distribution network at 5 minute intervals, the control cycle between successive OPF analysis was 15 minutes.

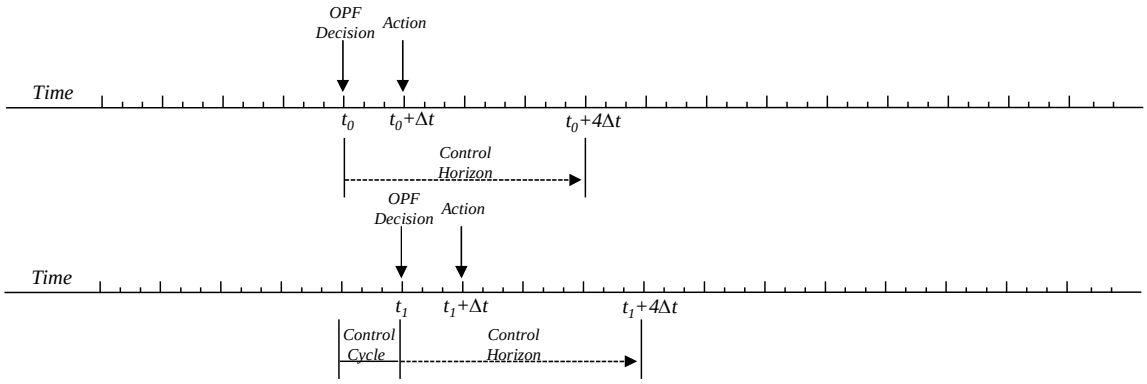

Figure 5.112: Time series of major events for RHOPF with DA control practices

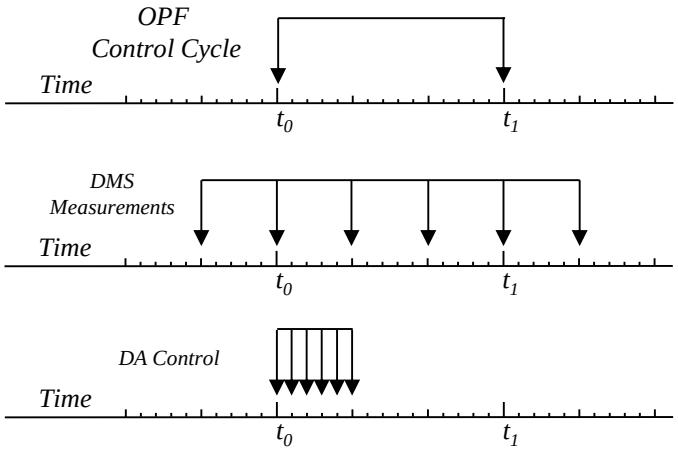

Figure 5.113: Analysis time scales of concurrent OPF, DMS and DA control elements

Forecast data for the RHOPF technique was generated in the same process as before; taking a weighted central moving average of the half hourly real time resource levels and linearly interpolating down to 15 minute intervals. In this analysis, the order and the weightings of the synthesising process were augmented to favour up-coming generation trends. This was to reflect the longer time steps and period of the finite control horizon.

For wind demand data, forecasts were generated by a 5th order weighted central moving average. The process favoured future resource levels by the following weights, in order from first (at t=-2) to last (t+2), 10%, 10%, 30%, 25%, 25%). For the tidal forecast data, a third order process was continued as the longer period began to distort the trends in production. Here, the persistence measurements account for 17% of the final forecast value, while the forth-coming and following measurement account for 50% and 33% respectively.

A comparison of the forecast data in each case is shown on Figure 5.114 and Figure 5.115. The figures illustrate an good correlation with real time resource and demand levels. The figures show the result of the WCMA smoothing process at each time step, for which the RHOPF-A forecast will follow and the t+1 forecast level for which the RHOPF-B will implement at each time step.

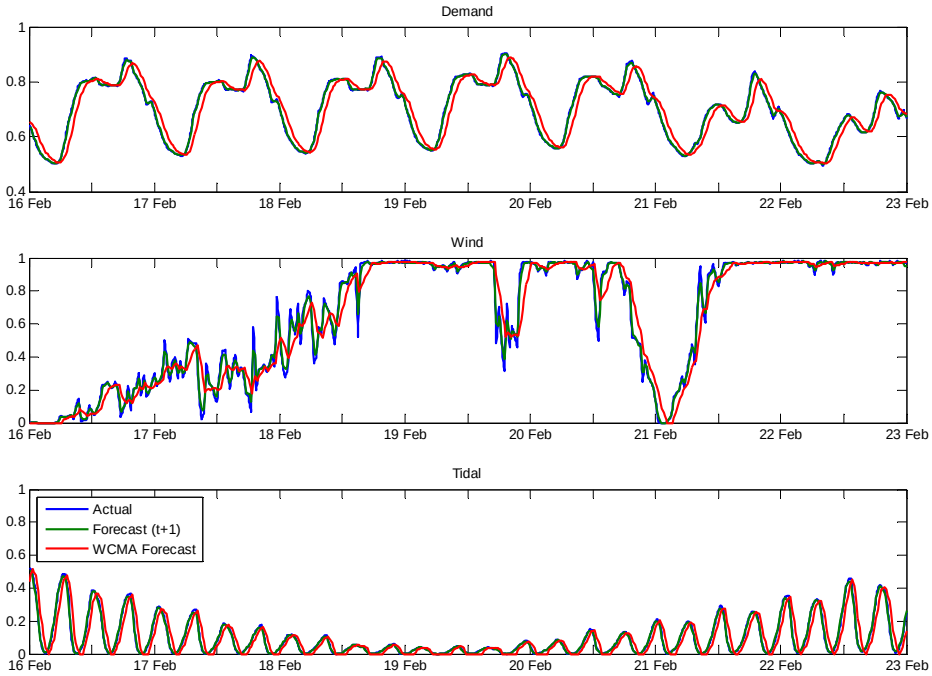

Figure 5.114: Comparison of forecast data case 1

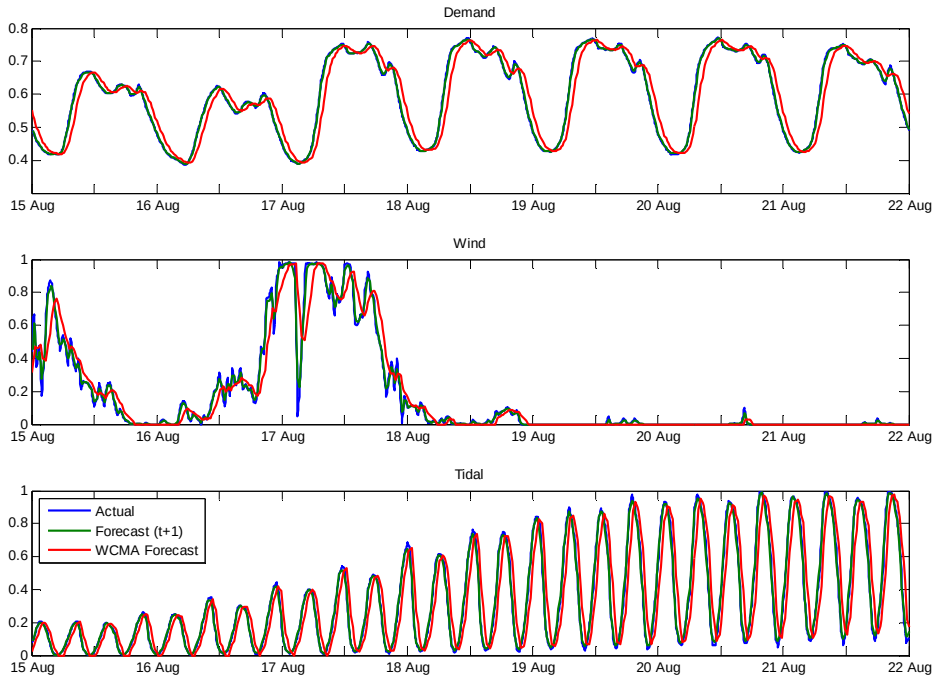

Figure 5.115: Comparison of forecast data case 2

The real power outputs for each DG in the RHOPF scenarios are illustrated in Figure 5.116 and Figure 5.123. Table XXV and Table XXVI show the respective energy yield for each DG.

Table XXV: EHV1 DG energy yield – RHOPF1-A case 1

RHOPF	WTG 1105	WTG 1106	WTG 1108	Tidal 1113	Tidal 1114	Tidal 1115
MW	10	15	5	2	10	10
MWh	867.3	1334.5	448.9	32.0	159.0	159.0
MVArh	27.2	-45.8	12.1	4.8	8.7	14.0
EC MWh	222.2	299.3	95.9	1.3	7.6	7.4
EC (%)	20.4%	18.3%	17.6%	4.0%	4.6%	4.4%
Capacity Factor	51.6%	53.0%	53.4%	9.5%	9.5%	9.5%

Table XXVI: EHV1 DG energy yield – RHOPF1-A case 2

RHOPF	WTG 1105	WTG 1106	WTG 1108	Tidal 1113	Tidal 1114	Tidal 1115
MW	10	15	5	2	10	10
MWh	243.9	378.4	124.6	101.1	480.0	489.5
MVArh	1.2	-22.3	-3.5	-20.5	-83.1	-75.1
EC MWh	50.0	62.6	22.3	13.6	93.2	83.1
EC (%)	17.0%	14.2%	15.2%	11.9%	16.3%	14.5%
Capacity Factor	14.5%	15.0%	14.8%	30.1%	28.6%	29.1%

Table XXVII: EHV1 DG energy yield – RHOPF1-B case 1

RHOPF1	WTG 1105	WTG 1106	WTG 1108	Tidal 1113	Tidal 1114	Tidal 1115
MW	10	15	5	2	10	10
MWh	877.0	1349.7	453.8	32.6	164.2	163.9
MVArh	20.6	-58.2	15.5	2.3	28.0	27.4
EC MWh	211.9	284.0	90.7	0.7	2.4	2.4
EC (%)	19.5%	17.4%	16.7%	2.0%	1.4%	1.4%
Capacity Factor	52.2%	53.6%	54.0%	9.7%	9.8%	9.8%

Table XXVIII: EHV1 DG energy yield – RHOPF1-B case 2

RHOPF1	WTG 1105	WTG 1106	WTG 1108	Tidal 1113	Tidal 1114	Tidal 1115
MW	10	15	5	2	10	10
MWh	250.5	389.1	127.8	102.0	491.0	499.8
MVArh	5.1	-10.7	3.0	-18.2	-68.0	-81.7
EC MWh	42.6	50.9	18.9	12.6	81.1	72.4
EC (%)	14.5%	11.6%	12.9%	11.0%	14.2%	12.7%
Capacity Factor	14.9%	15.4%	15.2%	30.3%	29.2%	29.7%

The crux of the RHOPF technique was that the ANM OPF technique was determining appropriate network control actions based on upcoming levels of variable power flow, pro-actively adjusting network control settings to prevent variable power flow injections from violating system constraints and unnecessary control switching.

In the single scenario OPF formulations, rising levels of DG real power output were constrained by local active DG controls until the changing power injections were seen by the ANM OPF technique and the control settings were adjusted accordingly. One benefit of the RHOPF was a reduction in unnecessary real power curtailment on the ramp-up of renewable energy resource as the real time RHOPF technique operates in advance of changing power flow injections. The additional increase in energy yield was 2% in case 1 and 5% in case 2 for the RHOPF1-A analysis and 1% in case 1 and 3% in case 2 for the RHOPF1-B analysis.

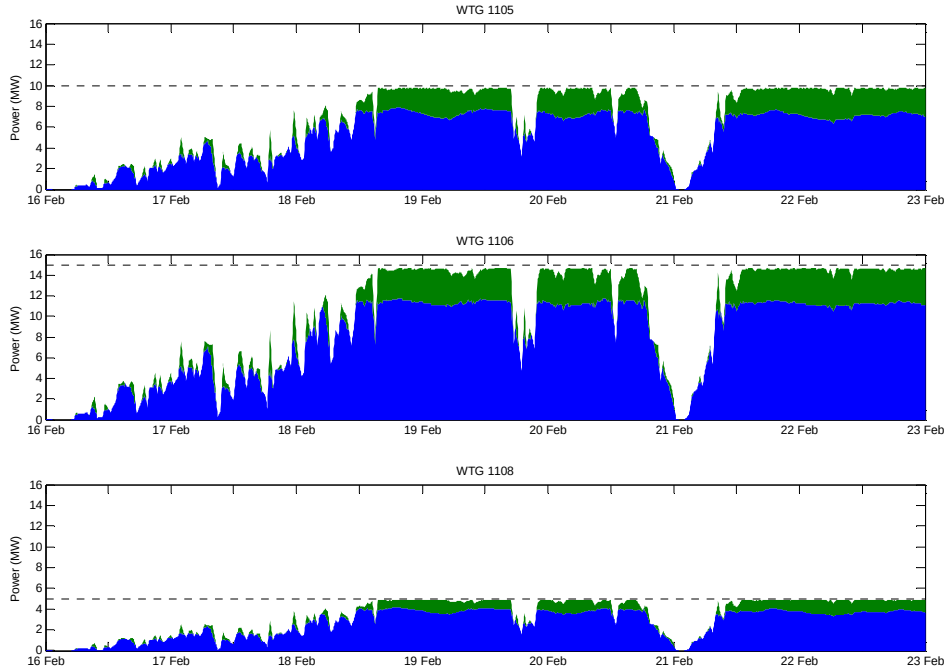

Figure 5.116: Wind farm real power production – RHOPF1-A case 1

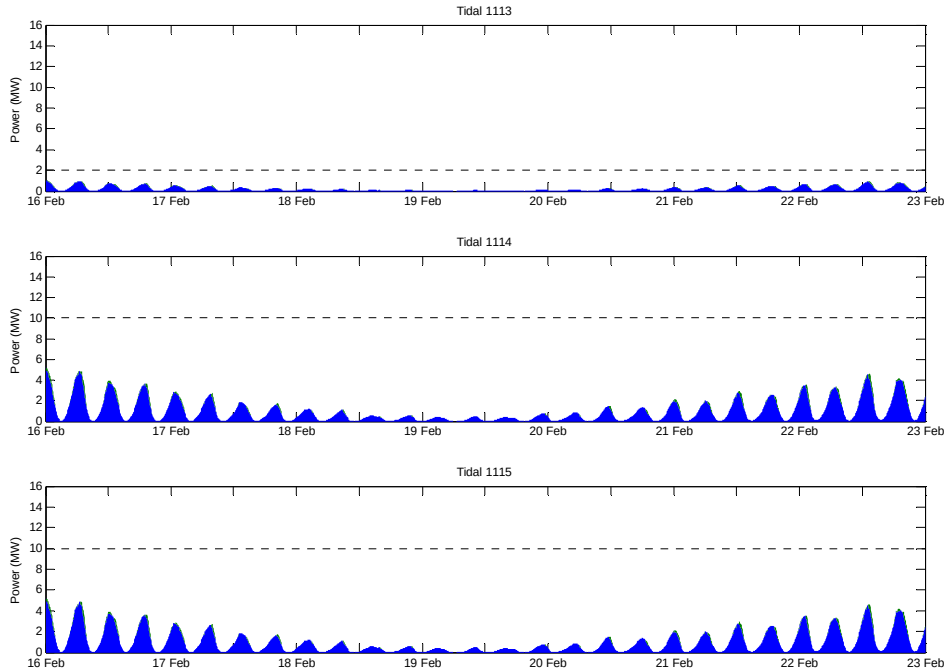

Figure 5.117: Tidal array real power production - RHOPF1-A case 1

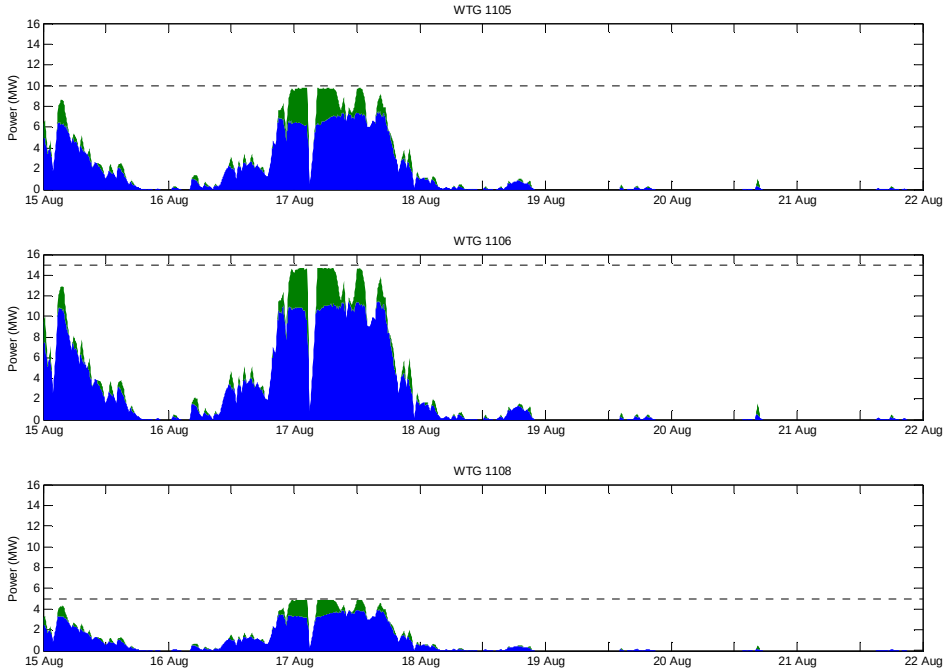

Figure 5.118: Wind farm real power production - RHOPF1-A case 2

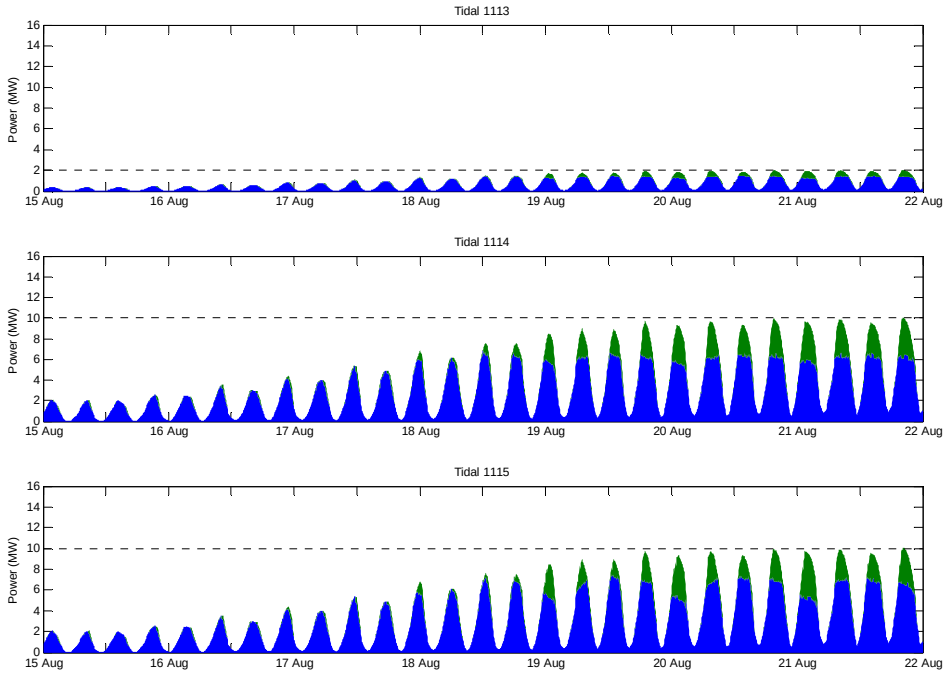

Figure 5.119: Tidal array real power production - RHOPF1-A case 2

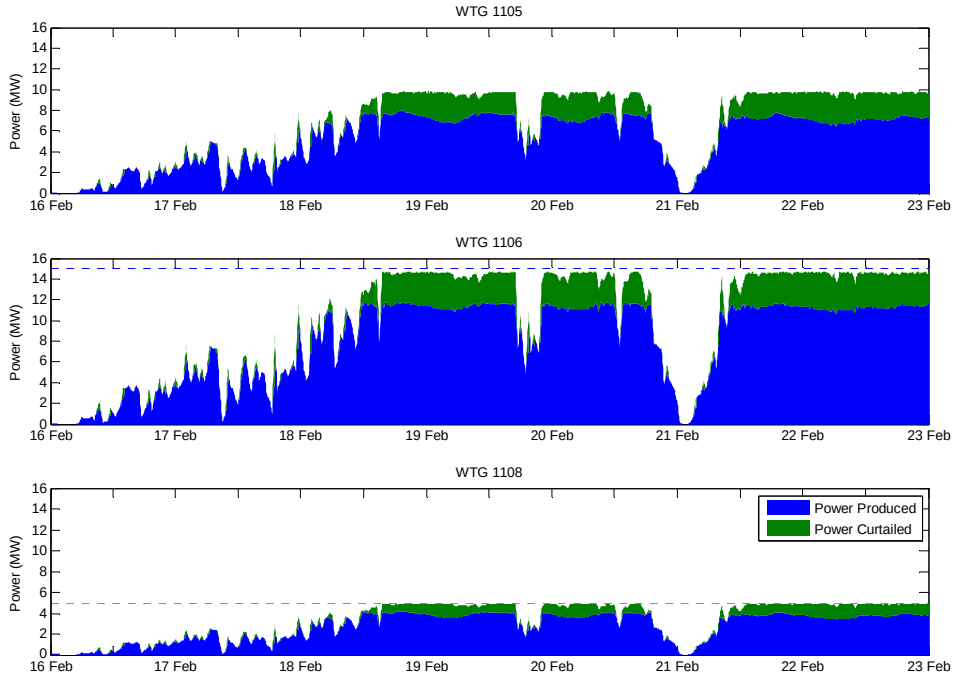

Figure 5.120: Wind farm real power production – RHOPF1-B case 1

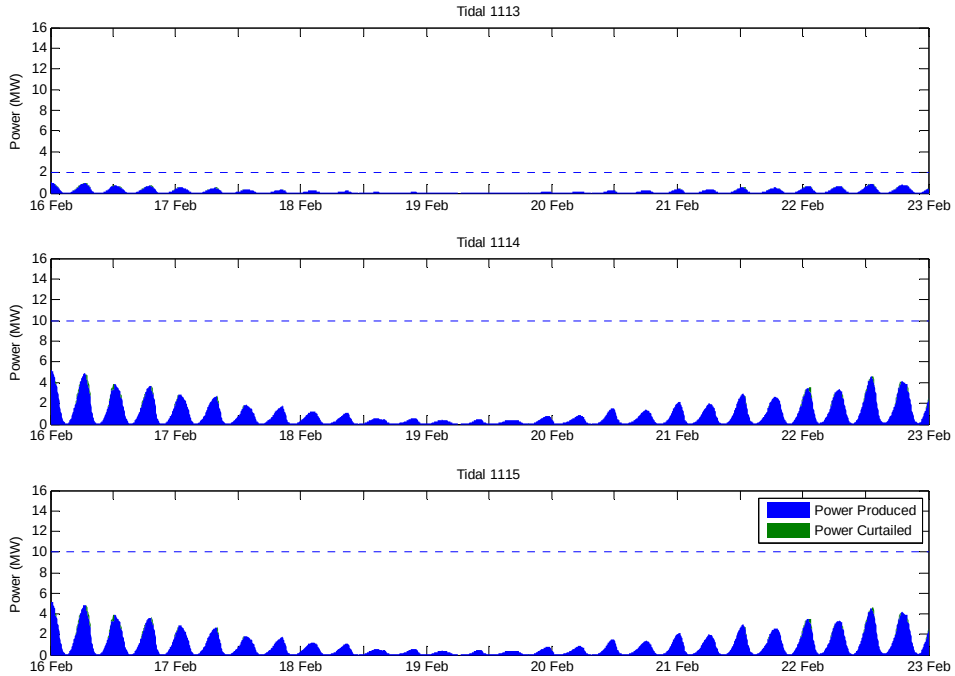

Figure 5.121: Tidal array real power production – RHOPF1-B case 1

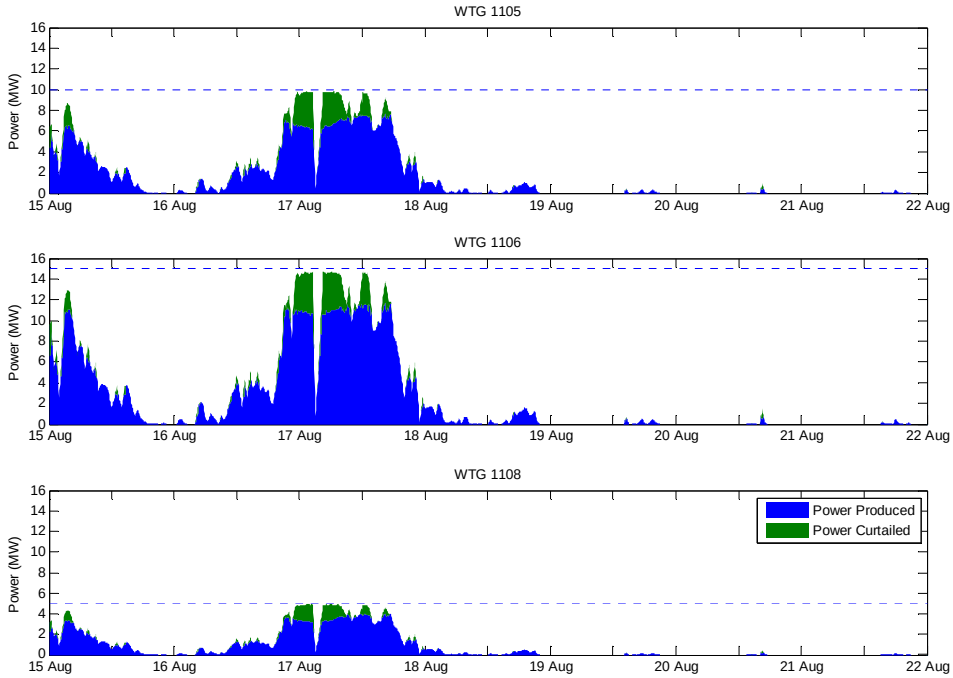

Figure 5.122: Wind farm real power production – RHOPF1-B case 2

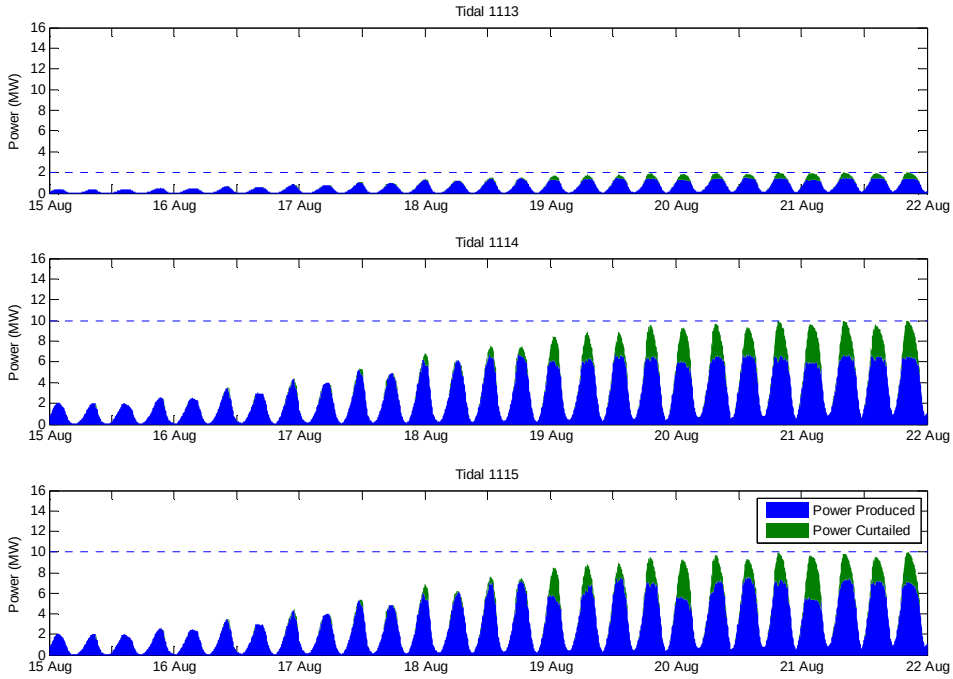

Figure 5.123: Tidal array real power production – RHOPF1-B case 2

In both test cases and for all formulations of the real ANM OPF, the network power flow solutions were within, or within recommendations of, the system technical and statutory constraints. The maximum instantaneous thermal loading level and the percentage of thermal overloading observed in each case is shown in Figure 5.124 and Figure 5.125.

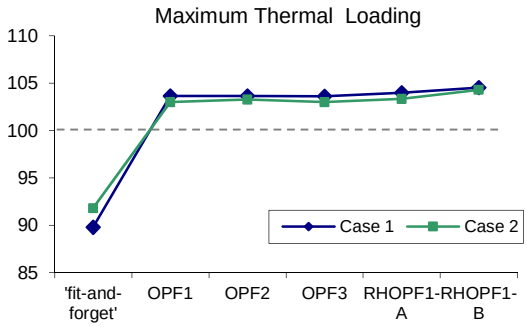

Figure 5.124: Maximum thermal loading

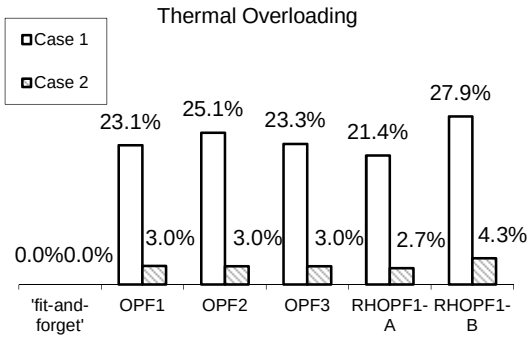

Figure 5.125: Overload occurrence

There was a large difference in the occurrence of overloading between each case; as was expected, given the large variation in wind power capacity factors between the two cases. Thermal overloading of network components was only evident on the distribution transformers connecting to the wind farm DGs. Again, there was a negligible difference in the thermal loading levels between the various formulations of the OPF. An example of the distribution of thermal loading levels in these transformers is shown in the box plots in Figure 5.126 to Figure 5.127, which extend to the 5^{th} and 95^{th} percentile. Overloading of this severity is considered acceptable, but if necessary, the OPF internal thermal loading constraints can be restricted to prevent residual variations in power flow from breaching the thermal limit.

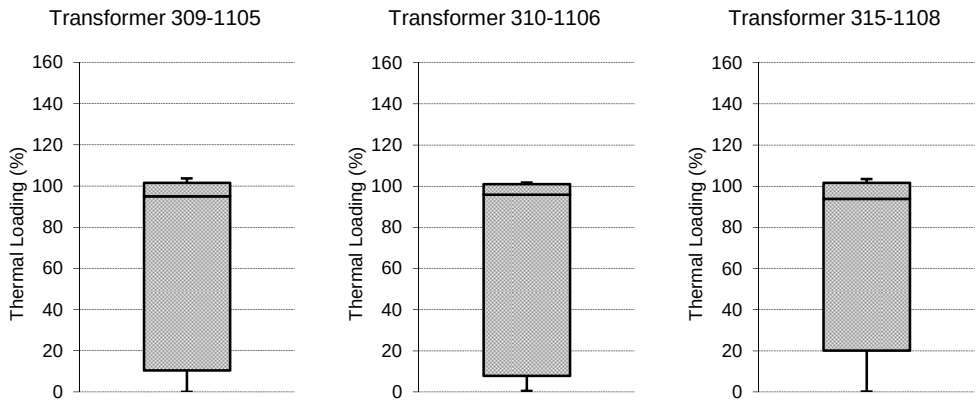

Figure 5.126: Box plot distributions of thermal loading levels in the wind farm DG distribution transformers OPF 1 case 1

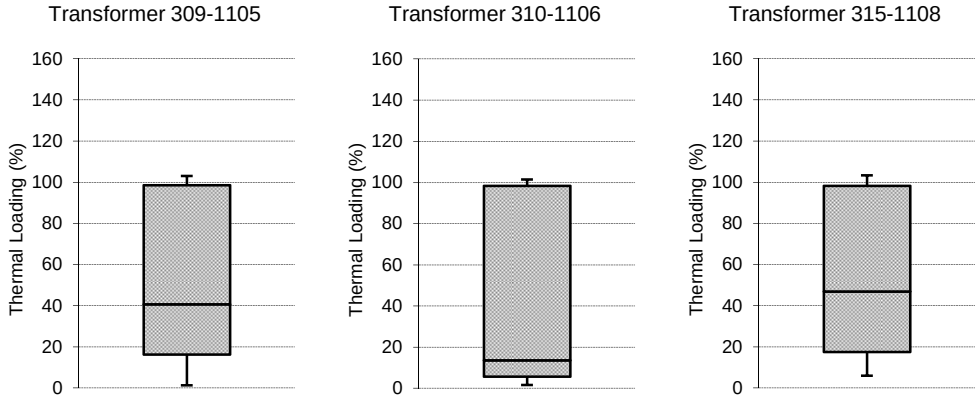

Figure 5.127: Box plot distributions of thermal loading levels in the wind farm DG distribution transformers OPF 1 case 2

Except for those discussed below, network voltage levels were within acceptable limits for all system buses in all configurations.

In the OPF1 formulation, significant instantaneous voltage excursions were high due to spurious switching of transformer tap positions. In all other formulations of the real time ANM OPF technique, residual voltage variation within the deadband of tap-changing transformer control practices lead to the minor voltage excursions shown in Figure 5.128 and Figure 5.129. Voltage excursions occurred explicitly on the primary winding of tap changing transformers, and went unchecked by upstream voltage

regulation as the severity of voltage excursion fell within the deadband of the upstream voltage control practices.

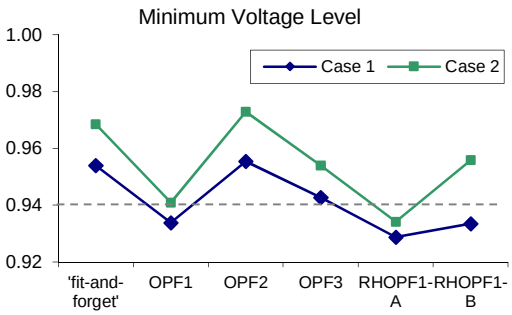

Figure 5.128: Minimum voltage

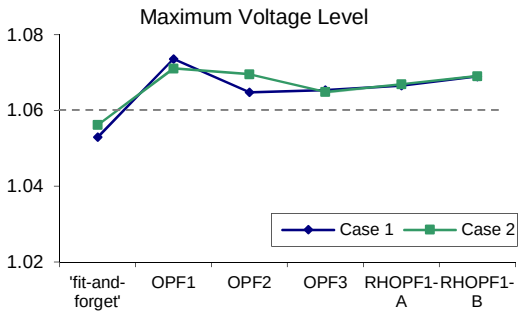

Figure 5.129: Maximum voltage

Excessive occurrences of voltage excursion were evident in case 1 for the OPF2 and OPF3 scenarios. In each formulation the corresponding voltage excursion was observed on bus 309 with a maximum level of 1.0655 pu. This high occurrence was due to the exceptional period of wind power resource enjoyed during this test case. The voltage profile for bus 309 is shown in Figure 5.132.

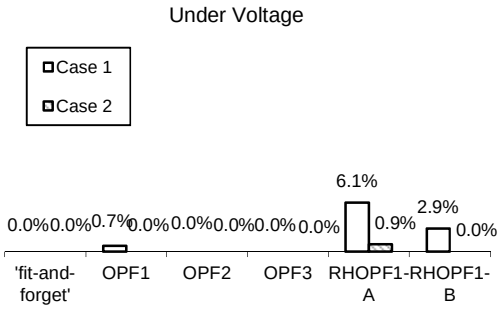

Figure 5.130: Under voltage occurrence

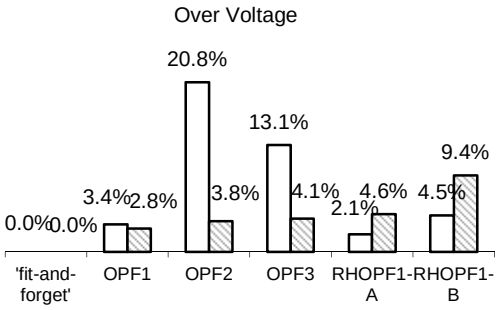

Figure 5.131: Overvoltage occurrence

The undervoltage excursion occurred on the primary winding of the VR transformer after the subsea cable to the island and before rectification and connection to any consumers. Under voltage excursion, besides that induced by spurious tap switching in the OPF1 formulation, was unique to the RHOPF formulation and caused by the combination of forecast errors and residual voltage variation. This was only evident at daily peaks in demand and during low real power output from the tidal array DGs, as shown in Figure 5.133. This was only of note in case 1, which occurs during the winter season.

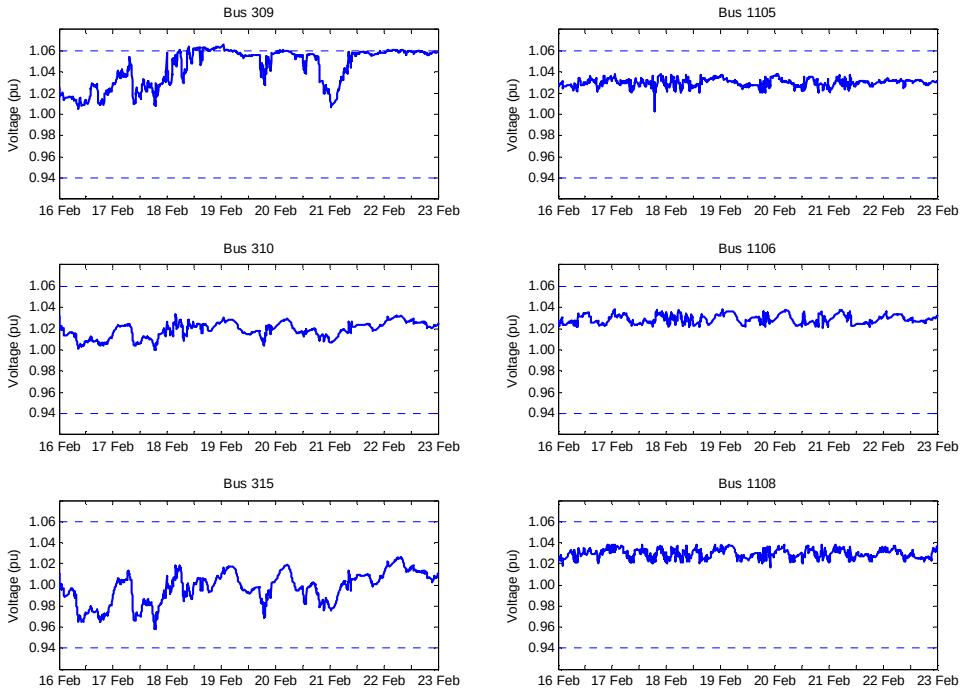

Figure 5.132: Voltage profiles wind farm DG distribution transformers - OPF3 case 1

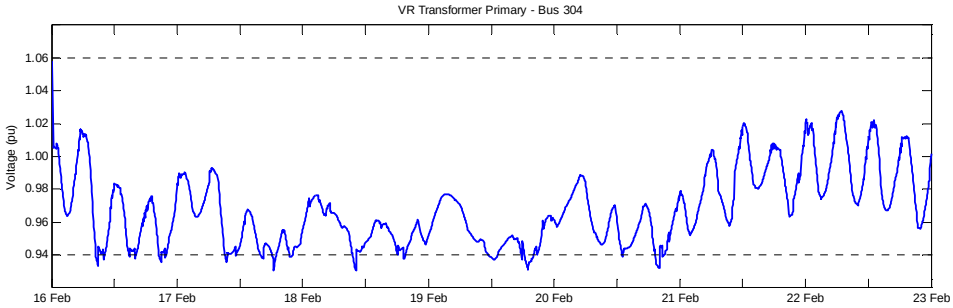

Figure 5.133: Voltage level on VR transformer primary – RHOPF1-A case 1

Results of the standard OPF1 formulation continued to be overshadowed by the spurious switching of network control practices. This switching of transformer tap positions caused a significant disturbance to voltage levels and would breach quality of supply regulations. Once again, a significant reduction in tap changing actions was again brought about with the multi-objective formulations and RHOPF technique, as illustrated by Figure 5.134 to Figure 5.143.

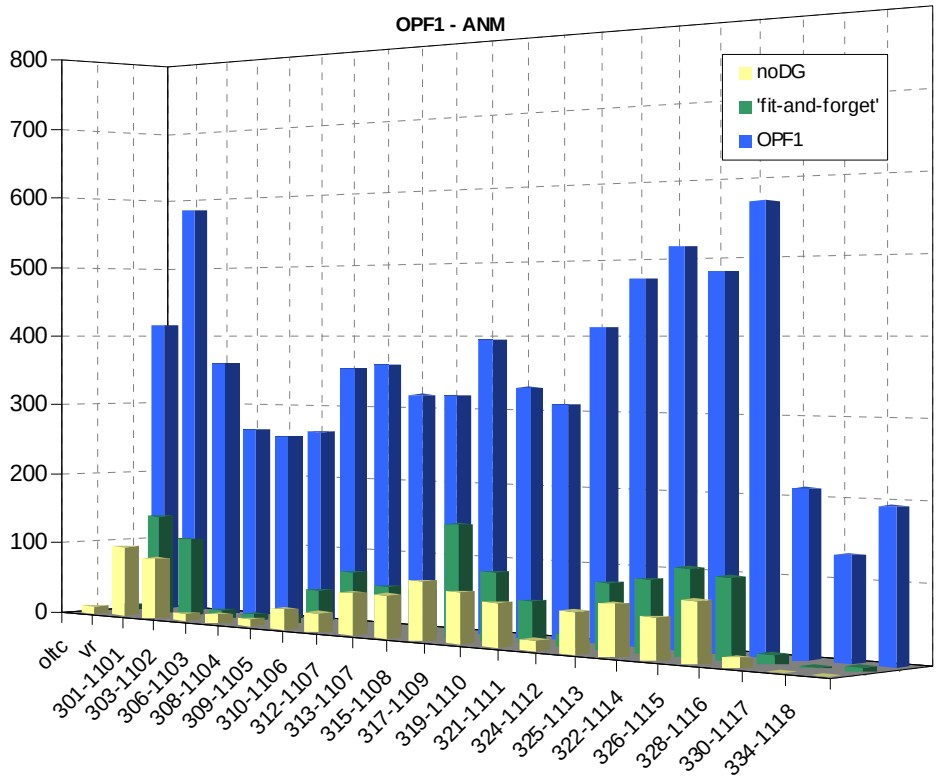

Figure 5.134: Total tap changing actions of all transformers - OPF1 case 1

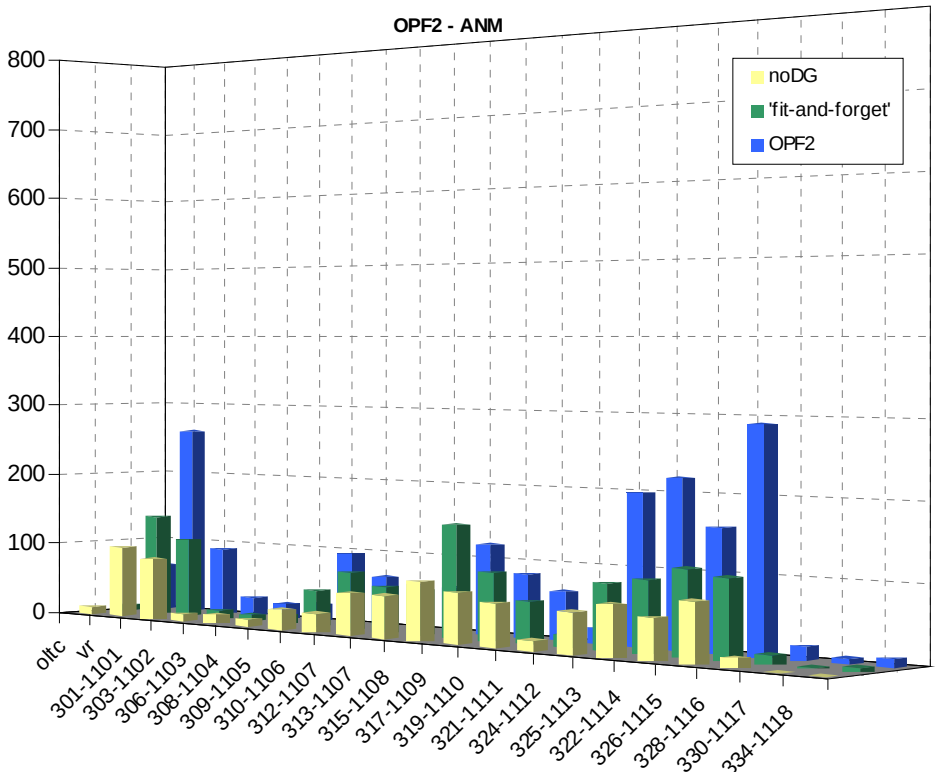

Figure 5.135: Total tap changing actions of all transformers - OPF2 case 1

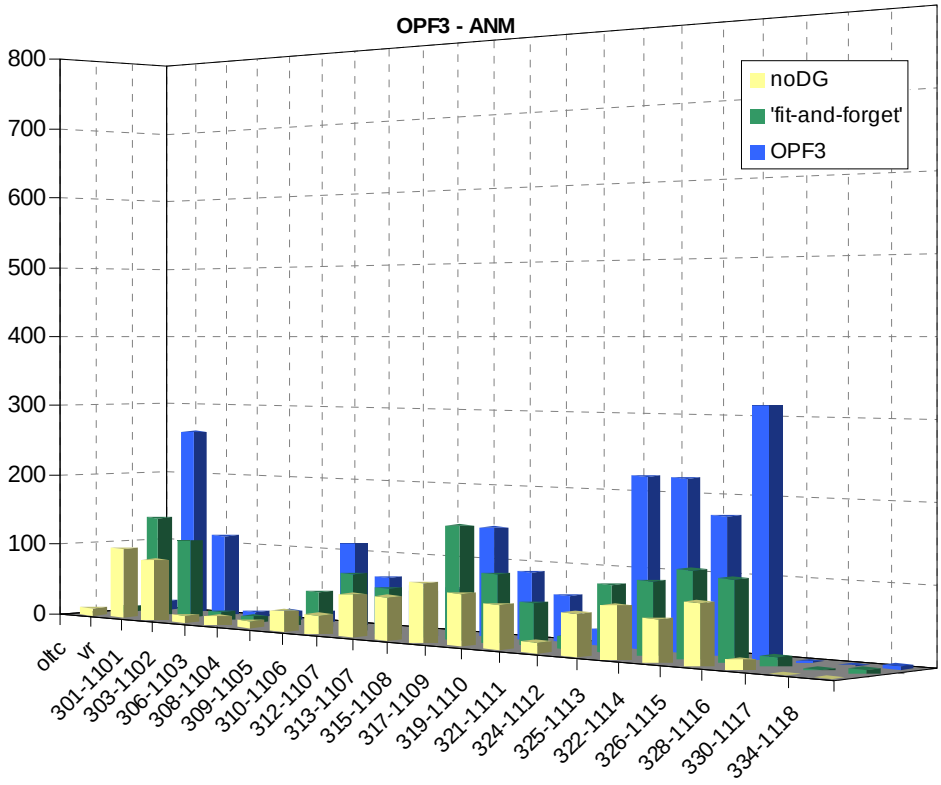

Figure 5.136: Total tap changing actions of all transformers - OPF3 case 1

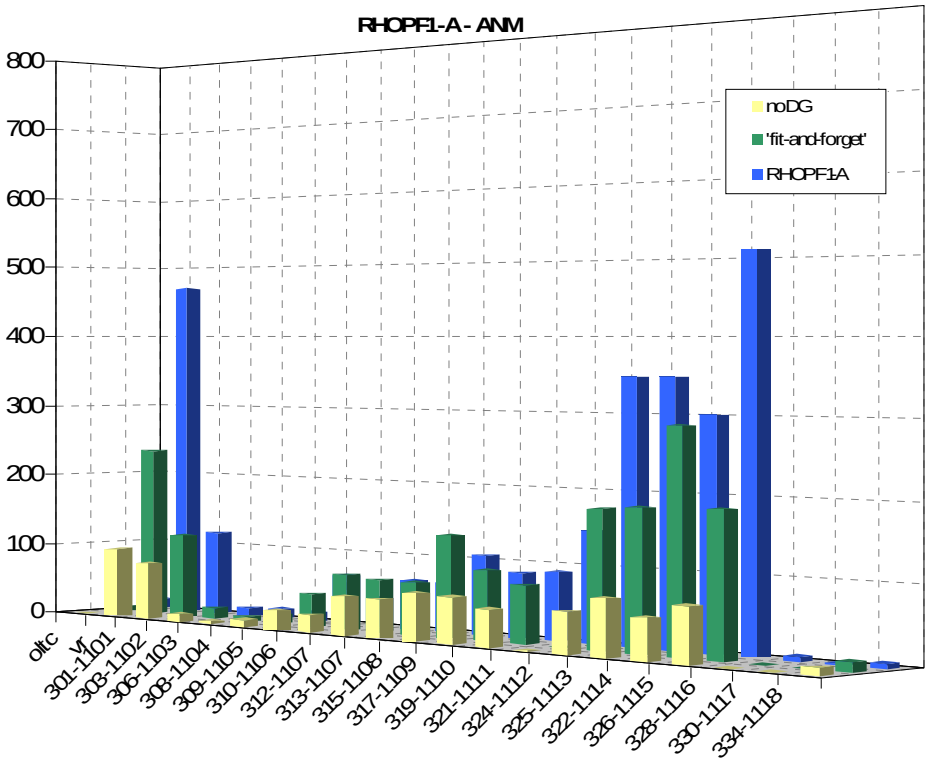

Figure 5.137: Total tap changing actions of all transformers – RHOPF1-A case 1

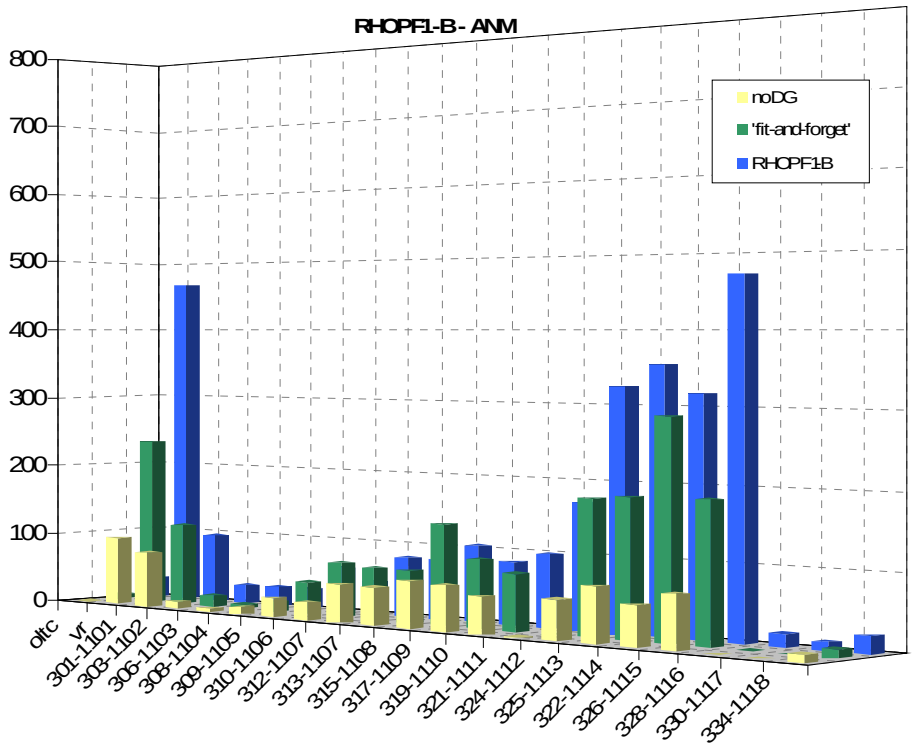

Figure 5.138: Total tap changing actions of all transformers – RHOPF1-B case 1

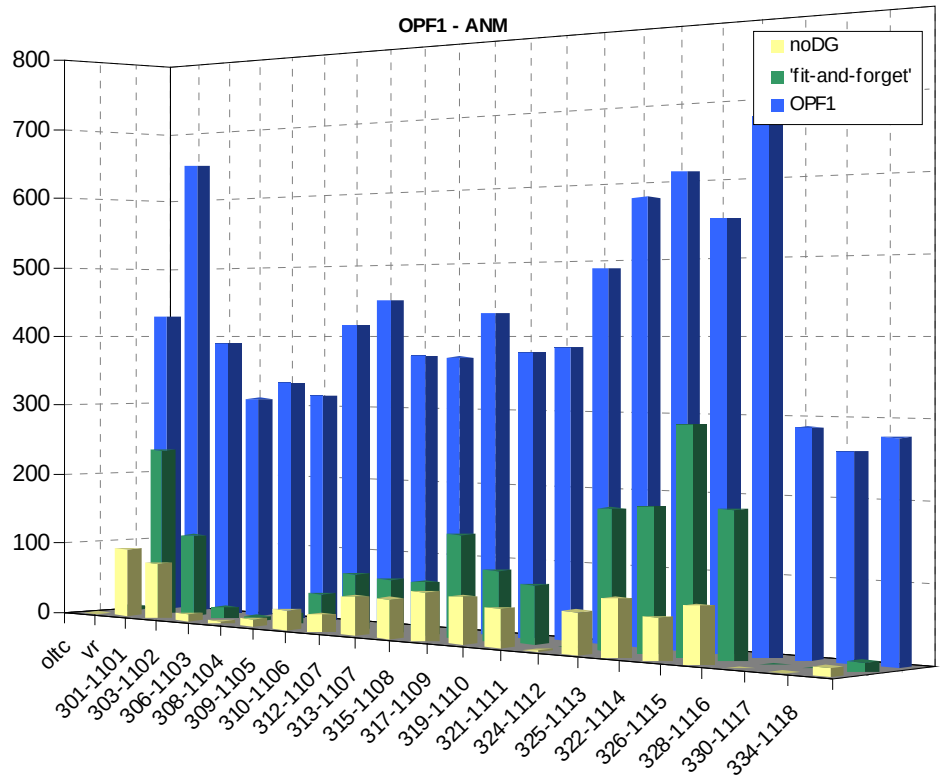

Figure 5.139: Total tap changing actions of all transformers - OPF1 case 2

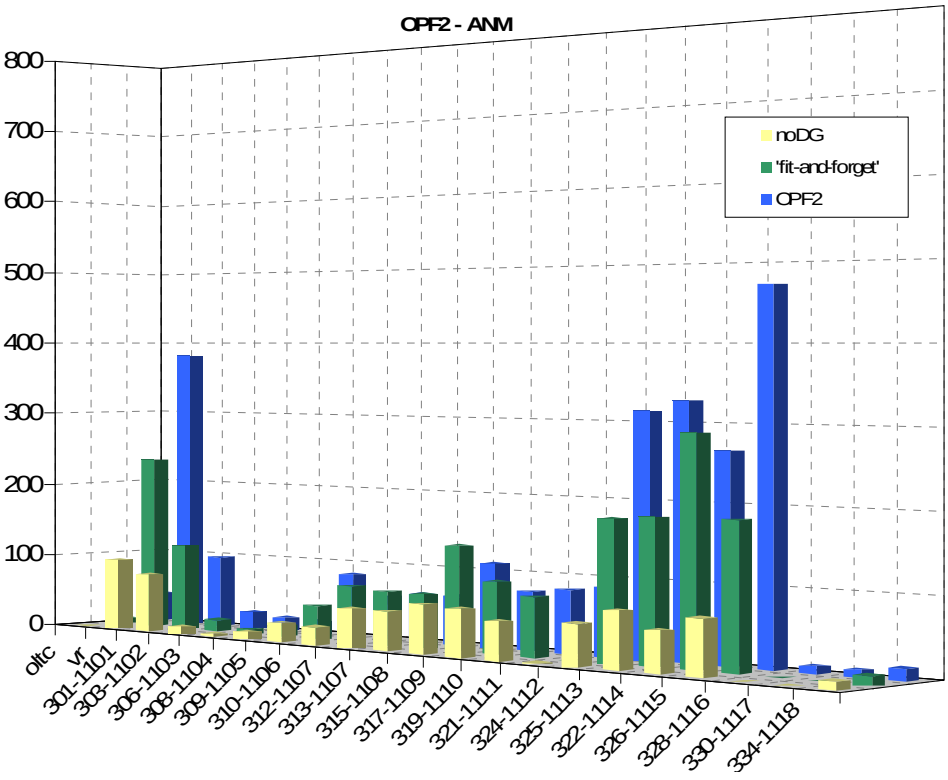

Figure 5.140: Total tap changing actions of all transformers - OPF2 case 2

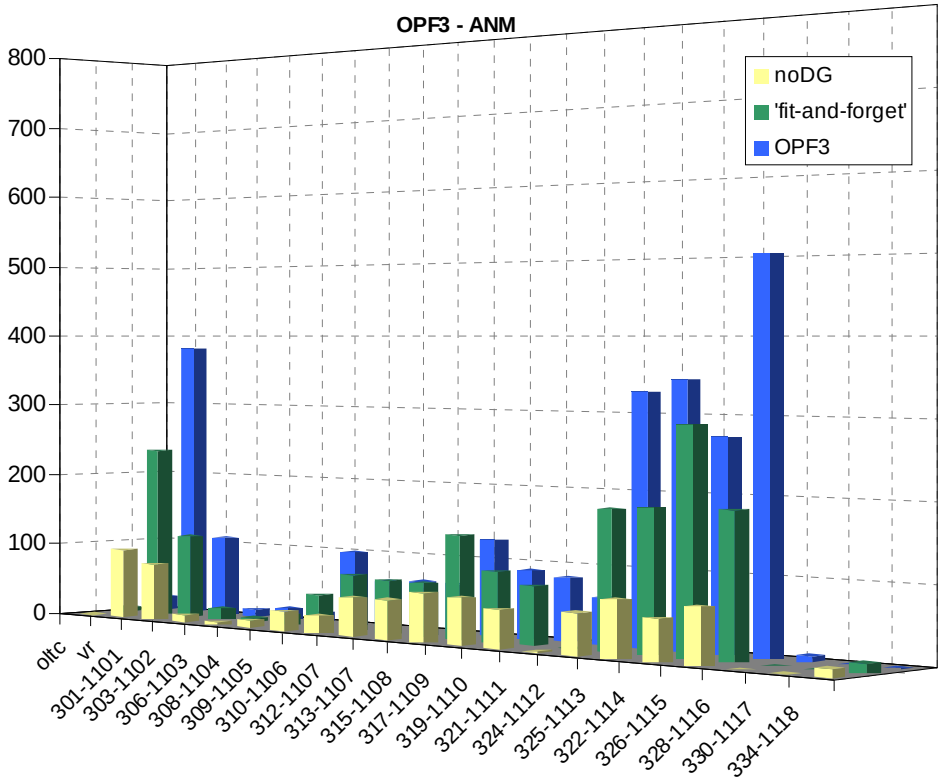

Figure 5.141: Total tap changing actions of all transformers - OPF3 case 2

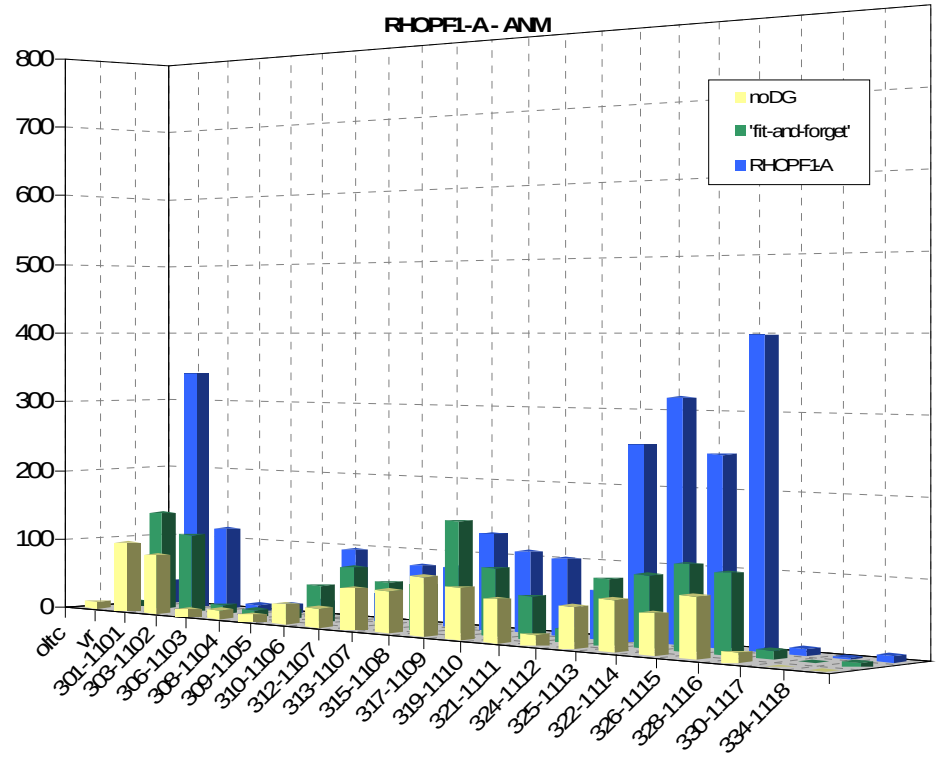

Figure 5.142: Total tap changing actions of all transformers – RHOPF1-A case 2

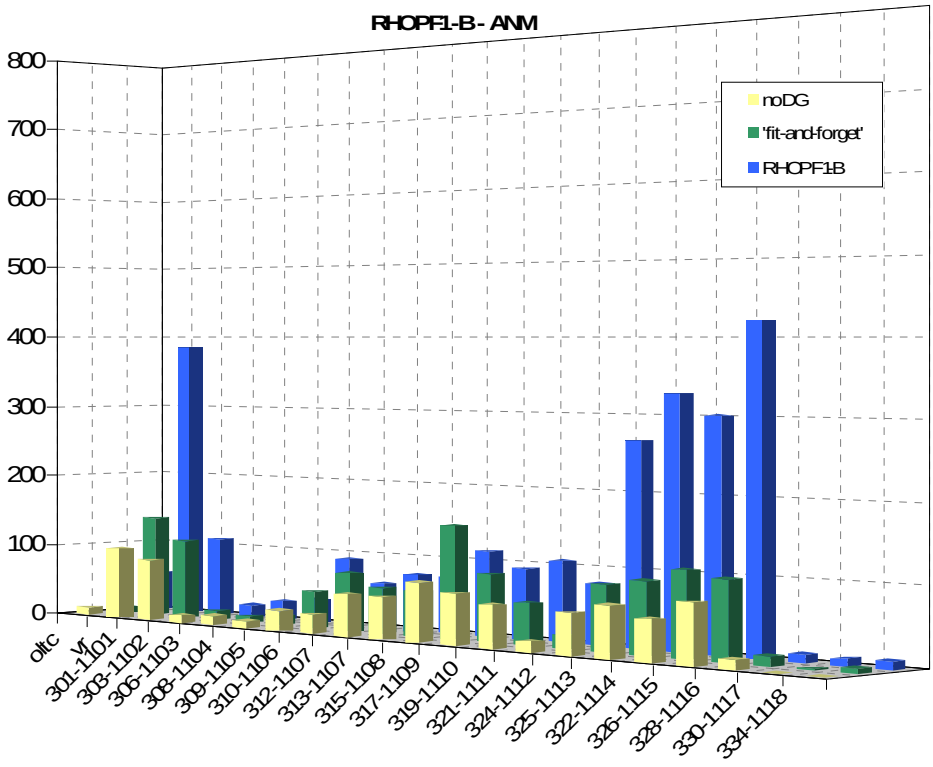

Figure 5.143: Total tap changing actions of all transformers – RHOPF1-B case 2

Figure 5.144 shows a summation of all tap-changing actions in all network transformers over the two, one-week simulation periods.

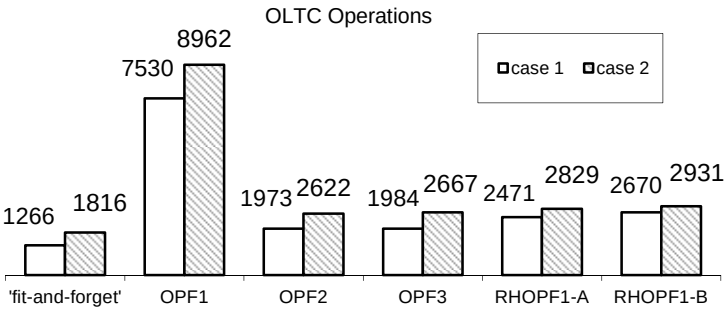

Figure 5.144: Summation of tap changing actions

Some infrequent evidence of additional short-term tap changing actions, brought about by short term switching of the DG power factor settings, was observed in the multi-objective formulations. This was greatly reduced by the larger time periods between OPF time steps. Application of the RHOPF was again demonstrated to prevent all

spurious switching, although there were more tap-changing actions in the RHOPF scenarios.

In both test cases the most frequently used tap-changing transformer was the 33/11-kV distribution transformer connecting to the tidal array at bus 1115. In case 1 tap-changing occurred on this transformer between 34.6 and 23.9 minutes on average for the OPF2, OPF3, RHOPF1-A and RHOPF1-B analyses. In case two this was between 23.7 and 20.8 minutes. In both cases the RHOPF1-B analysis produced the most frequent tap changing actions on this transformer.

5.4.7 SUMMARY AND CONCLUSIONS

The purpose of this subsection was:

- To test the combination of autonomous DG control practices with the centralised scheduling of active DG and responsive network asset control settings.
- To the test the real time OPF techniques over longer simulation periods with more varying power flow conditions.

This subsection has studied the effect of the real time OPF techniques over two 1-week simulation periods. The real time ANM OPF techniques had no difficulty in converging.

The impact of real time re-configurable ANM control practices on the network performance was similar to that witnessed over the shorter time scales at higher resolution. The combination of the ANM OPF technique with autonomous DG controllers improved the system performance with a minimisation of thermal overloading and voltage excursion.

The results have shown that the autonomous DG controllers can mitigate the most severe impacts from forecast data errors.

The RHOPF technique demonstrated a decrease in energy curtailment, over the single scenario formulations, by conditioning network control settings to suit upcoming power flow conditions based on forward looking data forecasts; negating energy curtailment by the autonomous DG controllers.

5.5 CHAPTER SUMMARY

In this chapter the application of the proposed OPF techniques to prescribe, in real time, appropriate network control pre-sets was investigated on more complex scenarios with a higher number of DG developments in two variations of a typical UK distribution network. The aim of this section was to test the proposed ANM OPF techniques and the development of advanced formulations in highly demanding scenarios.

Studies have demonstrated the robustness of the ANM OPF technique and the advanced formulations. Results have indicated that, compared with the 'fit-and-forget' approach, the ANM schemes raise the energy yield from DG substantially in each case and can therefore defer or remove the need for costly network reinforcement. The extent to which and for how long network reinforcement can be postponed is entirely dependent on specific network cases, with individual political and socio-economic factors.

In section 5.2 additional non-firm renewable DGs were added to the simplified EHV1 – ANM network and the testing procedures from chapter 4 repeated. Results showed an increase in energy yield over the fit-and-forget scenario. Similar impacts on network operation for each formulation of the ANM OPF technique were found, with unnecessary and spurious tap changing and DG power factor actions in the OPF1 scenario. Mitigation of this action was evident with the multi-objective formulations of OPF2 and OPF3. The frequency and severity of minor voltage excursions were reduced and controlled by the OPF3 formulation. Better temporal stability with no unnecessary or spurious switching was again found with the RHOPF formulation and implementation, however like the observations made in Chapter 4 imbalances and errors in the forecast data did lead to significant and sustained voltage excursion and thermal overloading of network components, particularly for the longer term forecasting routine in RHOPF1-A.

Section 5.3 presented and discussed validation and interpretation of the ANM OPF technique performance in the full EHV1 network. This system has significantly higher levels of installed renewable non-firm DG capacity.

Results showed the same benefits as in the two configurations of the simplified network indicating that the ANM OPF techniques are scalable and sustainable in larger and more complex network topologies. The potential scale of the ANM OPF techniques is only

limited by the number of constraints and variables generated in the mathematical program, and the ability of the solver to handle these. High resolution power flow solutions demonstrating the network impacts and system consequences identified the same limitations to each formulation of the ANM OPF.

In section 5.4 the ANM OPF technique was tested in combination with localised distributed automation embedded in the DG controllers. The DA controllers affect a cap on excess real power production at the DG so that power output does not significantly exceed the prescribed power output from the OPF solution between OPF time steps. This configuration allows the active DG controllers to regulate system power flows under varying power flow injections.

The simulation observation period was extended to cover a one week period, with a longer time step between successive solutions power flow solutions and an increase in the control cycle of active intervention from the ANM OPF technique was increased from 5 to 15 minutes.

Results showed that this combination of localised control regulation complimentary to the real time scheduling of active control settings maximised the system-wide energy yield while preventing extensive thermal overloading which was previously limiting the performance of the ANM OPF technique.

The RHOPF technique was shown to reduce power curtailment by autonomous DG controllers and increase energy yield by pro-actively prescribing network control settings in anticipation of upcoming power flow injections.

In conclusion, the validation, testing and interpretation presented in Chapter 5 shows the advanced ANM OPF techniques developed can provide a feasible and desirable maximisation of energy yield from renewable non-firm DGs.

Chapter 6

Discussion & Conclusions

6.1 THESIS SUMMARY

This thesis has presented an investigation into the use of OPF techniques to determine, in real time, the control settings of active DG and responsive network assets to better integrate DG from renewable energy resources; maximising energy yield and the network benefit from DG.

Chapter 2 reported on the literature survey and identified the need for technology and practices that would go beyond existing regulation of 'connect-and-manage' practices in distribution networks.

Chapter 3 discussed the enablers and procedures developed in the work reported in this thesis. It defined a new modelling environment, the underlying theory and advanced concepts used to increase the performance of real time OPF techniques for ANM.

Proof-of-concept and exploration of advanced formulations were presented in chapter 4. Simulations were performed on a simple demonstration network to examine the impacts and network response to the intervention of OPF techniques on variable control settings. Amendments to the OPF formulation to minimise the infeasible or adverse impacts and maximise the network benefits were demonstrated.

Chapter 5 extended the study to more complex network configurations with further DGs from different renewable energy resources. Studies were performed on the simplified EHV1 – ANM network with three clusters of DGs from three different resource patterns spread across parallel feeders and in the larger, significantly more complex, full EHV1 network for six renewable DGs from two areas of aggregated resource patterns. Investigations identified the boundaries of present OPF techniques and demonstrated

effective resolution through the innovative combination of the RHOPF formulation and more authoritative localised DG control practices.

6.2 ENABLERS

During the research, a number of innovative concepts were integrated to overcome the issues and limitations of scripting new formulations of OPF with the facility for real time data transfer and simulating the impacts and network response.

These enabling concepts were: a new modelling environment, suggestions for the necessary distribution network automation, a customised optimisation platform, and real time forecasting techniques.

6.2.1 MODELLING ENVIRONMENT

A challenge in this research was to identify the impacts and network responses to the variable network control settings under the intervention of real time scheduling techniques.

Power flow solutions, independent of the OPF solutions were necessary to enable the simulation and visualisation of real time distribution network control actions. This study created and demonstrated an innovative modelling environment using a suite of interconnected proprietary software. The modelling environment mimics the hardware-in-the-loop operation and each software package is interchangeable with alternative like-for-like packages or the real life network.

The modelling environment was composed of three distinct software packages: a non-specific optimisation platform with ability to script new formulations of the OPF problem, a dedicated power flow solver to emulate the impacts and network response, and a distribution management system (DMS) which managed the real time transfer of data and facilitated customised distribution network automation not presently available in the power flow solver.

6.2.2 DISTRIBUTION NETWORK AUTOMATION

OLTC transformers have operated autonomously in the distribution networks for a long time; the practice is well known and programmable in most power flow solvers.

Autonomous ANM control schemes for DG have previously been proposed and developed in other research but the practices to implement variable control settings is not well-established or standardised in power system modelling. Active DG control settings including real power curtailment and variable power factor settings were included in the power flow solutions through the DMS.

In section 5.4, secondary active DG controls were deployed to limit the DG real power output to the maximum real power production identified by the OPF solution. This provided more self-regulating control at the point of DG connection between successive solutions of the OPF scheduling and corrected network settings in response to errors in the forecast data and discrepancies in the network state information.

6.2.3 CUSTOM OPF SCRIPTING

The crux of the research presented in this thesis was the ability to script novel formulations of the OPF problem to maximise the energy yield and system benefit from renewable non-firm DG.

Manipulation and formulation of new OPF techniques for scheduling ANM control settings over multiple time intervals was denied by the limited number of problem parameters that were accessible in the common proprietary power flow software packages with ad-hoc OPF algorithms.

The non-specific optimisation platform used enabled a series of novel and customisable OPF formulations with ANM, including new multi-faceted objective functions and the potential to solve over a specific time period at multiple intervals.

This work developed an OPF technique with the facility for real time data transfer to schedule active DG and responsive network asset controller settings based on prevailing network parameters and power flow variations.

6.2.4 FORECASTING

Short term forecasting of variable demand and renewable energy resources became an additional specific aim of this thesis. The rationale behind the RHOPF technique mandated a credibility sequence of forward-looking forecast data. A series of auto-regressive forecasting techniques were explored to generate, in real time, short term

trends in variable demand and renewable DG resources. A sequence of synthetic forecast data was eventually generated to enable testing of the RHOPF technique.

6.3 FINDINGS

The findings of this study can be summarised as:

- Significant improvements in the energy yield from renewable non-firm DGs can be achieved with the real time scheduling of system-wide ANM control settings.
- Increases in energy yield were greater in distribution networks where voltage constraints restrict network headroom for the addition of new DG capacity.
- Minor violations of system constraints were evident due to network operating margins such as; deadbands, discrete tap steps, time delays, ramp rates and communication delays. These would not be sufficient to operate network protection and were brought within recommended limits. Customising of the OPF algorithms was able to reduce these occurrences and direct variable network control settings away from operational boundaries.
- Time sequential solutions of a standard, single scenario, OPF formulation could also lead to spurious and unnecessary switching of active control settings, which breached quality of supply limits.
- Multi-objective formulations of the OPF problem, penalising unnecessary deviation of variable control settings from pre-defined targets in tap-changing transformers, were successful in removing this spurious switching.
- RHOPF techniques were successful in improving the temporal stability of variable network control settings in all configurations of the distribution networks studied.
- Autonomous intervention of decentralised active DG controllers was successful in mitigating very short-term fluctuations in power flow injections from renewable energy resources without conflicting with other active network controllers.

- Innovative integration of centralised control scheduling with automated, coupled authoritative decentralised DG and controllers, significantly increased or maximised the system-wide energy yield and the network benefit from DG.

Further discussion of selected findings follows.

6.3.1 NETWORK BENEFITS

The use of new OPF techniques in real time has been demonstrated to increase the modelled energy yield from renewable non-firm DGs by acting on variable network control settings.

In chapter 4, testing of the real time OPF techniques showed that the energy yield for a single DG increased by 200% from the fit-and-forget scenario. In section 5.2, a second configuration of the simplified EHV1 – AM network with three DGs was tested. Results in this network configuration showed an increase of 216% from the fit-and-forget energy yield over both observed test case simulations.

In the larger EHV1 network, the increase in energy yield was more modest with increases between 30% and 60% over the fit-and-forget approach, for each observed test case. In the full EHV1 network, increases in energy yield were limited as the binding constraint on 58% of the installed DG capacity was thermal overloading of the network lines and transformers, for which there was no immediate alternative to real power curtailment.

Advanced formulations of the ANM OPF technique have identified simple, but effective augmentations to a standard OPF formulation that induced significant network disturbances.

6.3.2 MODELLING ENVIRONMENT

The optimisation algorithms deeply embodied in proprietary power flow solver packages lacked the freedom required to model new time-dependent formulations of OPF and independent power flow solutions to demonstrate the impact and network response to successive OPF solutions.

This work developed a simulation architecture to model the impact and network response to new OPF techniques and allowed the examination of the system consequences.

6.3.3 OPF IN REAL TIME

Real time analysis is defined as the evaluation of distribution network constraints based on prevailing network conditions rather than the speed of operation (as is commonly misunderstood). Real time OPF techniques evaluate network power flow conditions and determine appropriate network control settings to maintain network power flows within technical and statutory limits. OPF techniques were implemented in a range of network configurations and sizes for different operating applications with similar results.

Two initial limits on the use of OPF techniques in real time to schedule ANM control settings were found. These were; spurious switching of control settings leading to minor voltage excursions and thermal violation.

With the multi-objective objective function, deviation from the pre-existing voltage settings on tap changing transformers was penalised to reduce disturbance of network control settings.

Furthermore, by determining new voltage control settings from which to penalise voltage deviation, network operating settings can be directed away from the boundaries of network constraints. This was shown to reduce the frequency and severity of voltage excursions observed. It is important to recognise that these new target voltage settings were internal to the formulation of the OPF model and the active scheduling of network control settings was still determined by the converged OPF solutions.

Thermal overloading and voltage excursion were minimised in the RHOPF formulation by combining the centralised scheduling of control settings in the OPF with decentralised and autonomous secondary network automation of non-firm DGs. Secondary local control can be used to limit the real power production to levels prescribed by the OPF solution without conflicting with the operation of other autonomous network control.

6.3.4 *Combination of Localised Control and OPF*

Imbalances between the mathematical model of the OPF solution and power flow solutions of the distribution network were caused by fluctuations in resource levels and variation of the network state within the parameters of active network controllers. Real time adjustments of variable network control settings proved more difficult to regulate without the provision of autonomous localised control practices, at the point of DG connection.

In some instances, it may therefore be necessary to combine real time OPF with autonomous and decentralised active DG controllers to mitigate minor deviations from the 'optimally' prescribed state.

In this combination, the RHOPF technique was shown to reduce unnecessary curtailment on the ramp-up of renewable energy resources, which could not be distinguished from short-term spikes in resource production in the single scenario snapshot OPF formulations.

6.3.5 *Forecasting*

Forecasting was the single most significant parameter influencing the operation of the proposed RHOPF technique. A full investigation of short-term forecasting routines was beyond the scope of this project, but a basic understanding and knowledge of some plausible solutions was necessary.

Real time forecasting of renewable energy resources and variable demand patterns can be accomplished by auto-regressive forecasting techniques. This was demonstrated successfully for tidal power resource and system demand, but required further work beyond the scope of this project for wind power.

In this study a means of applying pseudo-forecasts that derived new control targets and appropriate system control pre-sets in real time was investigated as a significant improvement and evolution of control techniques in distribution networks. The pseudo-forecasts utilise the receding-horizon principle to smooth the variation in system control pre-sets. This results in a system where control actions are determined and issued to

follow the general trend in power generation and demand and not on the exact last step or current conditions, which vary frequently.

This has a major impact on the perception that short-term forecasting, particularly of wind generation, is not advantageous because it is not likely to improve on the accuracy of persistence forecasting on a sub 30 minute time frame. A clear finding from this thesis is that the very-short-term next step accuracy is secondary to the importance of the forthcoming short-term trend in power flow injections and demands when determining suitable network control actions. This demonstrated that OPF techniques for scheduling variable network control settings can benefit significantly from a more progressive means of forecasting.

6.4 CONCLUSIONS

The integration of high numbers and capacity of DG from various renewable energy resources requires a substantial change in the philosophy and operation of distribution networks. To increase or make best use of the headroom in existing distribution networks and avoid the need for expensive network reinforcement the principles of connection for DGs is changing from fit-and-forget to ‘connect-and-manage’.

To maximise the system-wide energy yield and network benefits from DG in a 'connect-and-manage' (or ANM) system, specific networks and regions of distribution networks may need to be centrally controlled and able to dispatch variable network control settings. In this thesis, OPF techniques which are well understood, transparent and adaptable, were identified as an effective tool for scheduling these control settings 'in-the-loop'.

Results illustrate that these techniques lead to significantly increased energy yield in constrained distribution networks.

ANM considers the real-time variation in generation and demand levels, rather than assuming the most onerous system conditions, therefore the reality of scheduling ANM control settings is that if the control settings are not exact and immediate local system conditions, there was the potential for network to experience thermal overloading or voltage excursions as a result of large, unseen and unchecked fluctuations in system resource. It is not feasible for the OPF to visualise and interpret the very short term

impacts and residual variability to control settings, which is why minor thermal overloading and voltage excursion was evident.

The application of more localised active DG control practices can effectively mitigate minor imbalances and discrepancies from the OPF solutions which minimised the severity and frequency of thermal overloading and voltage excursion.

The Receding-Horizon principle offered a feasible resolution against spurious and unnecessary switching of variable control settings and was demonstrated to increase the temporal stability of variable DG and responsive network asset control settings.

Hence, OPF techniques can be formulated and adapted to function online as an 'in-the-loop' decision engine. Which satisfies the hypothesis, introduced in Chapter 1, that:

"OPF techniques can be used in real time to determine appropriate active network control set-points to integrate more DG from renewable energy resources within the existing network infrastructure."

6.5 CONTRIBUTION TO KNOWLEDGE

The principle contributions to knowledge arising from this thesis were:

- The establishment and demonstration of a system wide ANM scheme to minimise the real power curtailment from multiple non-firm renewable DGs.
- The design and refinement of OPF techniques to provide the (artificial) control intelligence to a centralised distribution management system.
- A methodology and modelling environment to explore new and innovative formulations of the OPF problem and determine the impact and real time network response to active management of variable network control settings.
- The formulation of customised OPF techniques for determining better active DG and responsive network control settings in real time.
- The development and successful application of a RHOPF technique with the facility to determine pro-active (preventative) control actions to manage probable network constraints based on the temporal variation of power flow injections from renewable energy DGs.

- An assessment of localised and authoritative active DG controllers to determine re-active (corrective) control actions to manage short term fluctuations of power injections from renewable energy DGs in combination with the centralised scheduling of variable control settings.
- The demonstration that the proposed ANM OPF schemes can provide an intelligent and valid technical and economic alternative to network upgrades from the increased capacity and number of renewable DGs.

6.6 LIMITATIONS

6.6.1 DATA

This work has assumed that the production levels and available resource are linearly scalable for each test case. This is limited by the provision of data available for this project, but is not considered to detract from the operation or findings of the study.

Equally, analysis of generation and demand data with higher sampling intervals is required to test more vigorously the true performance of the ANM OPF algorithms.

6.6.2 FORECASTING

Methods of forecasting renewable energy resources at short time scales were also limited by the availability of specific case data. Auto-regressive methods of forecasting wind power resource, investigated in this thesis, were not compatible with needs of the RHOPF.

A limitation in this study was the potential to further investigate means of real time forecasting to improve the forecast data for the RHOPF technique. Significant improvements over the synthetic forecast data generated are possible by developing forecasting techniques in real time.

6.6.3 CONNECTION AGREEMENTS

The assumption of free DNO control over the prescription of DG settings is also subject to the terms and conditions of the connection agreement between the network operator and the DG developer, the parameters of which were not explored in this thesis. In the current climate operational control parameters for DG developments are determined

offline by the DNO as part of the connection agreement. Therefore there is a natural opportunity for the DNO to evaluate and schedule these in real time.

6.6.4 INCREASED USE OF ASSETS

Despite the advancements made in mitigating excessive tap operations, enhanced penetration of DG does increase the frequency of tap changing actions, particularly with any coordinated voltage control scheme. This has the potential to reduce the lifetime of network infrastructure such as the load tap changing transformers. The potential increase in maintenance costs are, with good practice in the scheme design, anticipated to be significantly lower than the cost of traditional network reinforcement [70].

6.6.5 NETWORK OBSERVABILITY

Accurate information for each distribution network is required to properly formulate and implement the ANM OPF techniques. Static data on network topology, such as transmission line and transformer: resistance, reactance and thermal capacity are vital to correlate the OPF solutions with the real distribution network. In addition, real time network observability is necessary for the basic snapshot OPF and the real time double input forecasting routine for the RHOPF-B analysis. This work has assumed that all network measurements are 100% observable and reliable. In order to deploy the proposed techniques, only real time network sampling of generation and demand levels are necessary in order to solve the OPF. It may be necessary, for full deployment, to incorporate state estimation in order to supplement or enhance limited network observability.

6.7 SUGGESTIONS FOR FURTHER WORK

During this project, several avenues of further research were identified as potentially beneficial to the current and future challenges of deploying real time OPF control in distribution networks. These themes are discussed briefly below.

- At present the loading and renewable energy resource production patterns are scaled over a large geographical area due to limitations in available generation and demand data. With more accurate description of these patterns, further

simulation would be able to identify any further benefits or limitations to the system operations.

Further analysis with generation and demand data with a higher sampling resolution is also advantageous.

- Much of this work has evolved to consider the advantages and impacts of data forecasting on the performance of the ANM OPF scheme. In an initial attempt to broaden the work on data forecasting included in this thesis, a literature survey and investigation into auto-regressive methods of time series forecasting was conducted. In combination with the findings on the use of synthetic forecast data, this has culminated in the provision of a strong platform for the development of real time data forecasting to identify substantial changes and ramps in the DG production levels that warrants further investigation.

  It was not reported because RH forecasting techniques were considered efficient to demonstrate the principle and advantages.

- As part of the literature review of this thesis, dynamic line rating methods were identified as a proven technology that can enhance system thermal capacity and deliver extended headroom capacity of DG. In the networks studied, after the alleviation of voltage rise (and drop) constraints, the next barrier to further DG capacity and energy harvest became thermal overloading of system components. In the OPF scheme development the functionality to incorporate dynamic line ratings was discussed but not modelled due to a lack of real time weather data influencing heat loss. Real time relaxation of the fixed thermal capacity limits can easily be accommodated by the transformation of the thermal limit to a variable-constraint. The inclusion of dynamic line ratings to the simulation could provide crucial information of the best potential location and use of the technology.

- Energy Storage and Demand Side Management technologies are important developments in distribution network evolution. The potential of these technologies to flatten the profile of either demand or generation (or both) is a key enabling technology to accommodate a shift in the generation mix to one

with a majority of the generation capacity embedded within the distribution networks. Energy storage and demand side management could be used to improve system operation, mitigate the impacts of variable DG and reduce levels of energy curtailment. Deploying the proposed ANM OPF scheme as a system aggregator, flexible demand and storage options could be utilised to aid operation of sections of distribution network as a virtual power plant, or even facilitate intentional system islanding.

- Based on the findings of this research, detailed economic evaluation of the benefit of ANM OPF scheme is required to back-up the case for a new control philosophy in distribution networks. The economic evaluation should contrast aggregate income from additional yield with the capital expenditure on new communication infrastructure and protocols, any additional operation and maintenance costs and a comparison of the standard network reinforcement cost.

  Further simulation of the ANM OPF algorithms, with reduce network observability will help to identify critical communication infrastructure

.

References

[1] United Nations Framework Convention on Climate Change: Key Steps. Accessed May 2013, from http://unfccc.int/2860.php

[2] Group of Eight (G8), *Gleneagles Plan of Action: Climate change, clean energy and sustainable development*, 2005. Available: https://www.gov.uk/government/uploads/system/uploads/attachment_data/file/48584/gleneagles-planofaction.pdf

[3] Department of Trade and Industry, *Meeting the Energy Challenge: A White Paper on Energy*, 2007. Available: http://webarchive.nationalarchives.gov.uk/+/http://www.berr.gov.uk/energy/whitepaper/page39534.html

[4] Climate Change Act (c. 27); Available: http://www.opsi.gov.uk/acts/acts2008/ukpga_20080027_en_2#pt1-pb2-l1g4

[5] Commission of the European Communities, *"20 20 by 2020: Europes's Climate Change Opportunity"*, COM(2008) 19 final. Available: http://eur-lex.europa.eu/LexUriServ/LexUriServ.do?uri=COM:2008:0030:FIN:en:PDF

[6] House of Lords – European Union Committee, *"The EU's Target for Renewable Energy: 20% by 2020 - Volume I: Report"*, 27th Report of Session 2007-08, 2008. Available: http://www.publications.parliament.uk/pa/ld200708/ldselect/ldeucom/175/175.pdf

[7] The Scottish Government, *"2020 Routemap for Renewable Energy in Scotland"*, July 2011

[8] Department for Energy and Climate Change, *"The UK Renewable Energy Strategy"*, 2009. Available: http://www.official-documents.gov.uk/document/cm76/7686/7686.pdf

[9] Department for Energy and Climate Change, *"The UK Renewable Energy Roadmap"*, 2011. Available: https://www.gov.uk/government/uploads/system/uploads/attachment_data/file/48128/2167-uk-renewable-energy-roadmap.pdf

[10] IET. Hydroelectric Power Factfile. Available: http://www.theiet.org/factfiles/energy/hydro-power.cfm

[11] G. P. Harrison, A. E. Kiprakis and A. R. Wallace, "A new era for mini-hydro"', *International Water Power and Dam Construction*, **54** (11), November 2002.

[12] Renewable UK Website: http://www.renewableuk.com/en/renewable-energy/wind-energy/offshore-wind/ Accessed: July 2014.

[13] Repower Systems, Repower MM82 WTG product brochure. Available: http://www.senvion.com/fileadmin/download/produkte/repower_PP_MM82_EN.pdf?fromold=1

[14] MacKay, David J.C.; *Sustainable Energy – without the hot air*; UIT Cambridge; 2008. Available: www.withouthotair.com

[15] Carbon Trust – Marine Energy. Available: http://www.carbontrust.com/resources/reports/technology/marine-energy

[16] Department for Energy and Climate Change, "Solar Photovoltaic Deployment" 2014. Available: www.gov.uk/government/statistics/solar-photovoltaics-deployment Accessed January 2014.

[17] Machowski, J., Bialek, J. and Bumby, J.R. "Power system dynamics: stability and control", Second Edition, John Wiley & Sons, Ltd, 2008

[18] Department for Energy and Climate Change, "Digest of United Kingdom energy statistics (DUKES) – Chapter 5: Electricity," 2012. Available:

https://www.gov.uk/government/publications/electricity-chapter-5-digest-of-united-kingdom-energy-statistics-dukes

[19] National Grid plc., “GB Electricity Ten Year Statement”, 2013.

[20] E. Lakervi and E.J. Homes, *Electric distribution network design*, Second ed.: IEE Power Engineering, Series 21, 2003.

[21] Hadi Saadat, “Power System Analysis,” *McGraw-Hill Series in Electrical and Computer Engineering*, 1999.

[22] R.C. Dugan and T.E. McDermott, "An Open Source Platform for Collaborating on Smart Grid Research," *IEEE PES General Meeting*, 2011.

[23] J.D. Glover, M.S. Sarma and T.J. Overbye, “Power System Analysis and Design, ” Fourth Edition, Cengage Learning, 2010.

[24] National Grid, “The Grid Code”, Issue 5, Revision 3 – 2 April 2013. Available: http://www.nationalgrid.com/uk/Electricity/Codes/

[25] *Statutory Instruments: The Electricity Safety, Quality and Continuity Regulations*., The National Archives, HM Government. Available: http://www.legislation.gov.uk/uksi/2002/2665/contents/made, 2002.

[26] C. M. Stahl, “Economic Loading of Generating Stations,” *Electrical Engineering*, vol. 50, no. 9, pp. 722 – 727, 1931.

[27] R. B. Squires, “Economic Dispatch of Generation Directly From Power System Voltages and Admittances,” *Transactions of the American Institute of Electrical Engineers. Part III: Power Apparatus and Systems*, vol. 75, no. 3, pp. 398–1244, Apr. 1960.

[28] W.F. Dommel and W.F. Tinney, "Optimal Power Flow Solutions," *IEEE Transactions on Power Apparatus and Systems*, vol. 87, 1968, pp. 1866-1876.

[29] M. Huneault and F. D. Galiana, “A Survey of the Optimal Power Flow Literature,” *IEEE transactions on Power Systems*, vol. 6, no. 2, pp. 762–770, 1991.

[30] J. F. Dopazo, O. a. Klitin, G. W. Stagg, and M. Watson, "An optimization technique for real and reactive power allocation," *Proceedings of the IEEE*, vol. 55, no. 11, pp. 1877–1885, 1967.

[31] J. Peschon, D. S. Piercy, W. F. Tinney, O. J. Tveit, and M. Cuenod, "Optimum Control of Reactive Power Flow," *IEEE Transactions on Power Apparatus and Systems*, vol. 87, no. 1, pp. 40–48, 1968.

[32] Harrison G.P & Wallace A.R.; "*Maximising Renewable Energy Integration within Electrical Networks";* World Renewable Energy Congress *(WREC2005)*; 22-27 May 2005; Aberdeen.

[33] Barker, P. P. & de Mello, R. W., *Determining the Impact of DG on Power Systems: Part 1 – Radial Distribution Systems*, IEEE. 2000.

[34] Embedded Generator Working Group, "Report into Network Access Issues," *Volume 1*, *Main Report and Appendices*, 2001

[35] K. Jarrett, J.Hedgecock, R.Gregory, and T.Warham, "Technical guide to the connection of generation to the distribution network: Appendix c.", February 2004.

[36] Masters C.L; Voltage Rise, *The big issue when connecting embedded generation to long 11kV overhead lines*; Power Engineering Journal, vol. 16; Feb-02.

[37] Weedy, B.M. & Cory, B.J.; *Electrical Power Systems*; 4th ED.; John Wiley and sons.; April 1999; ISBN 0 471 97677 6

[38] KEMA ltd. "The Contribution of Distribution Network Fault Levels from the Connection of Distributed Generation", DTI Publication DG/CG/00027/00/00, 2005.

[39] Energy Networks Association, "The Distribution Code", Issue 19 – December 2012. Available: http://www.dcode.org.uk/

[40] R. A. F. Currie, G. W. Ault, C. E. T. Foote, and J. R. Mcdonald; *Active power-flow management utilising operating margins for the increased*

connection of distributed generation, in *Proc. IEE Generation, Transmission and Distribution*, 2007, pp. 197–202.

[41] Jenkins, N., Allan, R., Crossley, P., Kirschen, D., and Strbac, G.; *Embedded Generation*; IEE Power and Energy Series 31; 2000.

[42] Walling, R.A., Saint, R., Dugan, R.C., Burke, J. and Kojovic, L.A.; "Summary of distributed resources impact on power delivery systems," *IEEE Transactions on Power Delivery*, vol.23, no.3, pp. 1636-1644, 2008.

[43] Calleja, H. And Jimenex, H.; *Performance of grid connected PV system used as an active filter*; Elsevier; 2004.

[44] F. C. Schweppe, R. D. Tabors, J. L. Kirtley, H. R. Outhred, F. H. Pickel, and A. J. Cox, "Homeostatic Utility Control," *IEEE Transactions on Power Apparatus and Systems*, vol. 99, no. 3, pp. 1151–1163, 1980.

[45] Embedded Generator Working Group, *"Future Network Design, Maintenance and Business Environment,"* 2000.

[46] EA Technology; *A Technical Review and Assessment of Active Network Management Infrastructures and Practices*; United Kingdom Department of Trade and Industry Technology Programme: New and Renewable Energy Contract Number: DG/CG/00068/00/00, URN Number: 06/1196, 2006

[47] D. A. Roberts, "Network Management Systems for Active Distribution Networks – A Feasibility Study"; 2004, Contractor: SP Power Systems Ltd, ScottishPower Plc, Report Number K/EL/00310/REP, URN 04/1361, DTI Technology Programme: New and Renewable Energy

[48] Department for Energy and Climate Change, *Smarter Grids: The Opportunity*; 2050 Roadmap: Discussion Paper 2009.

[49] A. Collinson, F. Dai, A. Beddoes, & J. Crabtree, "Solutions for the connection and operation of distributed generation," DTI – Distributed Generation Co-ordinating Group, Technical Steering Group; July 2003.

[50] R. A. F. Currie, G. W. Ault, R. W. Fordyce, D. F. Maclenan, M. Smith, and J. R. Mcdonald, “Actively Managing Wind Farm Power Output,” *IEEE Transactions on Power Systems*, vol. 23, no. 3, pp. 1523–1524, 2008.

[51] Q. Zhou, & J.W. Bialek, “Generation curtailment to manage voltage constraints in distribution networks,” IET Proceedings on Generation Transmission & Distribution, 1,(3), pp.492-498, 2007.

[52] A.E. Kiprakis and A.R. Wallace, "Maximising Energy Capture from Distributed Generators in Weak Networks," *IEE Proceedings - Generation, Transmission and Distribution*, vol. 151, 2004, pp. 611-618.

[53] T. Sansawatt, L.F. Ochoa, and G.P. Harrison, "Integrating Distributed Generation Using Decentralised Voltage Regulation," *IEEE Power and Energy Society General Meeting*, 2010.

[54] G. Strbac, N. Jenkins, M. Hird, P. Djapic & G. Nicholson, “Integration of operation of embedded generation and distribution networks,” DTI Publication K/EL/00262/REP, 2002.

[55] M. Hird, N. Jenkins & P. Taylor, “An Active 11 kV voltage Controller: Practical Considerations,” CIRED 17th International Conference on Electricity Distribution, 2003.

[56] M. Fila, D. Reid, P. Lang, J. Hiscock, and G. A. Taylor, “Flexible Voltage Control in Distribution Networks with Distributed Generation – Modelling Analysis and Field Trial Comparison,” CIRED *20th International Conference on Electricity Distribution*, 2009, no. 0411.

[57] S. White, “GenAVC: Active Local Distribution Network Management for Embedded Generation,” DTI Publication K/EL/00271/REP, 2005.

[58] S. N. Liew and G. Strbac, “Maximising penetration of wind generation in existing distribution networks,” *IEE Proceedings - Generation, Transmission and Distribution*, vol. 149, no. 3, pp. 256–262, 2002.

[59] L. F. Ochoa, C. J. Dent, and G. P. Harrison, "Distribution Network Capacity Assessment: Variable DG and Active Networks," IEEE Transactions on Power Systems, vol. 25, pp. 87-95, 2010.

[60] A. Michiorri, P.C. Taylor, S.C. Jupe, and C.J. Berry, "Investigation into the influence of environmental conditions on power system ratings," *Proceedings of the Institution of Mechanical Engineers, Part A: Journal of Power and Energy*, vol. 223, 2009, pp. 743-757

[61] T. Yip, G. Lloyd, M. Aten, B. Ferris, and C. An, "Dynamic Line Rating Protection for Wind Farm Connections," CIRED 20th International Conference on Electricity Distribution, 2009, pp. 8-11.

[62] N. C. Scott, D. J. Atkinson and J.E Morrell, "Use of Load Control to Regulate Voltage on Distribution Networks with Embedded Generation," IEEE Transactions on Power Systems, vol. 17, no.2, 2002.

[63] D. Westermann and A. John, "Demand Matching Wind Power Generation with Wide-Area Measurement and Demand-Side Management," IEEE Transactions on Energy Conversion, vol.22, no.1, 2007.

[64] T. Logenthiran, D. Srinivasan and T. Z. Shun, "Demand Side Management in Smart Grid Using Heuristic Optmization," IEEE Transactions on Smart Grid, vol.3, no.3. 2012.

[65] S. Rahman and G.B. Shrestha, "An investigation into the impact of electric vehicle load on the electric utility distribution system," IEEE Transactions on Power Delivery, vol.8, no.2, 1993.

[66] M. Yilmaz and P. T. Krein, "Review of the Impact of Vehicle-to-Grid Technologies on Distribution Systems and Utility Interfaces," IEEE Transactions on Power Electronics, vol.28 no.12 2013.

[67] T.S. Ustun, C.R. Ozansoy and A. Zayegh, "Implementing Vehicle-to-Grid (V2G) Technology with IEC 61850-7-420," IEEE Transactions on Smart Grid, vol.4 no.2, 2013.

[68] L.F. Ochoa and D.H. Wilson, “Angle constraint active management of distribution networks with wind power,” *IEEE PES: Innovative Smart Grid Technologies Conference Europe*, 2010

[69] T. Sansawatt, L. F. Ochoa, and G. P. Harrison, “Smart Decentralized Control of DG for Voltage and Thermal Constraint Management,” *IEEE Transactions on Power Systems*, vol. 27, no. 3, pp. 1637–1645, 2012.

[70] J. O’Donnell, *“Voltage Management of Networks with Distributed Generation,”* Doctor of Philosophy Dissertation, Institute for Energy Systems, University of Edinburgh, 2007.

[71] P. N. Vovos, A. E. Kiprakis, A. R. Wallace, and G. P. Harrison, “Centralized and Distributed Voltage Control: Impact on Distributed Generation Penetration,” *IEEE Transactions on Power Systems*, vol. 22, no. 1, pp. 476–483, Feb. 2007.

[72] A. Hughes, D.I. Sun, B. Ashley, B. Brewer, B. Wa, N. Way, and W.F. Tinney, "Optimal Power Flow by Newton Approach," *IEEE Transactions on Power Apparatus and Systems*, vol. 103, 1984, pp. 2864-2880.

[73] O. Alsac, J. Bright, M. Prais, and B. Stott, "Further Developments in LP-Base Optimal Power Flow," *IEEE Transactions on Power Systems*, vol. 5, 1990, pp. 697-711.

[74] L. Vargas, V. Quintana, and a. Vannelli, "A tutorial description of an interior point method and its applications to security-constrained economic dispatch," *IEEE Transactions on Power Systems*, vol. 8, 1993, pp. 1315-1324.

[75] V.H. Quintana and M. Santos-Nieto, "Reactive-Power Dispatch by Successive Quadratic Programing," *IEEE Transactions on Energy Conversion*, vol. 4, 1989, pp. 425-435.

[76] B. Stott, O. Alsac, and A. Monticelli, "Security Analysis and Optimization," *Proceedings of the IEEE*, vol. 75, 1987, pp. 1623-1644.

[77] A. Sasson and H. Merrill, "Some applications of optimization techniques to power systems problems," *Proceedings of the IEEE*, vol. 62, 1974, pp. 959-972.

[78] M. Huneault and F.D. Galiana, "A Survey of the Optimal Power Flow Literature," *IEEE transactions on Power Systems*, vol. 6, 1991, pp. 762-770.

[79] G. P. Harrison and A. R. Wallace, “Maximising Distributed Generation Capacity in Deregulated Markets,” *IEEE PES: Transmission and Distribution Conference and Exposition*, pp. 527–530, 2003.

[80] G. P. Harrison and A. R. Wallace, "Optimal power flow evaluation of distribution network capacity for the connection of distributed generation," IEE Proc.-Gener. Transm. Distrib, vol. 152, pp. 115-122, 2005.

[81] P. N. Vovos, G. P. Harrison, A. R. Wallace, and J. W. Bialek, “Optimal Power Flow as a Tool for Fault Level-Constrained Network Capacity Analysis,” *IEEE Tranactions on Power Systems*, vol. 20, no. 2, pp. 734–741, 2005.

[82] T. Boehme, G. P. Harrison, and A. R. Wallace, “Assessment of distribution network limits for non-firm connection of renewable generation,” *IET Renewable Power Generation*, vol. 4, no. 1, pp. 64–74, 2008.

[83] J. Dent, L. F. Ochoa, and G. P. Harrison, “Network Distributed Generation Capacity Analysis Using OPF With Voltage Step Constraints,” *IEEE Transactions on Power Systems*, vol. 25, no. 1, pp. 296–304, 2010.

[84] L. F. Ochoa and G. P. Harrison, “Minimizing Energy Losses: Optimal Accommodation and Smart Operation of Renewable Distributed Generation,” *IEEE Transactions on Power Systems*, vol. 26, no. 1, pp. 198–205, Feb. 2011.

[85] L. F. Ochoa, A. Keane, and G. P. Harrison, “Minimizing the Reactive Support for Distributed Generation: Enhanced Passive Operation and Smart Distribution Networks,” *IEEE Transactions on Power Systems*, vol. 26, no. 4, pp. 2134–2142, Nov. 2011.

[86] A. R. Ahmadi and T. C. Green, “Optimal power flow for autonomous regional active network management system,” *2009 IEEE Power & Energy Society General Meeting*, pp. 1–7, Jul. 2009.

[87] M. J. Dolan, E. M. Davidson, I. Kockar, G. W. Ault, and S. D. J. McArthur, “Distribution Power Flow Management Utilizing an Online Optimal Power Flow Technique,” *IEEE Transactions on Power Systems*, vol. 27, no. 2, pp. 790–799, 2012.

[88] L. Yu, D. Czarkowski, and F. D. León, “Optimal Distributed Voltage Regulation for Secondary Networks With DGs,” *IEEE Transactions on Smart Grid*, vol. 3, no. 2, pp. 959–967, 2012.

[89] T. Sansawatt; *Adaptive Control for Active Distribution Networks*; PhD Thesis; The University of Edinburgh; 2012

[90] J. Robertson, G.P. Harrison & A.R. Wallace, *“A Pseudo-Real Time Distribution Network Simulator for Analysis of Coordinated ANM Control Strategies”*, Proceedings CIRED workshop 2012: Integration of Renewables into the Distribution Grid, no. 0285.

[91] J. Bisschop and M. Roelofs, *"AIMMS, Paragon Decision Technolog, 2006.*

[92] W.H. Kersting, *“Distribution System Modelling and Analysis”*, Second Edition, CRC Press – Taylor & Francis Group, 2007.

[93] Maciejowski, J.M., “Predictive Control with Constraints,” Prentice Hall, 2002.

[94] L. Xie and M. D. Ilic, “Model Predictive Economic / Environmental Dispatch of Power Systems with Intermittent Resources,” *IEEE Power & Energy Society General Meeting*, 2009.

[95] X. Xia, J. Zhang, and A. Elaiw, "An application of model predictive control to the dynamic economic dispatch of power generation," *Control Engineering Practice*, vol. 19, no. 6, pp. 638–648, Jun. 2011.

[96] M. Glavic, S. Member, M. Hajian, and S. Member, "Receding-Horizon Multi-Step Optimization to Correct Nonviable or Unstable," *IEEE transactions on Power Systems*, vol. 26, no. 3, pp. 1641–1650, 2011.

[97] T. Boehme, J. Taylor, A. R. Wallace, and J. W. Bialek, "*Matching Renewable Electricity Generation With Demand,"* Edinburgh, U.K.: Scottish Executive, Feb. 2006.

[98] A.Sankaran Iyer, S.J. Couch, G.P. Harrison & A.R. Wallace; *Phasing of tidal current energy around the UK and the potential contribution to electricity generation*; 9th European Wave and Tidal Energy Conference; 2011.

[99] G. Giebel, R. Brownsword, G. Kariniotakis, M. Denhard and C. Darxl, *"The State of the Art in Short-Term Prediction of wind Power: A Literature Overview, 2nd Edition"*, Deliverable report of the ANEMOS Consortium, 2011.

[100] T.S. Nielsen, A. Joensen, H. Madsen, L. Landberg and G. Giebel, *"A New Reference for Predicting Wind Power,"* Wind Energy 1, 1998.

[101] X. Jiang, B. Dong, L. Xie and L. Sweeney, "*Adaptive Gaussian Process for Short-Term Wind Speed Forecasting*", Proceedings of the 19th European Conference on Artificial Intelligence, 2010.

[102] C. Lowery and M. O'Malley, *"Impact of Wind Forecast Error Statistics Upon Unit Commitment,"* IEEE Trans on sustainable Energy vol. 3 no. 4, 2012.

[103] M. Milligan, M. Schwartz and Y. Wan, *"Statistical Wind Power Forecasting for U.S. Wind Farms,"* 17th Conference on Probability and Statistics in the Atmospheric Sciences, American Meteorological Society Annual Meeting, 2004.

[104] Makridakis S., Wheelwright S.C. & Hyndman R.J.; *Forecasting Methods and Applications*; Third Edition; John Wiley & Sons; 1998.

[105] Parkpoom Suchao Jake; *The Impact of Climate Change on Electricity Demand in Thailand*; PhD Thesis; The University of Edinburgh; 2007

[106] Box G.E.P., Jenkins G.M. & Reinsel G.C.; Time Series Analysis Forecasting and Control; Third Edition; Prentice-Hall, Inc; 1994.

[107] Distributed Generation and Sustainable Electrical Energy Centre, United Kingdom Generic Distribution System (UK GDS). [Online]. Available: http://www.sedg.ac.uk/.

[108] Power Quality Application Guide, 5.4.2 Voltage Disturbances Standard EN 50160: Voltage Characteristics in Public Distribution Systems, 2004.

[109] The Distribution Code and the Guide to the Distribution Code of Licensed Distribution Network Operators of Great Britain: Issue 19: December 2012. Available: http://www.dcode.org.uk/

Appendix A: OPF Formulation

Sets

B	Buses (indexed by *b*)
L	Lines (indexed by *l*)
G	Generators (indexed by *g*)
T	Control Horizon (indexed by *t*)
X	External sources (indexed by *x*)

Parameters and Variables

Parameters:

p_g	Rated DG capacity at each generator *g*
d_b^P	Maximum real power demand at each network bus *b*
d_b^Q	Maximum reactive power demand at each network bus *b*
$\eta(t)$	Variable demand level (pu of peak demand)
$\omega(t)$	Variable renewable energy resource (pu of installed capacity)

State Variables:

$V_b(t)$	Voltage magnitude at each bus *b*
$\delta_b(t)$	Voltage phase angle at each bus *b*
$p_{b_i b_j}(t)$	Real power injection from bus *i* to bus *j*
$p_{b_j b_i}(t)$	Real power injection from bus *j* to bus *i*
$q_{b_i b_j}(t)$	Reactive power injection from bus *i* to bus *j*
$q_{b_j b_i}(t)$	Reactive power injection from bus *j* to bus *i*
$p_b^L(t)$	Total real power injection into lines at bus *b*
$q_b^L(t)$	Total real power injection into lines at bus *b*

$p_x(t)$	Real power import/export at network boundary *x*
$q_x(t)$	Reactive power import/export at network boundary *x*

Control Variables:

$p_g^{curt}(t)$	Real power curtailment of generator *g*
$\phi_g(t)$	Power factor angle of generator *g*
$V_{OLTC}(t)$	Voltage settings on regulated buses (subset of *b*)
$\tau_l(t)$	Tap ratio on tap-changing transformer *l*

Optimisation Problem

Objective function(s):

OPF1:
$$Min \sum_{g \in G} p_g^{curt}(k+j|k)$$

OPF2:
$$Min \sum_{g \in G} p_g^{curt}(k+j|k) + \sum_{b \in B} (V_{OLTC}(k+j|k) - V_{OLTC}^{t\arg et})^2$$

Constraints:

The power balance equations (Kirchhoff's current law):

$$\sum_{l \in L | \beta_l^{1,2}=b} p_b^L(t) + d_b^P \eta(t) = \sum_{g \in G | \beta_g=b} \left[p_g \omega_g(t) - p_g^{curt}(t) \right] + \sum_{x \in X | \beta_g=b} p_x(t)$$

$$\sum_{l \in L | \beta_l^{1,2}=b} q_b^L(t) + d_b^Q \eta(t) = \sum_{g \in G | \beta_g=b} \left[p_g \omega_g(t) - p_g^{curt}(t) \right] \tan(\phi_g(t)) + \sum_{x \in X | \beta_g=b} q_x(t)$$

The thermal limits of the network infrastructure:

$$(p_{b_i b_j}(t))^2 + (q_{b_i b_j}(t))^2 \le (s_l)^2$$

The statutory voltage envelope constraint:

$$V_b^- \le V_b(t) \le V_b^+ \quad \forall b \in B$$

With the Grid Supply Point (GSP) taken as reference bus b_0 and the voltage angle set to zero:

$$V_{b_0} = 1.00 \quad \delta_{b_0} = 0.00$$

Kirchhoff's voltage law:

$$p_{b_i b_j}(t) = g_l\left(\frac{V_i(t)}{\tau_l(t)}\right)^2 - \frac{V_i(t)V_j(t)}{\tau_l(t)}\left[g_l\cos(\delta_i(t)-\delta_j(t)) + b_l\sin(\delta_i(t)-\delta_j(t))\right]$$

$$q_{b_i b_j}(t) = -b_l\left(\frac{V_i(t)}{\tau_l(t)}\right)^2 - \frac{V_i(t)V_j(t)}{\tau_l(t)}\left[g_l\sin(\delta_j(t)-\delta_i(t)) - b_l\cos(\delta_j(t)-\delta_i(t))\right]$$

$$p_{b_j b_i}(t) = g_l V_j^2 - \frac{V_j(t)V_i(t)}{\tau_l(t)}\left[g_l\cos(\delta_j(t)-\delta_i(t)) + b_l\sin(\delta_j(t)-\delta_i(t))\right]$$

$$q_{b_j b_i}(t) = -b_l V_j^2 - \frac{V_j(t)V_i(t)}{\tau_l(t)}\left[g_l\sin(\delta_j(t)-\delta_i(t)) - b_l\cos(\delta_j(t)-\delta_i(t))\right]$$

Where g_l and b_l are the conductance and susceptance of *l*, respectively.

The limits of variable network controls:

Real power curtailment:

$$0 \le p_g^{curt}(t) \le p_g\,\omega_g(t)$$

Power factor angle

$$\phi_g^- \le \phi_g(t) \le \phi_g^+$$

Variable voltage settings:

$$V_{OLTC}^- \le V_{OLTC}(t) \le V_{OLTC}^+$$

Tap ratio:

$$\tau_l^- \le \tau_l(t) \le \tau_l^+$$

Appendix B: Simplified EHV1 – ANM Data

Bus Data:

Bus Name	Voltage (kV)	P Load (MW)	Q Load (MVAr)
1	132	0	0
2	33	5.41	1.09
3	33	1.93	0.39
4	33	0.06	0.01
5	33	18.4	3.74
6	33	1.96	0.4
7	33	1.9	0.39
8	33	0	0
9	33	0.55	0.11
10	33	2.7	0.55
11	33	2.85	0.58
12	33	0.81	0.16
13	33	1.01	0.2
14	33	0.58	0.12
15	33	0	0
16	33	0	0

Transformers:

Transformer Name	From Bus	To Bus	MVA	R (pu)	X (pu)
Substation OLTC	1	2	60	0	0.125
VR	8	9	15	0.0728	0.1039

Transmission Lines:

Line Name	From Bus	To Bus	MVA	R (pu)	X (pu)
Line_2-3	2	3	25	0.198	0.446
Line_2-4	2	4	45	0.187	0.299
Line_3-4	3	4	20	0.216	0.287
Line_4-5	4	5	40	0.0305	0.029
Line_4-6	4	6	15	0.517	0.376
Line_6-7	6	7	15	0.394	0.348
Line_4-8	4	8	15	0.441	0.392
Line_9-10	9	10	15	0.538	0.733
Line_10-11	10	11	15	0.944	0.657
Line_10-12	10	12	15	1.59	1.21
Line_2-13	2	13	20	0.213	0.284
Line_2-14	2	14	15	0.506	0.532
Line_13-15	13	15	15	0.265	0.281
Line_14-15	14	15	15	0.4	0.291
Line_15-16	15	16	15	0.401	0.292

Appendix C: Full EHV1 Data

Bus Data:

Bus Name	Voltage (kV)	P Load (MW)	Q Load (MVAr)
100	132	0	0
301	33	0	0
302	33	0	0
303	33	0	0
304	33	0	0
305	33	0	0
306	33	0	0
307	33	0	0
308	33	0	0
309	33	0	0
310	33	0	0
311	33	0	0
312	33	0	0
313	33	0	0
314	33	0	0
315	33	0	0
316	33	0	0
317	33	0	0
318	33	0	0
319	33	0	0
320	33	0	0
321	33	0	0
322	33	0	0
323	33	0	0
324	33	0	0
325	33	0	0
326	33	0	0
327	33	0	0
328	33	0	0
329	33	0	0
330	33	0	0
331	33	0	0
332	33	0	0
333	33	0	0
334	33	0	0
335	33	0	0
336	33	0	0
337	33	0	0
338	33	0	0
339	33	0	0
340	33	0	0

Bus Name	Voltage (kV)	P Load (MW)	Q Load (MVAr)
341	33	0	0
342	**33**	**0**	**0**
1101	11	1.9	0.39
1102	11	1.5	0.3
1103	11	0.28	0.06
1104	11	0.32	0.06
1105	11	3.31	0.67
1106	11	1.93	0.39
1107	11	18.4	3.74
1108	11	1.9	0.39
1109	11	0.06	0.01
1110	11	0.06	0.01
1111	11	0.55	0.11
1112	11	0.04	0.01
1113	11	0.77	0.15
1114	11	2.7	0.55
1115	11	2.85	0.58
1116	11	0.8	0.16
1117	11	0.21	0.04
1118	11	0.58	0.12

Transformers:

Transformer Name	From Bus	To Bus	MVA	R (pu)	X (pu)
100-302	100	302	60	0.000	0.125
301-1101	301	1101	2.5	0.381	2.978
303-1102	303	1102	2	0.517	4.019
304-321	304	321	15	0.073	0.104
306-1103	306	1103	0.5	1.579	12.120
308-1104	308	1104	0.5	1.579	12.120
309-1105	309	1105	5	0.151	1.614
310-1106	310	1106	10	0.092	1.055
312-1107	312	1107	25	0.034	0.893
313-1107	313	1107	25	0.034	0.893
315-1108	315	1108	2.5	0.384	2.997
317-1109	317	1109	0.5	2.714	20.781
319-1110	319	1110	0.5	2.714	20.781
321-1111	321	1111	1	0.797	6.175
322-1114	322	1114	5	0.192	1.498
324-1112	324	1112	0.5	2.714	20.781
325-1113	325	1113	1	0.743	5.760
326-1115	326	1115	10	0.094	1.087
328-1116	328	1116	1	0.743	5.760
330-1117	330	1117	1.5	0.580	4.492
334-1118	334	1118	1	1.010	7.791

Transmission Lines:

Line Name	From Bus	To Bus	MVA	R (pu)	X (pu)
302-303	302	303	35	0.000	0.001
302-327	302	327	17	0.213	0.284
302-331	302	331	17	0.091	0.121
302-340	302	340	17	0.227	0.302
302-341	302	341	22	0.104	0.199
303-305	303	305	13	0.128	0.094
303-339	303	339	22	0.100	0.225
305-306	305	306	26	0.000	0.001
305-307	305	307	13	0.056	0.041
307-308	307	308	13	0.002	0.001
307-309	307	309	13	0.507	0.374
310-311	310	311	17	0.216	0.287
311-312	311	312	17	0.030	0.026
311-313	311	313	17	0.031	0.032
311-314	311	314	13	0.517	0.376
311-338	311	338	17	0.079	0.106
314-315	314	315	13	0.009	0.007
314-316	314	316	13	0.166	0.121
316-301	316	301	13	0.228	0.227
316-317	316	317	26	0.000	0.001
318-304	318	304	13	0.336	0.270
318-319	318	319	26	0.000	0.001
320-321	320	321	26	0.000	0.001
320-322	320	322	13	0.538	0.733
322-323	322	323	13	1.126	0.873
322-326	322	326	13	0.944	0.657
323-324	323	324	9	0.045	0.020
323-342	323	342	13	0.238	0.173
327-328	327	328	9	0.053	0.023
327-329	327	329	13	0.094	0.110
329-330	329	330	13	0.039	0.039
329-337	329	337	13	0.083	0.083
331-332	331	332	13	0.113	0.100
332-333	332	333	17	0.153	0.203
334-333	334	333	13	0.149	0.108
335-334	335	334	13	0.400	0.291
335-336	335	336	13	0.401	0.292
337-335	337	335	13	0.088	0.088
338-318	338	318	13	0.026	0.016
339-310	339	310	22	0.098	0.221
340-311	340	311	17	0.216	0.287
341-311	341	311	22	0.208	0.398
342-325	342	325	13	0.226	0.164